University of Glasgow | College of Medical, Veterinary & Life Sciences

Dissecting the Role of T-Follicular Helper Cells in Experimental Atherosclerosis

Mr Suleman Rahman Sabir

BSc (Hons) Pharmacology

MRes Integrated Mammalian Biology

Thesis Submitted to the University of Glasgow for the degree of Doctor of Philosophy

Research Conducted in The Institute of Infection, Immunity and Inflammation, the College of Medical, Veterinary & Life Sciences, the University of Glasgow, G12 8TA

December 2015

Abstract

The immune system plays a key role in atherosclerosis, and to date several immune cells have been characterised as having pro-atherogenic or athero-protective properties. In particular, great attention has been paid to the study of CD4+ T-cells in lesion formation and progression.

In recent times, the role of a new T-cell subset termed T-follicular helper (Tfh) cells has gained attention in atherosclerosis related autoimmune conditions. Involved in aiding germinal centre (GC) B-cells in the production of high affinity, isotype switched antibodies; Tfh cells comprise a fundamental proportion of both homeostatic and pathologic GCs. Of importance, the role of the Tfh cell : GC B-cell axis has not been fully elucidated in atherosclerosis. Therefore, as part of this thesis, the role of the Tfh cell : GC B-cell axis in experimental models of atherosclerosis was dissected.

Apolipoprotein-E knock out (apoE$^{-/-}$) mice fed chow or high fat diet (HFD) for variable lengths of time (1, 2, 4, 8 and 12 weeks) displayed an increasing trend in Tfh cell number, peaking at 12 weeks post-diet. In contrast, GC B-cell populations peaked at 4 weeks post-diet. Importantly, immunohistochemcal studies demonstrated that apoE$^{-/-}$ mice fed HFD for 12 weeks comprised the sole group to express the Tfh cell transcription factor – B-cell lymphoma-6 (Bcl-6). Therefore indicating hyperlipidemia as a driver in bonafide Tfh cell marker expression.

Interleukin (IL)-21 enhances Tfh cell and GC B-cell differentiation *in vivo*. In an attempt to modulate the Tfh cell : GC B-cell axis, as part of chapter 4, an IL-21 receptor (IL-21R) deficient hyperlipidemic chimeric mouse model (IL-21R$^{-/-}$: LDLR$^{-/-}$) was generated. Loss of IL-21R significantly attenuated both Tfh cell and GC B-cell populations, alongside total and oxidised low-density lipoprotein specific antibody titres. Interestingly, loss of IL-21R enhanced lesion formation and pro-inflammatory cell infiltration. Taken together, the results described in chapter 4 demonstrate the potential athero-protective role of Tfh cell and GC B-cells in atherosclerosis.

In conclusion, the results presented in this thesis provide evidence indicative of Tfh and GC B-cells cells playing an important role in atherosclerosis. By affecting antibody production *in vivo*, Tfh cells may regulate lesion formation and subsequent

pathological progression. As such, Tfh cells may form an attractive target in the development of effective therapeutics for atherosclerosis.

Table of Contents

Chapter 3: Characterising Tfh cell & GC B-cell Populations in the apoE⁻ᐟ⁻ Mouse Model of Atherosclerosis. 87

List of Tables

Chapter 1 – General Introduction

Chapter 4 – Results

Chapter 4 – Discussion

Chapter 5 – Results

List of Figures

Chapter 1 – General Introduction

Chapter 2 – Materials and Methods

Chapter 3 – Results

Chapter 4 – Results

Chapter 5 –Introduction

Chapter 5 – Results

Chapter 5 – Discussion

List of Published Material

Peer Reviewed Published Papers

Hu D, Mohanta SK, Yin C, Peng L, Ma Z, Srikakulapu P, Grassia G, MacRitchie N, Dever G, Gordon P, Burton FL, Ialenti A, **Sabir SR**, McInnes IB, Brewer JM, Garside P, Weber C, Lehmann T, Teupser D, Habenicht L, Beer M, Grabner R, Maffia P, Weih F, Habenicht AJ. Artery Tertiary Lymphoid Organs Control Aorta Immunity and Protect against Atherosclerosis via Vascular Smooth Muscle Cell Lymphotoxin β Receptors. *Immunity.* 2015;42(6):1100-15.

Sage AP, Murphy D, Maffia P, Masters LM, **Sabir SR**, Baker LL, Cambrook H, Finigan AJ, Ait-Oufella H, Grassia G, Harrison JE, Ludewig B, Reith W, Hansson GK, Reizis B, Hugues S, Mallat Z. MHC Class II-restricted antigen presentation by plasmacytoid dendritic cells drives proatherogenic T cell immunity. *Circulation.* 2014;130(16):1363-73.

Macritchie N, Grassia G, **Sabir SR**, Maddaluno M, Welsh P, Sattar N, Ialenti A, Kurowska-Stolarska M, McInnes IB, Brewer JM, Garside P, Maffia P. Plasmacytoid dendritic cells play a key role in promoting atherosclerosis in apolipoprotein E-deficient mice. *Arterioscler Thromb Vasc Biol.* 2012;32(11):2569-79.

Conference Proceedings

Cambrook H, MacRitchie N, Grassia G, **Sabir S**, Ialenti A, Maddaluno M, Brewer J, Garside P, Maffia P. Antigen presenting cell phenotype is altered in the aorta of apolipoprotein-E deficient mice during atherosclerosis. European Atherosclerosis Society Congress 2015, MARCH 22-25, Glasgow, United Kindgom. *Atherosclerosis.* 2015;241(1):e62.

Sabir SR, MacLeod MKL, Garside P, Maffia P. Investigating the role of T-follicular helper cells in experimental atherosclerosis. Annual Congress of the British Society for Immunology. Liverpool, UK. DEC 02-05, 2013. *Immunology.* 2013;140(Suppl.1):58.

Sage A, Murphy D, Masters L, **Sabir S**, Grassia G, Maffia P, Ludewig B, Reith W, Hansson G, Reizis B, Hugues H, Mallat Z. MHC class II deficiency on Plasmacytoid Dendritic cells reduces atherosclerosis. Annual Congress of the British Society for Immunology. Liverpool, UK. DEC 02-05, 2013. *Immunology*. 2013;140(Suppl.1):188.

Acknowledgements

I dedicate this thesis to the strongest woman I know, my mother. Without her belief, and encouragement I would not have attained what I throughout life. I can't repay you for the sacrifices you've made but I hope my hard work and dedication makes you proud. Thank you for everything. Thank you for listening to me when I was down and making me copious amounts of food to make me feel better! You are my number one. Love you mum!

I would also like to thank my grandmother, for her endless love and unique personality. It's been hard without you and I miss you every day. I won't be able to tell you in person that your mana has become a doctor; I'll leave that one to the angels. Love you nannie and I miss you every day.

Finally, to end the soppy bit, I'd like to thank the best friend a guy can ever have. Tanya I did it! I know you'd be proud of me.

I would like to thank my supervisor, Dr Pasquale Maffia, for his help and encouragement throughout the years. You have been a great source of inspiration. I will miss our late night meetings and being your favourite PhD student! I look forward to continuing our friendship.

I would also like to thank my secondary supervisor, Professor Paul Garside. I am grateful for your help and will miss your grillings at lab meeting. I won't miss, however, Bob constantly telling me that you're looking for me. You have helped me immensely in my critical thinking and my general scientific development. Thank you very much.

I also owe a lot to the postdocs and fellows of the lab, specifically Gianluca, Megan and Bob. Thank you for always being there when I needed a moan or when I didn't quite know what I was doing. You've helped me a lot and I will always remember what you have taught me. Gianluca, I will miss your Italian flare and our late night chats. I hope you will miss my midnight singing. You have helped me so much throughout the years and you are a true friend. Thank you so much.

I have met so many amazing PhD students throughout my PhD. I would specifically like to thank Shafqat. You two have been there when I needed cheered up or when I

just needed someone to go to lunch with. I will specifically miss our ventures to the south side and our fix of Biryani. Thank you for everything you've done for me. I will never forget it. 14

I would also like to thank my funding body, The Nuffield Foundation, Oliver Bird Rheumatism Programme. I am grateful to have been part of such a prestigious programme and will not forget the amazing people I have met. I would specifically like to thank Dr Vicki Hughes and Professor Iain Mcinnes for their continual support and encouragement.

Authors Declaration

I declare that the work presented in this thesis is my own work. I declare that, to the best of my knowledge, it contains no material previously submitted for the award of another degree. Unless stated elsewhere, this thesis does not contain the work from any published studies.

Mr. Suleman Rahman Sabir

Signature: _____

Date: _____

Abbreviations

AD	Alzheimer's Disease
AID	Activation Induced Cytidine Deaminase
Anti-CCP	Anti-Cyclic Citrullinated Peptide
APC	Antigen Presenting Cell
Apo (various)	Apolipoprotein
apoE	Apolipoprotein-E
Ascl-2	Achaete-scute homologue-2
ATLO	Aortic Tertiary Lymphoid Organ
ATLO	Aortic Tertiary Lymphoid Organ
BATF	Basic Leucine Zipper Transcription Factor, ATF-like
Bcl-6	B-cell Lymphoma-6
BCR	B-cell Receptor
C-maf	Musculoaponeurotic Fibrosarcoma Oncogene Homolog
CAD	Coronary Artery Disease
CAMs	Cellular Adhesion Molecules
CCL19	(C-C Motif) Ligand-19
CCL2	(C-C Motif) Ligand 2
CCL21	(C-C Motif) Receptor-21
CCR7	(C-C Motif) Receptor-7
CD (various)	Cluster of Differentiation
CETP	Cholesteryl Ester Transfer Protein
CFA	Complete Freund's Adjuvant
CM	Chylomicron
CO_2	Carbon Dioxide
CTLs	Cytotoxic Lymphocytes
CVD	Cardiovascular Disease
CXCL12	(C-X-C Motif) Ligand-12
CXCL13	(C-X-C Motif) Ligand-13
CXCR5	(C-X-C Motif) Ligand-5
DC	Dendritic Cell
DNA-PK	DNA-Dependent Protein Kinase
DZ	Dark Zone
EAE	Experimental Autoimmune Encephalomyelitis

EDTA	Ethylenediaminetetraacetic Acid
ELISA	Enzyme Linked Immunosorbent Assay
Fab	Fragment Antigen Binding
Fc	Fragment Crystallisable
FCS	Foetal Calf Serum
fDC	Follicular Dendritic Cell
FSC	Forward Scatter
GC	Germinal Centre
GWAS	Genome Wide Association Study
HA	Hyaluronic Acid
HBSS	Hanks Buffers Saline Solution
HDL	High Density Lipoprotein
HFD	High Fat Diet
HRP	Horse Radish Peroxidase
HSP	Heat Shock Protein
HSP-60	Heat Shock Protein-60
HSP-65	Heat Shock Protein-65
ICAM-1	Intracellular Adhesion Molecule-1
ICOS	Inducible T-cell Co-stimulator
ICOSL	Inducible T-cell Co-Stimulator Ligand
IDL	Intermediated Density lipoprotein
IF	Immunofluorescence
IFN-γ	Interferon-Gamma
Ig (Various)	Immunoglobulin
IL (Various)	Interleukin
IL-21R	Interleukin-21 Receptor
IL-21R$^{-/-}$	Interleukin-21 Receptor Knock Out
iT-reg	Inducible T-regulatory Cell
JAK	Janus Activated Kinase
LCAT	Lecithin Cholesterol Acyltransferase
LDL	Low Density Lipoprotein
LDLR	Low Density Lipoprotein Receptor
LDLR$^{-/-}$	Low Density Lipoprotein Knock Out
LN	Lymph Node
LOX-1	Lectin-Like Oxidised Low-Density Lipoprotein Receptor-1

LPS	Lipopolysaccharide
LTβR	Lymphotoxin Beta Receptor
LZ	Light Zone
MAPK	Mitogen-activated Protein Kinase
MCP-1	Monocyte Chemotactic Protein-1
MDA	Malondialdehyde
MDA-Ox-LDL	Malondialdehyde Oxidised Low-Density Lipoprotein
MFI	Mean Fluorescent intensity
MHC (I/II)	Major Histocompatibility Complex-I/II
MI	Myocardial Infarction
Myd88	Myeloid Primary Differentiation Gene-88
MZ	Marginal Zone
NF-κβ	Nuclear Factor Kappa Light-Chain-Enhancer of Activated B-cells
NK Cell	Natural Killer Cell
nLDL	Native Low-Density Lipoprotein
NO	Nitric Oxide
nT-reg	Natural T-regulatory Cell
OD	Optical Density
ORO	Oil Red O
OVA	Ovalbumin
Ox-LDL	Oxidised Low Density Lipoprotein
PAD	Peripheral Artery Disease
Pao-LN	Para-aortic Lymph Node
PC	Phosphorylcholine
PD-1	Programmed Death Ligand-1
PDL-1	Programmed Death Ligand-1
PDL-2	Programmed Death Ligand-1
PI3K / Akt	Phosphoinositide 3-kinase /
pLN	Peripheral Lymph Node
PLO	Peripheral Lymphoid Organ
PNA	Peanut Agglutinin
R.L.U	Relative Light Unit
RA	Rheumatoid Arthritis
RAG	Recombinase Activating Gene
Rag-1	Recombinase Activating Gene-1

RAG-1	Recombination Activating Gene-1
RAG-2	Recombination Activating Gene-2
RSS	Recombination Signal Sequences
SCF	Stem Cell Factor
SCID	Severe Combined Immunodeficiency
SHC	SRC homology 2-Domain Containing
SLAM	Signalling Lymphocytic Activation Molecule
SLE	Systemic Lupus Erythematosus
SLO	Secondary Lymphoid Organ
SMC	Smooth Muscle Cell
SOCS	Suppressors of Cytokine Signalling
SR	Scavenger Receptor
SR-A	Scavenger Receptor-A
SSC	Side Scatter
SSC	Side Scatter
STAT	Signal Transducer and Activator of Transcription
T-bet	T-Box Transcription Factor
T-reg	T-regulatory
T1	Transitional-1
T2	Transitional-2
Tap-1	Transported Associated with Antigen Processing 1
TCR	T-cell Receptor
Tfh cell	T-Follicular Helper
Tfr cell	T-Follicular Regulatory Cell
TGF-β	Transforming Growth Factor-Beta
Th1	T-helper 1 Cell
Th17	T-helper 17 Cell
Th2	T-helper 2 Cell
TLO	Tertiary Lymphoid Organ
TLO	Tertiary Lymphoid Organ
TNF-α	Tumour Necrosis Factor-Alpha
TNT	TRIS NaCl Tween-20
VCAM-1	Vascular Adhesion Molecule-1
VLA-4	Very Late Antigen-4
VLDL	Very Low Density Lipoprotein

VLDLR	Very Low-Density Lipoprotein Receptor
WT	Wild Type
αβ T-cell	Alpha-Beta T-cell
γδ T-cell	Gamma-Delta T-cell

Chapter 1: General Introduction

1.1 Cardiovascular Disease (CVD)

Cardiovascular Disease (CVD) is now the leading cause of death worldwide. Accounting for approximately 17.5 million deaths in 2012 [1], CVD can manifest in various forms, from myocardial infarction (MI), stroke and peripheral artery disease (PAD). Closer to home, Scotland has the highest death rate from CVD than any other British nation (347 per 100,0000) [2]. In combination with other non-communicable diseases, Glasgow is said to suffer from the phenomenon termed the "the Glasgow effect" [3], where diseases with significant death rates affect the city's inhabitants.

Strikingly, CVD is fast becoming an epidemic in developing countries [4]. Traditionally viewed as regions with low CVD incidence, developing nations now have extensive access to westernised, high fat diets [5]. Helped by an increase in disposable income, developing countries are now witnessing the beginning of a cardiovascular crisis [5]. Unless effective therapeutics are developed and developing nations receive appropriate education on CVD, such nations face a future similar to that of their developed counterpart's.

Common to all branches of CVD is the arterial disease – atherosclerosis. Atherosclerosis is a chronic immune disease of small and medium sized arteries [6]. Characterised by the gradual accumulation of low-density lipoprotein (LDL) in the sub-endothelial space, affected arteries house dense populations of both innate and adaptive immune cells [6]. Proliferating and secreting immune mediators, these cells orchestrate the pro-atherogenic immune response to oxidised forms of LDL, as well as other implicated antigens. As a result of sustained inflammation, luminal plaques become increasingly complex, with additional immune cells being recruited. Following a breach in the protective smooth muscle / collagenous cap that encapsulates all plaques, plaques may rupture and release their pro-thrombic contents into the luminal space. Affected arteries consequently lose their patency, resulting in reduced blood flow to end organs. Individuals affected by such events may experience a stroke or MI, resulting in organ necrosis and/or death.

1.2 Risk Factors

Factors that influence atherosclerosis may comprise both physiological and life style components. Termed risk factors, risk factors comprise a range of traits, habits or conditions that may increase ones likelihood of developing atherosclerosis. The term risk factor was first coined at the start of the 1960's, when the presence of specific factors or conditions were found to be linked to an individual's susceptibility to lesion formation [7]. Risk factors are now divided into either traditional and non-tradition risk factors.

Traditional risk factors comprise a comprehensive list including, smoking, diet, race, high blood pressure and genetics. Although stand-alone, traditional risk factors are insufficient in predicting lesion formation; their cumulative presence is associated with approximately 75 % - 90 % of cardiovascular events [8]. In testament to the pro-atherogenic effects of traditional risk factors, cigarette smoking has been linked to reduced nitrous oxide (NO) production, enhanced adhesion molecule expression and increased lipid peroxidation [9-11]. Moreover, genetic abnormalities - such as familial hyperlipidemia – result in increased serum LDL levels, leading to increased retention and oxidation. High blood pressure can significantly enhance endothelial dysfunction and adhesion molecule expression by increasing sheer stress on endothelial surfaces. Table 1 below outlines the various traditional risk factors linked to atherosclerosis formation.

Of those discussed above, diabetes has emerged as a major risk factor for the development of CV morbidities [12]. Using large data sets, collected over a period of two decades, researchers have identified that diabetes doubles and triples CV risk in men and woman respectively [13]. Although rates of CVD in patients with diabetes have steadily decreased, the relative risk of CVD in diabetic cohorts remains unchanged [14]. As a result, diabetes has now become an integral component of CV treatment regimes, with a strong focus on prevention.

Traditional Risk Factors
Diabetes
Smoking
High Fat Diet
Age
Sex
Race
Genetics
High Blood Pressure

Table 1: Traditional Risk Factors involved in Atherosclerosis.

Although active inflammation plays an important role on atherosclerosis, several lifestyle and hereditary factors may influence plaque development.

1.3 Atherosclerosis – Accumulation to Inflammation

Atherosclerosis was, for decades, considered to be a vapid disease of lipid accumulation that resulted in lumen occlusion and end organ necrosis. This notion soon gave way to a new theory based heavily on the involvement of the immune system [15]. Using a combination of animal models and clinical observations, scientists identified a fundamental association between the immune system and atherosclerosis progression. Using genetically modified animal models of atherosclerosis (discussed elsewhere); researchers now understand the fundamental role of immune cells such as, T-cells, B-cells, macrophages and dendritic cell in atherosclerosis.

As part of this section, the natural progression of atherosclerosis will be discussed. Particular focus will be given to the role of immune cells in plaque progression and the pathological processes involved.

1.4 Structure of Arteries

To understand the pathological processes that lead to the formation of intra-arterial plaques, it is important to appreciate the structure of arteries. Arteries represent the body's network of vessels that carry oxygenated blood from the heart to peripheral organs. Without their plentiful supply of blood to organs, organs - and subsequent physiological processes - would cease, resulting in multi-organ failure and eventual death.

Structurally, arteries are designed to withstand the force of blood moving at high velocity. All arteries are composed of three structurally distinct areas. The innermost layer, or the tunica intima is composed largely of connective tissue with an overlying layer of endothelial cells [16]. This layer is continuously exposed to blood flow and plays an important role in the initiation and progression of inflammatory atherosclerosis. Separating the tunica intima from the middle layer – or the tunica media – is a thin layer of elastic tissue called the elastic lamina [17] [16]. The tunica media comprises a large component of arteries and consists mainly of smooth muscle cells and underlying elastic tissue [17]. The outermost layer, or the tunica externa or adventitia, is composed of collagen and another layer of elastic lamina tissue.

Taken together, the components of each layer allow arteries to withstand pressure from circulating blood, while maintaining a plentiful supply of oxygen rich blood to end organs. Due to the pathological nature of atherosclerosis, lesion formation significantly alters the anatomy and function of these layers, with the intense infiltration of immune cells and structural augmentation.

1.5 Development and Progression of Atherosclerosis

For decades, atherosclerosis was viewed as a physiological disease of aging. In testament to this theory, nascent stages of atherosclerosis can be found in young children [18]. Whether these early stages develop into mature plaques is heavily dependent on the presence of risk factors including, genetics, smoking, diet, lifestyle and co-morbidity (discussed elsewhere). In general terms, atherosclerosis is the result of impaired clearance of LDLs coupled with a chronic inflammatory response. Although other factors play an important role in plaque progression, LDL's role in the initiation and progression of atherosclerosis is fundamental.

LDL are homeostatic transport molecules composed of triglycerides, cholesterol and free fatty acids [19]. As such, LDL's transport components of energy metabolism and cellular construction to their relevant locations throughout the body [19]. Under physiological conditions, LDL infiltrate artery walls, where they release their components and are transported away from arteries via another lipoprotein pathway [20]. This pathway, or the reverse cholesterol transport pathway, is dependent on another class of plasma lipoproteins – termed high-density lipoproteins (HDL) [21]. HDL, as such remove excess cholesterol from the sub-endothelial layer of arteries and transports it to the liver, from where it is excreted in bile [21]. In cases where the homeostatic balance between LDL infiltration and removal is favoured in the balance of the former, LDLs accumulate in the sub-endothelial layer and initiate the formation of nascent atherosclerotic plaques. Such cases can arise when individuals lead sedentary life styles coupled with fat enriched diets, or in cases of genetic disorders such as familial hyperlipidemia.

Once in the sub-endothelial layer, LDL particles are exposed to a wealth of oxidising agents that progressively modify native LDL (nLDL) into pathogenic oxidised-LDL (Ox-LDL) [22]. Due to the progressive oxidation of nLDL, Ox-LDL particles are more "immune-obvious" than their native counterparts. In particular, tissue resident macrophages display high affinity for the newly formed molecules. By their nature, phagocytising macrophages bind and uptake Ox-LDL via a range of innate receptors called scavenger receptors (SR)s on their surface. SRs comprise a diverse group of innate receptors involved in binding pattern molecules located on the surface of pathogens, apoptotic cells and altered physiological molecules [23]. To date, several

SRs have been implicated in Ox-LDL recognition and uptake by arterial macrophages. These include, CD36, scavenger receptor-A (SR-A) and lectin-like oxidised low-density lipoprotein receptor-1 (LOX-1) [24-26]. Highlighting the importance of SRs to lesion formation, some have shown that loss of SR function significantly ameliorates lesion formation [27-29]. Conversely, others have demonstrated that loss of SR function in fact enhances lesion formation [30]. As such, these findings suggest that several Ox-LDL uptake mechanisms may exist to promote lesion formation.

As arterial macrophages progressively uptake and internalise Ox-LDL molecules, they become overwhelmed and cease functioning as local phagocytes. As a result, arterial macrophages readily transform into pathological structures termed foam cells. Seen under the microscope, foam cells are characteristically yellow in colour, due to the excessive cholesterol products contained in their cytoplasm. As such, foam cells were one of the first immune cells to be linked with atherosclerosis and form the characteristic signs of nascent plaque formation [31, 32]. When aggregated together, foam cells form structures called fatty streaks. Found at early stages of disease, fatty steaks can be found in stillborn babies as well as infants [33]. Once completely overwhelmed, foam cells release their toxic contents through apoptosis and contribute to the formation of a necrotic core [34].

Diverging from the original descriptions of atherosclerosis as a simple disease of accumulation, the past few decades have provided evidence indicating the important role of Ox-LDL in initiating pro-inflammatory, atherogenic events. Importantly, remnants of oxidation have been implicated in the up-regulation of various leukocyte adhesion molecules and chemokines. Specifically, Ox-LDL can induce the expression of vascular cellular adhesion molecule-1 (VCAM-1), intracellular cellular adhesion molecule-1 (ICAM-1), P-selectin and the chemokine (C-C motif) ligand 2 (CCL2) or also referred to as monocyte chemotactic protein 1 (MCP-1) on endothelial cells [35, 36]. Facing the lumen, adhesion molecules bind circulating leukocytes via specific receptors. As a result, bound leukocytes roll along the endothelial surface and migrate towards the sub-endothelial space, where they contribute to the evolving inflammatory response. Highlighting the importance of adhesion molecules and their receptors to lesion formation, loss of adhesion molecule expression in apoE$^{-/-}$ mice significantly attenuates atherosclerosis [37].

As well as affecting adhesion molecule expression, Ox-LDL activates arterial macrophages, resulting in the secretion of pro-inflammatory cytokines. The release of these cytokines induces a pro-inflammatory cascade in which further adhesion molecule expression is induced, resulting in increased leukocyte migration [35]. Supporting this, Ox-LDL has been implicated in the up regulation of various macrophage associated pro-inflammatory genes. This continuous cycle of activation and infiltration contributes significantly to plaque progression and evolution of the local immune response. Highlighting the importance of Ox-LDL to macrophage activation, loss of human SRs has been shown to attenuate pro-inflammatory tumour necrosis factor-alpha (TNF-α) and IL-1β production in a nuclear factor kappa-light chain enhancer of activated B-cells (NF-$\kappa\beta$) dependent manner [38].

As well as macrophages, T-cells are well-characterised components of atherosclerotic plaques [39-41]. Responding to a single antigen via T-cell receptor (TCR) – major histocompatibility complex (MHC)-I/II interaction, T-cells secrete vast amounts of pro-inflammatory cytokines [42] [43]. These cytokines consequently influence the pro-inflammatory processes involved in cell recruitment and plaque progression. Moreover, T-cells can help B-cells in the production of high affinity antibodies [44]. Several products required for this process have been identified in aortic tertiary lymphoid organs (ATLO)s [45] – ectopic structures found in the adventitia of aged atherosclerotic mice. Upon engagement of antigen, T-cells home to affected arteries using adhesion molecules such as VCAM-1 and ICAM-1. Binding of such molecules to the endothelial expressed integrins, very-late antigen-4 (VLA-4) and lymphocyte function associated antigen-1 (LFA-1) mediates this process [46] [47]. Upon migration to the sub-endothelial space, T-cells proceed to secrete toxic cytokines, thereby increasing endothelial dysfunction, adhesion molecule expression and migration of additional leukocytes.

Collectively, debris from dying foam cells, cholesterol products and immune cells form a structure termed the necrotic core. A hallmark of advanced disease, the necrotic core houses a range of potential neo-antigens for resident immune cells to recognise and react to. Driven by the secretion of inflammatory mediators, the necrotic core continues to grow in size, resulting in the gradual occlusion of the artery in question. Secreted products also enhance smooth muscle phenotypic transition from contractile to pathological in function. Specifically, smooth muscle cells migrate

from the tunica media to the sub-endothelial space, where they accumulate and deposit extra-cellular matrix components into forming lesion cap. Exposure to pro-inflammatory stimuli and persistent erosion of the smooth muscle cap may breach plaque integrity and allow the pro-thromic contents of spill into the luminal space. If such an event occurs, it is most likely to result in stroke or MI by inducing thrombus formation.

1.6 Antigen Specificity and Molecular Mimicry

To date, various antigens have been implicated in the induction of atherosclerosis, including, Ox-LDL, heat shock protein 60 (HSP-60) and various microbes. In particular, Helicobacter pylori can be found in a significant proportion of human lesions, with a strong correlation to adhesion molecule expression [48, 49]. Chlamydia Pneumoniae can also be detected in atherosclerotic lesions [48, 50, 51]. Moreover, inoculation of both mice and rabbits with Chlamydia Pneumoniae has been shown to drive lesion formation [52].

Interestingly, some have suggested that common motifs between different pathological molecules may drive atherosclerosis. Termed, molecular mimicry, several studies have studied the potential significance of this notion. Supporting molecular mimicry, immunization of low-density lipoprotein receptor knock out (LDLR$^{-/-}$) mice with Streptococcus Pneumoniae induces Ox-LDL specific antibody production [53]. Importantly, these antibodies bind pneumococcal components effectively [53], therefore indicating a common motif.

It is well documented that antigens play an important role in atherosclerosis. Of importance to this notion however, the location in which a T-cell become activated and subsequently exerts their pro-atherogenic affects is contested. Conforming to traditional views, T-cells become activated in secondary lymphoid organs and travel to arteries, where they exert their pro-atherogenic effects. In contrast, some have provided data suggesting that antigen presentation and subsequent T-cell activation may in fact occur locally within the aorta [54]

1.7 Animal Models of Atherosclerosis

Due to the location of plaques and the importance of arteries to life, researchers are restrained to studying human atherosclerosis post-mortem or by using surgical biopsies. As such, the pathophysiological processes that lead to plaque development may only be studied when plaques are the cause of death. To study the multifaceted nature of atherosclerosis, and the role of various processes in plaque formation, researchers have utilised animal models throughout the decades. In testament to the role of animal models in atherosclerosis research, much of what researchers understand about plaque formation is a direct result of animal experimentation.

To date, several species have been used in the study of atherosclerosis, including, mice, pigs, rabbits and non-human primates. Like all models of disease, these models have advantages and limitations to their use. In recent times, mouse models have dominated atherosclerosis research. However, in using these models, it is important to acknowledge the differences between mice and humans and their subsequent effect on atherosclerosis.

Humans develop lesions mainly in the carotid, coronary and peripheral arteries, whereas mice develop lesions more commonly in the aortic root and aortic arch. Although plaque location may differ, many of the pathophysiological processes required for lesion formation are common to both humans and mice. This coupled with the short time needed for plaque formation; low cost and high litter numbers has resulted in mouse models dominating atherosclerosis research.

Although mouse models have dominated atherosclerosis research, larger animal species have also contributed to our understanding of atherosclerosis formation and progression. As with mouse models, these models represent their own advantages and disadvantages as faithful models of atherosclerosis. Unlike mice, pigs develop spontaneous atherosclerosis that can be enhanced with the use of atherogenic diets [55-57]. Moreover, pigs develop lesions at sites more commonly affected in humans [58], display human-like lipoprotein profiles and are big enough for minimally-invasive interventional studies [59]. As such, pigs may be viewed as a robust model of atherosclerosis. However, pigs are expensive to maintain and display little susceptibility to genetic manipulation. In contrast to this, however, pig models have

provided valuable data with regards to the transcriptional regulation of genes at sites susceptible and resistant to atherosclerosis [60].

Rabbits have been used extensively throughout the literature as another model of atherosclerosis. Rabbits are most sensitive to cholesterol burden [61], cheap to maintain and share some of the characteristics found in pigs. Moreover, rabbits have been instrumental in the study of lipoprotein fractions and genetic conditions affecting lipoprotein metabolism [62] [63].

Perhaps most controversially, non-human primates have been used in the study of atherosclerosis. Non-human primates display the advantage of expressing humanoid lipoproteins and lipoprotein metabolism. Males are more susceptible to lesion formation and plaques occur in areas more applicable to human disease [63]. Moreover, non-human primates display enhanced vasa vasorum density and increased intimal thickening [64] - a feature of human disease not commonly found in lower animal models. The size, maintenance cost, lack of genetic diversity and time taken for plaque development represent a limitation to the use of non-human primates in atherosclerosis research.

In comparison to large animals, the mouse has remained the animal of choice in atherosclerosis research. In comparison to humans, wild type (WT) mice are relatively resistant to plaque formation. This is mainly due to variations in rodent and human cholesterol metabolism. Mouse cholesterol is composed mainly of athero-protective HDL particles, while humans display a more pro-atherogenic LDL profile. One reason for this difference can be found in the expression of cholesterol ester transfer protein (CETP) in the mouse [65]. Involved in the transport of LDL constituents to HDL particles, CETP significantly reduces circulating levels of atherogenic LDL in the mouse. Moreover, humans absorb approximately 50% of cholesterol derived from dietary sources, while the mouse does not absorb significant amounts [66]. A combination of these two processes allows mice to express HDL dominant (athero-protective) lipid profiles.

To address these issues, early researchers used genetic approaches to ablate components of cholesterol transport. In doing so, scientists were able to skew mouse lipoprotein kinetics from athero-protective profiles to atherogenic ones. Although

32

these approaches yielded a variety of transgenic animals, two models have predominated and are in common use today. These models were termed the apoE$^{-/-}$ and LDLR$^{-/-}$ mouse models.

As part of this section, both the apoE$^{-/-}$ and LDLR$^{-/-}$ mouse models will be discussed. Particular attention will be given to their advantages in atherosclerosis research, as well as their disadvantages as a model of human disease.

1.7.1 ApoE$^{-/-}$ Mouse Model of Atherosclerosis

The apoE$^{-/-}$ mouse model lacks the 34 kD glycoprotein apoE and is perhaps the most used animal model of atherosclerosis [67]. Involved in chylomicron remnant and LDL metabolism, apoE displays high affinity for LDL receptors in the liver, where receptor mediated endocytosis results in lipid clearance [67]. Lack of functional apoE in apoE$^{-/-}$ mice results in enhanced serum very low-density lipoprotein (VLDL), LDL, intermediate density lipoprotein (IDL) levels with a concomitant decrease in HDL levels. As such, apoE$^{-/-}$ mice display lipoprotein levels that are favourable to lesion development. In testament to this, apoE$^{-/-}$ mice develop lesions typical of a more advanced stage of human pre-atherosclerotic lesions when fed standard laboratory diet [68]. When fed diets enriched with cholesterol and fat, apoE$^{-/-}$ mice develop arterial lesions in an accelerated manner [68]. However, lesions induced in such a manner, display reduced cellularity and contain primarily lipid laden foam cells [69]. The short time frame in which apoE mice breed, coupled with their large litters, has allowed scientists to employ several genetic approaches to study immune cell involvement in atherosclerosis. In particular, the apoE$^{-/-}$ mice crossed with immuno-deficient recombinase activation gene (RAG) or severe combined immuno-deficient (SCID) mice have been instrumental in our understanding of the role of T-cells and B-cells in atherosclerosis.

Although used throughout the literature as a reliable model of atherosclerosis, the apoE$^{-/-}$ mouse model has several disadvantages. In particular, atherogenesis in the apoE$^{-/-}$ mouse is dependent on lipoprotein remnants, rather than the larger LDL particles that are causative in humans. Moreover, apoE has been suggested to have important roles in macrophage, immune and adipose tissue biology [70]. As such, loss of apoE may affect these processes in a manner independent of cholesterol kinetics. Irrespective of these disadvantages, the apoE mouse model has become one of the gold standard models of experimental atherogenesis.

1.7.2 LDLR$^{-/-}$ Mouse Model of Atherosclerosis

Unlike apoE, loss of low-density lipoprotein receptor (LDLR) expression in LDLR$^{-/-}$ solely affects lipoprotein uptake and clearance. Due to the lack of hepatic LDLRs, LDLR$^{-/-}$ are unable to remove and metabolise atherogenic lipoprotein molecules via apoE-LDLR mediated endocytosis. As such, LDL predominates in the circulation of animals, leading to vascular accumulation and atherosclerosis formation. Interestingly, LDLR$^{-/-}$ mice do not develop spontaneous atherosclerosis and are dependent on the use of cholesterol and fat enriched HFDs [71, 72]. When fed HFD for extended periods of time, LDLR$^{-/-}$ mice develop advanced lesions throughout the aortic tree, aortic root and innominate arteries [73]. Unfortunately, studies using LDLR$^{-/-}$ mice use a variety of atherogenic diets, with varying cholesterol content. As such, studies using the LDLR$^{-/-}$ model are often not standardised, making comparisons difficult. A major advantage of the LDLR$^{-/-}$ model is that these mice are ideal for the generation of chimeras. Repopulation of irradiated apoE$^{-/-}$ mice with bone marrow cells from apoE$^{+/+}$ donors ablated atherosclerosis. On the contrary, LDL receptor phenotype of the donor cells does not significantly impact atherosclerosis when used to repopulate LDLR$^{-/-}$ mice [74].

Despite their limitations, the apoE$^{-/-}$ and LDLR$^{-/-}$ models have proven invaluable in our understanding of the complex nature of atherosclerosis. Both models have been used in this thesis.

1.8 T-cells in Atherosclerosis

Although found in healthy arteries [75], T-cells are greatly expanded in the context of atherosclerosis, where they accumulate mainly within the adventitia of affected arteries. The majority of T-cells found in atherosclerotic plaques are of memory/effector phenotype, express the $\alpha\beta$-TCR [39, 76] and are found in close proximity to dendritic cells (DCs) in humans [77]. As well as this, atherosclerotic lesions house dense populations of Ox-LDL and HSP specific T-cells, thus indicating local activation and proliferation [78, 79].

The importance of CD4+ T-cells in atherosclerosis has been demonstrated in studies using the immune-deficient recombinase activating gene-1 (Rag-1) and SCID mouse strains [80, 81]. Crossed with LDLR$^{-/-}$ or apoE$^{-/-}$ mice, these mice develop attenuated lesions, with one study reporting a 54% reduction in lesion formation [82]. Consequently, and reinforcing the importance of T-cells in atherosclerosis, adoptive transfer of T-cells into apoE$^{-/-}$ scid/scid mice enhances lesion formation; with one study demonstrating a 164% increase [81]. Highlighting the importance of oxidised forms of LDL, malondialdehyde modified LDL (MDA-Ox-LDL) specific T-cells preferentially enhance lesion formation when transferred into apoE$^{-/-}$ scid/scid mice [83].

1.9 T-helper 1 Cells & Atherosclerosis

T-helper 1 cells (Th1) represent the most studied lymphocyte population in atherosclerosis. In testament to this, atherosclerosis is now considered to be a Th1 mediated disease. The prominence of Th1 responses may be explained by the Th1 skewed animal models used to study lesion development [84]; therefore the importance of other immune cells should not be ignored.

Using apoE$^{-/-}$ and LDLR$^{-/-}$ mice scientists have been able to study the involvement of Th1 mediated pathways in disease progression. Research into the role of Th1 cells in atherosclerosis has followed two directions – modulation of signature Th1 cell cytokines and the modulation of CD4+ Th1 cells *in vivo.* As result, we now have an extensive understanding of the role Th1 cells (and their signature cytokines) play in atherosclerosis.

In this section, the role of Th1 associated cytokines and Th1 cells in atherosclerosis will be discussed.

1.9.1 IFN-γ

Interferon-gamma (IFN-γ) is perhaps the most noted and discussed cytokines secreted by activated Th1 cells. Interestingly, *in situ* and immunohistochemical analysis of human plaques has demonstrated that presence of IFN-γ secreting cells in human plaques (10, 11).

IFN-γ has been documented to have various pro-atherogenic effects. These effects include, reduced collagen fibre production, enhanced major MHC-II expression, elevated cytokine secretion and increased protease production [42, 85]. As well as this, IFN-γ contributes to the feedback loop between adaptive and innate immune systems, by enhancing VCAM-1 and ICAM-1 expression on smooth muscle cells, macrophages and endothelial cells [86-88].

Moreover, exogenous administration of IFN-γ increases lesion size, MHC-II expression and CD4+ T-cell expansion in apoE$^{-/-}$ mice *in vivo* [89]. Further supporting a pro-atherogenic role of IFN-γ, apoE$^{-/-}$ or LDLR$^{-/-}$ mice deficient in IFN-γ receptor develop reduced atherosclerosis [42, 90]. Exerting its effects throughout atherosclerosis development, IFN-γ also enhances oxidised LDL uptake into THP-1 macrophages *in vitro* [91] and induces SR-1 expression on THP-1 macrophages and vascular smooth muscle cells (SMCs) [91, 92].

It is important to consider that other cell types secrete IFN-γ, including macrophages and natural killer (NK) cells. The effect of T-cell independent IFN-γ secretion must, therefore, be considered. Indeed, IFN-γ can enhance atherosclerosis formation in the absence of T and B-cells in vivo, via modulation of smooth muscle cells *in vivo* [93]. Irrespective of this, IFN-γ is secreted in vast amounts by activated Th1 cells – a source that contributes significantly to pathology.

Taken together, the studies described above provide evidence that implicates IFN-γ as an important cytokine in atherosclerosis development. They also indicate that IFN-γ functions to exert its effects throughout atherosclerosis development, and as such is an important mediator in all stages of the pro-atherogenic immune response.

1.9.2 IL-18

IL-18, along with IL-12, is an important cytokine in the formation of effector Th1 cells [39]. The importance of IL-18 to Th1 cell function is demonstrated by the finding that IL-18 deficient mice develop significantly reduced Th1 responses *in vivo* [94]. IL-18 is believed to exert its pro-atherogenic effects via enhanced IFN-γ production [95]. Using IL-18$^{-/-}$/apoE$^{-/-}$ mice, researchers have demonstrated that IL-18 ablation reduces I-A^b and IFN- γ expression, as well as reducing lesion formation in an IFN-γ dependent manner [96].

Interestingly, IL-18$^{-/-}$ apoE$^{-/-}$ mice display elevated serum cholesterol and triglyceride levels [96], thus providing enhanced native LDL for oxidation and uptake by arterial macrophages.

Taken together, these studies indicate that IL-18 is an important mediator in the pro-atherogenic immune response and mediates its effects via IFN-γ production. As well as this, these studies indicate that IL-18 can function to enhance early stage atherogenesis by modulating cholesterol metabolism *in vivo*.

1.9.3 IL-2

IL-2 belongs to a super family of cytokines, which – in combination with different subunits – signal via the type-1 receptor family. IL-2 exerts a range of effects on different immune subsets, with T-cells being the most prominent. Upon activation, T-cells express copious amounts of IL-2, followed by increased expression of the IL-2R. Working in a paracrine manner, IL-2 influences the expansion of antigen experienced effector T-cell populations *in vivo* [97]. As well as inducing effector T-cell responses, IL-2 maintains immune tolerance by influencing CD4+ CD25+ T-regulatory (T-reg) cells in the thymus [98-100].

The role of IL-2 in atherosclerosis was first addressed in studies using apoE$^{-/-}$ mice treated with IL-2 or IL-2 blocking antibodies. IL-2 was found to exacerbate atherosclerosis formation, while blockade of IL-2 protein resulted in atheroprotection [101]. In contrast to these findings, IL-2 has been shown by some to reduce atherosclerosis formation *in vivo*, in a T-reg dependent manner [102]. Recent studies have supported this finding, with anti-CD3/IL-2 therapy being effective in reducing atherosclerosis in apoE$^{-/-}$ mice via a T-reg dependent manner [103].

Together, these studies provide evidence indicating the role of IL-2 in maintaining a balance between pro-atherogenic effector T-cell and athero-protective T-reg responses *in vivo*.

1.9.4 T-bet

T-box transcription factor TBX21 (T-bet) is attributed as the Th1 cell master regulator of function. Particularly, T-bet induces the expression of IFN-γ in naïve T-cells [104]. Furthermore, T-bet has been shown to re-direct lineage-committed T-helper 2 (Th2) cells to a Th1 cell programme, thus suppressing Th2 development [104].

Due to its effects on IFN-γ production and role in Th1 cell development, T-bet has received considerable attention in cardiovascular research. Using T-bet deficient LDLR$^{-/-}$ mice, some have shown that T-bet deficiency significantly reduces plaque formation *in vivo* [105]. Coupled with this, T-bet deficiency also results in enhanced Th2 cell expression, resulting in increased athero-protective E06 antibodies [105]. As well as affecting Th1 cell responses *in vivo,* these studies indicate that T-bet deficiency functions to promote athero-protective antibody responses *in vivo*. As such, T-bet modulation *in vivo* may prove to be a powerful tool in modulating atherosclerosis.

1.10 T-helper 2 Cells in Atherosclerosis

Th2 cells are generally perceived to convey an athero-protective function in atherosclerosis, via their influence on antibody production and cytokine secretion. In testament to the athero-protective effects of Th2 cells, BALB/c mice – which are characterised by a Th2 cell response – are resistant to atherosclerosis formation [106]. In contrast to this, C57BL6/J mice – which are characterised by a Th1 cell response - are susceptible to atherosclerosis formation [106]. As Th2 cells exert their athero-protective effects via the production of cytokines, this section will discuss the influence of Th2 derived cytokines on atherosclerosis.

1.10.1   IL-4

IL-4 represents one of the signature Th2 cytokines and its role in atherosclerosis is debated. Exogenous administration of IL-4 to apoE$^{-/-}$ mice has been reported to afford no athero-protective or pro-atherogenic effect, with no change in T-cell or macrophage infiltration compared to control mice [107]. Moreover, both IL-4$^{-/-}$/apoE$^{-/-}$ and IL-4$^{-/-}$/LDLR$^{-/-}$ mice do not display increased or decreased plaque formation [107]. In contrast to this, long-term studies using HFD fed IL-4$^{-/-}$/apoE$^{-/-}$ mice have reported a 27% reduction in lesion area in comparison to control groups [108]. Adding to this, IL-4$^{-/-}$: LDLR$^{-/-}$ chimeric mice display significantly reduced lesion formation than respective control animals [109].

Together, these studies suggest that the role IL-4 In atherosclerosis is controversial.

1.10.2 IL-5

In contrast to IL-4's role in atherosclerosis, IL-5's role is more defined and consistent throughout the literature. A variety of studies have reported the athero-protective functions of IL-5 *in vivo*. In particular, vaccination with MDA-Ox-LDL in apoE$^{-/-}$ mice results in reduced atherosclerosis in an IL-5 dependent manner [110]. Moreover, this reduction is associated with enhanced natural, athero-protective IgM production [110]. Using a chimeric approach, some have reported that IL-5$^{-/-}$: LDLR$^{-/-}$ mice develop enhanced atherosclerosis, coupled with reduced natural IgM production [110].

Taken together, these studies suggest that IL-5 may play variable roles in atherosclerosis. They also suggest that IL-5 exerts is effects via modulation of natural IgM antibodies that convey protective roles in atherosclerosis. As such, modulation of IL-5 may be a powerful tool in the induction of athero-protective antibody responses.

1.10.3 IL-33

Attributed as another Th2 cell cytokine, IL-33 is present in the arteries of both healthy and diseased arteries [111]. *In vivo* administration of IL-33 in apoE$^{-/-}$ mice induces a switch from dominant Th1 cell to Th2 cell response [111]. This switch is complimented by a rise in IL-4, IL-5 and IL-13 production and a reduction in pro-inflammatory IFN-γ production [111]. Influencing early atherogenesis, IL-33 has been shown to reduce pathological foam cell formation [112], a process attributed to IL-33's ability to reduce CD36 expression and enhance cholesterol efflux in macrophages [112]. As such, these studies suggest that IL-33 may function to inhibit pro-atherogenic processes while promoting athero-protective mechanisms.

1.11 T-helper 17 Cells in Atherosclerosis

After the initial discovery of T-helper 17 (Th17) cells, their role in atherosclerosis was quickly addressed. IL-17 secreting cells have been described in both mouse [113, 114] and human lesions [115, 116]. Although initially associated with plaque stability in humans [117], subsequent studies reported that IL-17A production was linked to plaque instability [116].

Animal studies have provided contradictory data as to the role of Th17 cells in atherosclerosis. Suggesting a pro-atherogenic role, apoE$^{-/-}$/Fcγ$^{-/-}$ mice display reduced lesion formation, associated with inhibition of Th17 cells [118]. As well as this, apoE$^{-/-}$ mice treated with anti-IL-17A antibodies display reduced lesion formation [113] , as well as reduced VCAM-1, IL-6 and TNF-α production [119].

Supporting an athero-protective role of Th17 cells, some have reported that neutralisation of IL-17 – with anti-IL-17A antibodies – enhances atherosclerosis formation [120]. Subsequent studies, using apoE$^{-/-}$ IL-17A$^{-/-}$ mice, have supported these findings [121]. More recently, IL-17A has been linked to induction of a stable plaque phenotype [122]

1.12 ϒδ T-cells in Atherosclerosis

γδ T-cells comprise approximately 5% of all T-cell populations and are specifically found in areas exposed to antigen, such as the skin and the gastrointestinal tract [123]. Interestingly, γδ T-cell numbers are greatly expanded in context of infection and autoimmunity [124-126] and respond rapidly to infection. Believed to be a link between both innate and adaptive immune systems, γδ T-cells do not require antigen processing and presentation on MHC molecules [127].

γδ T-cells are found in the atherosclerotic arteries of both humans and mice [128]. Data from early and more recent work has suggested the redundant role of γδ T-cells in plaque formation and progression [129, 130], with classical αβ T-cells being responsible for lesion formation [129]. These findings are however conflicted by studies using apoE$^{-/-}$/γδ$^{-/-}$ double knock out mice, in which loss of γδ T-cell expression significantly attenuates lesion formation by up to 44% [128].

1.13 T-regulatory Cells in Atherosclerosis

T-reg cells represent the suppressive arm of the adaptive immune system and function to prevent aberrant T-helper cell responses that may result in breach of tolerance and detrimental processes [131]. T-regs can be classified as natural T-regs (nT-regs), where thymic processes lead to the development of T-reg populations, or inducible T-regs (iT-regs), where peripheral stresses induce their formation [132]. T-regs exert their effects via cell-cell interactions, as well as the production of anti-inflammatory cytokines such as, IL-10 and TGF-β [132]. As a consequence of their function, T-regs play an important role in maintaining balance between effective and detrimental T-cell responses [132].

Several studies have addressed the role of T-regs in the development of arterial lesions. Particularly, hypercholesterolemic apoE$^{-/-}$ mice display reduced T-reg expression patterns than C57BL/6 control mice [133], a finding associated with deficient suppressor activity [133]. Subsequent transfer of T-regs into apoE$^{-/-}$ mice is sufficient to reduce atherosclerosis formation [133]. Complimenting this finding, enhanced Th17 profiles in apoE$^{-/-}$ mice has been linked to defective T-reg expression patterns [114].

1.14 IL-10

A range of immune cells secrete IL-10, however, its T-reg role has gained significant attention. In testament to its anti-atherogenic role, LDLR$^{-/-}$ mice transplanted with IL-10$^{-/-}$ bone marrow cells display enhanced atherosclerosis, coupled with increased inflammatory cell infiltrates [134]. Conversely, over-expression of IL-10 in lymphocytes, from LDLR$^{-/-}$ mice, has been shown to significantly reduce atherosclerosis formation [135].

1.15 CD8+ T-cells in Atherosclerosis

Unlike CD4+ T-helper cells, CD8+ cytotoxic T-cells have gained little attention in the area of atherosclerosis. Surprisingly, CD8+ T-cells represent the biggest leukocyte population in advanced human lesions [136]. In animal models, CD8+ T-cells are readily found at early stages of disease [137] and increase in number as lesions become more advanced [138]. Initial studies, using β-2-microglobluin deficient mice, in which MHC-I expression was inhibited, mice developed enhanced lesions [139]. Questions over the exclusivity of this approach in depleting all CD8+ T-cell populations has cast doubt over its validity. Moreover, mice deficient in MHC-I - via Tap-I ablation – do not show modified atherosclerosis formation [140].

With the development of more refined approaches, involving anti-CD8 depleting antibodies, researchers have demonstrated the true role of CD8+ T-cells in atherosclerosis. Using this approach, CD8+ depletion has been shown to significantly reduce lesion formation *in vivo* by reducing apoptosis, macrophage accumulation, VCAM-1 expression and IFN-γ production to name a few [41]. Furthermore, transfer of CD8+ T-cells into apoE$^{-/-}$ mice results in enhanced lipid and macrophage accumulation, as well as necrotic core formation [41]. Adding to this, CD8+ T-cells deficient in perforin and granzyme B are unable to enhance atherosclerosis formation *in vivo* [41].

More recently, the role of CD8+ CD25+ T-regs in atherosclerosis has gained extensive attention. Depletion of regulatory CD8+ CD25 T-regs has been shown to enhance the cytolytic activity of CD8+ T-cells in atherosclerosis [141]. In contrast to this, adoptive transfer of CD8+ CD25+ T-cells functions to limit CD4+ T-cell expansion [141]. Suggesting a protective effect in atherosclerosis, CD8+ T-regs have also been suggested to regulate atherogenic T-cell responses via a modulation of the Tfh cell : GC B-cell axis – where high affinity isotype antibodies are produced [142].

Taken together, these studies suggest that CD8+ T-cells function to enhance apoptosis induced necrotic debris formation. As such, CD8+ T-cells may represent an important population in atherosclerosis. Reinforcing the heterogeneous effects of immune cells in atherosclerosis, these studies also elude to the therapeutic potential of CD8+ CD25+ T-regs in atherosclerosis.

1.16 B-cells in Atherosclerosis

Along with T-cells, B-cells represent an important component of the adaptive immune system. Phenotypically, B-cells are distinguished from all other leukocytes by their expression of a B-cell receptor (BCR). Involved in binding to cognate antigen presented in context of major MHC, B-cells are charged with the task of immunoglobulin production. Peripherally, B-cells can be classified as B1 cells or B2 cells, with B1 cells being further refined into B1a and B1b cells [143]. In mice, the surface marker CD5 is commonly used to distinguish between subsets, with B1a cells being CD5+ and B1b and B2 cells being CD5-. B1 cells arise early in development and produce vast amounts of natural IgM antibodies in a T-cell independent manner [144]. Enriched in the peritoneal and pleural cavities, B1 cells are rarely found in secondary lymphoid organs [143, 145]. In comparison to this, B2 cells – also called conventional B-cells – express a variety of diverse BCRs and are responsible for the production of isotype switched antibodies [146]. Crucially, B2 cells require T-cell help for the production of switched antibodies and as a result are found in significant numbers in secondary lymphoid organs.

1.17 Antibodies – Structure and Function

Antibodies – or Immunoglobulins (Igs) – are Y-shaped glycoproteins produced by B-cells *in vivo*. Specific for a single antigen, or a group of related epitopes, antibodies are responsible for the effective neutralisation of invading pathogens [147]. To protect from infection, antibodies may initiate a range of processes. The first of these is referred to as the complement pathway, where antibodies bind pathogens and initiate degrading complement proteins in the blood [147]. Moreover, antibodies may potentiate the uptake of pathogens by additional cell types (e.g. macrophages), resulting in pathogen neutralisation [147]. As such, antibodies comprise an important component of the adaptive immune response to invading pathogens.

Structurally, all antibodies are composed of two heavy and two light chains (Fig 1). Following recombination of germ line DNA, a single antibody may be composed of two λ or two κ light chains as well as two γ, δ, α, μ or ε heavy chains (Fig 1) [148]. Both light and heavy chains may be subdivided into variable and constant regions. Variable regions are responsible for antigen binding, while constant regions are conserved throughout subtypes [148]. Based on variations in the amino acid sequence of the constant region of the heavy chain, Immunoglobulins can be subdivided into 5 major classes – IgG, IgD, IgA, IgM and IgE. Expression of the γ, δ, α, μ or ε heavy chain corresponds to the production of IgG, IgD, IgA, IgM and IgE antibodies respectively [148]. These classes may be divided further based on subtle changes in the amino acid sequence of the heavy chain, thus providing enhanced specificity.

Common to all immunglobulins is the fragment antigen binding (Fab) region and fragment crystallisable (Fc) region [148]. The variable region of the Fab segment is responsible for antigen specificity, while the constant region of the heavy chain is responsible for Fc receptor mediated effector functions and activation of the complement cascade (Fig 1) [148]. As such, antibodies are important in the recognition of foreign antigen as well as the activation of host cells for eradication of pathogens. An example of this may be found in the actions of IgE. IgE are secreted at epithelial barriers and play an important role in allergic reactions. Binding of IgE Fc regions to mast cells and other granulocytes significantly enhances degranulation and the release of effector chemicals such as histamine. As such, IgE plays an important

role in antigen recognition (Fab mediated), as well as effector cell activation (Fc mediated).

Hv = Variable Segment of Heavy Chain

Lv = Variable Segment of Light Chain

Hc = Constant Segment of Heavy Chain

Lc = Constant Segment of Light Chain
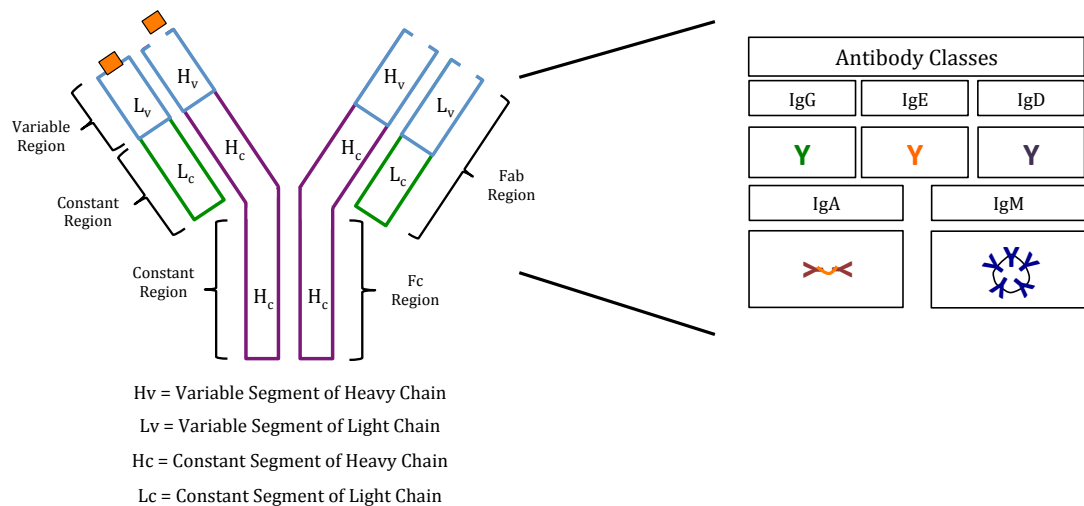
Figure 1: Subunit composition of antibody classes

Immunoglobulins share a common 4-chain structure. Arranged in various conformations, these subunits comprise the more readily distinguished antibody subsets, IgG, IgE, IgD, IgA and IgM. All units comprise 2 heavy chains and 2 light chains that, following germ line recombination, yield functional antibody subunits. Located distal to the antibody, the Fab region is responsible for antigen recognition, while the proximal end (Fc region) is responsible for antibody mediated effector functions.

1.17.1   Role of Antibodies in Atherosclerosis

Antibodies have long been associated with protective immunity against infectious disease. Exploiting this notion, many modern vaccinations influence the immune system to produce vast quantities of protective antibodies. As a result, hosts may display lifelong immunity to potentially lethal pathogens.

As well as infection, antibody mediated immunity has gained significant attention in atherosclerosis. Clues to the importance of antibodies in atherosclerosis can be found in human studies, where patients with atherosclerosis display antibody titres to Ox-LDL and other atherogenic antigens [149-152]. Moreover, mice immunized with atherogenic molecules display increased antibody responses *in vivo* [153, 154]. Animal studies have also provided an insight into the role of antibodies in regulating atherosclerosis formation. Specifically, splenectomised apoE$^{-/-}$ mice develop significantly aggravated atherosclerosis [155, 156]. Interestingly, the adoptive transfer of B-cells remedies this effect, thus suggesting an athero-protective effect of B-cells [156]. Moreover, in comparison to WT mice, B-cell deficient mice display a 30 % - 40 % increase in lesion size [157]. As such, the notion that B-cells confer protective immunity in atherosclerosis, via antibody production, has gained significant attention.

Although B-cells may confer athero-protective properties, B-cells may also produce large amounts of potentially pro-atherogenic antibodies. As such, it is important to consider antibody classes and B-cell subsets involved in their production. To date, specific attention has been focused on the atherogenic role of IgM and IgG in atherosclerosis. Although much debate remains as to their atherogenic role, IgM has more frequently been linked to reduced CV risk, while IgG has been linked to enhanced risk [158, 159].

Using anti-CD20 antibodies, some have shown that B-cell depletion is athero-protective [120]. Importantly, this protection was conferred by reduced B2 B-cell responses, while maintaining protective IgM responses. Highlighting the association between T-cells, B2 cells and pathology, anti-CD20 depletion of B2 B-cells significant attenuates pro-atherogenic T-cell responses [120]. Supporting the notion that B1a cells are atheroprotective, adoptive transfer of B1a B-cells into splenectomised apoE$^-$

/- mice has been shown to significantly attenuate necrotic core and lesion formation *in vivo* [160]. Conversely, adoptive transfer of B2 B-cells enhances lesion formation [160]. Further supporting a protective role of IgM and B1 cells, LDLR$^{-/-}$ mice deficient in serum IgM display significantly aggravated atherosclerosis [161]. Adding to the differential protective role of IgM in atherosclerosis, several studies have provided evidence indicative of an inverse correlation between IgM titres and clinical manifestations of arterial disease [162, 163]. Together, these findings confirm the differential effects of both IgM and IgG antibodies in atherosclerosis.

Functionally, IgM antibodies, specific for Ox-LDL epitopes, have been shown to be important in maintaining lipid equilibrium in atherosclerosis. Specifically, the EO6 IgM clone prevents Ox-LDL binding to CD36 and SR-B1 in vitro [164]. As such, EO6 antibodies may be important in preventing Ox-LDL accumulation and foam cell formation. In contrast, conclusive data demonstrating a functional pro-atherogenic effect of IgG antibodies remain elusive.

1.17.2   New Players in Atherosclerosis?

Interestingly, over the past few years the role of T-cell dependent antibody responses has gained significant attention in autoimmune disease such as Rheumatoid Arthritis (RA) and Systemic Lupus Erythematosus (SLE). This may, in part, be due to the success of biologic therapies, and in particularly those that target B-cell populations and antibody production.

As part of these developments, a new subset of T-cells, called T follicular helper cells has been documented and characterised. Involved in high affinity, class switched antibody production; Tfh cell numbers are increased in the blood of RA and SLE patients [165-167]. Interestingly, although antibodies play an important role in plaque progression, the role of Tfh cells in atherosclerosis remains to be fully determined.

1.17.3   T-follicular Helper Cells

Tfh cells were first described at the start of the 21st century. At the time, two studies described the presence of a CD4+ T-helper cell population in human tonsil tissue [44, 168]. This population was subsequently described as being able to migrate to B-cell follicles and help GC B-cells in the production of high affinity, isotype switched antibodies [44, 168]. Taking into account their location and function, these CD4+ T-cell populations became known as Tfh cells. Dissecting their role further, Tfh cells became define as,

"The T-helper cell subset, able to migrate to B-cell follicles in a C-X-C motif ligand-13 (CXCL13) dependent manner and aid GC B-cells in the production of high affinity, isotype switched antibodies".

Tfh cells differ from other T-cell subsets by their constitutive expression of membrane bound C-X-C chemokine receptor type 5 (CXCR5) [169]. Coupled with this, Tfh cells up-regulate a wealth of additional co-stimulatory molecules, including the signalling lymphocytic activation molecule (SLAM), programmed cell death protein-1 (PD-1) and inducible co-stimulatory molecule (ICOS), which bind to their respective ligands on B-cells [169]. As well as this, Tfh cells express enhanced amounts of their implicated transcription factor - B-cell lymphoma-6 (Bcl-6) and secrete vast quantities of their signature cytokine IL-21. Both Bcl-6 and IL-21 function to enhance Tfh cell and GC B-cell differentiation *in vivo* [170, 171].

Functionally, Tfh cells provide help to GC B-cells in the form of TCR : MHC engagement, co-stimulation and paracrine IL-21. Initiating a range of effects, the importance of Tfh cells to GC B-cell biology will be discussed herein.

1.18 T-follicular Regulatory (Tfr) Cells

Alongside Tfh cells, another subset of CD4+ T-cells is able to migrate to and participate in GC processes. Termed T-follicular Regulatory (Tfr) cells, Tfrs function to control and limit aberrant Tfh cell and GC B-cell responses *in vivo* by preventing IL-21 production and class switching [172]. Highlighting the role of Tfr cells, absence of Tfr cells results in enhanced GC B-cell numbers, resulting in reduced antigen specific clones and aberrant antibody production [173, 174]. Interestingly, Tfr cells express markers characteristic of both Tfh cell and conventional T-reg populations, including CXCR5, ICOS, PD-1 and Bcl-6 (Tfh), GITR, FoxP3 and CTLA-4 (T-reg) [173-176] and display memory capacity [172]. Moreover, conventional Tfh cell differentiation signals are also required for Tfr formation [173], as well as the expression of Bcl-6 [174]. Adding evidence to their disconnect from both Tfh cell and T-reg lineages, however, Tfr cells maintain distinct transcriptional and lineage differences from both populations [173] and arise from thymic derived precursors [173, 174]. Of importance to this thesis, Tfr cells may play an integral role in regulating both Tfh cell and GC B-cell responses in the atherogenic process. Indeed, recently, CD8+ T-regs have been shown to limit aberrant Tfh cell responses in atherosclerosis [142], however the atherogenic significance of Tfr cells remains to be elucidated. It is clear however, that modulation of the Tfr cells may hold therapeutic and research significance. Whether these compartments are affected in the studies discussed throughout this thesis remains to be determined.

1.19 B-cell Development and Maturation

Essential to the adaptive immune response, B-cells play important roles in antibody production, antigen presentation and cytokine secretion *in vivo* [177, 178]. To participate in such processes, B-cells differentiate in a multi-stage developmental pathway. Subdivided, these stages are referred to as the antigen independent and antigen dependent phases [179]. The antigen independent stage occurs within the bone marrow and results in the formation of a mature membrane bound BCR via a tightly controlled set of processes termed V(D)J recombination (Figure 2). In contrast, the antigen dependent phase occurs peripherally within secondary lymphoid organs (SLO), where immature B-cells meet their cognate antigen, resulting in memory B-cell and plasma cell formation.

Interactions with bone marrow resident somatic cells are crucial for the antigen independent phase. In particular, bone marrow resident stromal cells play a pivotal role in the initial differentiation of B-cells from B-cell precursors to pro-B-cells and then pre-B-cells [179]. Supporting the antigen independent pathway, stromal cells express adhesion molecules, including VCAM-1 and other CAMs (cellular adhesion molecules) [179]. Binding of the integrin VLA-4 on progenitor B-cells to VCAM-1 ensures tight binding and long-lived interactions with stromal cells, thus ensuring sufficient access to growth factors. Following adhesive interactions, pro-B-cell bound receptor tyrosine kinase KIT binds to stromal bound stem cell factor (SCF), inducing kinase activity and cellular proliferation, therefore expanding B-cell numbers. Towards late stage pro-B-cell development, secreted cytokines play an important role in terminal differentiation. In particular, stromal derived IL-7 binds to IL-7Rs located on late-pro-B-cells, resulting in enhanced proliferation and pro-B-cell growth. Highlighting the importance of IL-7 and adhesion molecules to the antigen independent pathway, loss of either molecules result in impaired or absent B-cell development [180, 181].

In addition to stromal cell : B-cell interactions, the bone marrow is the site of intrinsic changes to DNA encoding the BCR of developing B-cells. Termed VDJ recombination, these changes allow for a wealth of antigen specificities and BCR diversity. As such, this section will discuss the process in which VDJ recombination occurs.

All Immunoglobulins are composed of the same basic units – two heavy chains and two light chains (discussed elsewhere). This structure is identical to that which forms the BCR. The germ line DNA that encodes for heavy and light chains is comprised of multiple gene segments, termed V (variable), D (diversity) and J (joining) [179]. Ensuring a range of specificities, many different copies of V, D and J genes exist, combinations of which yield approximately 10^{14} different BCRs [182]. Resulting heavy and light chain recombination, results in the expression of a functional and unique BCR specific for a unique antigen [182].

When transitioning from progenitor B-cell to early B-cell stage, developing B-cells first undergo heavy chain recombination (Figure 2). As part of this process, D segments are initially recombined with J segments, followed by subsequent recombination of DJ segments with V segments. To participate in recombination, V, D and J segments are flanked by a sequence of DNA termed recombination signal sequences (RSS) [182]. These sequences recognise two enzymes termed (recombination activating gene-1) RAG-1 and (recombination activating gene-2) RAG-2. Forming a complex with each other, RAG-1 and RAG-2 cleave DNA strands at RSS sites, creating a resulting DNA hairpin [183]. Additional enzymes – involved in DNA repair – including DNA ligase IV, DNA-dependent protein kinase (DNA-PK) and Ku - cleave the resulting DNA hairpin and join open ends, yielding a linear length of DNA containing one D segment and one J segment (Figure 2). Highlighting the importance of both RAG-1 and RAG-2, loss of the gene encoding their expression results in impaired B-cell development and subsequent immunodeficiency [184, 185]. Utilizing this, scientists commonly use RAG1$^{-/-}$ and RAG2$^{-/-}$ mice to study the pathological importance of lymphocytes in disease.

To complete VDJ recombination, DJ segments are subsequently recombined with a single V segment. Using the same enzymes described above, recombined DJ segments are combined with a single V gene copy. As a result, this process yields a linear strand of DNA, encoding the heavy chain and contains a single V, D and J gene (Figure 2).

Following recombination of the heavy chain, the light chain of the antibody glycoprotein is recombined. Unlike the heavy chain, DNA encoding the light chain does not comprise D segments and contains copies of V and J genes only. Following

the same process described above, a single V gene is recombined with a single J gene, yielding a bonafide BCR light chain comprised of 2 heavy and 2 light chains (Figure 2).

Successful recombination of heavy and light chains of the BCR results in the expression of a mature, membrane bound BCR – usually IgM as well as IgD [186]. As a result, B-cells (immature) are permitted to continue development as part of the antigen dependent phase.

To participate in the antigen dependent phase of B-cell differentiation, B-cells must egress from the bone marrow and migrate to SLOs. Although variations in B-cell transition state exist between spleen and pLNs, this section will discuss the entry and movement of B-cells in the pLNs.

Entry into pLNs is a precise and regulated set of processes controlled by the interactions of various chemokines and chemokine receptors. As with T-cells, naïve B-cells express CCR7, and use this receptor to travel along a CCL19 and CCL21 gradient in high endothelial venules (HEVs), where both ligands are expressed at high levels [187, 188]. Although some dispute the importance of CCR7 and its ligands in B-cell migration [189, 190], others have shown its importance alongside CXCR4 in B-cell re-location [191]. Further supporting B-cell migration; B-cells use CXCR4 to migrate along a CXCL12 gradient towards B-cell follicles. To partake in GC processes and complete their differentiation, B-cells must migrate to B-cell follicles. Using membrane bound CXCR5; B-cells migrate along a CXCL13 gradient to B-cell follicles [192, 193], where they remain positioned for terminal differentiation and involvement in GC processes. Upon recognition of MHC bound antigen, B-cells differentiate towards plasma cell and memory B-cell phenotypes in an anatomically segregated GC reaction (discussed elsewhere). Importantly, chemokine mediated retainment in the GC allows B-cells to receive differentiation signals from follicular dendritic cells and Tfh cells.
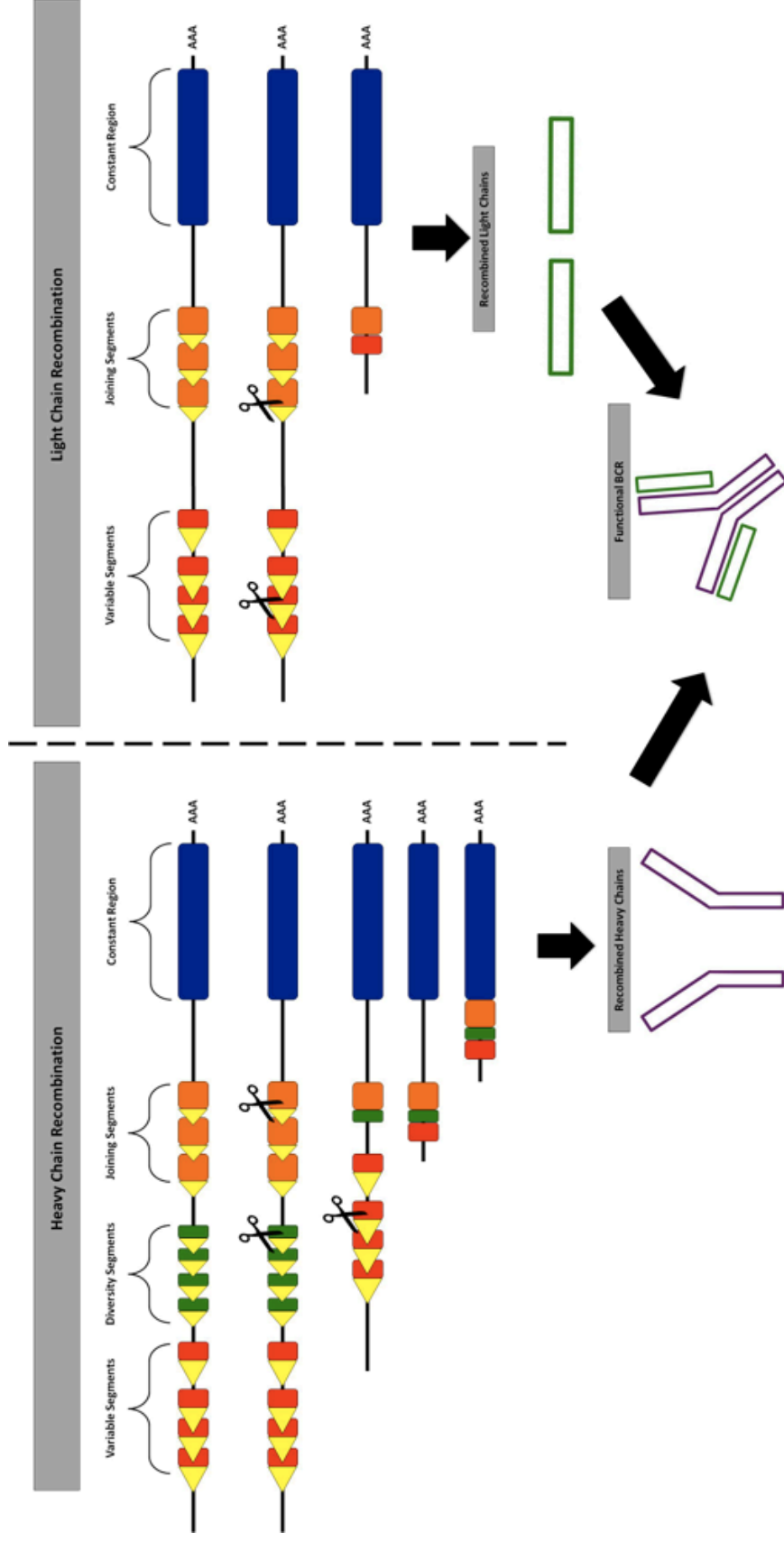
Figure 2: Schematic representation of VDJ recombination of the BCR.

To ensure B-cells are capable of recognising a range of antigens, the germ line DNA encoding both heavy and light chains of the BCR is recombined. Termed VDJ recombination; un-mutated DNA encoding the BCR contains multiple copies of V, D and J sequences. Following enzymatic processes, BCR DNA is recombined to contain a single V, D and J sequence (heavy chain) or a single V and J sequence. As a consequence of VDJ recombination, the immune system is able to encode BCRs capable of recognising approximately 10^{14} different antigens.

1.20 B-cell Tolerance

As with T-cells, B-cells become educated so as not to react to self-antigen when in circulation. This system of education can be subdivided into two anatomically distinct processes, termed central and peripheral tolerance. Central tolerance occurs within the bone marrow, where circulating antigen can bind to BCRs, resulting in clonal deletion of B-cell clones or the reorganisation of germ line DNA in a process termed receptor editing. BCR signalling strength has been shown to play an important role in determining these fates, where strong BCR-auto-antigen binding results in deletion or editing, while intermediate binding permits B-cell survival and progression [186] [194].

In contrast, peripheral tolerance occurs within the periphery and functions to eliminate self-reacting clones that bypass central tolerance mechanisms or are specific for self-antigen absent in the bone marrow. As part of these processes, self-reactive B-cells – in competition with foreign specific B-cells - may be prevented from entering B-cell follicles and thus involvement in GC processes. Moreover, if B-cell clones bind self-antigen with high affinity they may enter a state of anergy, characterised by substantial down regulation of IgM [195]. In the event that a T-cell clone, specific for the same auto-antigen as an auto-reactive B-cell develops, B-cells may use FAS-FASL interactions to induce cellular apoptosis.

Taken together, central and peripheral tolerance function to reduce the risk of aberrant B-cell responses *in vivo*. In the absence of such checkpoints, aberrant B-cell clones survive and seed the basis of autoimmunity.

1.21 Germinal Centre B-cells

GCs are distinct, transient structures found in the B-cell follicles of secondary lymphoid organs [196]. First described over 100 years ago, we now understand the importance of GC reactions to the formation of protective and aberrant adaptive immune responses. In particular, GCs are sites in which the processes of clonal expansion, somatic hypermutation and affinity maturation occur [196]. As part of this section, the importance of these processes to B-cell development will be discussed. As well as this, the role Tfh cells play in guiding B-cell development will also be discussed.

On leaving the bone marrow, immature B-cells migrate to secondary lymphoid organs, where they acquire antigen form follicular dendritic cells (fDCs) and in turn present it to cognate CD4+ Tfh cells at the border between T cell zone and B cell follicles (Fig 2). Upon activation by a T-cell dependent antigen, B-cells being the process of translocation to B-cell rich areas in the cortex of lymph nodes (LNs) (Fig 2). This movement initiates a process in which a new GC reaction is formed.

Specific for a single antigen, activated B-cells – now called centroblasts – initiate a programme of intense proliferation termed clonal expansion (Fig 2) [197]. At the same time, centroblasts up regulate the production of activation induced cytidine deaminase (AID) – an enzyme involved in introducing point mutations in the variable region of antibodies, in a process termed somatic hypermutation (Fig 2) [198] Located in the dark zone (DZ) of the GC, so called due to the high nucleus to cytoplasm ratio of resident B-cells [199], DZ centroblasts represent the beginnings of high affinity antibody production.

As a result of clonal expansion and somatic hypermutation, activated centroblasts significantly alter their range of affinity for a single antigen. Due to the random nature of AID, not every centroblast is of improved affinity for its respective antigen. This, therefore, conveys a disadvantage. To preserve high specificity, low binding centroblasts are removed in a selection process termed affinity maturation in the light zone (LZ) of the GC (Fig 2) [197].

Upon moving to the LZ, centroblasts (now termed centrocytes) interact with resident fDCs and Tfh cells that present cognate antigen on their surface (Fig 2). Depending on the affinity of their surface antibody to the antigen, developing centrocytes acquire two different fates. These fates are described below.

1. Centrocytes of low affinity for cognate antigen presented in the LZ
   ➢ Cannot make contact with resident fDCs or Tfh cells
      ➢ Become apoptotic

2. Centrocytes of high affinity for cognate antigen presented in the LZ
   ➢ Can make contact with resident fDCs or Tfh cells
      ➢ Selected for class switching and differentiation
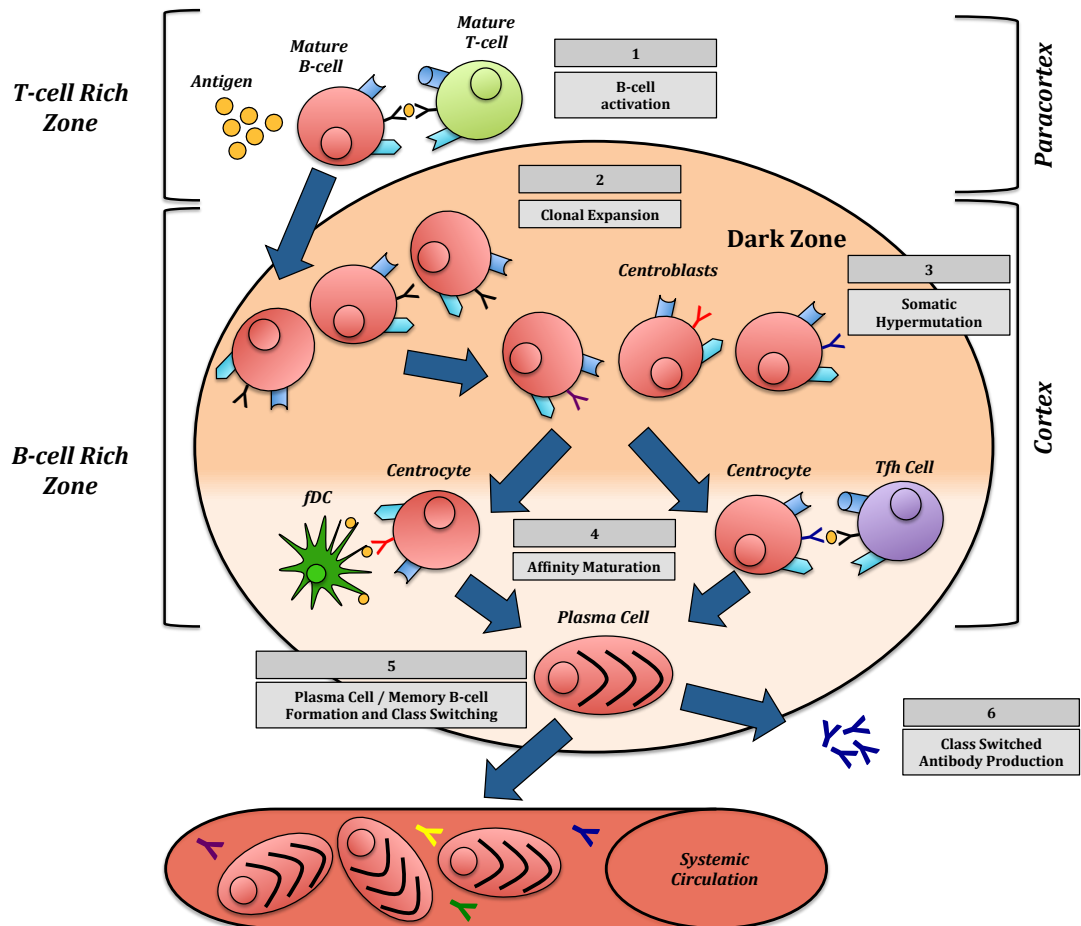
Figure 3: Schematic representation of B-cell differentiation through the germinal centre reaction

Upon encountering its cognate antigen in the paracortex **(1)**, mature B-cells develop down a differentiation programme that results in the formation of antibody secreting plasma cells and B-cell memory. Leaving the paracortex, activated centroblasts enter the dark zone of the germinal centre, where they proliferate in a process known as clonal expansion **(2)**. Subsequent somatic hypermutation **(3)** of heavy and light chains results in a range of antigen affinities. In a process termed affinity maturation **(4)**, centrocytes are tested by Tfh cells and fDCs for their relative affinity for a single cognate antigen. Those of low affinity are eliminates via apoptosis, while those of high affinity are selected for plasma cell, memory B-cell and class switching **(5-6)**.

1.22 Importance of Tfh cells in the GC Reaction

Although the number of GC T-cells is relatively low in comparison to GC B-cells, their role in the GC reaction is one of great importance. Testament to this, athymic nude mice fail to develop functional GC reactions [200]. Moreover, GC formation is restored solely by the adoptive transfer of thymocytes [200]. Adding further evidence to the role of T-cells in the GC, CD40-CD40L interaction is required for the formation of GCs, with CD40-CD40L blockade being sufficient to drive GC dissolution *in vivo* [201]. In humans, deficient CD40 or CD40L expression results in the absence of GC formation. Coupled with the presence of excess amounts of low-affinity, un-switched antibodies, such individuals are highly susceptible to infection [202, 203].

The role of Tfh cells in the GC has more recently been addressed. GC resident Tfh cells secrete large amounts of their signature cytokine – IL-21. Working in both an autocrine and paracrine manner, IL-21 exerts a multitude of effects via its dedicated IL-21R. Located on the surface of both GC B-cells and Tfh cells, IL-21R has been shown to affect both cell subtypes and activates important molecules required for cellular function – most notably Bcl-6 [204]. The importance of Tfh cell derived IL-21 is demonstrated by the finding that IL-21 deficient or IL-21R deficient mice display reduced GC formation, antibody production and B-cell proliferation [205, 206] (Fig 3).

As well as influencing GC reactions via the secretion of IL-21, Tfh also provide crucial co-stimulatory signals to GC B-cells [207-212]. Binding B-cell expressed ligands, engagement of co-stimulatory molecules facilitates Tfh cell – B-cell interactions, as well as Tfh cell and GC B-cell activation. Specifically ICOS – inducible t-cell co-stimulator ligand (ICOSL) interaction enhances the production of B-cell stimulating cytokine IL-21 [206]. Loss of co-stimulation not only alters Tfh cell responses but also significantly affects the productivity and integrity of GC B-cells and GC reactions in mice and humans [207, 210, 213, 214].
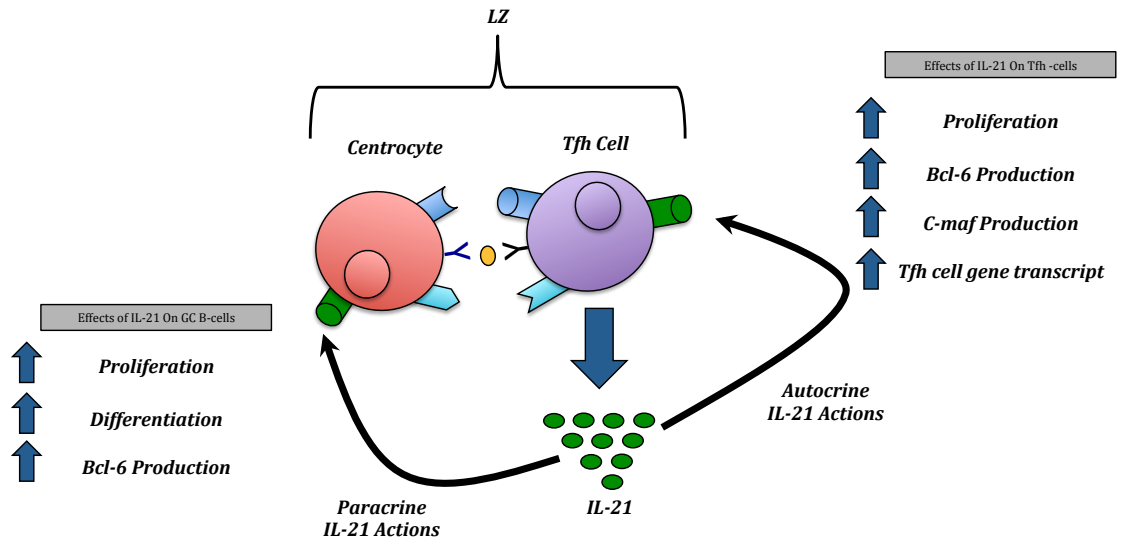
Figure 4: Schematic representation of the effects Tfh cell derived IL-21 has on both GC B-cells and Tfh cells

Working in both an autocrine and paracrine manner, IL-21 exerts its effects directly upon both GC B-cells and Tfh cells. Acting via a dedicated IL-21R, IL-21 indices GC B-cell and Tfh cell differentiation, B-cell class switching, Bcl-6 up-regulation and the up-regulation of other related nuclear transcripts.

1.23 Aortic Tertiary Lymphoid Organs (ATLOs)

Throughout development, structures termed primary and secondary lymphoid organs direct lymphocyte development and differentiation. Primary lymphoid organs (PLOs), such as the thymus and bone marrow direct T-cell and B-cell development respectively, while SLOs, including pLNs and the spleen, orchestrate the differentiation of T-cells and B-cells towards various terminal fates.

Until recently, PLOs and SLOs were considered the sole sites of T-cell and B-cell development and differentiation. More recently however, the formation of highly organised tertiary lymphoid organs (TLOs) have been identified in various conditions [215-218]. Differing from SLOs, TLOs do not form during ontogeny but form in an undetermined manner at sites of chronic, non-resolving inflammation. In common with SLOs, TLOs are highly organised and are characterised as containing T-cell, B-cell and GC zones. In context of this thesis, aortic tertiary lymphoid organs (ATLOs) have also been identified in animal models and in biopsy samples from aortic aneurysms [45, 142, 219, 220]. Moreover, ATLOs comprise a wealth of innate and adaptive immune subsets, including CD4+ T-cells, CD8+ T-cells, B-cells, GC B-cells, and dendritic cells [45].

ATLOs form preferentially within the abdominal aorta in aged chow fed apoE$^{-/-}$ mice [45]. Interestingly, recent data has indicated a lymphotoxin-beta receptor (LTβR) pathway that orchestrates cellular organisation within ATLOs [45]. Activation of intimal smooth muscle cells via LTβR has been shown to enhance expression of the lymphorganogenic chemokines CXCL13 and CCL21 [45]. The receptor and ligand for CXCR5 and CCR7 respectively, CXCL13 and CCL21 are pivotal to the homing of B-cells and T-cells to SLOs and, in this case, ATLOs. As such, the LTβR mediated pathway is crucial to lymphocyte homing and accumulation in advanced atherosclerosis. Importantly, ATLOs have been confirmed to be sites of active naïve T-cell recruitment and induced T-reg formation [219].

Although present in late stage atherosclerosis, the pathological significance of ATLOs was not eluded to until recently. Working in a SMC LTβR dependent manner, ATLOs have been shown to confer protective functions *in vivo* [219]. Indicative of this, loss of LTβR expression has been shown attenuate ATLO formation, while enhancing luminal

lesion formation and atherosclerosis progression [219]. Of importance to this thesis, ATLOs have been shown to contain the relevant lymphogenic and anatomical subdivisions for Tfh cell and GC B-cell processes [219]. Moreover, human studies have identified Tfh cells in the ATLOs [142].

1.24 Scope of Current Study

Despite sharing common inflammatory signatures with other autoimmune conditions, the role of Tfh cells and GC B-cells have not been fully addressed in context of atherosclerosis. As such, the studies described herein aimed to address whether the Tfh cell : GC B-cell axis is of pathological significance in atherosclerosis.

Employing a question and answer approach, the studies presented in this thesis aimed to:

1. Determine whether Tfh cell, GC B-cell and antibody kinetics followed a pattern in line with atherosclerosis progression in the apoE$^{-/-}$ mouse;
2. Determine whether the results obtained in point 1 were the result of pathology and not the loss of functional apoE protein;
3. Study the effects of IL-21R deficiency on the Tfh cell : GC B-cell axis and pathology in the LDLR$^{-/-}$ mouse.

Figure 5 overleaf summarises the aims and objectives, as well as the methodological approach, of each results chapter.

Chapter 3: Characterising Tfh cell & GC B-cell Populations in the apoE$^{-/-}$ Mouse Model of Atherosclerosis

Aim and Objectives:
To determine whether Tfh cell and GC B-cell kinetics change in line with atherosclerosis formation *in vivo*.

Methods:
1. *Flowcytometry analysis* of Tfh cells and GC B-cells from SLOs of apoE$^{-/-}$ mice fed chow or HFD for variable lengths of time (1, 2, 4, 8 & 12 weeks).
2. *Histochemical analysis* to determine Tfh cell location and marker expression.
3. *ELISA analysis* to determine functional consequences of differential Tfh cell : GC B-cell kinetics.
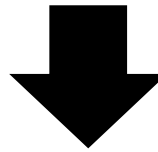
Chapter 4: Elucidating the Role of Apolipoprotein-E in Adaptive Immunity

Aim and Objectives:
To determine whether loss of apolipoprotein-E affects Tfh cell and GC B-cell populations in the apoE$^{-/-}$ mouse.

Methods:
1. *Flowcytometry analysis* of Tfh cells and GC B-cells from SLOs of apoE$^{-/-}$ mice immunised with ovalbumin (OVA) and complete freund's adjuvant (CFA).
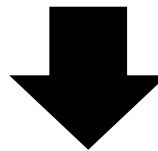
Chapter 5: Effects of IL-21R Deficiency on the Development of Atherosclerosis

Aim and Objectives:
To modulate Tfh cell integrity *in vivo* via IL-21R ablation and determine its effects on atherosclerosis formation.

Methods:
1. *Flowcytometry analysis* of Tfh cells and GC B-cells from SLOs of C57BL/6NJ : LDLR$^{-/-}$ and IL-21R$^{-/-}$: C57BL/6NJ chimeric mice.
2. *Histochemical analysis* of Tfh cell marker expression and location in splenic tissue
3. *Histochemical assessment* of lesion composition and plaque burden following IL-21R ablation
4. *ELISA analysis* of antibody kinetics following IL-21R ablation.

Figure 5: Flow diagram depicting the aims, objectives and direction of the chapters described herein.

Chapter 2: Materials and Methods

1.25 Animals

Twelve-week-old B6.129P2-Apoe(tm1Unc)/J (apoE$^{-/-}$) mice (originally purchased from Jackson Laboratories, Bar Harbor, Maine, USA) were bred in house (central research facility, The University of Glasgow, Scotland, United Kingdom), or purchased from Charles Rivers Laboratories (Margate, England, United Kingdom). Age-matched C57BL/6 mice were purchased from Charles Rivers Laboratories (Margate, England, United Kingdom) and used as respective controls. For other experiments, five to eight week old C57BL/6NJ, IL-21R$^{-/-}$ and B6.129S7-Ldlr^{tm1Her}/J (LDLR$^{-/-}$), mice were obtained from Jackson Laboratories (Bar Harbor, Maine, USA) and housed at central research facility (The University of Glasgow, Scotland, United Kingdom).

Unless stated elsewhere, animals were allowed free access to food and water and maintained in a 12/12- hour light/dark cycle. All procedures were performed in accordance to local ethical and UK Home Office guidelines.

1.26 High Fat Diet (HFD)

Where relevant, mice were allowed free access to high fat diet (HFD) (Special Diet Services, Essex, United Kingdom). For a full description of the diet composition, please refer to appendix 1. For studies conducted as part of chapter 3, mice were allowed access to diet for 1, 2, 4, 8 and 12 weeks (Fig 6). For studies conducted as part of chapter 5, mice were allowed access to diet for 14 weeks.

3 Groups   **Mice aged 12 weeks at time zero**
1. C57BL/6   Chow Fed
2. apoE$^{-/-}$ Chow Fed
3. apoE$^{-/-}$ High Fat Diet Fed

Tissue harvest at each time point
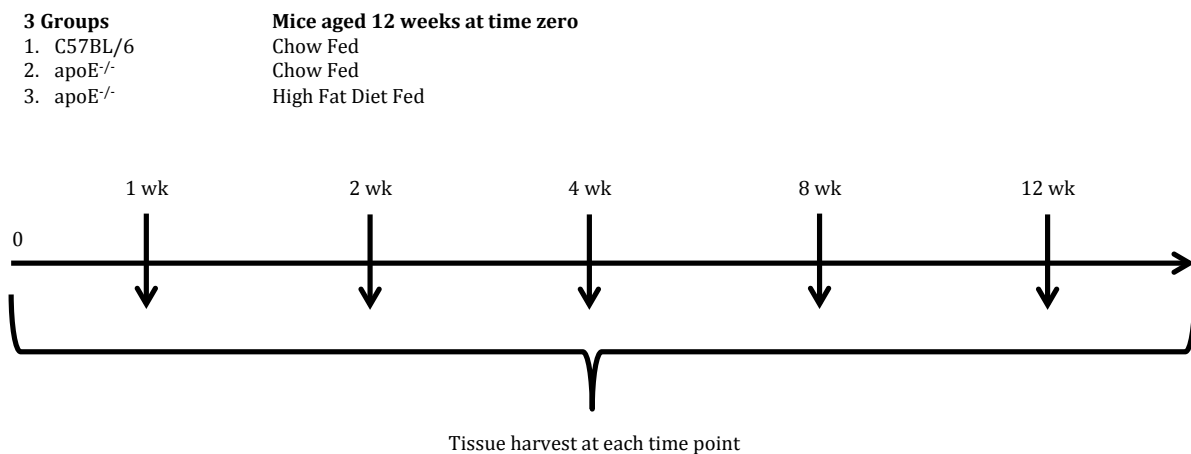
Figure 6: Experimental protocol and time line for the assessment of Tfh cell and GC B-cell kinetics in apoE$^{-/-}$ mice

Three groups of mice, aged 12 weeks at time point 0, were supplied with chow (C57BL/6 and apoE$^{-/-}$) or HFD (apoE$^{-/-}$) for varying lengths of time (1wk, 2wks, 4wks, 8wks and 12wks). Upon completion of each respective time point, secondary lymphoid organs (pLNs, spleen and pao-LNs) were harvested and processed for staining via flow cytometry and/or IF (half of spleen). As well as this, serum samples from all groups were tested for anti-MDA-Ox-LDL IgM, IgG, IgG$_1$ and IgG$_{2c}$ antibody titres.

1.27 Preparation of Tissue Samples for Flow Cytometry Staining

Mice were placed under terminal anaesthesia. Following ablation of the hind-limb flexor withdrawal reflex, peripheral lymph nodes (pLNs) (inguinal, axillary, brachial and cervical), spleen and para-aortic lymph nodes (pao-LNs) were dissected and placed in hanks balanced salt solution (HBSS) (Life Technologies, Paisley, United Kingdom) containing 10% foetal calf serum (FCS) (Life Technologies, Paisley, United Kingdom). Samples were subsequently disrupted through a 40 μm cell strainer (Corning, New York, USA). The resulting cell suspensions were centrifuged at 400 g for 5 mins in preparation for flow cytometry staining.

1.28 Flow Cytometry Staining

After washing cell suspensions in HBSS containing 10% FCS, samples were incubated in FC-Receptor block (2.4G hybridoma supernatant) for 20 mins at 4^oC degrees. Samples were subsequently incubated with antibodies for the detection of cells of interest. For a full description of the antibodies used, please refer to appendix 2. After incubation, cells were washed twice in HBSS containing 10% FCS and resuspended in the same buffer. Samples were analysed using the MACSQuant Analyzer (Miltenyi Biotech, Bisley, United Kingdom) and data analysis was performed using FlowJo software (Tree Star Inc, Olten, Switzerland).

1.29 Enzyme Linked Immunosorbent Assays (ELISAs)

This section refers to ELISAs conducted as part of chapter 3.

1.29.1　Antigen Specific Antibody Titres

For the detection of anti-MDA-Ox-LDL specific antibodies, microtitre plates (Thermo Scientific, England, United Kingdom) were coated with 100 µl of 12.5 µg/ml MDA-Ox-LDL (Nordic Biosite, Sweden) in PBS overnight at 4°C degrees. The next day, plates were washed in PBS containing 0.05% tween. Plates were subsequently incubated with serum samples diluted 1:25 in PBS for 24 hours at 4°C degrees.

The next day, plates were washed 4 times in PBS containing 0.05% tween and incubated with horseradish peroxidase (HRP) conjugated goat anti-mouse IgG, IgM, IgG$_1$ or IgG$_{2c}$ for 1 hour at room temperature. To account for intra-plate variation, serum from 8 week-old C57BL/6 WT mice was included on each plate and used to normalise OD readings. After washing in PBS containing 0.05% tween, 100 µl of SureBlue™ TMB microwell peroxidase substrate (KPL, Gaithersburg, MD, USA) was added to each well. To stop the reaction, 100 µl of 10% hydrochloric acid was added to each well.

Using the sunrise ELISA reader (Tecan, Mannedorf, Switzerland), plates were read at 450 nm with a reference of 630 nm. Results were normalised to internal control C57BL/6 serum and expressed as normalised relative light units (R.L.U). R.L.Us were obtained by dividing the optical density (OD) of each samples with the OD yielded from the highest dilution of C57BL/6 serum.

For a full description of the antibodies used to detect antibody subtypes, please refer to appendix 3.

This section refers to ELISAs conducted as part of chapter 5.

For the detection of anti-MDA-Ox-LDL specific antibodies, microtitre plates (Thermo Scientific, England, United Kingdom) were coated with 100 µl of 12.5 µg/ml MDA-Ox-LDL (Nordic Biosite, Propellervagen, Sweden) in PBS overnight at 4°C degrees. The next day, plates were washed in PBS containing 0.05% tween and blocked using 10 % FCS for 2 hours at 37°C. After another washing step, plates were incubated overnight with serial dilutions of serum from either C57BL/6NJ : LDLR$^{-/-}$ or IL-21R$^{-/-}$: LDLR$^{-/-}$ mice. Dilutions started from 1:25 to 1:600 for IgM and IgG and 1:10 to 1:640 for IgG$_{2C}$, IgG$_1$ and IgG$_3$. The next day, plates were washed and subsequently incubated with horseradish peroxidase (HRP) conjugated goat anti-mouse IgG, IgM, IgG$_{2C}$ or IgG$_1$ for 1 hour at room temperature. After a final washing step, 100 µl of SureBlue™ TMB microwell peroxidase substrate (KPL, Gaithersburg, MD, USA) was added to each well. To stop the reaction, 100 µl of 10% hydrochloric acid was added to each well.

To account for intra-plate variation, serum from 8 week-old C57BL/6 WT mice was included on each plate and used to normalise OD readings.

For a full description of the antibodies used to detect antibody subtypes, please refer to appendix 4.

1.29.2   Total Serum Antibody ELISAs

1.29.2.1   Total IgM and IgG

For the detection of total IgM, microtitre plates (Thermo Scientific, England, United Kingdom) were coated with serially diluted serum from C57BL/6NJ : LDLR$^{-/-}$ or IL-21R$^{-/-}$: LDLR$^{-/-}$ mice (1:400 – 1:10240) in PBS overnight at 4°C. The next day, plates were washed in PBS containing 0.05% tween and subsequently blocked using 10 % FCS for 2 hours at 37°C. Plates were subsequently washed and incubated with HRP conjugated rat anti-mouse IgM for 1 hour at room temperature.

For the detection of total IgG, plates were coated with 100 µl of 20 µg/ml goat-anti-mouse IgM/G capture antibody (Jackson ImmunoResearch Laboratories, Sohan, United Kingdom) in PBS overnight at 4°C. The next day, plates were washed in PBS containing 0.05% tween and subsequently blocked using 10% FCS for 2 hours at

37°C. Plates were subsequently washed and incubated overnight with serially diluted of serum from either C57BL/6NJ : LDLR$^{-/-}$ or IL-21R$^{-/-}$: LDLR$^{-/-}$ mice. Dilutions ranged from 1:400 to 1:5120.

To account for intra-plate variation, serum from 8 week-old C57BL/6 WT mice was included on each plate and used to normalise OD readings.

1.29.2.2   Total IgE

For the detection of total IgE a Ready-SET-Go Kit was used (Affymetrix, eBioscience). Briefly, plates were coated with 100 µl of 1X anti-mouse IgE monoclonal antibody and incubated at 4°C degrees overnight. The next day, plates were washed in PBS containing 0.05% tween and incubated with 200 µl of 2X blocking buffer at room temperature for 2 hours. After washing, plates were incubated overnight with serial dilutions of serum from C57BL/6NJ : LDLR$^{-/-}$ or IL-21R$^{-/-}$: LDLR$^{-/-}$ mice. Dilutions started from 1:50 to 1:3200. The next day, plates were washed and incubated with 100 µl of 1X biotin conjugated anti-mouse monoclonal antibody at room temperature for 1 hour. After washing, plates were incubated with 100 µl of streptavidin-HRP at room temperature for 30 mins. After a final washing step, wells were incubated with 100 µl of substrate solution. To stop the reaction, 100 µl of stop solution was added to each well.

For a full description of the antibodies used to detect antibody subtypes, please refer to appendix 4.

1.30 ELISA Plate Development and Normalisation

All microtitre plates, from each chapter, were read using the sunrise ELISA reader (Teacan, Mannedorf, Switzerland). Plates were read at 450 nm with a reference of 630 nm. Resulting OD readings were normalised to internal control C57BL/6 serum and expressed as normalised R.L.Us. R.L.Us were obtained by dividing the ODs of each sample with the OD from the highest dilution of C57BL/6 internal control serum.

1.31 Immunofluorescence

1.31.1   Identification of Tfh cells and GC B-cells

Spleen sections from 12 week old and 4 week old mice were stained for Tfh cells and GC B-cells respectively. Prior to staining, 8 micron thick frozen sections were fixed in 100% acetone for 10 mins and allowed to air dry for a further 5 mins. Sections were subsequently re-hydrated in PBS for 10 mins and incubated in FC-receptor block (2.4G2 hybridoma supernatant) for 30 mins at room temperature. Following another washing step, sections were incubated in 10% horse serum for 30 minutes.

Sections from the 12-week time point were subsequently incubated with antibodies for the detection of Tfh cells, while sections from the 4 week time point were incubated with antibodies for the detection of GC B-cells. Samples were incubated overnight at 4°C degrees, after which sections were rinsed in PBS for 20 mins and mounted in Prolong Gold mountant (Life Technologies, Paisley, United Kingdom) containing DAPI (where appropriate). Samples were analysed using the LSM510 metaconfocal microscope (Zeiss, Germany) and assessed on Volocity (Perkin Elmer, USA) quantification software.

For a full description of the antibodies used to detect Tfh cells and GC B-cells via IF, please refer to appendix 5.

1.31.2   Quantitate Analysis of GC Formation

Following staining with respective antibodies (see appendix 5), spleen sections were visualised using the LSM510 metaconfocal microscope (Zeiss, Germany). Three sections from each mouse (n = 5 in each group) were analysed for GC formation using the image quantification software - Volocity (Perkin Elmer, USA). Total splenic area, B220+ areas and PNA+ areas were measured using the area tool and the value for each measurement recorded.

1.31.3   Qualitative Analysis of Tfh Cell Formation

Confocal microscopy was used to determine whether Tfh cells migrated to B-cell follicles in the spleen of mice, and expressed important markers for Tfh cell function (Bcl-6). Using marker expression and anatomical location, bonafide Tfh cells were identified.

1.31.4   En Face Analysis

Whole aortas were dissected from C57BL/6NJ : LDLR$^{-/-}$ and IL-21R$^{-/-}$: LDLR$^{-/-}$ mice and fixed in 10% formalin solution for 24 hours. Samples were subsequently bathed in filtered oil-red-o (ORO) solution, made with 3-parts concentrated ORO (0.5% in isopropanol) and 2-parts distilled water. After incubation for 2 hours, samples were rinsed in 100% isopropanol to remove excess ORO stain and then in distilled water. Using fine dissection, the intimal surface was exposed by a single longitudinal cut through the aortic arch towards the anterior edge of the aorta. Using dissection needles, aortas were pinned on a black rubber dissection board. Images were captured using a standard 8-mega-pixel camera.

Total aortic area and ORO stained plaque area was measured using ImageJ quantification software (National Institutes of Health Imagining: http://rsbweb.nih.gov/ij) and calculated in mm^2. Using the calculation shown in figure 7, percentage area of aorta covered in ORO positive plaque was measured.
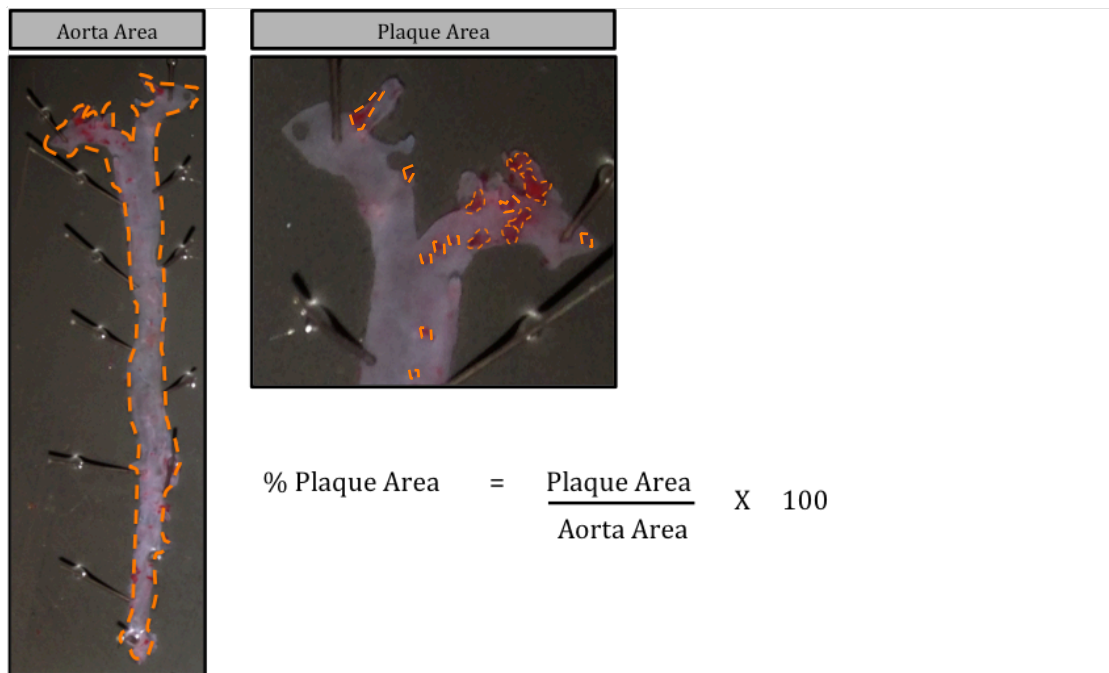
Figure 7: Schematic representation of En Face approach used to quantify the percentage of aorta comprised of ORO positive plaques

Aortas from both C57BL/6NJ : LDLR$^{-/-}$ and IL-21R$^{-/-}$: LDLR$^{-/-}$ mice were fixed in 10% formalin and stained in ORO solution for 2 hours. Total aorta area was measured alongside plaque area positive for ORO stain. Using these two parameters, the percentages of aorta comprised of ORO stained plaques was calculated.

1.31.5   Aortic Sinus Plaque Quantification

Aortic sinuses were harvested from both and C57BL/6NJ : LDLR$^{-/-}$ and IL-21R$^{-/-}$: LDLR$^{-/-}$ mice and placed in an OCT medium filled moulds. Eight-micron thick sequential sections were subsequently cut, starting at 0 microns and finishing at 660 microns.

Sections were fixed in 100% acetone for 10 minutes, after which they were re-hydrated in PBS. Sections were stained for 1 hour in an ORO solution containing 3-parts concentrated ORO (0.5 % ORO in isopropanol) and 2-parts distilled water. Sections were subsequently rinsed in 100% isopropanol, followed by distilled water and mounted using a water soluble mounting medium (Vector Labs, California, USA).

Total area positive for ORO was measured using ImageJ quantification software (National Institutes of Health Imaging: http://rsbweb.nih.gov/ij) and calculated in mm^2. Plaque burden was measured every 60 microns (from 0 microns to 660 microns) and the average area plotted for every animal at each point. The process of aortic sinus plaque quantification is shown in figure 8.
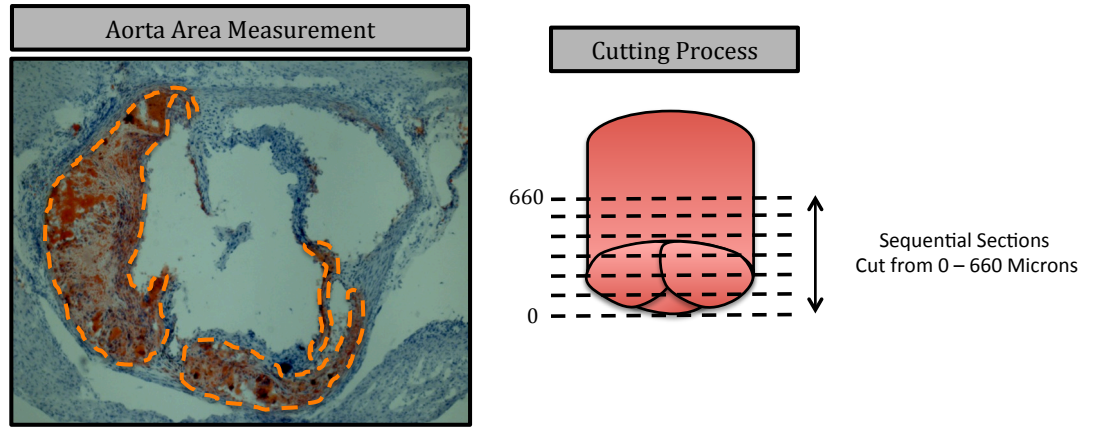
Figure 8: Schematic representation of approach used to quantify ORO positive area of aortic sinus sections

Aortic sinus sections from both C57BL/6NJ : LDLR$^{-/-}$ and IL-21$^{-/-}$: LDLR$^{-/-}$ mice were fixed in 10% formalin and stained in ORO solution for 2 hours. Using a total 12 sections per animal, mean ORO positive plaque area was measured using Imagej quantification software. These values were plotted in 60 micron increments, starting from 0 to 660 microns.

1.31.6　CD68+ Macrophage Staining

Eight micron thick sections from C57BL/6NJ : LDLR$^{-/-}$ and IL-21R$^{-/-}$: LDLR$^{-/-}$ mice were fixed in 100% acetone for 10 minutes. Sections were subsequently air dried and rehydrated in PBS. After washing in PBS, sections were incubated in FC-receptor block (2.3G2 hydridoma supernatant) for 15 mins and subsequently washed twice in PBS for 10 minutes. To detect CD68, samples were stained with rat-anti-mouse CD68 antibody (AbD Serotec, Oxford United kingdom) in 1% blocking reagent (Perkin Elmer, Cambridge, United kingdom) and 0.3% Triton X-100 in PBS overnight. The next day, samples were washed in TNT buffer (Tris-HCL; pH 7.5; 0.15 mol/L NaCl; and 0.05% Tween-20), dried and incubated with Texas Red-donkey anti-rat IgG (Jackson ImmunoResearch Laboratories, Sohan, United Kingdom) for 30 mins. After washing in TNT buffer, sections were dried and mounted in Prolong Gold containing DAPI (Life Technologies, Paisley, United Kingdom).

Respective isotype controls were prepared in an identical manner as described above, with rat-anti-mouse CD68 being replaced with rat-IgG$_{2a}$ (AbD Serotec, Oxford, United Kingdom). For a full description of the antibodies used to detect CD68 staining, please refer to appendix 6.

Sections were viewed using the Axioimager M2 epifluorescent microscope (Zeiss, Germany) and CD68+ macrophage content was quantified using ImageJ quantification software (National Institutes of Health Imaging: http://rsbweb.nih.gov/ij).

Colour thresholds determined CD68+ positive staining and results are presented as percentage area of sinus positive for CD68 staining. A total of thirteen sections per animal were used for quantification purposes.

1.31.7　Collagen Staining

Eight micron thick sinus sections from C57BL/6NJ : LDLR$^{-/-}$ and IL-21R$^{-/-}$: LDLR$^{-/-}$ mice were fixed in 10% formalin for 10 minutes. Sections were subsequently re-hydrated in distilled water for a further 10 minutes. Using a Picro Sirius Red kit (Abcam, Cambridge, United Kingdom), sections were stained in a 1X solution of Picro

Sirius Red for 1 hour at room temperature. To differentiate the Picro Sirius Red stain, sections were rinsed in two changes of 0.5% acetic acid. Sections were subsequently de-hydrated in 3 changes of 100% alcohol and mounted using DPX mounting media (ThermoFisher Scientific, Loughborough, United Kingdom).

Sections were viewed using the AxioStar Plus transmitted light microscope (Zeiss, Germany) with the aid of polarised lenses. Picro Sirius Red staining was quantified using ImageJ quantification software (National Institutes of Health Imaging: http://rsbweb.nih.gov/ij). Picro Sirius Red staining was determined by discrimination of threshold staining and results are presented as percentage of sinus comprising collagen. A total of thirteen sections per animal were used for quantification purposes.

1.32 Immunization Protocol

C57BL/6 (n = 6) and apoE$^{-/-}$ (n = 6) were immunised s.c. with 100 μg of ovalbumin (OVA) emulsified in 100 μl of complete freund's adjuvant (CFA). Mice were allowed to recover for 9-days, throughout which they were allowed free access to food and water. After 9-days, both groups were culled via CO_2 inhalation and scruff-draining lymph nodes removed for flow cytometry analysis.

Figure 9 summarises the immunization protocol employed.

1.33 Bone Marrow Processing and Retrieval

Using complete RPMI (Life Technologies, Paisley, United Kingdom), bone marrow was flushed from the femurs and tibias of donor mice (C57BL/6NJ and IL-21R$^{-/-}$). Expelled bone marrow was subsequently passed through a 40-μm nylon cell strainer (Falcon, New York, USA). The resulting cell suspension was centrifuged at 400 g for 5 minutes and re-suspended in complete RPMI, ready for i.v. Injection of 4 X 10^6 cells per mouse.
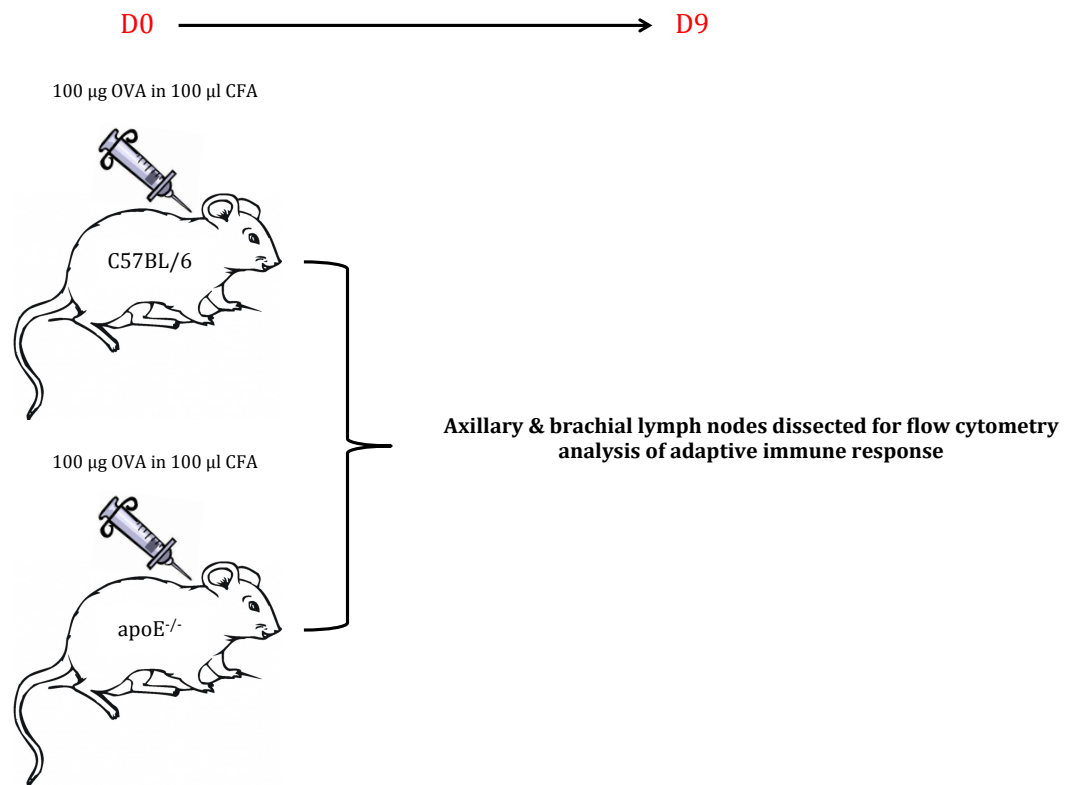
Figure 9: Schematic representation of Immunization protocol used to induce an adaptive immune response in C57BL/6 WT and apoE$^{-/-}$ mice

Two groups of mice [C57BL/6 WT (n = 6) and apoE$^{-/-}$ (n = 6)] were immunized s.c. with 100 µg of OVA protein in 100 µl CFA. Nine days later, draining lymph nodes (axillary and brachial) were dissected and prepared for flow cytometry analysis.

1.34 Chimera Generation

Two groups of recipient LDLR$^{-/-}$ mice were lethally irradiated with a single dose with 10.5 Grays X-ray Radiation (Precision X-ray, Connecticut. USA). Mice were subsequently injected i.v. with 4×10^6 bone marrow derived haematopoietic stem cells from donor C57BL/6NJ or IL-21R$^{-/-}$ mice. Mice were allowed to recover for 4 hours and subsequently placed on HFD (Special Diet services, Essex, United Kingdom) for a period of 14 weeks (for composition refer to appendix 1). Chimeric mice were administered 1% Enrofloxacin in drinking water for the duration of the study (Henry Schein, Dumfries, United Kingdom).

Resulting chimeras generated were as follows,

1. IL-21R$^{-/-}$: LDLR$^{-/-}$ $\qquad$ (n = 9)
2. C57BL/6NJ : LDLR$^{-/-}$ $\qquad$ (control) $\quad$ (n = 10).

Figure 10 summarises the process in which chimeric mice were generated.
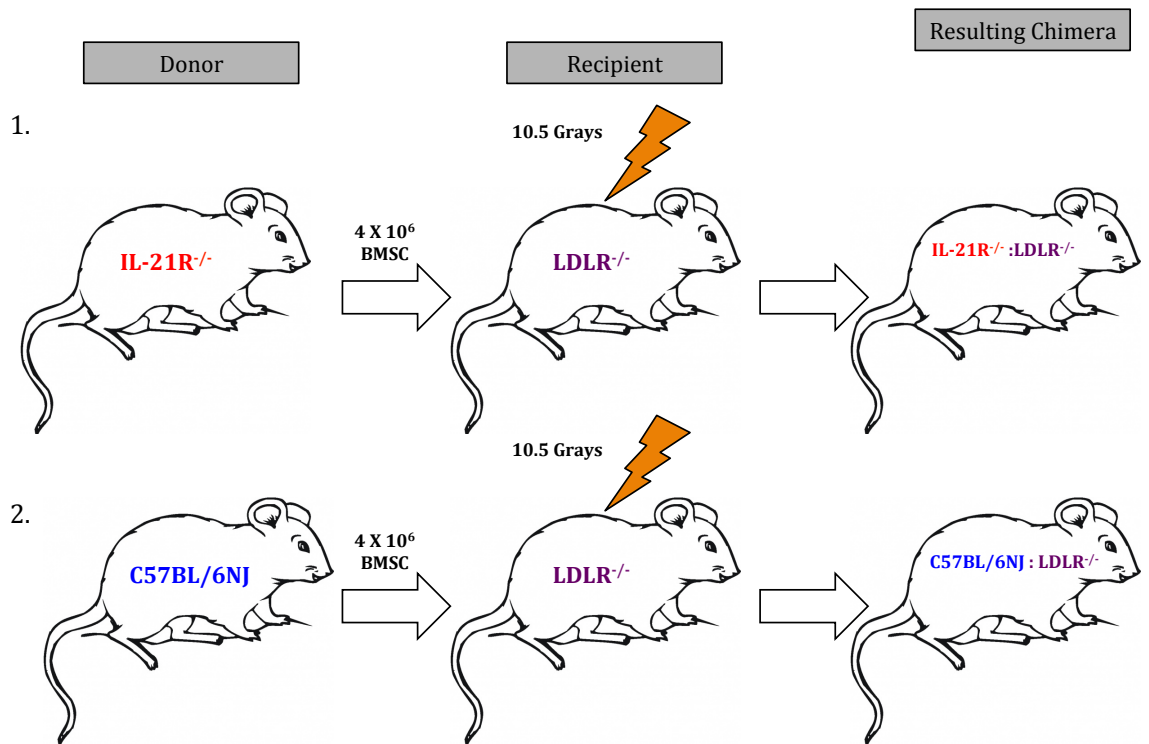
Figure 10: Schematic representation of approach used to develop C57BL/6NJ : LDLR$^{-/-}$ and IL-21R$^{-/-}$: LDLR$^{-/-}$ chimeric mice

Two groups of LDLR$^{-/-}$ mice were lethally irradiated with 10.5 Grays of X-ray radiation. One group was reconstituted i.v. with bone marrow derived from IL-21R$^{-/-}$ mice, while the other group was reconstituted with bone marrow from C57BL/6NJ mice. As a consequence, two chimeric animals were formed – 1. IL-21R$^{-/-}$: LDLR$^{-/-}$ and 2. C57BL/6NJ : LDLR$^{-/-}$.

1.35   Confirmation of Chimera Status

LDLR expression was determined on the surface of peripheral blood monocytes 10 weeks post-reconstitution. Blood was retrieved via tail vein puncture and collected into a vial containing 50 µl of ethylenediaminetetraacetic acid (EDTA). Red blood cells were lysed by adding 2 ml of red blood cell lysis buffer (Ebioscience, San Diego, USA) and subsequently washed in HBSS (Life Technologies, Paisley, United Kingdom) ready for flow cytometry staining.

1.35.1   Statistics

Statistical analysis was performed using GraphPad Prism. An unpaired student's t-test was performed when comparing two groups * $P < 0.05$, ** $P < 0.01$, *** $P < 0.001$. When comparing three or more groups, a one-way-ANOVA was conducted with a post-hoc-tukey's test. * $P < 0.05$, ** $P < 0.01$, *** $P < 0.001$.

Chapter 3: Characterising Tfh cell & GC B-cell Populations in the apoE$^{-/-}$ Mouse Model of Atherosclerosis.

1.36 Introduction

With over two decades of research into the immunological basis of atherosclerosis, researchers have gained an extensive understanding of the fundamental processes that lead to lesion development. As a result, a range of immune cells have been identified as being attractive therapeutic targets. Interestingly, although much research has been dedicated to the role of CD4+ T-cells in atherosclerosis, the role of Tfh cells is only just being addressed. Recent studies have indicated the potential significance of Tfh cells in driving lesion formation *in vivo* [142], indicating an increase in Tfh cell kinetics with lesion progression. Involved in helping GC B-cells in the production of isotype switched, high affinity antibodies, Tfh cells play an important role in GC B-cell differentiation and the formation of protective and pathological antibodies. Therefore, this chapter determined Tfh cell and GC B-cell kinetics in context of atherosclerosis by using the apoE$^{-/-}$ mouse model of atherosclerosis.

1.36.1 Aims

The aims of this chapter were to:

1. Determine whether Tfh cell and GC B-cell kinetics changed in line with atherosclerosis progression in apoE$^{-/-}$ mice fed diet for varying lengths of time;

2. Assess whether antibody titres to modified forms of low-density lipoprotein (LDL) changed in line with atherosclerosis progression and Tfh cell / GC B-cell kinetics.

1.37 Results

1.38 Gating Strategies for The Detection of Tfh cells *in vivo*

To date, there remains much confusion as to the exact phenotypic markers to be used for Tfh cell analysis. As a result, there is little consistency between published studies. In an attempt to address this issue, the studies described herein characterised Tfh cells using two gating strategies. Both strategies took into account that Tfh cells originate from the CD4+ T-cell lineage and migrate to B-cell follicles in a CXCR5 dependent manner [44, 168]. As such, both strategies included CD4 and CXCR5. Moreover, the fact that GC Tfh cells express high levels of PD-1 [171, 221, 222] was taken into account. With this in mind, PD-1 was included as a marker of Tfh cells in both strategies.

1.38.1   First Gating Strategy – CD4+ CXCR5+ PD-1+ Tfh Cells

The first approach involved using the gating style shown in figure 11. Lymphocytes were gated for on the basis of forward and side scatter (FSC) (SSC) parameters (Fig 11). This was followed by a subsequent CD4+ T-cell gate, upon which CXCR5+ PD-1+ cells were gated (Fig 11). In combination, the first gating strategy defined Tfh cells as CD4+ CXCR5+ PD-1+ expressing cells.

1.38.2   Second Gating Strategy – CD4+ CD44hi CXCR5+ PD-1+ Tfh cells

As well as profiling Tfh cells as CD4+ CXCR5+ PD-1+ cells, the cell surface glycoprotein CD44 was included in the second gating strategy. Involved in cell-cell interaction by binding extracellular hyaluronic acid (HA) [223], CD44 is up regulated on the surface of antigen experienced and activated T-cells [223]. As Tfh cells encounter antigen and subsequently migrate to B-cell follicles for participation in the GC reaction, they up-regulate CD44 on their surface. Moreover, CD44 has previously been used – in combination with other markers – as a faithful representation of Tfh cell phenotype [222].

Therefore, as part of the second gating strategy, Tfh cells were characterised as CD4+ CXCR5+ CD44hi PD-1+ cells.

Using the gating style shown in figure 12, lymphocytes were gated for on the basis of FSC and SSC parameters. This was followed by a subsequent CD4+ T-cell gate, upon which CD4+ CD44hi T-cells were selected. CXCR5+ PD-1+ Tfh cells were then gated for (Fig 12).
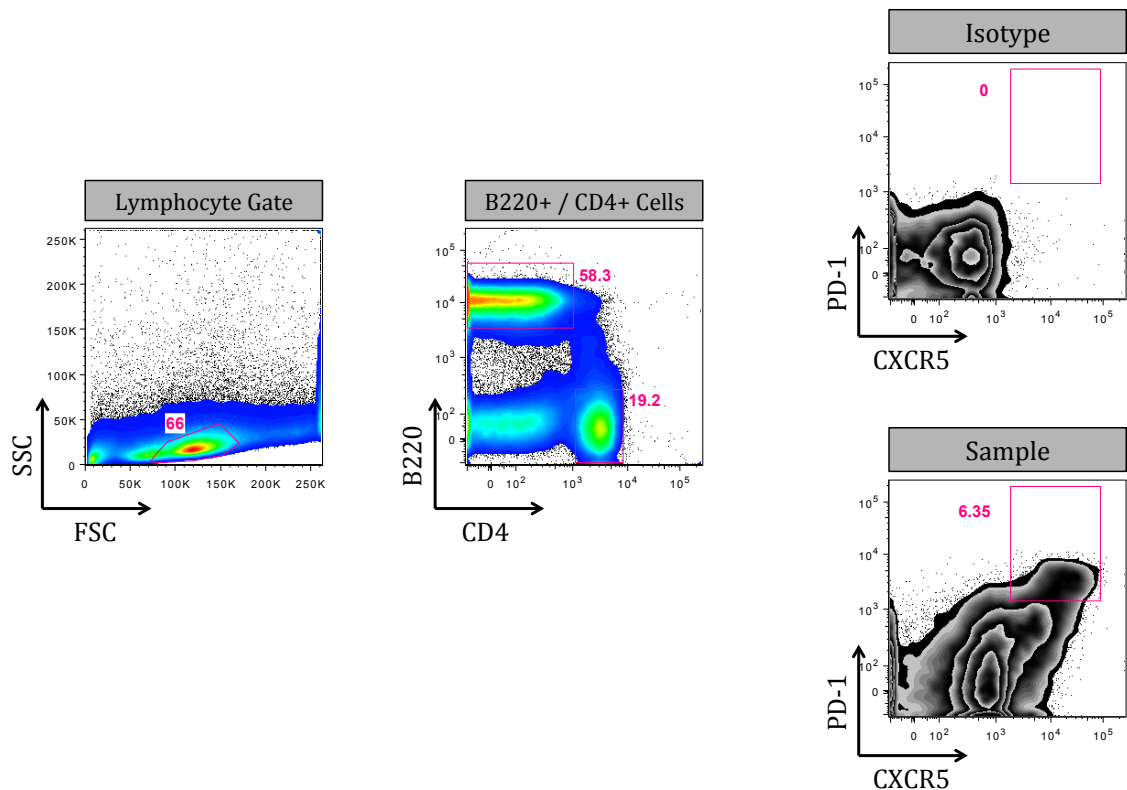
Figure 11: Generation of CD4+ CXCR5+ PD-1+ Tfh cell gating strategy

Lymphocytes were gated for on the basis of FSC and SSC parameters. Using a B220 / CD4 gate to exclude B220+ cells, CD4+ were selected. Using this parent gate, CXCR5+ PD-1+ Tfh cells were selected for. Using this gating strategy, Tfh cells were defined as CD4+ CXCR5+ PD-1+ Tfh cells. Representative plots were obtained from analysis of pao-LN samples.
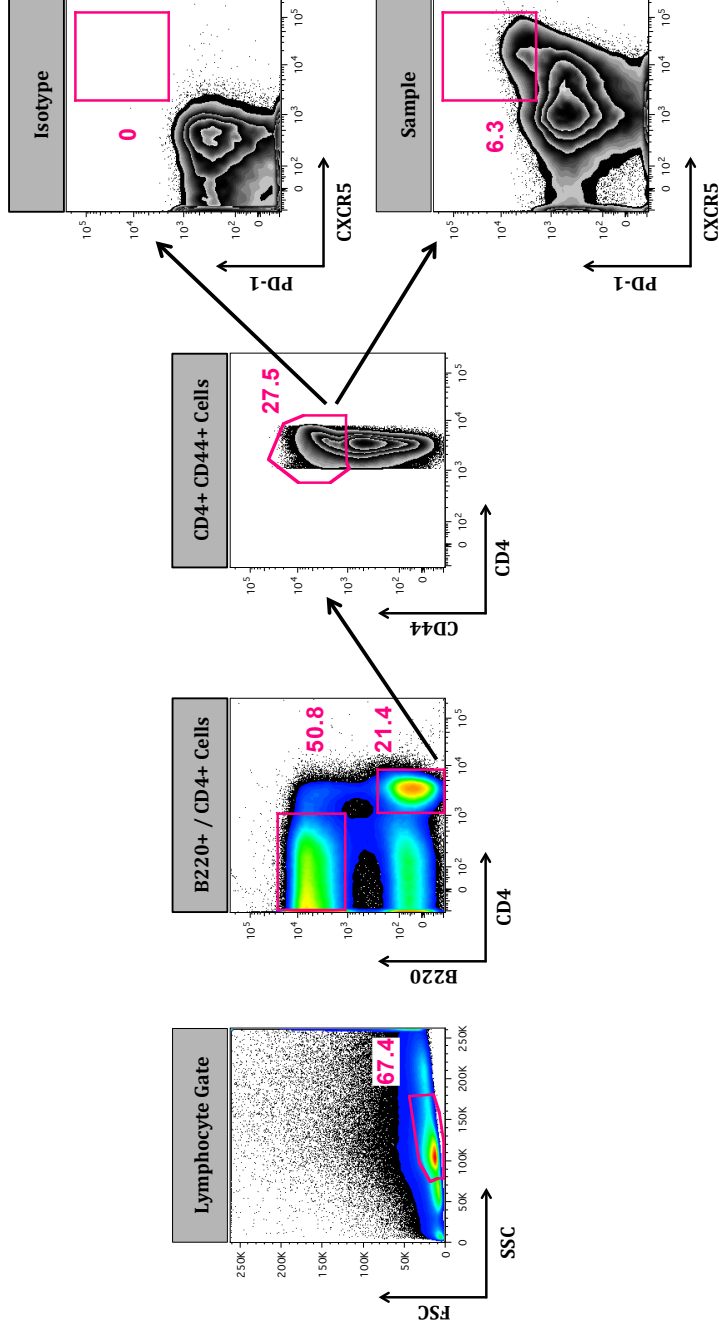
Figure 12: Generation of CD4+ CD44hi CXCR5+ PD-1+ Tfh cell gating strategy

Lymphocytes were gated for on the basis of FSC and SSC parameters. Using a B220 / CD4 gate to exclude B220+ cells, CD4+ were selected. Using this parent gate, CD4+ CD44hi T-cells were selected for. CD4+ CD44hi cells were subsequently gated for their doublet expression of CXCR5 and PD-1. Using this strategy, Tfh cells were defined as CD4+ CD44hi CXCR5+ PD-1+ Tfh cells. Representative plots were obtained from analysis of pLN samples.

1.39 Tfh cell Kinetics in Atherosclerosis

1.39.1 Peripheral Lymph Node CD4+ CXCR5+ PD-1+ Tfh Cell and CD4+ CD44hi CXCR5+ PD-1+ Tfh Cell Populations Increase in Line with Atherosclerosis Progression

PLNs represent an important network of structures that allow for the peripheral circulation of immune cells. As such, lymph nodes represent an important location where antigen presenting cells (APCs) uptake and present cognate antigen to resident T-cells. To determine whether pLN Tfh cell populations changed in line with atherosclerosis progression, Tfh cell expression patterns were assessed in the pLNs of C57BL/6 wild type (WT) and apoE$^{-/-}$ mice fed chow or HFD for variable lengths of time.

Using the first gating strategy, no difference in the percentage of pLN CD4+ CXCR5+ PD-1+ Tfh cells was observed in WT at any time point (Fig 13A). In contrast, a peak in CD4+ CXCR5+ PD-1+ Tfh cell populations in the pLNs of apoE$^{-/-}$ mice fed chow or HFD for 12 weeks was observed (Fig 13A).

In comparing intra-group variation, apoE$^{-/-}$ mice fed HFD for 12 weeks displayed a significant increase in the percentage of CD4+ CXCR5+ PD-1+ Tfh cells than WT and apoE$^{-/-}$ mice fed chow for the same length of time (Fig 13A). In contrast, pLN CD4+ CXCR5+ PD-1+ Tfh cell populations peaked in apoE$^{-/-}$ mice fed chow or HFD for 12 weeks (Fig 13A).

When including CD44hi cells, a similar trend in Tfh cell expression – as found using gating strategy one – was observed. Remaining low throughout, no difference in the percentage of CD4+ CD44hi CXCR5+ PD-1+ Tfh cells in the pLNs of WT mice (Fig 13B) was found. In contrast, both apoE$^{-/-}$ chow and HFD fed mice peaked in CD4+ CD44hi CXCR5+ PD-1+ Tfh cell formation at 12 weeks post-diet (Fig 13B). Mirroring the results obtained via gating strategy one, apoE$^{-/-}$ mice fed HFD for 12 weeks displayed

significantly enhanced percentages of CD4+ CD44hi CXCR5+ PD-1+ Tfh cell than WT and apoE$^{-/-}$ mice fed chow for the same length of time (Fig 13B).
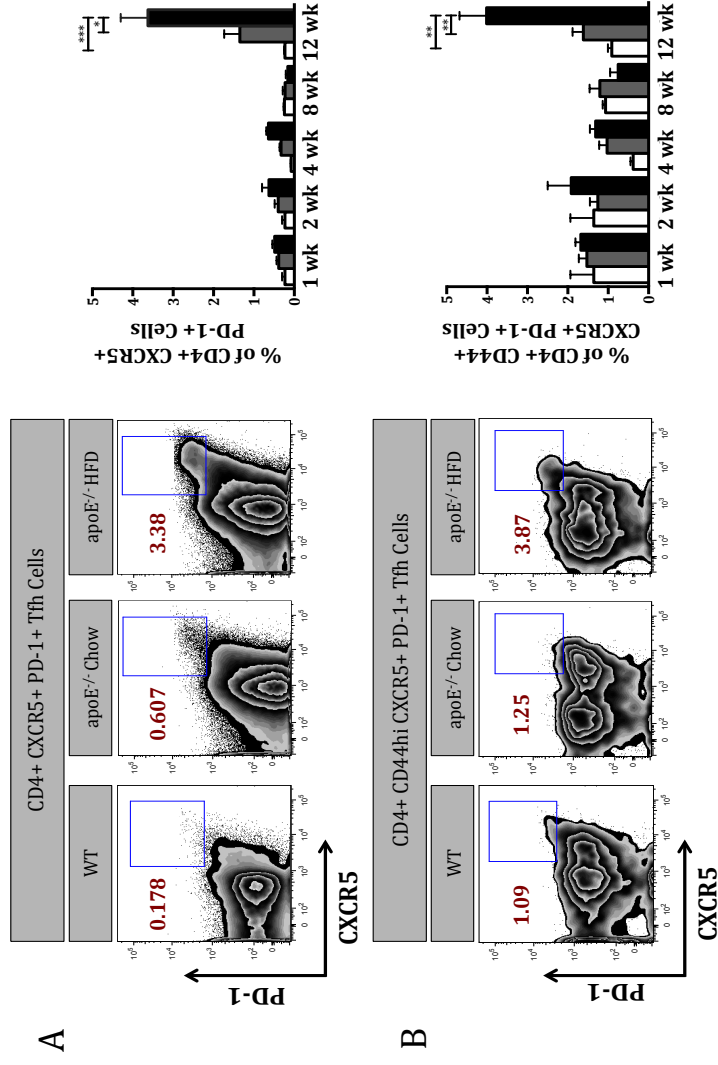
Figure 13: Percentage of CXCR5+ PD-1+ Tfh cells in pLNs of mice following administration of chow or HFD for variable lengths of time

Individual groups of mice were provided with HFD (apoE⁻/⁻) or chow diet (apoE⁻/⁻ and C57BL/6 WT) for a period of 1, 2, 4, 8 and 12 weeks. Pao-LNs were harvested at each time point and using two gating strategies, Tfh cell populations were assessed. Tfh cells were characterised as CD4+ CXCR5+ PD-1+ **(A)** and CD4+ CD44hi CXCR5+ PD-1+ **(B)** expressing cells. Representative plots display the 12 week time point. Open bars represent C57BL/6 WT (n = 5 - 6) mice fed standard laboratory chow diet. Shaded grey and black bars represent apoE⁻/⁻ mice fed standard laboratory chow diet (n = 3 - 5) or HFD (n = 3 - 5), respectively. Statistical analysis was performed using GraphPad Prism and by conducting a one-way-ANOVA with a post-hoc-tukey's test. * $P < 0.05$, ** $P < 0.01$, *** $P < 0.001$

1.39.2 Spleen CD4+ CXCR5+ PD-1+ Tfh Cell and CD4+ CD44hi CXCR5+ PD-1+ Tfh Cell Populations Increase in Line with Atherosclerosis Progression

The spleen is a multifunctional organ with roles in red blood cell metabolism, immunity and blood filtration [224]. Underlining the role of the spleen in atherosclerosis, splenectomised mice develop enhanced lesions, with significantly lower antibody titres [155, 156]. As well as this, and of particular relevance to Tfh cell biology, the spleen is a major site of antibody production *in vivo* [224]. As atherogenic antigens (oxidised forms of low density lipoprotein) circulate in the blood, the percentage of Tfh cell populations in spleen of all three groups was assessed. As such, it was determined whether the spleen housed significant Tfh cell populations, in the context of atherosclerosis.

Little variation in the percentage of CD4+ CXCR5+ PD-1+ Tfh cells in the spleen of WT mice at early time points (1wk – 4wk) (Fig 14A) was observed. This was followed by a slight increase towards later time points (8wk – 12wk) (Fig 14A). As observed in pLN samples, CD4+ CXCR5+ PD-1+ Tfh cell populations peaked in apoE$^{-/-}$ mice fed HFD for 12 weeks (Fig 14A). This peak was significantly greater than the percentage of CD4+ CXCR5+ PD-1+ Tfh cells in the spleen of WT and apoE$^{-/-}$ mice fed chow diet for the same length of time (Fig 14A). Mirroring this, apoE$^{-/-}$ mice fed chow or HFD at early time points (1wk) also displayed enhanced CD4+ CXCR5+ PD-1+ Tfh cell percentages when compared to WT and apoE$^{-/-}$ mice fed chow diet (Fig 14A).

When including CD44+ cells, apoE$^{-/-}$ mice fed chow or HFD for 1 week displayed significantly enhanced percentages of CD4+ CD44hi CXCR5+ PD-1+ Tfh cells than WT mice (Fig 14B). In comparing apoE$^{-/-}$ groups, this rise was significantly greater in apoE$^{-/-}$ mice fed HFD (Fig 14B). Following a similar pattern, apoE$^{-/-}$ mice fed chow diet for 4 weeks displayed significantly enhanced percentages of CD4+ CD44hi CXCR5+ PD-1+ Tfh cells than WT mice (Fig 14B).

Interestingly, WT mice fed diet for 8 weeks displayed significantly enhanced percentages of CD4+ CD44hi CXCR5+ PD-1+ Tfh cells than apoE$^{-/-}$ mice fed chow or HFD for the same length of time (Fig 14B)

Figure 14: Percentage of CXCR5+ PD-1+ Tfh cells in spleen of mice following administration of chow or HFD for variable lengths of time

Individual groups of mice were provided with HFD (apoE$^{-/-}$) or chow diet (apoE$^{-/-}$ and C57BL/6 WT) for a period of 1, 2, 4, 8 and 12 weeks. Pao-LNs were harvested at each time point and using two gating strategies, Tfh cell populations were assessed. Tfh cells were characterised as CD4+ CXCR5+ PD-1+ **(A)** and CD4+ CD44hi CXCR5+ PD-1+ **(B)** expressing cells. Representative plots display the 12 week time point. Open bars represent C57BL/6 WT (n = 5 - 6) mice fed standard laboratory chow diet. Shaded grey and black bars represent apoE$^{-/-}$ mice fed standard laboratory chow diet (n = 3 - 5) or HFD (n = 3 - 5), respectively. Statistical analysis was performed using GraphPad Prism and by conducting a one-way-ANOVA with a post-hoc-tukey's test. * $P < 0.05$, ** $P < 0.01$, *** $P < 0.001$

97

1.39.3 Para-aortic CD4+ CXCR5+ PD-1+ Tfh Cell and CD4+ CD44hi CXCR5+ PD-1+ Tfh Cell Populations Increase in Line with Atherosclerosis Progression

The inflammatory response that occurs within the aortic vessel is important to the development and progression of lesions [225]. During established pathology, cells from both the adaptive and innate compartments converge to orchestrate the progression of luminal plaques [225]. Acting via cell-cell interaction and the secretion of chemical mediators (to recruit more cells), the delicate balance of arterial inflammation can have a profound effect upon pathological outcome. In testament to this, modulation of many immune cells discussed in the introduction of this chapter significantly affect lesion progression.

To obtain immune cells from highly fibrous aortas, aortas must be subjected to enzymatic digestion, using a cocktail of collagenase, hylauronadase and DNAse. Unfortunately, from previous experiments, it became apparent that this very process results in diminished aortic CXCR5 detection (data not shown).

To confirm this finding wasn't a result of deficient CXCR5 expression in the aorta, pLN and spleen samples were assessed for CXCR5 expression post-digestion. Confirming our findings, no CXCR5 positive staining was detected after digestion (data not shown). To address this issue, a variety of techniques were used, including biotinylated CXCR5 antibody and streptavidin treatment, and fluorescently labelled CXCL13 (the ligand for CXCR5). Unfortunately, these techniques were insufficient in detecting CXCR5 expression (data not shown).

As such, to gain an understanding of what Tfh cell expression may be like in a local environment, Tfh cell populations were assessed in the para-aortic lymph nodes (pao-LNs) of mice.

The pao-LNs are a group of lymph nodes that lie parallel to the abdominal aorta. Of particular importance to atherosclerosis, these LNs receive drainage from the aortic trunk, and hence plaques [219].

Both WT and apoE$^{-/-}$ mice fed chow diet for 1 – 12 weeks displayed little variation in pao-LN CD4+ CXCR5+ PD-1+ Tfh cell populations. (Fig 15A). In contrast, apoE$^{-/-}$ mice fed HFD for 12 weeks, displayed a significant peak in the percentage of CD4+ CXCR5+ PD-1+ Tfh cells (Fig 15A).

In comparing earlier time points, apoE-/- mice fed chow diet for 1 week displayed enhanced percentages of CD4+ CXCR5+ PD-1+ Tfh cells than WT control mice (Fig 15A). Following a similar pattern, both apoE$^{-/-}$ chow and apoE$^{-/-}$ HFD mice fed diet for 4 weeks displayed significantly enhanced percentages of CD4+ CXCR5+ PD-1+ Tfh cells than their respective WT controls (Fig 15A).

When including CD44, WT mice displayed no difference in the expression of CD4+ CD44hi CXCR5+ PD-1+ Tfh cells at any time point (Fig 15B). In contrast, apoE$^{-/-}$ mice fed chow diet for 8 weeks displayed a significant peak in pao-LN CD4+ CD44hi CXCR5+ PD-1+ Tfh cell populations (Fig 15B).

Moreover, apoE$^{-/-}$ mice fed HFD for 12 weeks displayed a significant peak in pao-LN CD4+ CD44hi CXCR5+ PD-1+ Tfh cell populations (Fig 15B). This peak was significantly greater than WT and apoE$^{-/-}$ mice fed chow diet for the same length of time   (Fig   15B).
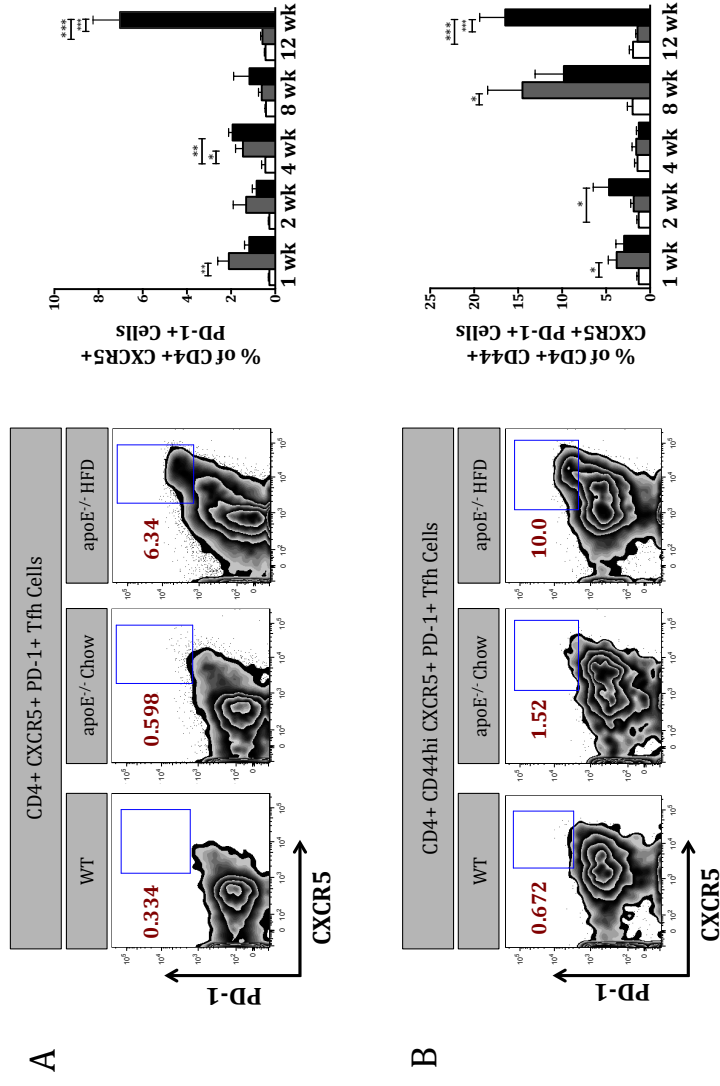
Figure 15: Percentage of CXCR5+ PD-1+ Tfh cells in pao-LNs of mice following administration of chow or HFD for variable lengths of time

Individual groups of mice were provided with HFD (apoE$^{-/-}$) or chow diet (apoE$^{-/-}$ and C57BL/6 WT) for a period of 1, 2, 4, 8 and 12 weeks. Pao-LNs were harvested at each time point and using two gating strategies, Tfh cell populations were assessed. Tfh cells were characterised as CD4+ CXCR5+ PD-1+ **(A)** and CD4+ CD44hi CXCR5+ PD-1+ **(B)** expressing cells. Representative plots display the 12 week time point. Open bars represent C57BL/6 WT (n = 5 - 6) mice fed standard laboratory chow diet. Shaded grey and black bars represent apoE$^{-/-}$ mice fed standard laboratory chow diet (n = 3 - 5) or HFD (n = 3 - 5), respectively. Statistical analysis was performed using GraphPad Prism and by conducting a one-way-ANOVA with a post-hoc-tukey's test. * $P < 0.05$, ** $P < 0.01$, *** $P < 0.001$

1.39.4 Summary of Tfh cell Kinetics in Experimental Atherosclerosis

In summary, remaining consistently low, WT mice displayed little variation in Tfh cell populations in all organs assessed. Interestingly, apoE$^{-/-}$ mice fed HFD for 12 weeks displayed significantly enhanced Tfh cell percentages in all organs assessed. Peaking at 12 weeks, this time point co-insides with the formation of advanced plaques, enhanced arterial inflammation and established pathology in the apoE$^{-/-}$ mouse model. As such, Tfh cells may comprise a significant population at advanced stages of atherosclerosis. Moreover, our data suggests that extreme hyperlipidaemia may function to drive Tfh cell formation *in vivo*.

1.40 Gating Strategies for The Detection of GC B-cells *In vivo*

As well as Tfh cells, GC B-cells comprise an important component of every GC reaction. Via cell-cell interactions and production of IL-21, Tfh cells guide GC B-cells through their differentiation programme, to form antibody-secreting memory B-cells and plasma cells [226]. The interaction between GC B-cells and Tfh cells is therefore essential to the successful mounting of adaptive immune responses.

Using surface flow cytometry staining, GC B-cell populations were assessed in the pLNs, spleen and pao-LNs of apoE$^{-/-}$ mice fed chow or HFD for 1, 2, 4, 8 and 12 weeks. Using this data, we aimed to determine whether GC B-cell kinetics followed a pattern in line with the Tfh cell kinetics described above.

As a means of determining GC B-cell kinetics in the pLNs, spleen and pao-LNs of mice, the gating strategy shown in figure 16 was devised. Using an initial lymphocyte gate, B220+ cells were gated for alongside a CD4 exclusion gate. B220+ cells were subsequently gated for their expression of the GC B-cell markers – peanut agglutinin (PNA) and FAS.
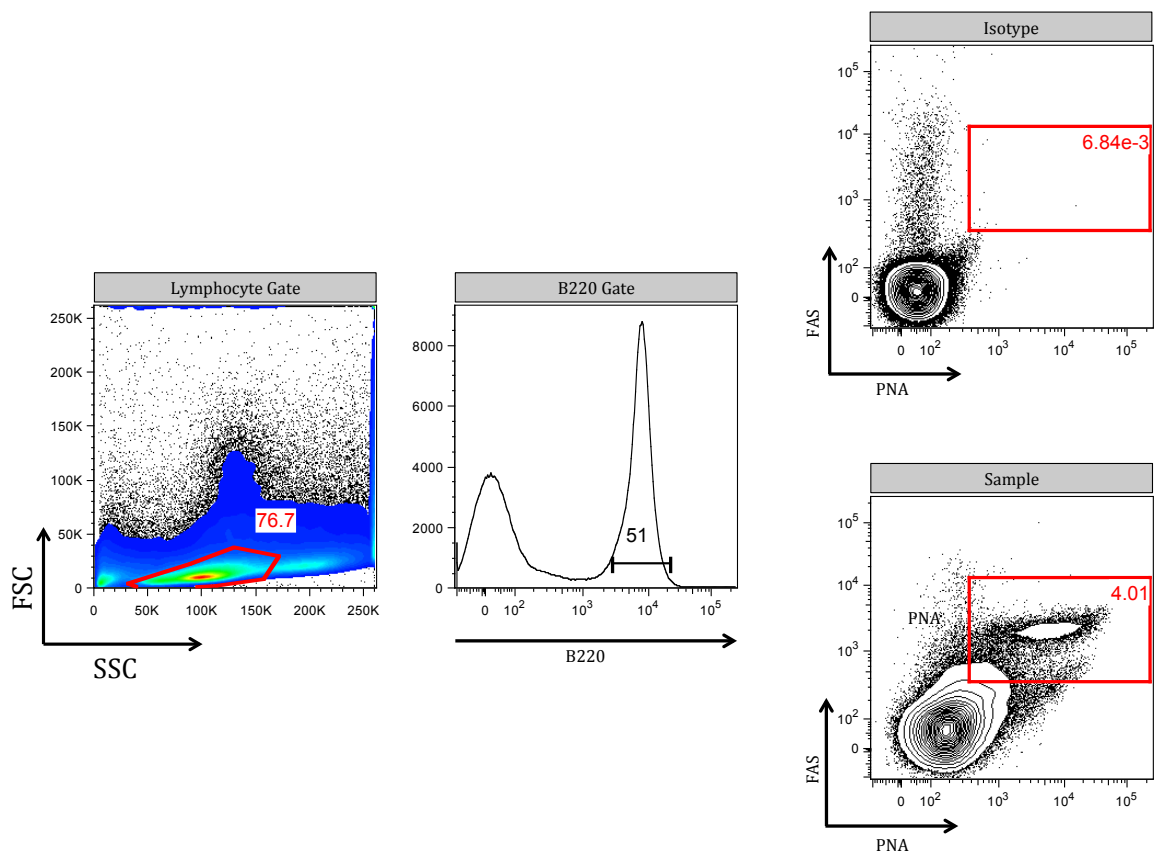
Figure 16: Generation of B220+ PNA+ FAS+ GC B-cell gating strategy

Lymphocytes were gated for on the basis of FSC and SSC parameters. B220+ cells were subsequently gated. Doublet gating followed this, upon which PNA+ FAS+ expressing cells were gated.

1.40.1 Peripheral Lymph Node GC B-cell Populations Increase in Line with Atherosclerosis Progression

No difference in the percentage of WT pLN B220+ FAS+ PNA+ GC B-cell populations was observed at any time point (Fig 17). In comparison, a significant increase in the percentage of GC B-cells in the pLNs of apoE$^{-/-}$ mice fed chow or HFD diet for 4 and 12 weeks was observed (Fig 17). When comparing intergroup variation, apoE$^{-/-}$ mice fed HFD (for 4 or 12 weeks) displayed significantly greater percentages of GC B-cells than apoE$^{-/-}$ mice fed chow diet for the same length of time (Fig 17).
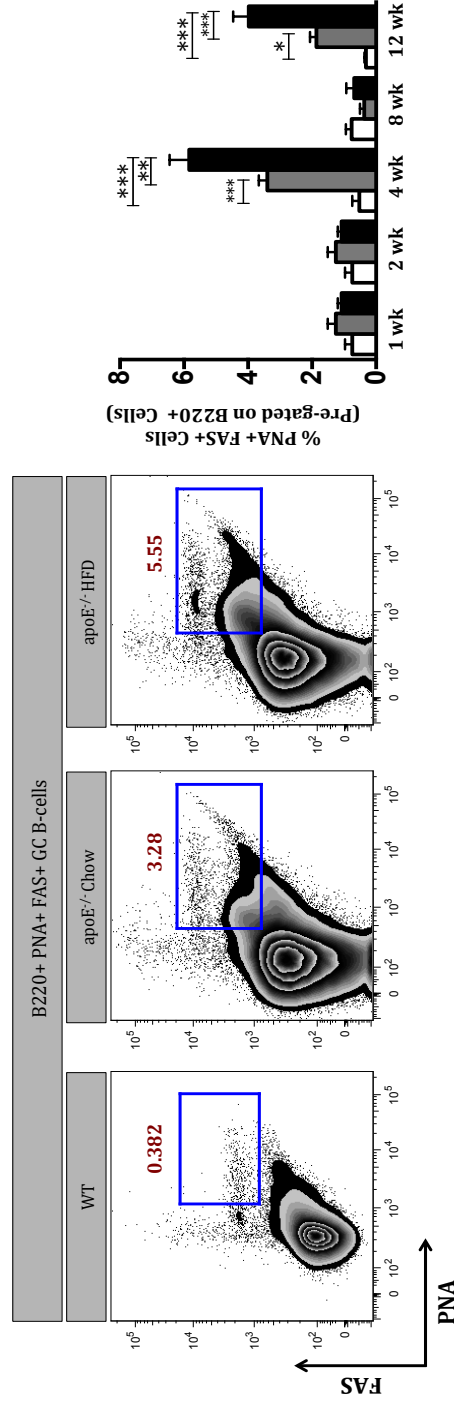
Figure 17: Percentage of B220+ FAS+ PNA+ GC B-cell in pLNs of mice following administration of chow or HFD for variable lengths of time

Individual groups of mice were provided with chow (C57BL/6 WT and apoE$^{-/-}$) or HFD (apoE$^{-/-}$) for a period of 1, 2, 4, 8 and 12 weeks. pLNs were harvested at each time point and GC B-cell populations assessed via surface flow cytometry staining. Lymphocytes were gated for on the basis of an initial FSC and SSC gate and a subsequent B220+ gate made. Using this parent gate, FAS+ PNA+ cells were gated. Open bars represent C57BL/6 WT mice (n = 5 -6) fed standard laboratory chow diet. Shaded grey and black bars represent apoE$^{-/-}$ mice fed chow (n = 4 - 10) or HFD (n = 5 - 9), respectively. Statistical analysis was performed using GraphPad Prism and by conducting a one-way-ANOVA with a post-hoc-tukey's test. * $P < 0.05$, ** $P < 0.01$, *** $P < 0.001$.

1.40.2 Splenic GC B-cell Populations Increase in Line with Atherosclerosis Progression

As with Tfh cell populations, we studied B220+ PNA+ FAS+ GC B-cell expression in systemic compartments. As such, we determined whether Tfh cell and GC B-cell kinetics followed a distinct pattern, thus suggesting active GC reaction formation.

As with pLNs, little variation in the percentage of splenic GC B-cells was observed in WT mice at any time point (Fig 18). In contrast, and in comparison to WT mice, apoE$^{-/-}$ mice fed chow diet displayed a significant peak in GC B-cell formation at 4 weeks post-diet (Fig 18).

Interestingly, mice fed HFD at early (1wk and 2wk) and late time points (12 wk) displayed significantly greater percentages of GC B-cells than respective WT and apoE$^{-/-}$ chow fed groups (Fig 18). This pattern was also observed between apoE$^{-/-}$ HFD and WT mice fed diet for 4 and 8 weeks (Fig 18).
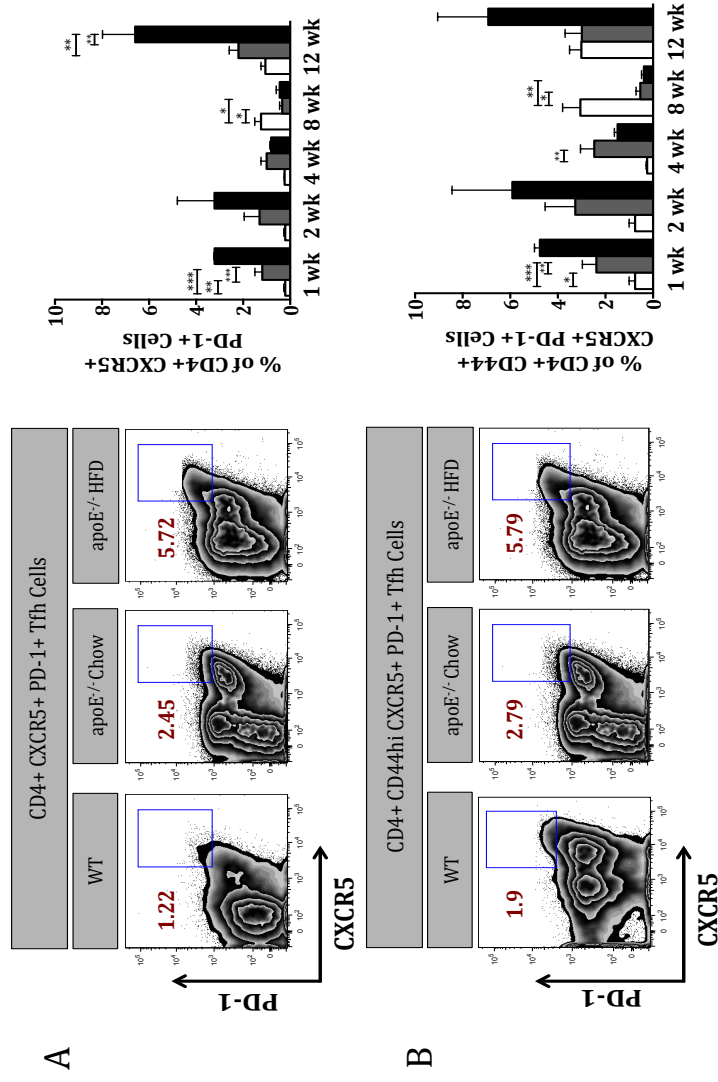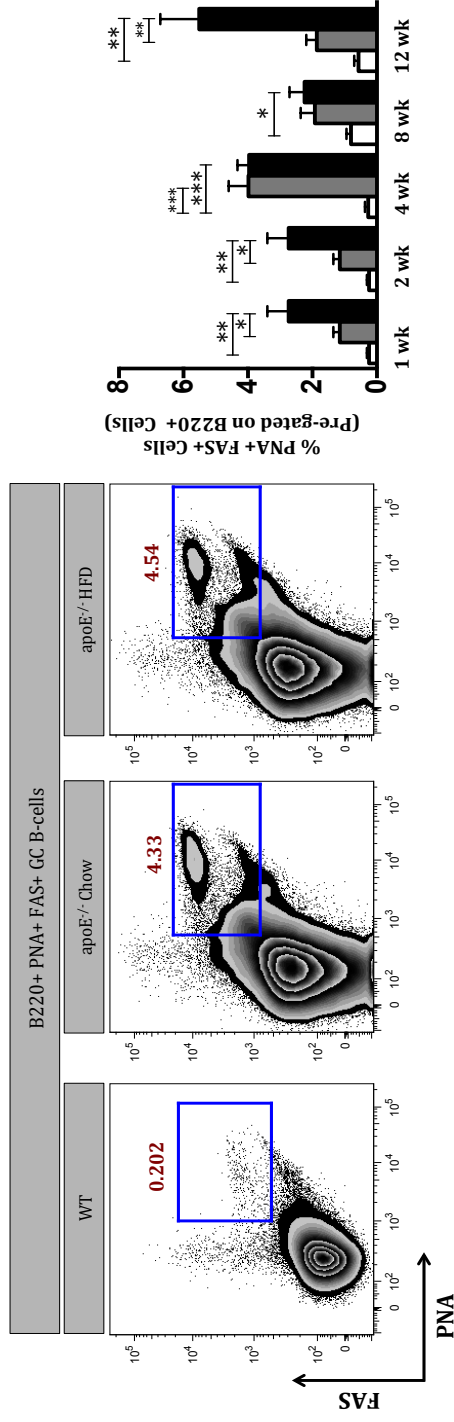
Figure 18: Percentage of B220+ FAS+ PNA+ GC B-cell in spleen of mice following administration of chow or HFD for variable lengths of time

Individual groups of mice were provided with chow (C57BL/6 WT and apoE−/−) or HFD (apoE−/−) for a period of 1, 2, 4, 8 and 12 weeks. Spleens were harvested at each time point and GC B-cell populations assessed via surface flow cytometry staining. Lymphocytes were gated for on the basis of an initial FSC and SSC gate and a subsequent B220+ gate made. Using this parent gate, FAS+ PNA+ cells were gated. Open bars represent C57BL/6 WT mice (n = 5 -6) fed standard laboratory chow diet. Shaded grey and black bars represent apoE−/− mice fed chow (n = 4 - 10) or HFD (n = 5 -10), respectively. Statistical analysis was performed using GraphPad Prism and by conducting a one-way-ANOVA with a post-hoc-tukey's test. * $P < 0.05$, ** $P < 0.01$, *** $P < 0.001$.

1.40.3 Para-aortic Lymph Node GC B-cell Populations Increase in Line with Atherosclerosis Progression

WT mice fed chow diet displayed consistently low percentages of GC B-cells throughout all time points (Fig 19). In contrast to this, both apoE$^{-/-}$ chow and apoE$^{-/-}$ HFD fed mice displayed a significant peak in the percentage of GC B-cells when fed diet for 4 weeks (Fig 19).

In comparing intergroup variation, apoE$^{-/-}$ mice fed HFD at all time points, with the exception of 8 weeks, displayed significantly greater percentages of GC B-cells than WT and apoE$^{-/-}$ mice fed chow diet for the same length of time (Fig 19).
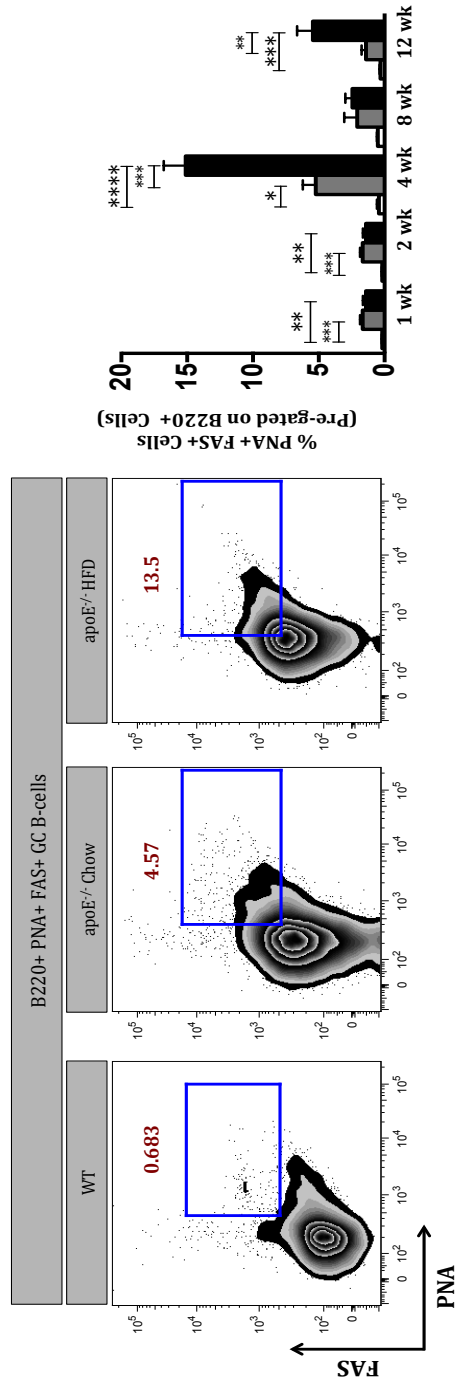
Figure 19: Percentage of B220+ FAS+ PNA+ GC B-cell in pao-LNs of mice following administration of chow or HFD for variable lengths of time

Individual groups of mice were provided with chow (C57BL/6 WT and apoE-/-) or HFD (apoE-/-) for a period of 1, 2, 4, 8 and 12 weeks. Pao-LNs were harvested at each time point and GC B-cell populations assessed via surface flow cytometry staining. Lymphocytes were gated for on the basis of an initial FSC and SSC gate and a subsequent B220+ gate made. Using this parent gate, FAS+ PNA+ cells were gated. Open bars represent C57BL/6 WT mice (n = 4 - 6) fed standard laboratory chow diet. Shaded grey and black bars represent apoE-/- mice fed chow (n = 4 - 6) or HFD (n = 5 -6), respectively. Statistical analysis was performed using GraphPad Prism and by conducting a one-way-ANOVA with a post-hoc-tukey's test. * $P < 0.05$, ** $P < 0.01$, *** $P < 0.001$.

1.40.4 Summary of GC B-cell Kinetics in Experimental Atherosclerosis

In summary, WT mice fed chow diet displayed little variation in the percentage of GC B-cell populations throughout all time points. Interestingly, however, pLN and pao-LNs from apoE$^{-/-}$ mice fed chow or HFD for 4 weeks displayed significantly enhanced GC B-cell populations. Moreover, in comparison to WT controls, apoE$^{-/-}$ chow or HFD fed mice displayed significantly enhanced splenic GC B-cells populations at all time points assessed. Taken together, our data suggests that hyperlipidemia may be a driving force in GC B-cell formation.

1.41 MDA-Ox-LDL antibody Titres

Both Tfh cells and GC B-cells play important roles in the production if isotype switched, high affinity antibodies. Specific for a single antigen, antibodies produced from the Tfh cell : GC B-cell axis are potent in their ability to recognise a specific target then their un-switched counterparts. This process, therefore, holds great importance in the area of disease and immunization. As such, many researchers have assessed the potential of modulating the Tfh cell : GC B-cell axis for better vaccine development.

Of the potential antigens described in atherosclerosis, one has gained extensive attention. Oxidised low-density lipid (Ox-LDL) is a modified form of the native, homeostatic transport molecule LDL. Implicated as an important molecule in the development of atherosclerosis, many have focused on studying its role in lesion formation.

Via exposure to a wealth of oxidising agents in diseased arteries, LDL becomes progressively oxidised and forms Ox-LDL. Attempting to resolve the Ox-LDL overload, resident macrophages engage Ox-LDL via SRs and become overwhelmed. Once overloaded, these macrophages cease to function and form the characteristic hallmark of atherosclerosis – the foam cell.

As a result of the intimate association between Tfh cells, GC B-cells and antibodies, we wished to determine serum antibody titres to the pathogenic molecule Ox-LDL. To obtain modified forms of LDL, native LDL can be incubated with one of two oxidising agents – malondialdehyde or Copper. Exposing oxidised sites, such as phosphorylcholine (PC), oxidation of LDL results in the formation of pathogenic Ox-LDL.

Once modified, prefixed MDA or Cu^{2+} refers to the method of oxidation. As part of our study, Cu^{2+} modified LDL bound variable levels of serum antibodies, and as such were unreliable (data now shown). To address this issue, MDA-Ox-LDL – which yielded more reliable and consistent results – was used throughout.

Using ELISAs, serum anti-MDA-Ox-LDL IgG, IgM, IgG_{2c} and IgG_1 antibody titres were measured.

1.41.1   Determining MDA-Ox-LDL Antigen Coating Concentration

To determine the concentration of MDA-Ox-LDL required for coating microtitre ELISA plates, plates were coated with varying concentrations of MDA-Ox-LDL (6.25, 12.5, 25, 50 and 100 µg/ml). Plates were subsequently incubated with serum from WT and apoE$^{-/-}$ mice fed chow or HFD for 12 weeks. Using HRP conjugated anti-IgM, IgG, IgG_{2C} and IgG_1, respective isotypes were detected. For a detailed description of the ELISA protocol used, please refer to the materials and methods section.

Equivalent detection of anti-MDA-Ox-LDL IgM, IgG, IgG_{2c} and IgG_1 was found across all antigen concentrations in all groups (WT, apoE$^{-/-}$ chow fed and apoE$^{-/-}$ HFD fed) (Fig 20). As a consequence, we used MDA-Ox-LDL at a concentration of 12.5 µg/ml was used for all ELISA coating purposes.
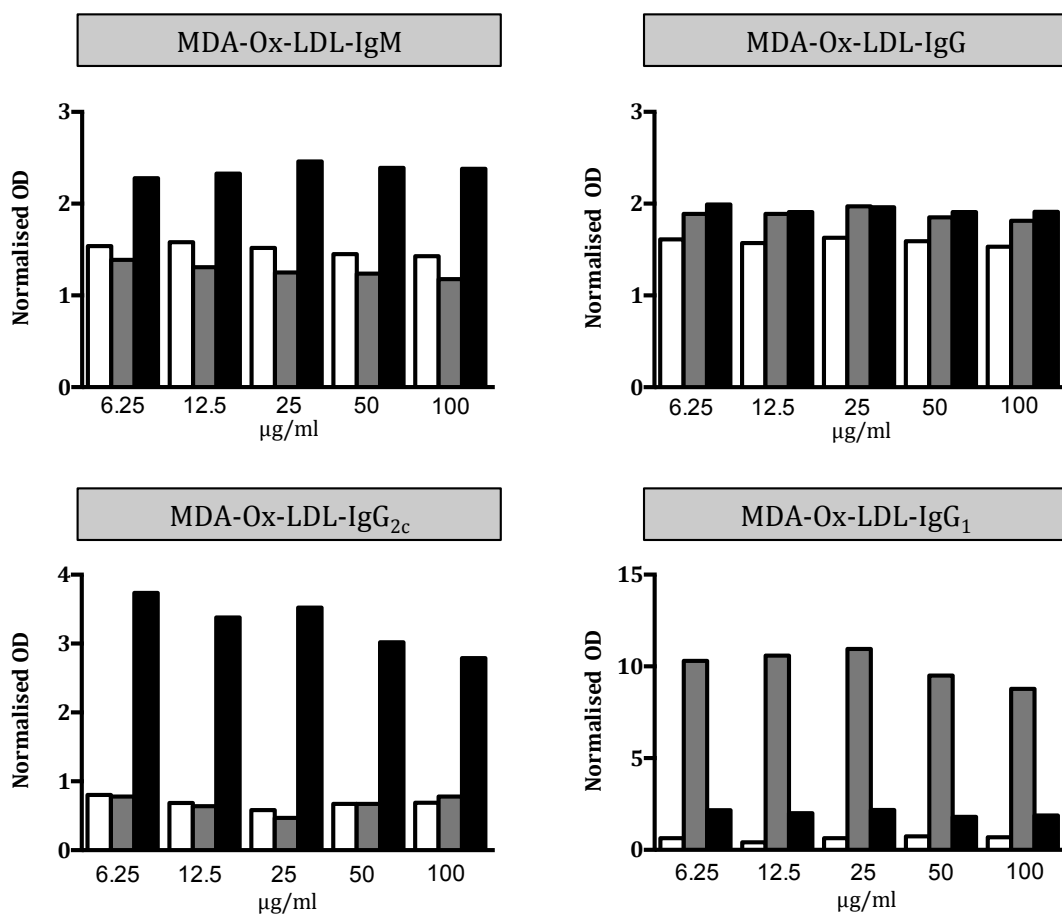
Figure 20: Optimising MDA-Ox-LDL antigen coating concentration

Microtitre plates were coated with varying concentrations of MDA-Ox-LDL (6.25, 12.5, 25, 50 and 100 μg/ml and incubated overnight at 4°C degrees. Serum samples from one C57BL/6 WT and apoE$^{-/-}$ mouse fed chow or HFD for 12 weeks was added and incubated overnight at 4°C degrees. IgM, IgG, IgG$_{2c}$ and IgG$_1$ antibodies isotypes were detected using HRP conjugated antibodies and subsequent incubation with TMB substrate. To account for intra-plate variation in OD readings, all values were normalised by dividing OD values with a fixed reading from C57BL/6 WT serum present on each plate. Graphs represent one animal from the 12 week time point. Open bars represent C57BL/6 WT mice fed chow diet, while shaded grey and black bars represent apoE$^{-/-}$ mice fed chow or HFD respectively.

1.41.2 Anti-MDA-Ox-LDL Serum Antibody Titres Change in Line with GC B-cell Kinetics

Following the increase in GC B-cell formation at 4 weeks, antibody titres to the pathogenic molecule MDA-Ox-LDL were assessed. Using a single point serum dilution of 1:25, anti-MDA-Ox-LDL serum antibody titres to IgM, IgG, IgG_{2c} and IgG_1 were determined.

Remaining consistently stable, no difference in serum MDA-Ox-LDL IgM titres was found between WT and $apoE^{-/-}$ groups at any time point.

Following a similar pattern, no difference in serum MDA-Ox-LDL IgG titres was observed between WT animals at any time point. In comparison, MDA-Ox-LDL IgG titres peaked in $apoE^{-/-}$ mice fed HFD mice for 12 weeks, with this peak being significantly greater than titres observed at earlier time points (4 weeks post-diet) (Fig 21). Although indifferent to levels detected in $apoE^{-/-}$ mice fed chow diet, $apoE^{-/-}$ mice fed HFD at later time points (8 week and 12 week post-diet) displayed significantly enhanced serum MDA-Ox-LDL-IgG titres than their respective WT controls (Fig 21).

Remaining low throughout, no change in basal MDA-Ox-LDL IgG_{2c} titres was observed in WT mice. Although not reaching significance, an increasing trend in MDA-Ox-LDL-IgG_{2c} titres in $apoE^{-/-}$ chow and HFD animals, with titres peaking at 12 weeks post-diet (Fig 21).

WT mice displayed a decreasing trend in MDA-Ox-LDL-IgG1titres (Fig 21). Although following a similar pattern, no change in MDA-Ox-LDL-IgG1 titres in $apoE^{-/-}$ chow or HFD fed mice was detected (Fig 21).
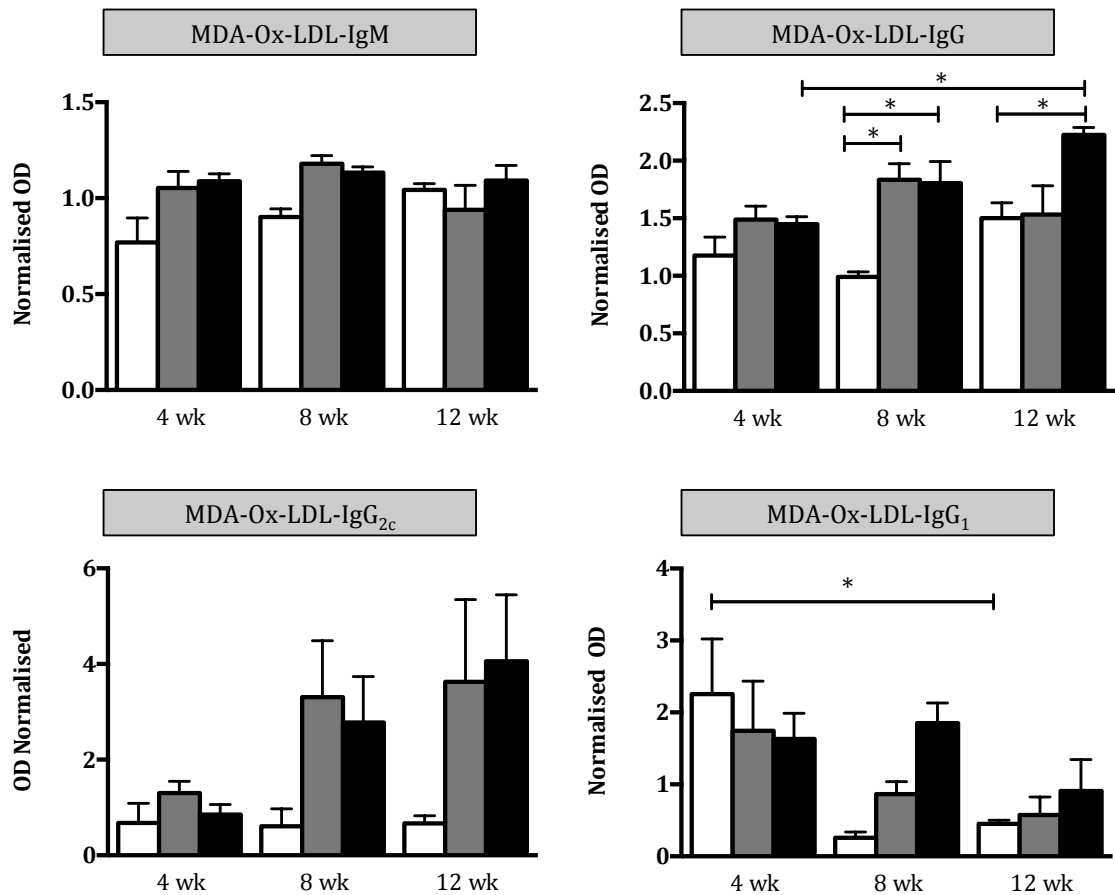
Figure 21: Anti-MDA-Ox-LDL antibodies in serum of mice fed diet for 4, 8 and 12 weeks

Microtitre plates were coated with 12.5 µg/ml MDA-Ox-LDL and incubated overnight for 4°C degrees. Serum samples from mice fed chow (C57BL/6 WT and apoE$^{-/-}$) or HFD (apoE$^{-/-}$) for 4, 8 or 12 weeks were added and incubated overnight at 4°C degrees. IgM, IgG, IgG$_{2c}$ and IgG$_1$ antibody isotypes were detected using HRP conjugated antibodies and subsequent incubation with TMB substrate. To account for intra-plate variation in OD readings, all values were normalised by dividing OD values with fixed an OD reading from C57BL/6 serum present on each plate. Open bars represent C57BL/6 WT mice (n = 5) fed chow diet, while shaded grey and black bars represent apoE$^{-/-}$ mice fed chow (n = 4 -5) or HFD (n = 4 -5), respectively. Statistical analysis was performed using prism graph pad and by conducting a one-way-ANOVA with a post-hoc-tukey's test. * $P < 0.05$, ** $P < 0.01$, *** $P < 0.001$.

1.41.3 Summary of Antibody Titres in Experimental Atherosclerosis

In summary, we have shown that anti-MDA-Ox-LDL serum antibody titres follow a pattern in line with GC B-cell kinetics. Specifically, we found a step wise increase in anti-MDA-Ox-LDL IgG_{2c} titres in the serum of $apoE^{-/-}$ mice fed chow or HFD fed. Coupled with this, we found a decreasing trend in anti-MDA-Ox-LDL serum IgG_1 titres in WT and $apoE^{-/-}$ mice. Interestingly, we found no variation in anti-MDA-Ox-LDL IgM serum titres in all groups.

1.42 Histochemical Analysis of Tfh cell and GC B-cell Populations

1.42.1 Qualitative Assessment of Tfh cell Populations

As well as using flow cytometry based approaches, early studies employed IF to visualise Tfh cell location and marker expression *ex vivo* [44]. Using this approach, early researchers characterised Tfh cells as CD4+ T-cells located within B-cell follicles [44]. With this in mind, we used IF to obtain a qualitative assessment of Tfh cell marker expression and anatomical location in the spleen of mice fed chow or HFD diet for 12 weeks (peak of Tfh cell response).

Using fluorochrome conjugated antibodies, we stained for CD4, B220, and Bcl-6. Using this combination, Tfh cells were defined as CD4+ Bcl-6+ T-cells located in B220+ areas. Taken together, we determined whether Tfh cells observed via flow cytometry were located in the follicle.

1.42.2 Spleen Sections from WT, apoE$^{-/-}$ chow and apoE$^{-/-}$ HFD fed Mice Show Variable Tfh Marker Expression Patterns

Spleen sections from WT mice fed chow diet for 12 weeks showed little CD4+ T-cell infiltration into B220+ areas (Fig 22). Of those CD4+ T-cell detected, none expressed Bcl-6 within their nuclei (Fig 22). In contrast, we found that spleen sections from apoE$^{-/-}$ mice fed chow diet for 12 weeks displayed enhanced CD4+ T-cell infiltration into B220+ areas (Fig 22). Similar to WT mice, these migrating T-cells did not, however, express Bcl-6 (Fig 22).

Interestingly, we found that spleen sections from apoE$^{-/-}$ mice fed HFD displayed enhanced CD4+ T-cell migration into B-cell follicles (Fig 22). Most importantly, migrating T-cells expressed the Tfh cell transcription factor – Bcl-6 – in their nuclei (Fig 22 and Fig 23).
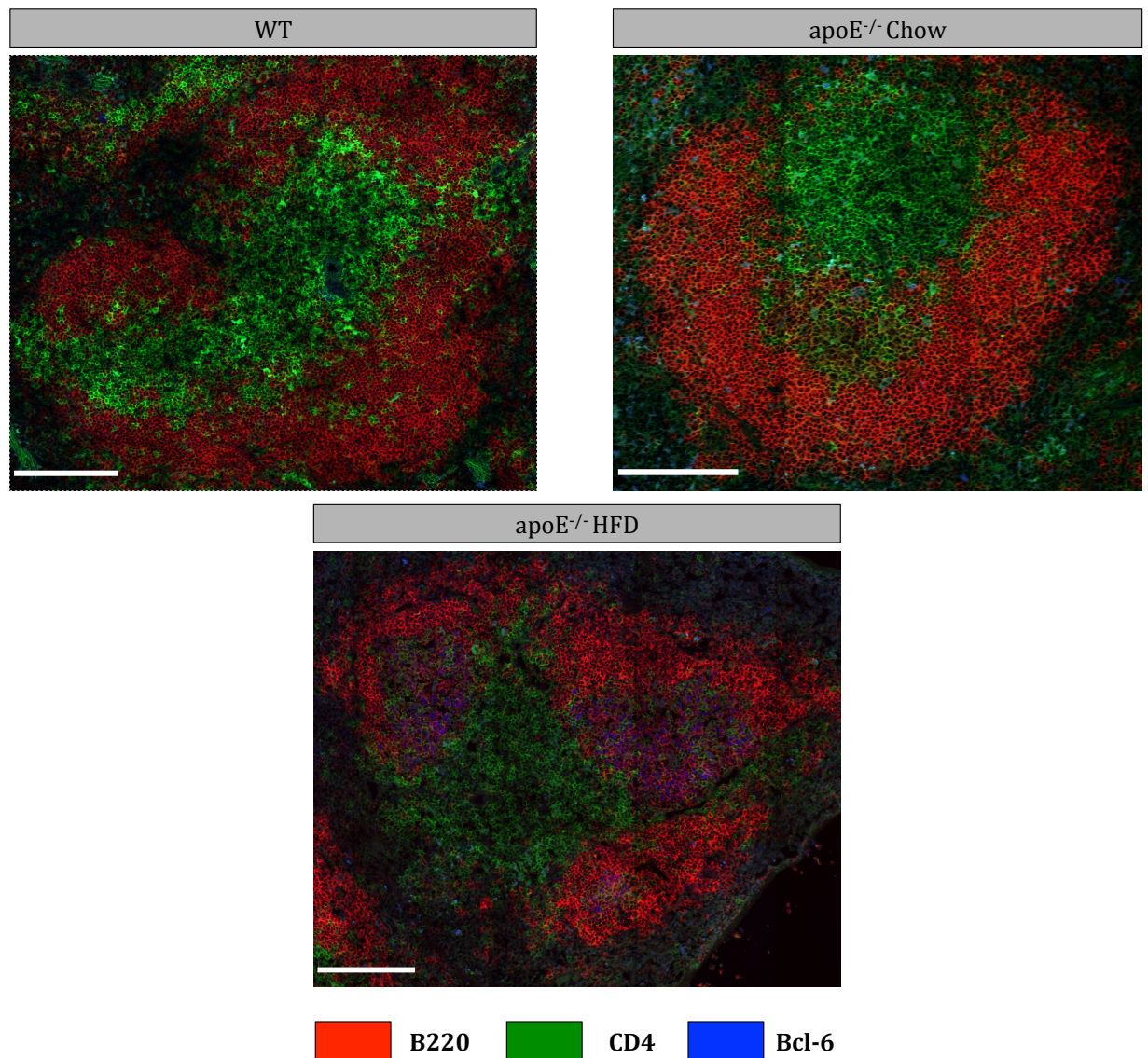
Figure 22: Qualitative analysis of Tfh cell marker expression and anatomical location in spleen of mice fed diet for 12 weeks

8 micron thick sections from mice fed chow (C57BL/6 WT and apoE$^{-/-}$) or HFD (apoE$^{-/-}$) for 12 weeks were assessed for Tfh cell infiltration into B220+ B-cell areas. Tfh cell phenotype was determined by using anti-mouse-CD4 and anti-mouse-Bcl-6. Anatomical location of Tfh cells was determined by the presence of CD4+ Bcl-6+ T-cells in B220+ B-cell areas. Images were acquired using the X40 objective of the LSM-510 meta-confocal microscope. Bar = 150 μm. Final images were analysed using volocity image analysis software.
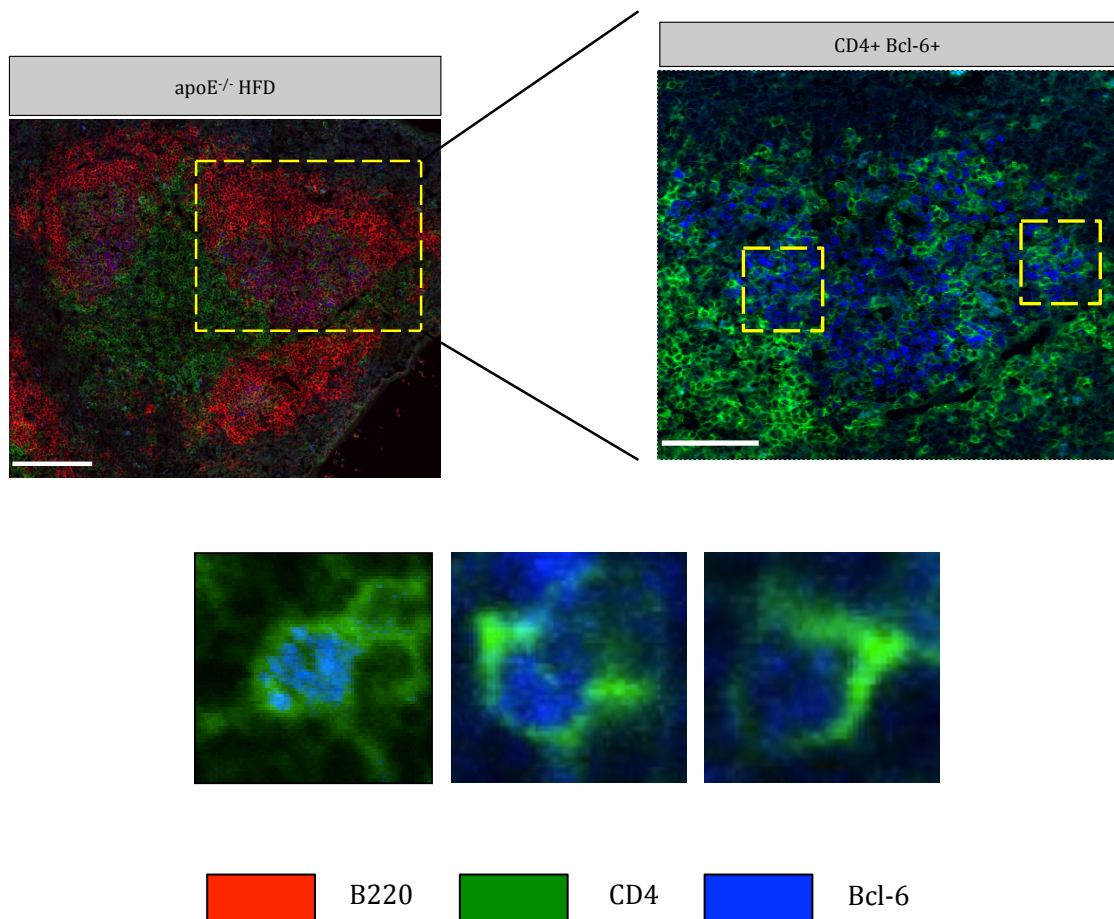
Figure 23: Cellular resolution of Bcl-6 expressing Tfh cells in spleen of apoE$^{-/-}$ mice fed HFD for 12 weeks

Spleen sections from apoE$^{-/-}$ mice fed HFD were assessed for Bcl-6 expression in the nuclei of CD4+ T-cells. Yellow boxes highlight areas containing Bcl-6 expressing CD4+ T-cells located in B220+ areas. Images were acquired using the X40 objective of the LSM-510 meta-confocal microscope. Bars = 150 μm. Right image shows red channel removed to reveal nuclear expression of Bcl-6 in CD4+ T-cells. Bottom panel displays high magnification images (X63) depicting Bcl-6 (blue) expression in nucleus of CD4+ T-cells (green) located in B220+ areas. Final images were analysed using volocity image analysis software.

1.42.3   Quantitative Assessment of GC Formation Via IF

Using a similar approach as described above, we stained spleen sections from mice fed chow or HFD diet for 4 weeks were assessed for GC formation. GCs were defined as PNA+ cells located in B220+ areas. Used as a marker of germinal centre B-cells, PNA binds to high levels of galactosyl residues found on GC B-cells and can therefore be used via flow cytometry and IF to identify GC B-cells [227]. To discriminate B-cell and T-cell areas, the T-cell marker CD4 was included in the staining panel. Using this approach, we determined whether GC size – and thus antibody producing capacity – varied between groups.

1.42.4   ApoE$^{-/-}$ mice fed HFD for 4 weeks Display Larger GCs than C57BL/6 WT Control Mice

Few and small PNA+ GCs were found in the spleens of WT mice fed chow diet for 4 weeks (Fig 24A). Although increasing in size, no significant difference in GC size between WT and apoE$^{-/-}$ mice fed chow diet for the same length of time was found (Fig 24A and 24B). Interestingly, apoE$^{-/-}$ mice fed HFD for 4 weeks displayed significantly larger GCs than C57BL/6 WT mice (Fig 24A and 24B). This increase was, however, not different from that observed in apoE$^{-/-}$ mice fed chow diet for the same length of time (Fig 24A and 24B).

A
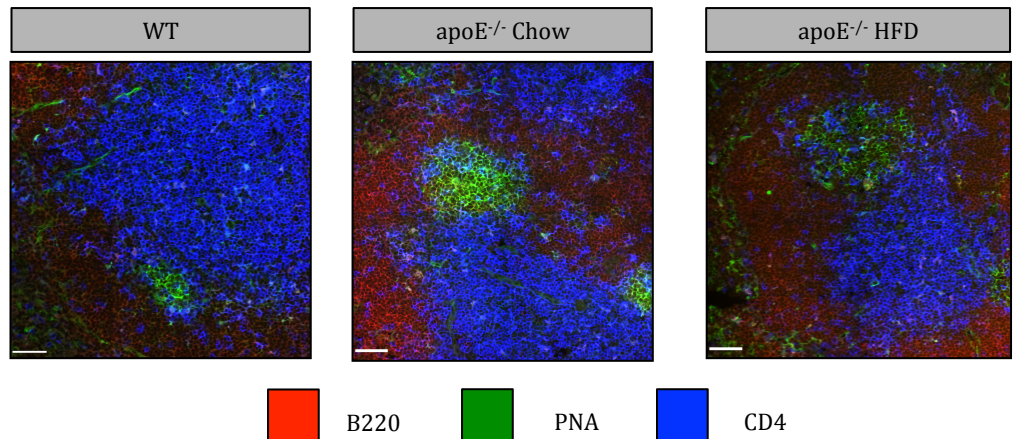
B
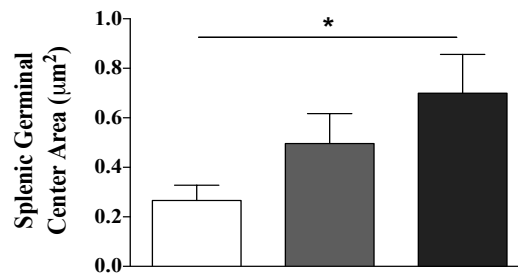
Figure 24: Quantitative analysis of GCs in spleen sections from mice fed chow or HFD diet for 4 weeks

Eight micron thick sections from mice fed chow (C57BL/6 WT and apoE$^{-/-}$) or HFD (apoE$^{-/-}$) for 4 weeks were assessed for GC formation. GCs were determined via IF by using fluorochrome conjugated PNA and anti-mouse-CD4 and B220 antibodies **(A)**. Images were acquired using the X40 objective of the LSM-510 meta-confocal microscope and final images were analysed using volocity image analysis software. Bars = 150 μm. Graph represents analysis of spleen area containing PNA+ GCs **(B)**. Statistical analysis was performed using GraphPad Prism and by conducting an unpaired student's t-test. * $P < 0.05$, ** $P < 0.01$, *** $P < 0.001$.

1.42.5 Summary of Tfh cell and GC B-cell Profiles Assessed via IF

In summary, we have shown that Tfh cells from WT and apoE$^{-/-}$ mice (chow and HFD fed) display the ability to translocate to B-cell rich areas in the spleen of mice. Interestingly, although all groups display this ability, only apoE$^{-/-}$ mice fed HFD display up-regulation of the Tfh cell transcription factor – Bcl-6. As such, our data supports the notion that hyperlipidemia may drive bonafide Tfh cell marker expression *in vivo*.

In addition to this, we have demonstrated that apoE$^{-/-}$ mice fed HFD display significantly larger GCs than WT mice. As such, our data suggests that apoE$^{-/-}$ mice fed HFD may display enhanced capacity for antibody production *in vivo*.

1.43 Discussion

1.43.1 Summary of Aims and Objectives

As part of this chapter, we aimed to assess whether Tfh cell and GC B-cell numbers changed in line with atherosclerosis formation in hyperlipidemic apoE$^{-/-}$ mice. We also determined whether variations in Tfh cell and GC B-cell populations had an impact on the production of high affinity, isotype switched antibodies. Using IF, we studied whether GC size varied between groups and if Tfh cells were distinguishable via marker expression and anatomical location.

1.43.2 Summary of Findings - Tfh cell, GC B-cell and Antibody Titres Increase in Line with Hyperlipidemia and Atherosclerosis Severity

Using surface flow cytometry staining we found that apoE$^{-/-}$ mice HFD for extended periods of time (12 weeks) displayed significantly enhanced Tfh cell populations in all organs assessed (pLNs, spleen and pao-LNs). Confirming an effect due to hyperlipidemia - and not age - we found little variation in Tfh cell percentages – in all compartments – in WT and apoE$^{-/-}$ mice fed chow diet at all time points.

Interestingly, the percentage of GC B-cells in apoE$^{-/-}$ chow and apoE$^{-/-}$ HFD fed mice peaked at 4 weeks post-diet, in all organs assessed. Again, indicative of the effects of hyperlipidemia and disease progression, few GC B-cells were detectable in the organs of WT mice fed chow diet at all time points.

Linking both Tfh cell and GC B-cell kinetics, we found that apoE$^{-/-}$ chow and apoE$^{-/-}$ HFD fed mice displayed an increasing trend in anti-MDA-Ox-LDL IgG$_{2C}$ serum titres, peaking at the 12-week time point.

Using IF, we found that apoE$^{-/-}$ mice fed HFD displayed significantly larger GCs than WT and apoE$^{-/-}$ mice fed chow diet. Along with their location in B-cell areas, apoE$^{-/-}$ mice fed HFD comprised the sole group that expressed bonafide Tfh cell markers (CD4+ and Bcl-6).

Taken together, we have provided evidence that indicates that Tfh cells and GC B-cells follow a pattern in line with atherosclerosis progression. Moreover, we have demonstrated that severe hyperlipidemia functions as an important cue in the induction of Tfh cell and antibody responses. As well as this, we have shown that hyperlipidemia is required for the optimal expression of Bcl-6 in bonafide Tfh cells.

1.43.3   T-follicular Helper Cells Represent a Significant Population in other Autoimmune Conditions

Supporting the pro-inflammatory nature of atherosclerosis, hyperlipidemia is linked to the expansion of various inflammatory immune cell subsets, including CD4+ T-cells, B-cells, macrophages and neutrophils [228-230].   Adding to this, we have demonstrated that Tfh cell and GC B-cells also increase in line with hyperlipidemia.

As such, we hypothesise that hyperlipidemia comprises an important driving force in the development of Tfh cells and GC B-cells in experimental atherosclerosis and that the Tfh cell / GC B-cell axis – via antibody production - may be important in the development of experimental atherosclerosis.

In line with our findings, others investigating the role of the Tfh cell / GC B-cell axis in autoimmunity have reported similar results to ours. In particular, elevated numbers of Tfh cells can be identified in the blood of both rheumatoid arthritis and systemic lupus erythematosus sufferers [165, 231]. Interestingly, Tfh cells have been identified in the inflamed joints in patients with RA [232]. Moreover, both RA and SLE sufferers show significantly elevated blood concentrations of the Tfh cell cytokine - IL-21; a finding that correlates with disease severity and antibody load [233]. Underlining the role of Tfh cells in autoimmunity, patients treated with the anti-arthritic drugs, methotrexate or methotrexate and sulfasalazine, display reduced serum IL-21 concentrations along with reduced disease severity [233].

Importantly, we have demonstrated that Tfh cell kinetics also follow a pattern in line with atherosclerosis progression. It is therefore plausible that Tfh cells may be important role in modulating the atherogenic immune response in atherosclerosis. As

such, Tfh cells may hold potential as therapeutic targets for the modulation of atherosclerosis formation *in vivo.*

1.43.4 T-follicular Helper Cell Expression in Atherosclerosis is Consistent with that from Published Studies

Much of what researchers know with regards to Tfh cell kinetics has been gained from studies using infection models [214, 221, 222, 234-237]. Given this, using published marker combinations, we have demonstrated that Tfh cell profiles found in our studies share similarities with those reported in such studies. In particular, Bcl-6 – the implicated transcription factor of Tfh cells – is required for the up-regulation of various Tfh cell molecules and as such is important to Tfh cell function [221]. We detected Bcl-6 expression solely in the spleen of apoE$^{-/-}$ mice with severe hyperlipidemia (12 week HFD), thus suggesting the need for hyperlipidemia for the induction of Tfh transcripts.

Used as a common method to induce Tfh cell formation, immunization induces profuse Tfh cell differentiation in an antigen dependent manner. Importantly, as part of our study we used no infection or immunization to induce Tfh cell formation. Our sole atherogenic stimulus was HFD fed to mice *ad libitum,* leading to increased levels of circulating antigens (such as Ox-LDL) overtime [238]. The finding that natural pathological progression is sufficient to drive Tfh cell differentiation indicates a potential involvement of Tfh cells in atherosclerosis formation and development. As such, the mechanisms by which Tfh cells may modulate atherosclerosis merit significant attention.

1.43.5 T-follicular Helper Cells Regulate the Germinal Centre Reaction and Antibody Production *in vivo*

We propose that Tfh cells represent an important subset that regulates pro-atherogenic antibody responses *in vivo*. We, therefore, hypothesise that Tfh cells and GC B-cells from HFD fed apoE$^{-/-}$ mice expand in response to cognate antigen (oxidised LDL), resulting in elevated pro-atherogenic serum antibody titres.

Supporting our findings, anti-Ox-LDL IgG$_{2c}$ antibodies have been suggested as important mediators in the pro-atherogenic immune response [120]. Moreover, depletion of B2 cells, responsible for IgG production, significantly attenuates atherosclerosis formation *in vivo* [120, 239, 240]. Interestingly, and of importance to Tfh cell kinetics, loss of B2 cells also significant reduces CD4+ T-cell proliferation and differentiation [240]. However the role of Tfh cells in this context has not been addressed.

In our hands, we found that anti-MDA-Ox-LDL IgG$_{2c}$ antibodies peak at advanced stages of atherosclerosis, concomitantly when CXCR5+ PD-1hi Bcl-6+ Tfh cell populations peak. It is therefore plausible that following elevated serum hyperlipidemia, bonafide CXCR5+ Bcl-6+ Tfh cells facilitate the production of enhanced anti-Ox-LDL IgG$_{2c}$ antibodies. Comprising a functional outcome of the GC reaction, these Ox-LDL specific IgG$_{2c}$ antibodies function to enhance atherosclerosis progression.

Further supporting the role of Tfh cells in atherosclerosis, CXCL13 - the ligand for membrane bound CXCR5 – is highly expressed in aortic tertiary lymphoid organs (ATLO) of aged atherosclerotic mice, as well as in human plaques [45, 241]. Specifically, loss of CXCL13 - CXCR5 interactions attenuates atherosclerosis formation in LDLR$^{-/-}$ mice, although the contributing role of Tfh cells to this finding has not been addressed. Confirming our findings, recent published data has reported findings correlating with those described in chapter 2. Specifically, Clement et al reported an increasing trend in Tfh cell kinetics, in line with pathology in an animal model of atherosclerosis. Indicating a potential role of Tfh cells in regulating antibody responses, the role of Tfh cells in atherosclerosis merits significant attention.

1.43.6   Summary of Findings

- Tfh cell expression follows a pattern in line with the development of advanced atherosclerosis
- Hyperlipidemia functions to drive bonafide Tfh cell formation
- GC B-cell expression increases in line with atherosclerosis formation
- Antibody titres to MDA-Ox-LDL follow Tfh cell and GC B-cell kinetics

1.43.7   Concluding Remarks

In combination, we have provided data to support the significant involvement of Tfh cells in atherosclerosis. We have demonstrated that hyperlipidemia functions as a driving force for the formation of such cells and their actions may be important in regulating pro-atherogenic antibody responses *in vivo*.

To report with certainty that Tfh cells are important in atherosclerosis, one must modulate their function *in vivo*. To address this issue, chapter 5 describes the development of a chimeric mouse, in which Tfh cell development is impaired by ablation of IL-21R in hyperlipidemic LDLR$^{-/-}$ mice.

Chapter 4: Elucidating the Role of Apolipoprotein-E in Adaptive Immunity

1.44 Introduction

1.44.1 Apolipoproteins – Multifunctional Proteins Involved in Lipid Metabolism

Apolipoproteins (apo) represent a class of proteins involved in lipoprotein transport, lipid clearance and enzyme activation [19, 242]. Synthesised in the liver and intestines, apolipoproteins are important to the homeostatic balance of plasma lipoproteins *in vivo* [242]. Embedded in the surface of lipoprotein molecules - composed of triglycerides, cholesterol esters, and phospholipids - apolipoproteins are fundamental to the movement of otherwise immiscible lipid molecules [19]. As a class of proteins, apolipoproteins are subdivided into 9 different subclasses, all with varying functions in lipid transport and metabolism. Designated, apoA(I-IV), apoB100, apoB48, apoC(I-III), apoD, apoE(I-IV), apoF, apoG and apoH, these isoforms are comprised at varying degrees in different lipoproteins [243]. To date, several factors have been implicated in the dynamic regulation of plasma apolipoproteins, including race, sex and genetic predisposition [243].

As part of this introduction, the role of apolipoproteins will be discussed. Particular focus will be given to apoE and its role in pathology and immunity, as well as its emerging roles in other conditions.

The aim of the current chapter was to investigate whether elevated Tfh cell and GC B-cell populations observed in apoE$^{-/-}$ HFD fed mice (chapter 2) was the result of disease progression or the effects of apoE ablation.

1.44.2 Apolipoproteins and Their Multifunctional Role in Lipoprotein Homeostasis

Apolipoproteins are intimately associated with spherical structures termed lipoproteins [19]. Composed of apolipoproteins, triglycerides, cholesterol and phospholipids, plasma lipoproteins can be classified into 6 broad groups based on their physical properties when separated via ultracentrifugation [19]. Classed as, chylomicrons (CM), VLDL, IDL, LDL and HDL, lipoproteins are highly dynamic and in many cases readily convert from one form to the other [19].

In testament to the dynamic regulation of lipoproteins and the multi-functional role of apolipoproteins, VLDL is converted to LDL via the enzyme activating properties of apoCI and apoCII. Specifically, apoCII activates lipoprotein lipase - an enzyme involved in triglyceride hydrolysis - thus yielding free fatty acids for use in energy metabolism [19, 244]. Alongside this, apoCI induces lecithin cholesterol acyltransferase (LCAT) activation, resulting in enhanced cholesterol ester formation from free cholesterol [242, 245]. As a consequence, VLDL molecules transform into LDL molecules via transitional ILDL molecules. The smallest of all lipoproteins, HDL particles measure from 120 - 70Å in diameter [19]. Unlike chylomicrons, VLDL, IDL and LDL, which transport triglycerides and cholesterol to tissues for use in cellular processes, HDL particles remove excess cholesterol from tissues for excretion in the bile [246]. Surface embedded apolipoproteins are fundamental to HDL functions. Of particular importance to HDL, apoA1 proteins facilitate a process termed reverse cholesterol transport, in which cholesterol is removed from peripheral tissues and transported to the liver [246].

1.44.3   Apolipoprotein-E – Function in Health and Disease

ApoE has gained significant attention in modulating plasma lipid levels and subsequent plaque formation [247]. As such, this section will discuss the role of apoE in modulating disease and the immune response.

ApoE is an arginine rich apolipoprotein that forms an integral component of many plasma lipoproteins [248]. Three apoE isoforms have been characterised, termed apoE2 (E2), apoE3 (E3), and apoE4 (E4) [249], all with varying affinity for LDLRs and receptors located on chylomicron remnants. Interestingly, unlike other apolipoproteins, apoE is produced widely throughout the body. Specific areas of production include, the brain, spleen, kidneys, smooth muscle cells and ovaries [250]. Due to its affinity for LDLRs in the liver, apoE plays an important role in endocytosis-mediated metabolism of LDL and chylomicron remnants in the liver [251].

Due to its fundamental role in the lipid metabolism, apoE has been linked to the progression of CVD and in particular atherosclerosis. Individuals with the hereditary condition familial dysbetalipoproteinemia - in which apoE2 synthesis is defective - display defective lipid clearance and enhanced atherosclerosis formation [252, 253]. Highlighting the role of apoE in lipid regulation, selective knock-out of apoE protein in rodents has formed the basis of the apoE knock out mouse model of atherosclerosis [254, 255]. ApoE$^{-/-}$ mice display elevated plasma cholesterol levels compared to wild type C57BL/6 mice [59]. Due to the absence of functional apoE proteins – and hence apoE mediated cholesterol clearance - cholesterol remnants accumulate in the circulation of apoE$^{-/-}$ mice. As a result, apoE$^{-/-}$ mice develop widespread atherosclerotic lesions, with many aspects of human disease, including inflammatory cell involvement [256]. As such, the apoE$^{-/-}$ mouse model has become the gold standard animal model of atherosclerosis. In particular, and relevant to this thesis, apoE$^{-/-}$ mice have been used to characterise the pro-atherogenic role of various immune cells, including T-cells, B-cells, and dendritic cells [81, 120, 156, 257, 258].

Interestingly, independent of its role in atherosclerosis, apoE has been implicated in the development of neurological conditions, specifically Alzheimer's disease (AD) [259]. Particularly, the E4 isoform is a recognised major risk factor for the development of AD [260]. Recent data have indicated that E4 functions to accelerate the formation of pathological alpha-beta amyloid structures in the brain [261]. Intriguingly, unlike E4, E2 and E3 are believed to convey neuro-protective functions [261]. Loss of E2 receptors of very low density lipoprotein receptors (VLDLr) is believed to impair the function of Reelin – a neuroprotective protein involved in neuron plasticity [262].

1.44.4   Apolipoprotein-E (apoE) – Roles in Immunity

Independent of its role in lipid homeostasis and neurobiology, apoE has been implicated as a modulator of peripheral inflammation. Interestingly, apoE$^{-/-}$ mice show increased susceptibility to a range of bacterial infections that readily develop into sepsis [263-265]. Underlining a role of apoE in inflammation, apoE has been shown to bind lipopolysaccharide (LPS) from gram-negative bacteria and re-direct it to the liver for excretion in bile [266]. Due to the absence of this process in apoE$^{-/-}$ mice, systemic LPS levels increase, resulting in cellular activation and secretion of pro-inflammatory cytokines. Although all lipoprotein classes are capable of binding endotoxin products [267-272], an approximate 8-fold increase in VLDL levels in apoE$^{-/-}$ mice is insufficient to protect against sepsis, thus reinforcing the importance of apoE in LPS removal.

Using *in vitro* approaches, early researchers identified apoE's particular ability to control lymphocyte expansion, cytolytic T-cell formation and neutrophil activation [273-277]. Reinforcing the role of apoE to these processes, other apolipoproteins failed to modulate lymphocyte activity [275]. In context of T-cell immunity, apoE has been reported to inhibit CD4+ and CD8+ T-cell proliferation *in vitro* [274, 275]. Providing a plausible explanation for these findings, some have suggested that apoE restricts the availability of bioactive IL-2 and IL-2R [274, 275]. As well as affecting IL-2 mediated pathways, apoE has been shown to significantly inhibit also IL-4 induced proliferation of lymphocytes [274]. Suggesting the involvement of a non-specific pathway, apoE has been shown to inhibit IL-2 / IL-4 induced proliferation by preventing G1 cell cycle processes [274].

Taken together, these studies highlight the pleotropic actions of apoE. As such, they reinforce the notion that apoE is important in controlling several aspects of peripheral inflammation.

Interestingly, some have provided evidence indicating the potential role of apoE in regulating T-cell and APC interactions [278]. Specifically, in comparison to WT cells, macrophages from apoE$^{-/-}$ mice injected i.p. with IFN-ɣ show enhanced ability to up-regulate CD40, CD80 and MHC-II [278]. Important for the initial priming of T-cells,

these molecules provide co-stimulation and TCR stimulation of T-cells. Due to the enhanced expression of such markers in the absence of apoE, researchers indicate that apoE may function to regulate initial T-cell – APC interactions *in vivo* [278].

Macrophages represent a major cell type involved in apoE protein synthesis. Of specific importance to atherosclerosis, arterial macrophages and foam cells express copious amounts of apoE [279]. Underlining the role of apoE in macrophage function and atherogenesis, loss of apoE expression in macrophages significantly enhances lesion formation [279]. Conversely, enhanced expression of macrophage apoE reduces many aspects of the pro-atherogenic immune response [247]. Adding further to this, others have shown the ability of apoE to induce an anti-inflammatory M2 phenotype over an M1 pro-inflammatory phenotype [280]. Translated *in vivo*, apoE$^{-/-}$ mice transplanted with apoE$^{+/+}$ bone marrow display a significant increase in the number of peritoneal M2 macrophages [280]. Underlining the protective role of apoE in atherosclerosis, apoE expression in LDLR$^{-/-}$ has been linked to enhanced apoA1+ HDL expression, reduced adhesion molecule expression and reduced monocyte lipid content [247].

Taken together, the studies described above provide strong evidence for the role of apoE in regulating various aspects of both adaptive and innate immunity. Of relevance to this thesis, they also provide evidence that modulation of such processes may affect disease progression.

As part of chapter 3, we used the apoE$^{-/-}$ mouse model to study Tfh cell, GC B-cell and antibody kinetics in context of hyperlipidemia. As discussed above, loss of functional apoE protein can affect immune cell function and subsequent pathological involvement. Therefore, to determine whether loss of apoE protein affected adaptive immunity, we assessed cell populations in C57BL/6 WT and apoE$^{-/-}$ mice immunized sub cutaneous (s.c.) with OVA emulsified in CFA and flow cytometry of dLNs conducted 9 days later.

1.44.5 Aims

1. Determine whether immunized C57BL/6 WT and apoE$^{-/-}$ mice displayed variable CD4+ T-cell and B220+ B-cell populations;

2. Assess whether CD4+ T-cell activation (CD44) varied between immunised groups;

3. Study if apoE deficiency affected CXCR5 expression on CD4+ and CD4+ CD44hi T-cells;

4. Determine whether loss of apoE affected Tfh cell and GC B-cell formation.

1.45 Results

In chapter 2 we used the apoE$^{-/-}$ mouse model to study Tfh cell, GC B-cell and antibody kinetics in context of hyperlipidemia. Using this approach, we found that Tfh cell, GC B-cell and antibody kinetics followed a pattern in line with atherosclerosis progression. As such, we attributed a potential role of the Tfh cell : GC B-cell axis in atherosclerosis.

Independent of its role in atherosclerosis, some have suggested that loss of apoE may significantly affect the immune response [247, 249, 274, 275, 277, 278, 280, 281]. To ensure the results obtained in chapter 2 were a result of disease progression, and not a consequence of apoE deficiency, we characterised T-cell and B-cell populations in C57BL/6 WT and apoE$^{-/-}$ mice immunized with OVA in CFA. Used commonly throughout the literature as a means of inducing a thymus dependent T-cell response, OVA / CFA injection induces enhanced T-cell proliferation in an antigen specific manner [235, 237, 282]. As such, we were able to characterise the differences in adaptive immune responses between C57BL/6 WT and apoE$^{-/-}$ mice.

As part of this chapter, we phenotyped various cell types in the draining lymph nodes of immunized C57BL/6 WT and apoE$^{-/-}$ mice. As this thesis is focused on the Tfh cell : GC B-cell axis, particular attention was given to the phenotyping Tfh cells and GC B-cells. Table 2 below summarises the populations assessed via flow cytometry.

Cell Population Phenotyped	Marker Combination
T-cells	CD4+
B-cells	B220+
Activated T-cells	CD4+ CD44hi
Tfh cells	CD4+ CXCR5+ ICOS+ CD4+ CXCR5+ PD-1+ CD4+ CXCR5+ Bcl-6+ CD4+ CD44hi CXCR5+ ICOS+ CD4+ CD44hi CXCR5+ PD-1+ CD4+ CD44hi CXCR5+ Bcl-6+
GC cells	B220+ PNA+ FAS+

Table 2: Adaptive Immune Cells Characterised in C57BL/6 WT and apoE$^{-/-}$ Immunized s.c. with OVA / CFA

Using flow cytometry staining, adaptive immune cells were phenotyped in the draining lymph nodes of C57BL/6 WT and apoE$^{-/-}$ mice immunized s.c. with 100 µg OVA emulsified in 100 µl CFA.

1.46 Effects of apoE deficiency on Adaptive Immune Cells

1.46.1 Apolipoprotein-E Deficiency does not Affect CD4+ T-cell and B220+ B-cell Responses *in vivo*

As part chapter 2, variations in the expression of Tfh cells and GC B-cells between C57BL/6 WT and apoE$^{-/-}$ mice fed diet for varying lengths of time was assessed. To phenotype these cells, Tfh cells were first gated for on a CD4+ pre-gate and GC B-cells were gated for on a B220+ pre-gate. To determine whether loss of apoE significantly altered the expression of CD4+ and B220+ cells, flow cytometry was used to stain for CD4+ T-cells and B220+ B-cells in the draining lymph nodes of mice immunized with OVA / CFA.

No difference in the percentage of B220+ B-cells between C57BL/6 WT and apoE$^{-/-}$ mice (25.02 % - vs - 27.60 %) immunized s.c. with OVA / CFA (Fig 25) was found. Coupled with this, little variation in the percentage of CD4+ T-cells between immunized C57BL/6 WT and apoE$^{-/-}$ mice (29.16 % - vs – 26.28 %) was found (Fig 25).
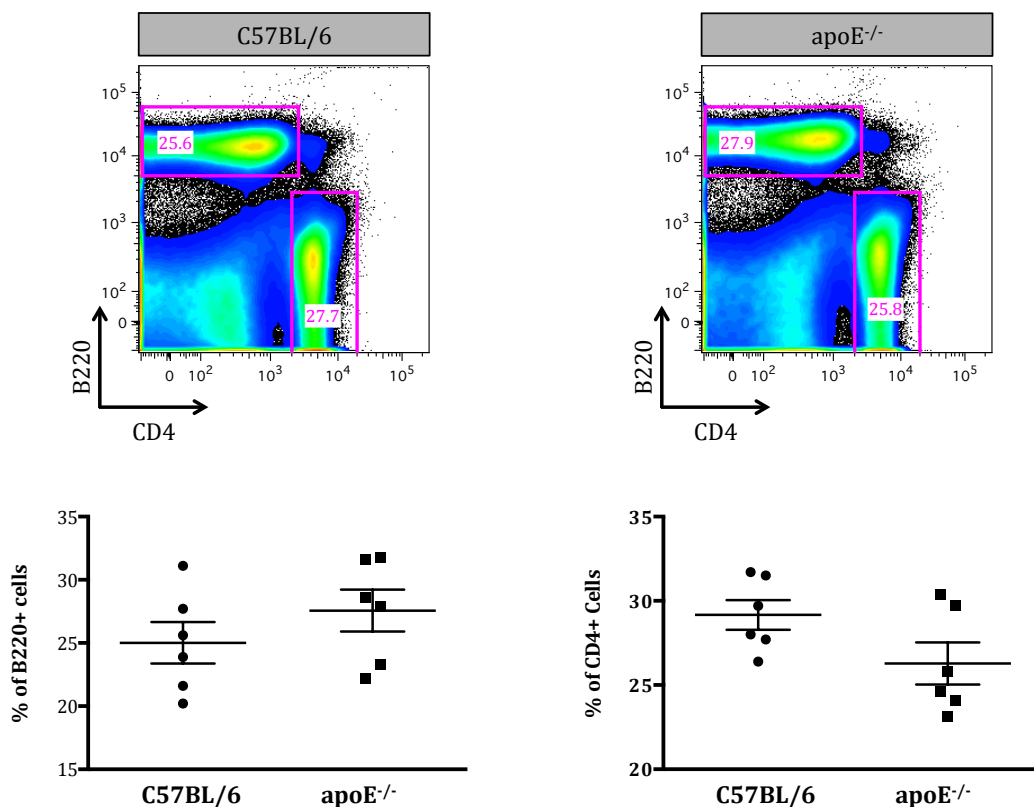
Figure 25: Flow cytometry analysis of B220+ B-cell and CD4+ T-cell populations in the draining lymph nodes of C57BL/6 WT and apoE$^{-/-}$ mice immunized S.C. with OVA / CFA

Two groups of mice [C57BL/6 WT (n = 6) and apoE$^{-/-}$ (n =6)] were immunized s.c. with 100 μg of OVA emulsified in 100 μl of CFA. Nine days after immunization, dLNs (axillary and brachial) were dissected and prepared for surface flow cytometry staining. Lymphocytes were gated for on the basis of FSC and SSC. Using these gates, CD4+ T-cell and B220+ B-cell expression was assessed. Statistical analysis was performed using GraphPad Prism and an unpaired students t-test. * P < 0.05, ** P < 0.01, *** P < 0.001.

1.46.2 Apolipoprotein-E Deficiency Significantly Enhances CD4+ CD44hi T-cell Responses *in vivo*

As well as using CD4 to pre-gate Tfh cells, a CD4+ CD44hi pre-gate was also included (gating strategy 2) (see chapter 3). Therefore, as part of chapter 4, the effect of apoE deficiency on CD4+ CD44hi T-cell expression in C57BL/6 WT and apoE$^{-/-}$ mice was also determined. In comparison to C57BL/6 WT mice, apoE$^{-/-}$ mice displayed a significant increase in the percentage of CD4+ CD44hi cells in the brachial and axillary lymph nodes 9 days after immunization (16.13 % - vs - 18.92%) (Fig 26).

Figure 26: Flow cytometry analysis of CD4+ CD44hi T-cell populations in the draining lymph nodes of C57BL/6 WT and apoE$^{-/-}$ mice immunized s.c. with OVA / CFA

Two groups of mice [C57BL/6 WT (n = 6) and apoE$^{-/-}$ (n =6)] were immunized s.c. with 100 μg of OVA emulsified in 100 μl of CFA. 9 days after immunization, dLNs (axillary and brachial) were dissected and prepared for surface flow cytometry staining. Lymphocytes were gated for on the basis of FSC and SSC parameters. Using these gates, CD4+ T-cells were selected, upon which CD44hi expression was assessed. Statistical analysis was performed using GraphPad Prism and an unpaired students t-test. * $P < 0.05$, ** $P < 0.01$, *** $P < 0.001$.

1.46.3 Summary of the Effects of Apolipoprotein-E Deficiency on CD4+ T-cell, B220+ B-cell and CD4+ CD44hi Populations

Taken together, our data indicates that apoE deficiency does not affect the percentage of CD4+ T-cells and B220+ B-cells *in vivo*. In comparison to this, our data also suggests that apoE deficiency results in the enhanced ability to up-regulate CD44 on CD4+ T-cells while supressing GC B-cell expression.

1.47 Effects of apoE Deficiency on Tfh Cell Populations

1.47.1 Apolipoprotein-E Deficiency Does not Affect CD4+ CXCR5+ ICOS+, CD4+ CXCR5+ PD-1+ or CD4+ CXCR5+ Bcl-6+ Tfh Cell Populations *in vivo*

In chapter 2, we studied Tfh cell kinetics in apoE$^{-/-}$ mice with varying degrees of hyperlipidemia. As such, we determined whether Tfh cell kinetics followed a pattern in line with atherosclerosis progression. In this chapter, we aimed to determine whether loss of apoE affected Tfh cell populations *in vivo* and as such could provide a plausible explanation of the findings in chapter 2. To do this, we phenotyped Tfh cell populations in the dLNs of immunized C57BL/6 WT and apoE$^{-/-}$ mice.

We phenotyped Tfh cells as follows:

1. CD4+ CXCR5+ ICOS+ Cells [206]
2. CD4+ CXCR5+ PD-1+ Cells [214, 222, 237]
3. CD4+ CXCR5+ Bcl-6+ Cells [214, 222]

As well as phenotyping Tfh cells using a CD4+ pre-gate, we also included the glycoprotein CD44 in our analysis. As a result of this, we were able to profile Tfh cells in the manner in which they were phenotyped in chapter 2.

Phenotyping Tfh cells in this manner, we determined Tfh cells as,

1. CD4+ CD44hi CXCR5+ ICOS+ Cells
2. CD4+ CD44hi CXCR5+ PD-1+ Cells [222, 283]
3. CD4+ CD44hi CXCR5+ Bcl-6+ Cells [222, 237]

Using this approach, no difference in the expression of CD4+ CXCR5+ ICOS+ (3.64 % - vs - 4.65 %), CD4+ CXCR5+ PD-1+ (2.19 % - vs - 2.45 %) or CD4+ CXCR5+ Bcl-6+ (1.83 % - vs - 2.43 %) Tfh cells was found in the draining lymph nodes of C57BL/6 WT *vs* apoE$^{-/-}$ mice (Fig 27).

Mirroring this, no difference in the percentage of CD4+ CD44hi CXCR5+ ICOS+ (15.25 % - vs - 16.73 %), CD4+ CD44hi CXCR5+ PD-1+ (6.30 % - vs – 4.66 %) or CD4+ CD44hi CXCR5+ Bcl-6+ (10.73 % - vs – 10.42 %) Tfh cells was found in the draining lymph nodes of C57BL/6 WT *vs* apoE$^{-/-}$ mice (Fig 28).
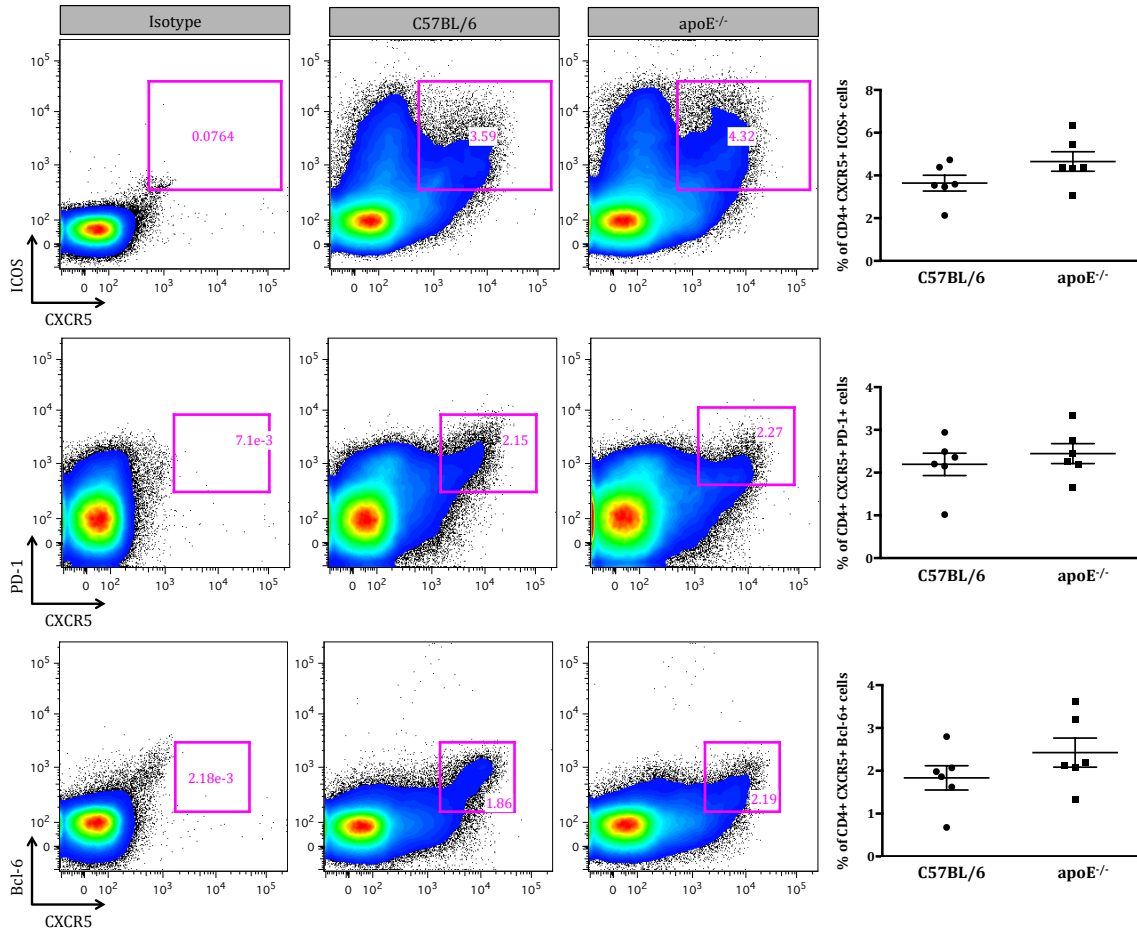
Figure 27: Flow cytometry analysis of CD4+ CXCR5+ ICOS+, CD4+ CXCR5+ PD-1+ and CD4+ CXCR5+ Bcl-6+ Tfh cell populations in the draining lymph nodes of C57BL/6 WT and apoE$^{-/-}$ mice immunized s.c. with OVA / CFA

Two groups of mice [C57BL/6 WT (n = 6) and apoE$^{-/-}$ (n =6)] were immunized s.c. with 100 µg of OVA emulsified in 100 µl of CFA. Nine days after immunization, dLNs (axillary and brachial) were dissected and prepared for surface flow cytometry staining. Lymphocytes were gated for on the basis of FSC and SSC parameters, after which single cells were selected for. Using these gates, CD4+ T-cells were selected. Using these parent gates, CXCR5+ ICOS+, CXCR5+ PD-1+ and CXCR5+ Bcl-6+ cells were gated. Statistical analysis was performed using GraphPad Prism and an unpaired students t-test. * $P < 0.05$, ** $P < 0.01$, *** $P < 0.001$.
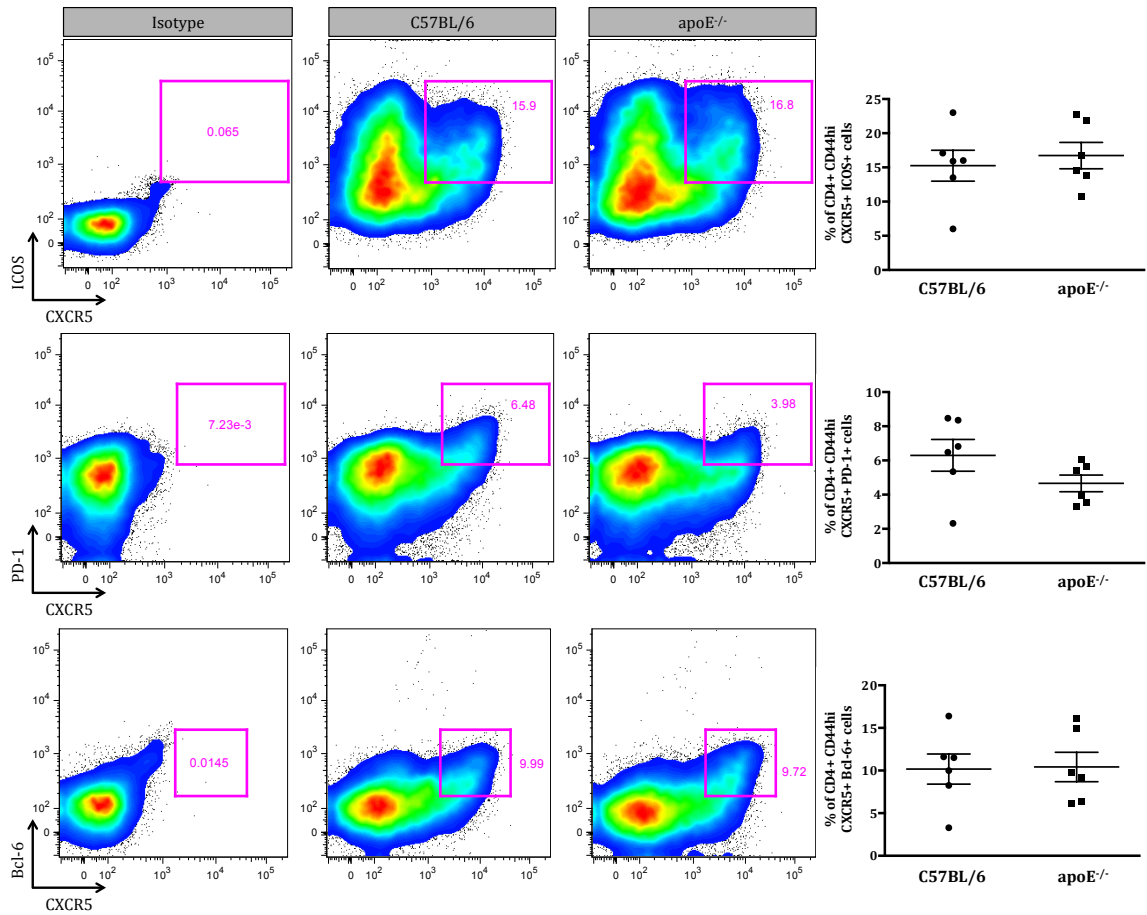
Figure 28: Flow cytometry analysis of CD4+ CD44hi CXCR5+ ICOS+, CD4+ CD44hi CXCR5+ PD-1+ and CD4+ CD44hi CXCR5+ Bcl-6+ Tfh cell populations in the draining lymph nodes of C57BL/6 WT and apoE$^{-/-}$ mice immunized s.c. with OVA / CFA

Two groups of mice [C57BL/6 WT (n = 6) and apoE$^{-/-}$ (n =6)] were immunized s.c. with 100 µg of OVA emulsified in 100 µl of CFA. Nine days after immunization, dLNs (axillary and brachial) were dissected and prepared for surface flow cytometry staining. Lymphocytes were gated for on the basis of FSC and SSC parameters, after which single cells were selected for. Using these gates, CD4+ T-cells were selected, followed by a subsequent CD44hi gate. Using these parent gates, CXCR5+ ICOS+, CXCR5+ PD-1+ and CXCR5+ Bcl-6+ cells were gated. Statistical analysis was performed using GraphPad Prism and an unpaired students t-test. * $P < 0.05$, ** $P < 0.01$, *** $P < 0.001$.

1.47.2   Apolipoprotein-E Deficiency Significantly Attenuates PD-1 and Bcl-6 Mean Fluorescence Intensity

To refine the experimental approach, the mean fluorescence intensity (MFI) of ICOS, PD-1 and Bcl-6 on pre-gated (CD4+ and CD4+ CD44hi) CXCR5+ ICOS, CXCR5+ PD-1+ and CXCR5+ Bcl-6+ Tfh cells was assessed respectively.

Used throughout the literature, MFI is a useful tool for the study of relative marker expression on a selected cell population. As such, variations in MFI can help determine whether selected markers are lowly or highly expressed under varying conditions.

Using this approach, no difference in the MFI of ICOS on both CD4+ CXCR5+ ICOS+ and CD4+ CD44hi CXCR5+ ICOS+ Tfh cells was found (Fig 29). Interestingly, in comparison to C57BL/6 WT mice, apoE$^{-/-}$ mice displayed a significant reduction in PD-1 MFI on both CD4+ CXCR5+ PD-1+ and CD4+ CD44hi CXCR5+ PD-1+ Tfh cells (Fig 29). Following a similar pattern, apoE$^{-/-}$ mice displayed a significant reduction in Bcl-6 MFI on CD4+ CXCR5+ Bcl-6+ and CD4+ CD44hi CXCR5+ Bcl-6+ Tfh cells (Fig 29).

147
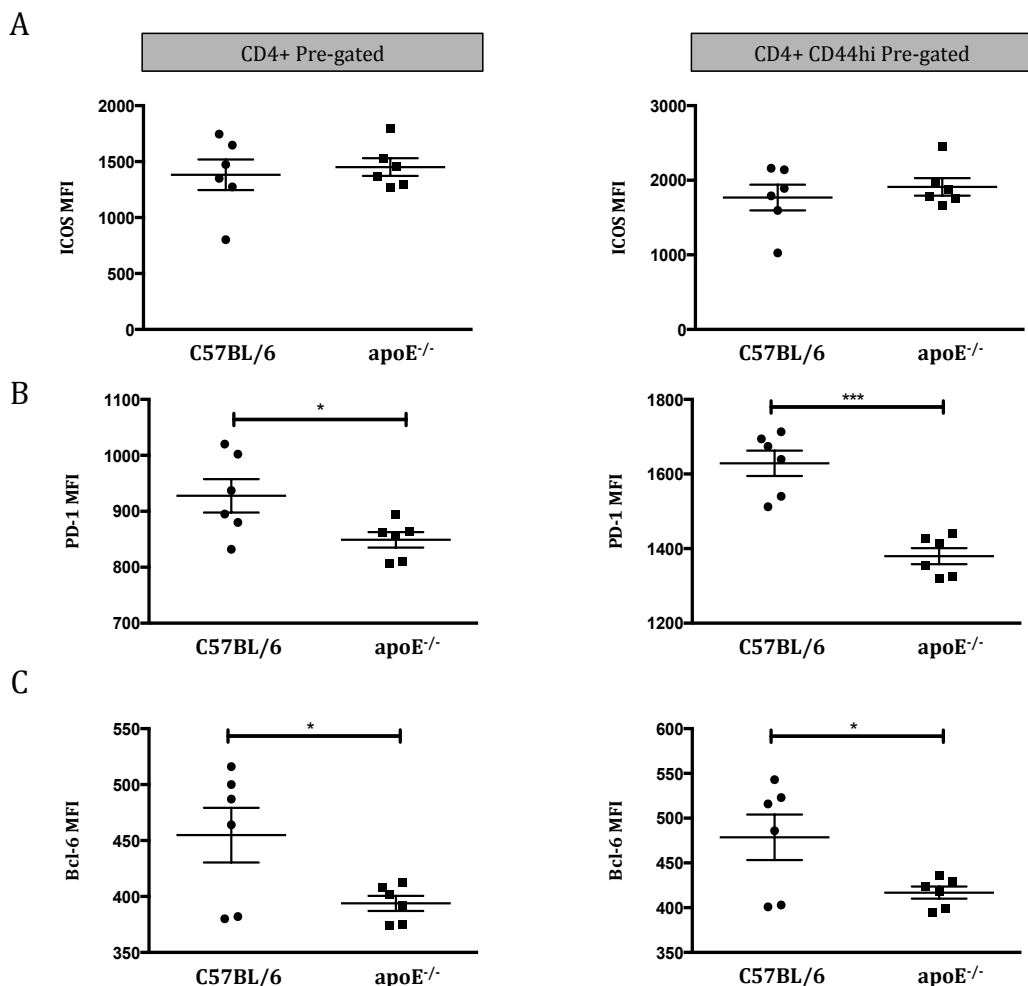
Figure 29: MFI of ICOS, PD-1 and Bcl-6 on CD4+ and CD4+ CD44hi pre-gated Tfh cells

Two groups of mice [C57BL/6 WT (n = 6) and apoE$^{-/-}$ (n =6)] were immunized s.c. with 100 µg of OVA emulsified in 100 µl of CFA. Nine days after immunization, dLNs (axillary and brachial) were dissected and prepared for surface flow cytometry staining. Lymphocytes were gated for on the basis of FSC and SSC parameters. Using these gates, CD4+ and CD4+ CD44hi T-cell were gated. Using these two parent gates, CXCR5+ ICOS+, CXCR5+ PD-1+ and CXCR5+ Bcl-6 Tfh cells were gated. ICOS, PD-1 and Bcl-6 MFI was subsequently measured on double positive CXCR5+ ICOS+ **(A)**, CXCR5+ PD-1+ **(B)** and CXCR5+ Bcl-6+ **(C)** cells respectively. Statistical analysis was performed using GraphPad Prism and an unpaired students t-test. * P < 0.05, ** P < 0.01, *** P < 0.001.

1.47.3 Apolipoprotein-E Deficiency does not Affect CXCR5 Expression on CD4+ and CD4+ CD44hi Cells

Membrane bound CXCR5 is fundamental to the migration of Tfh cells to B-cell rich areas in secondary lymphoid organs. As such, its expression is important to Tfh cell function, GC B-cell differentiation and GC productivity. To determine whether apoE deficiency significantly affected CXCR5 expression in apoE$^{-/-}$ mice, and thus affected Tfh cell migration, the MFI of CXCR5 on CD4+ and CD4+ CD44hi cells was determined.

No difference in the MFI of CXCR5 on CD4+ T-cells from C57BL/6 WT and apoE$^{-/-}$ mice was observed (Fig 30). Mirroring this, no difference in the MFI of CXCR5 on CD4+ CD44hi T-cells from C57BL/6 WT and apoE$^{-/-}$ mice was also found (Fig 30).
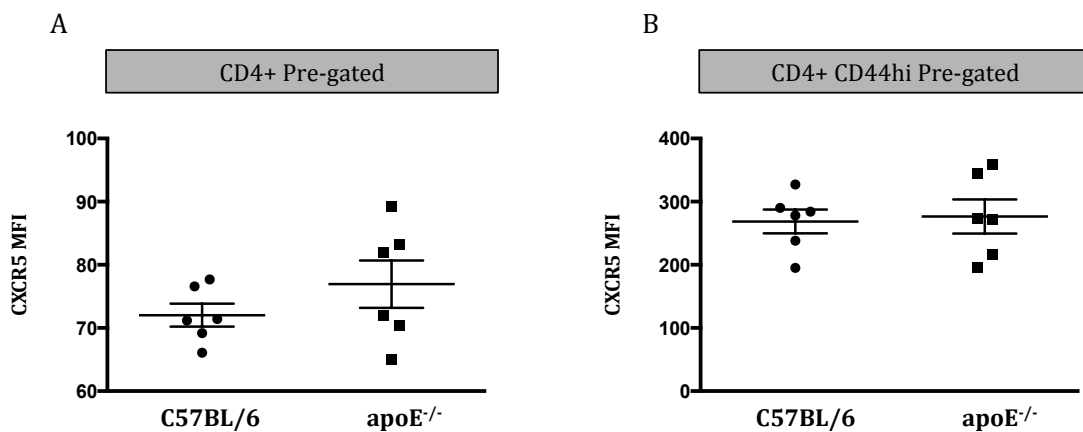
Figure 30: MFI of CXCR5 on CD4+ and CD4+ CD44hi T cells

Two groups of mice [C57BL/6 WT (n = 6) and apoE$^{-/-}$ (n =6)] were immunized s.c. with 100 μg of OVA emulsified in 100 μl of CFA. Nine days after immunization, dLNs (axillary and brachial) were dissected and prepared for surface flow cytometry staining. Lymphocytes were gated for on the basis of FSC and SSC parameters. CD4+ **(A)** and CD4+ CD44hi T-cells **(B)** were subsequently gated. Using these two gates, the MFI of CXCR5 was calculated **(A & B).** Statistical analysis was performed using GraphPad Prism and an unpaired students t-test. * $P < 0.05$, ** $P < 0.01$, *** $P < 0.001$.

1.47.4 Summary of the Effects of Apolipoprotein-E Deficiency on Tfh Cell Phenotype *in vivo*

Taken together, our results demonstrate that apoE deficiency does not affect Tfh cell formation but indicate that apoE$^{-/-}$ mice display reduced ability to express Tfh cell associated markers (PD-1 and Bcl-6). Importantly, our data also indicates that CD4+ and CD4+ CD44hi T-cells from apoE$^{-/-}$ mice up-regulate CXCR5 to the same level as C57BL/6 WT mice. As such, suggesting equivalent ability to migrate to B-cell follicles.

1.48 Effects of apoE Deficiency on GC B-cell Populations

1.48.1 Apolipoprotein-E Deficiency Significantly Attenuates Germinal Centre B-cell Populations

To study the effects of apoE deficiency on GC B-cell phenotype, GC B-cell expression was assessed in the draining lymph nodes of C57BL/6 WT and apoE$^{-/-}$ mice immunized s.c. with OVA / CFA.

Using this approach, apoE$^{-/-}$ mice displayed significantly reduced percentages of B220+ FAS+ PNA+ GC B-cells compared to C57BL/6 WT mice immunized in the same manner (4.23 % - vs – 2.30 %) (Fig 31).
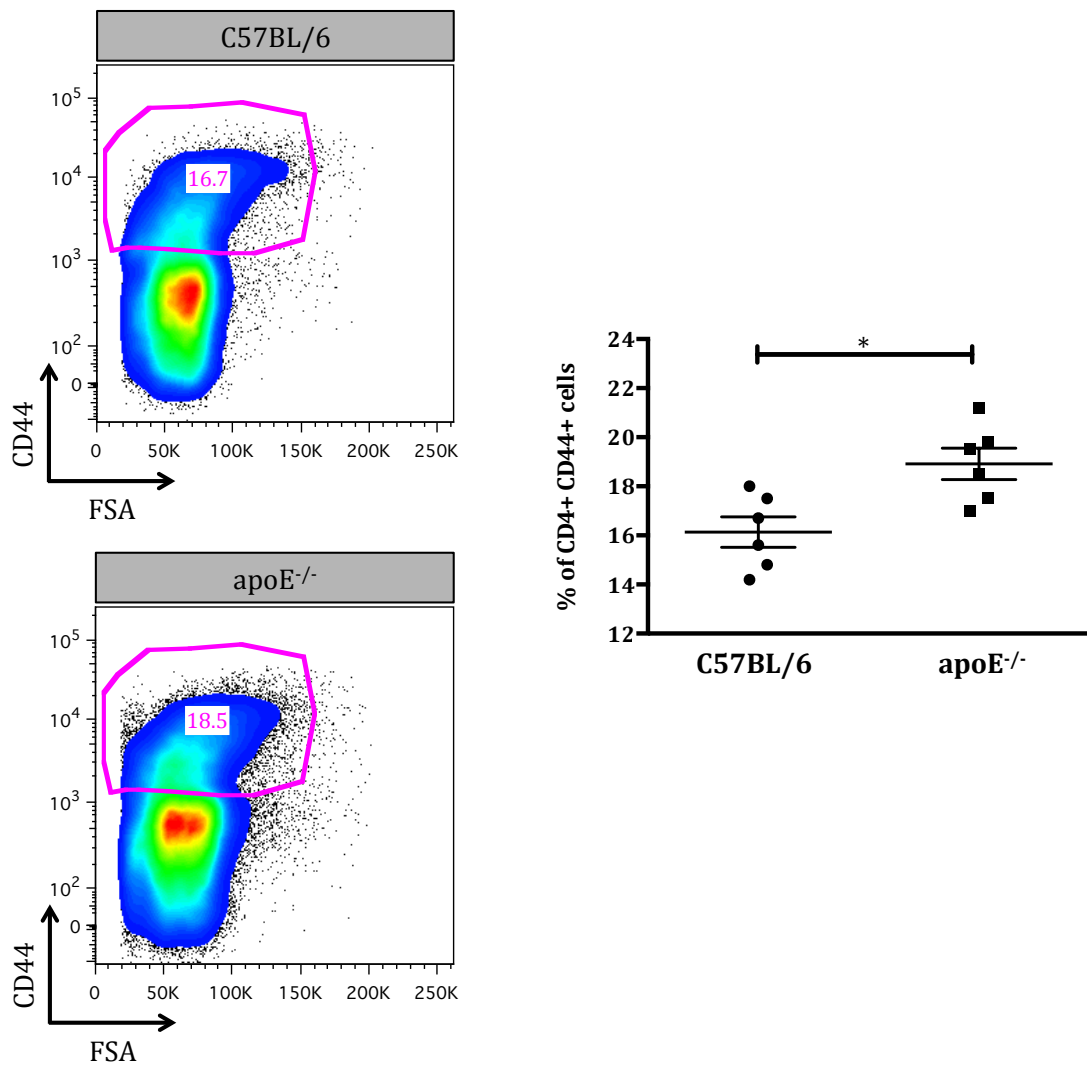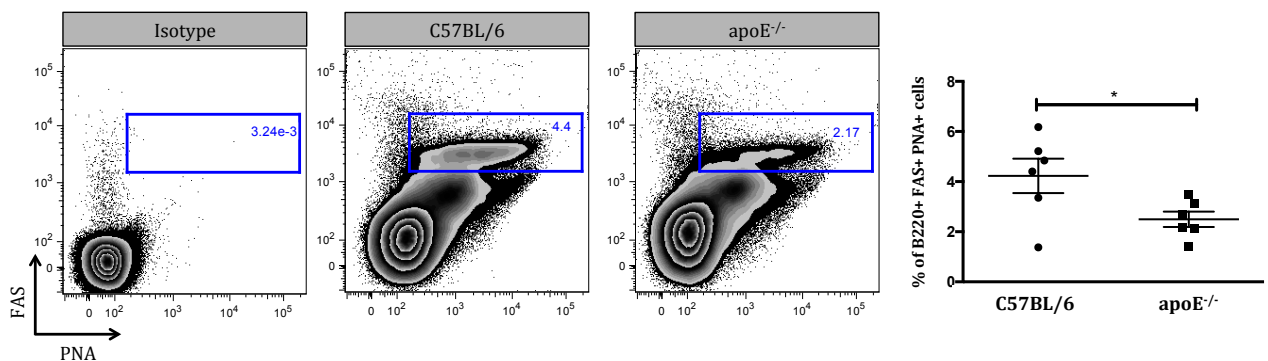

Figure 31: Flow cytometry analysis of B220+ FAS+ PNA+ GC B-cell populations in the draining lymph nodes of C57BL/6 WT and apoE$^{-/-}$ mice immunized s.c. with OVA / CFA

Two groups of mice [C57BL/6 WT (n = 6) and apoE$^{-/-}$ (n =6)] were immunized s.c. with 100 μg of OVA emulsified in 100 μl of CFA. nine days after immunization, dLNs (axillary and brachial) were dissected and prepared for surface flow cytometry staining. Lymphocytes were gated for on the basis of FSC and SSC parameters, after which single cells were selected for. Using these gates, B220+ cells were selected for on the basis of a B220 / CD4 exclusion gate. Doublet expression of FAS and PNA was subsequently assessed on single BB20+ cells. Statistical analysis was performed using GraphPad Prism and an unpaired students t-test. * *P* < 0.05, ** *P* < 0.01, *** *P* < 0.001.

1.48.2 Summary of the Effects of Apolipoprotein-E Deficiency on B220+ FAS+ PNA+ GC B-cell Populations

Taken together, our data suggests that apoE deficiency attenuates the expression of GC B-cell associated markers (FAS and PNA) on B220+ cells. As such, our data indicates that apoE$^{-/-}$ mice display reduced ability to form GC B-cell populations *in vivo*.

1.49 Discussion

1.49.1 Summary of Aims and Objectives

In this chapter, we studied the effects of apoE deficiency on the adaptive immune response *in vivo*. To do this, we immunized both C57BL/6 WT and apoE$^{-/-}$ mice with OVA antigen emulsified in complete freund's adjuvant CFA. Nine days later, we used surface flow cytometry to stain for a range of adaptive immune cells of particular interest. As such, we quantified the percentage of immune cells in the draining lymph nodes of both animals. The cellular subsets phenotyped in this study are summarised in table 3 below.

Cellular Subsets Analysed via Flow Cytometry	
Cell Phenotype	**Marker Combination**
B-cells	B220
T-cells	CD4
Activated T-cells	CD4+ CD44+
Tfh cells	CD4+ CXCR5+ ICOS+ CD4+ CXCR5+ PD-1+ CD4+ CXCR5+ Bcl-6+
Activated Tfh cells	CD4+ CD44+ CXCR5+ ICOS+ CD4+ CD44+ CXCR5+ PD-1+ CD4+ CD44+ CXCR5+ Bcl-6+

Table 3: Tabular documentation of cell types and marker combinations used to document adaptive immune cells

Using surface flow cytometry a range of adaptive immune cells were phenotyped in the draining lymph nodes of C57BL/6 WT and apoE$^{-/-}$ mice immunized s.c. with OVA/CFA.

1.49.2 Summary of Findings

In this chapter we found that C57BL/6 WT and apoE$^{-/-}$ mice displayed equivalent percentages of B220+ B-cells and CD4+ T-cells in the draining lymph nodes 9 days post-immunization. In contrast to this, apoE$^{-/-}$ mice displayed significantly greater percentages of CD4+ CD44+ T-cells than C57BL/6 WT mice.

We detected no difference in the percentage of Tfh cells between C57BL/6 WT and apoE$^{-/-}$ mice. Conversely, we found that apoE$^{-/-}$ Tfh cells expressed PD-1 and Bcl-6 at lower levels than C57BL/6 WT Tfh cells. As well as this, loss of apoE protein significantly attenuated GC B-cell formation. Reassuringly, loss of apoE did not affect the ability of T-cells to translocate to B-cell follicles – a finding evident by equivalent CXCR5 expression on CD4 T-cells from C57BL/6 WT and apoE$^{-/-}$ mice.

Taken together, our results confirm that apoE deficiency *in vivo* does not affect CD4+ T-cell, B220+ B-cell and Tfh cell percentages. Our data also indicates that apoE deficiency may function to depress GC B-cell formation *in vivo*, as well as reduce available co-stimulation on Tfh cells. As such, our results provide an interesting insight into the potential modulation of adaptive immunity by apoE *in vivo*. The implications of such variations on disease progression must therefore be taken into account and will be discussed herein.

1.49.3 Apolipoprotein-E Deficiency Does Not affect the Percentage of B220+ B-cell, CD4+ T-cell and Tfh Cells in Draining lymph Nodes of Mice

Both CD4 and B220 are important markers for the pre-gating of Tfh cells and GC B-cells. As such, we determined whether loss of apoE affected CD4+ T-cell and B220+ B-cell populations. We found no difference in CD4+ T-cell or B220+ B-cell populations *in vivo.* We can, therefore, be confident that CD4+ T-cell and B220+ B-cell gates used in chapter 2 were not inadvertently affected by the loss of apoE expression. In support of our data, others have shown that loss of apoE does not affect T-cell or B-cell percentages *in vivo* [249].

While apoE functions to inhibit lymphocyte expansion *in vitro* [274, 275], the use of non-physiological antigen doses and cultured cell lines in studies complicates extrapolation of *in vitro* data to an *in vivo* setting. In support of the notion that apoE regulates lymphocyte proliferation and activation, we found that apoE$^{-/-}$ mice display significantly enhanced expression of the activation marker CD44 (CD4+ CD44hi cells).

As a model, apoE$^{-/-}$ mice express enhanced levels of T-cell activation [54, 137, 284]. It is likely that loss of apoE and the developing pro-atherogenic immune response both contribute to the presence of enhanced T-cell activation. However the individual contribution by apoE deficiency to T-cell activation *in vivo* is unknown.

1.49.4 Apolipoprotein-E Deficiency Does not Affect the Percentage of Tfh Cells or CXCR5 Expression but Attenuates PD-1 and Bcl-6 Expression

In previous chapters we phenotyped Tfh cells using a variety of published marker combinations. Using the same marker combinations, with the addition of Bcl-6, we characterised the difference in Tfh cell percentages between C57BL/6 WT and apoE$^{-/-}$ mice immunized s.c. with OVA / CFA. We found no difference in Tfh cell percentage between both groups. As such, we propose that differences in Tfh cell kinetics observed in chapter 2 were as a result of diet-induced atherosclerosis and not due to the effects of apoE deficiency. This is supported by the finding that, in comparison to chow diet, HFD induced the largest increase in Tfh populations (chapter 3). To date, no published data exists studying the difference in Tfh cell populations between C57BL/6 WT and apoE$^{-/-}$ mice and the role of apoE in such processes. Adding to this area, we can confirm that apoE deficiency does not inadvertently affect Tfh cell percentages *in vivo,* in context of hyperlipidemia.

Interestingly, we found that apoE$^{-/-}$ mice displayed significantly less GC B-cell populations than C57BL/6 WT mice. Strikingly, as with T-cells, little data exists assessing the role of apoE in regulating GC B-cells. Importantly, our finding that apoE$^{-/-}$ mice display reduced GC B-cell populations following immunization supports our hypothesis that atherosclerosis and hyperlipidemia and not apoE deficiency are major drivers of the enhanced GC responses observed in atherosclerotic mice.

As well as assessing cell percentages, we studied the expression of Tfh cell associated molecules (ICOS, PD-1 and Bcl-6). Using mean MFI, marker expression was assessed on CD4+ and CD4+ CD44hi Tfh cells. Interestingly, we found that Tfh cells from immunized apoE$^{-/-}$ mice expressed significantly less PD-1 and Bcl-6. Both PD-1 and Bcl-6 are important Tfh cell markers [237, 283, 285]. Specifically, PD-1 is involved in co-stimulation and interacts with its ligand on GC B-cells and APC in the GC [286, 287]. Moreover, Bcl-6 is well characterised as the Tfh cell master regulator of function and plays an important role in the up-regulation of Tfh cell associated genes [236, 285]. As such, our data suggest that apoE deficiency does not affect Tfh cell percentages but significantly attenuates Tfh cell associated marker expression. To

determine the functional consequences of such a finding *in vivo*, future studies may determine switched antibody production and IL-21 secretion in response to mitogenic stimuli.

Importantly, PD-1 provides negative signals during T-cell : APC interactions [287], thus regulating T-cell activation. As such, it is plausible that loss of PD-1 may affect the ability of Tfh cells to interact with APCs. Adding to this, loss of PD-1 or its ligands (programmed death ligand-1/2 (PD-L1 and PD-L2)) has been shown to significantly enhance atherosclerosis formation *in vivo* by affecting both CD4+ and CD8+ T-cell activation [288-291]. Moreover, Bcl-6 has been implicated in the regulation of macrophage activation in animal models of atherosclerosis [292]. In summary, we can conclude that the Tfh cell and GC B-cell kinetics observed in chapter 2 were the result of atherogenic processes in apoE$^{-/-}$ HFD fed mice and not due to apoE deficiency.

1.49.5 Summary of Findings

- C57BL/6 WT and apoE$^{-/-}$ display equivalent percentages of CD4+ T-cells and B220+ B-cells
- Loss of apoE protein significantly enhances expression of CD44 on CD4+ T-cells in apoE$^{-/-}$ mice
- Loss of apoE does not affect Tfh cell percentages *in vivo*
- Loss of apoE does not affect CXCR5 expression on CD4+ T-cells
- Loss of apoE significantly attenuates PD-1 and Bcl-6 expression on Tfh cells
- Immunised apoE$^{-/-}$ mice display impaired expression of B220+ PNA+ FAS+ germinal centre B-cells

1.49.6 Concluding Remarks

Together, our findings indicate that apoE mice do not display impaired ability to express CD4+, B220+ or Tfh cell populations *in vivo*. As such, they support our hypothesis that the data presented in chapter 2 are a result of atherosclerosis progression. We have also demonstrated that CD4+ T-cells from apoE mice express CXCR5 to the same level as C57BL/6 WT mice. As such, we are confident that Tfh cells from apoE$^{-/-}$ mice display equivalent ability to migrate to B-cell follicles.

In contrast to this our data also indicates that apoE deficiency may alter the expression of Tfh cell associated markers (PD-1 and Bcl-6). The functional effects of this deficiency should form the basis of a follow up study, assessing antibody formation and Tfh cell helper function.

Chapter 5: Effects of IL-21R Deficiency on the Development of Atherosclerosis

1.50 Introduction

The role of IL-21 in regulating the adaptive immune response has gained extensive attention over the past few years. In particular, its importance in the formation of Tfh cells, GC B-cells and consequently GC reactions has been the topic of many publications. With direct relevance to the area of infection and immunity, these publications have provided insights into the potential benefits of IL-21R signal modulation in optimising vaccine production and biological immunity. As well as this, IL-21 has been implicated as an important molecule in the pathogenesis of many autoimmune diseases. Interestingly, although closely related to RA and other autoimmune conditions, the role of the IL-21 in atherosclerosis remains to be elucidated.

We have shown in chapter 2 that Tfh cell and GC B-cell kinetics follow a pattern in line with atherosclerosis progression *in vivo*. As part of this chapter we aimed to modulate Tfh cell and GC B-cell populations – in the context of hyperlipidemia - via IL-21R ablation on haematopoietic stem cells. Moving on from this, we studied the effects of IL-21R ablation on atherosclerosis formation and antibody production.

As part of this introduction, IL-21 and its receptor structure will be discussed, with focus on the intercellular signalling molecules involved. In addition to this, the importance of IL-21 to both Tfh cells and GC B-cells will be discussed, as well as its role in other autoimmune conditions. Finally, the scope of the current study will be introduced, as well as the rationale behind our approach.

1.50.1   IL-21 & the IL-21 Receptor

IL-21 belongs to the IL-2 family of cytokines that includes other cytokines such as, IL-4, IL-7, IL-9 and IL-15 [293]. In combination with the common γ-receptor subunit – shared with the aforementioned cytokines – IL-21 signals via a heterodimeric receptor comprising an IL-21 specific subunit [294] (Figure 32). First cloned at the start of the 21st century, the IL-21R [295] is expressed by a variety of immune cells, including NK cells, T-cells, B-cells and DCs [296-298]. In contrast to its receptor, IL-21 secretion is mainly conserved to activated T-cells [206, 299-301]. Functioning in both autocrine and paracrine manners, IL-21 is able to exert its effects on a wide range of cell types.

More recently, the importance of IL-21 in immune cell expansion has been studied in detail. IL-21 is pivotal to the expansion of both CD4+ and CD8+ T-helper cells, with over-expression being linked to CD8+ T-cell memory [302]. In particular, IL-21 has been shown to influence the formation of activated cytotoxic lymphocytes (CTLs), via up-regulation of t-bet in T-cells [303, 304]. Adding further to the pleiotropic effects of IL-21, IL-21 supports B-cell differentiation into antibody secreting plasma cells and memory B-cell formation [204, 205, 305, 306].
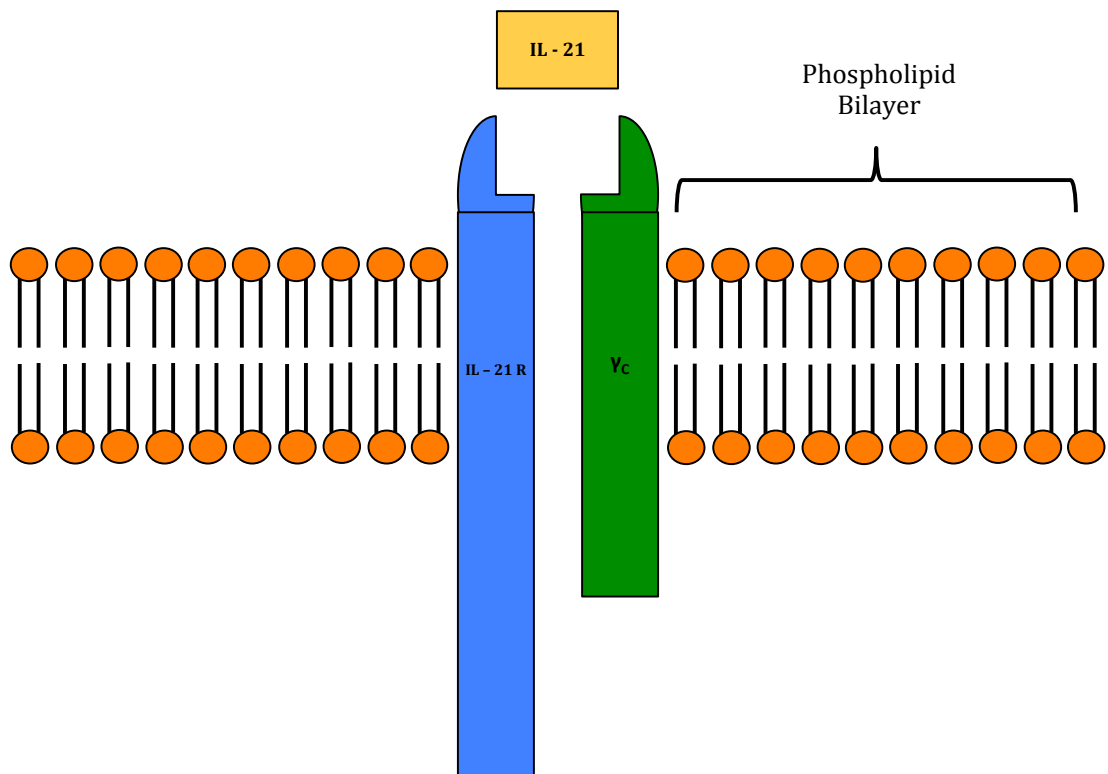
Figure 32: Structural composition of the functional IL-21R receptor

The IL-21R belongs to the family of receptors that share the common-γ (γ$_C$) chain receptor. The γ$_C$ chain receptor forms a heterodimer with an IL-21R specific subunit, giving form to a functional IL-21R receptor. In the absence of an IL-21 signal, both the γ$_C$ chain receptor and IL-21R specific subunit remain separate from one another. When in the presence of IL-21, both subunits combine to form a functional IL-21R.

1.50.2   IL-21R Signal Propagation

Binding of IL-21 to the IL-21R results in the activation of the janus kinase / signal transducer and activator of transcription (JAK / STAT) pathway (Figure 33). Using *in vitro* approaches, both JAK1 and JAK3 have been shown to propagate the initial IL-21 – IL-21R signal [294, 307]. Subsequent phosphorylation of STAT3 – and to a lesser extent STAT1 – results in nuclear transcription and Tfh cell / GC B-cell expansion [308-311].

Independent of the JAK / STAT pathway, common-γ chain receptor cytokines have been reported to activate phosphatidylinositol-4,5-bisphosphate 3-kinase / protein kinase B (P13K/Akt) and RAS and mitogen activated protein kinase (RAS/MAPK) [310]. It is therefore plausible that IL-21 may initiate other signalling pathways independent of the JAK/STAT. True to this, IL-21 has been shown to induce phosphorylation of both SRC homology 2-domain containing (SHC) and Akt, with the subsequent induction of T-cell proliferation [310]. Reinforcing the potential significance of SHC and Akt, blockade of these results in abolition of IL-21 induced T-cell proliferation [310].

Taking these findings into account, it is likely that messaging systems – other than the JAK / STAT pathway – are involved in IL-21R signal propagation. The importance of these pathways to IL-21R function is, however, in its infancy and may help to explain the range of effects IL-21 exerts.
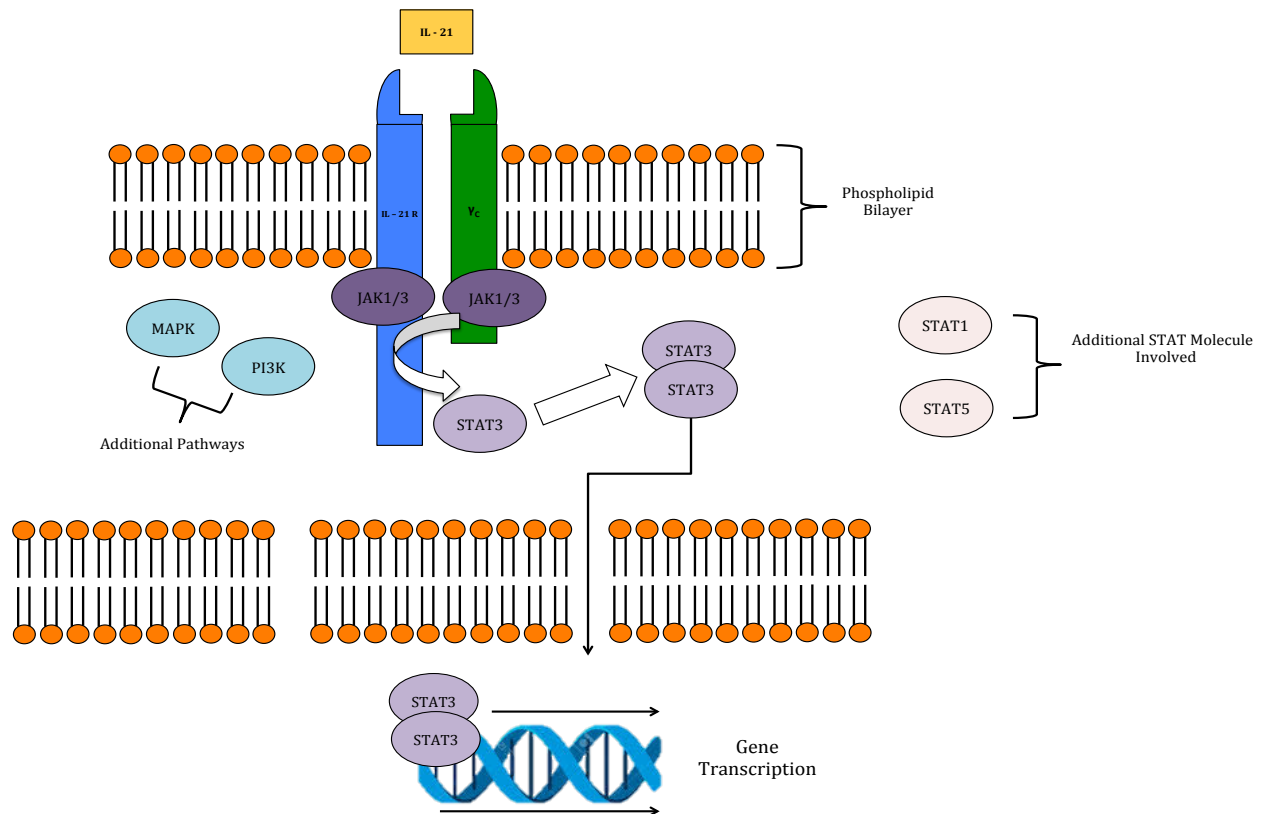
Figure 33: Signalling pathways involved in IL-21R signalling

Binding of IL-21 to the functional IL-21R – composed of an IL-21R specific subunit and the common -γ receptor chain – results in the activation of various intracellular signalling processes. IL-21 activates the JAK/STAT pathway, particularly JAK1, JAK3 and STAT 3, although STAT1 and STAT5 can also be activated to varying degrees. Phosphorylation of STAT molecules results in dimer formation and subsequent translocation to the nucleus, where gene transcription leads protein production. Additional pathways, such as the MAPK and PI 3-kinase can also be activated.

1.50.3   The Role of IL-21 in Modulating T-Follicular Helper Cells

More recently, IL-21 has been characterised as the signature cytokine of the Tfh cell subset [312]. Characterised by the expression of CXCR5, ICOS, PD-1, Bcl-6 and IL-21, Tfh cells aid GC B-cells in the production of high affinity, isotype switched antibodies [313]. Adding to the importance of IL-21 to Tfh cells, IL-21 functions to enhance Bcl-6 expression and Tfh cell associated gene expression in naïve T-helper cells [235, 305]. Acting in an autocrine and paracrine manner, IL-21 affects the activation and differentiation of Tfh cells, as well as other cells within vicinity.

With developments in Tfh cell biology, researchers now understand the complex interplay between various nuclear transcripts and Tfh cell formation. Although originally Bcl-6 was perceived as being the master regulator of transcription, recent studies have casted doubt upon its exclusive role in Tfh cell formation. More recently, the transcription factor musculoaponeurotic fibrosarcoma oncogene homolog (c-maf) has been shown to be important in optimal Tfh cell formation and IL-21 production [285]. Working in cooperation with Bcl-6, c-maf is essential to optimal IL-21 production by Tfh cells *in vivo.* Highlighting the importance of c-maf to IL-21 production*,* c-maf deficient mice are void of IL-21 production *in vivo* [314, 315]. Interestingly, transcription factors – other than c-maf and Bcl-6 - have been implicated in the IL-21 production and Tfh cell formation. Specifically, the transcription factor – basic leucine zipper transcription factor (BATF) – has been shown to enhance IL-21 production, as well as Bcl-6 and c-maf expression [316].

Intriguingly, some have provided evidence that IL-21 is dispensable in the formation of Tfh cells, thus raising questions over the importance of this cytokine to Tfh cell development [205]. The role of varying signalling pathways, the diverse actions of IL-21 and the methods used in such studies are likely to explain these findings. Raising questions with regards to subset plasticity, others have demonstrated that Tfh cells secrete large amounts of cytokines associated with other T-helper cell subsets, including IL-4 and IFN-γ [312, 317].

Recent studies have pointed to a novel mechanism of action for IL-21. Acting via Vav1 – a signalling molecule involved in TCR signalling – IL-21 can co-stimulate alongside the TCR, at a level that surpasses conventional co-stimulation [206, 296].

Taken together, the studies described above provide strong evidence for the role of IL-21R signalling in the development of Tfh cells. They also reinforce the complex nature in which IL-21 secretion is regulated in Tfh cell transcripts, as well as the range of cells IL-21 can target.

1.50.4 The Role of IL-21 in Modulating Germinal Centre B-cells

Independent of its effects on Tfh cells, IL-21 has been shown to play an important role in the formation and function of GC B-cells, memory B-cells and plasma cells *in vivo* [170, 204, 205, 305, 306]. In terms of GC reactions, the primary source of IL-21 is derived from activated Tfh cells found within the local vicinity [205], thus reinforcing the intimate association between both cell types.

B-cells express IL-21R at varying degrees throughout their developmental programme. Immature transitional (T1) B-cells and marginal zone (MZ) B-cells express low levels of IL-21R [318]. Subsequent progression to transitional 2 (T2) stages confers enhanced levels of expression, similar to that found on follicular B-cells [318]. Of most importance to the GC reaction, human GC B-cells express IL-21R at high levels, with memory B-cells being void of expression [319].

Intriguingly, IL-21 exerts a multitude of effects, depending on the presence of other secreted factors and the context of stimulation. IL-21 induces death of resting B cells while it promotes differentiation of B cells into plasma cells depending on the signalling context.

In recent times, IL-21 has been shown to act directly upon GC B-cells *in vivo.* Specifically, IL-21 regulates Bcl-6 expression in GC B-cells [204], as well as working alongside other cytokines to up-regulate AID - an important enzyme involved in antibody isotype switching [320, 321]. Further highlighting the importance of IL-21 and its receptor to GC B-cell and GC formation, loss of IL-21 or IL-21R results in

inefficient GC reaction production, reduced antibody production and reduced GC B-cell populations [204, 205].

Taken together, the studies described above provide evidence for the role of IL-21R signalling in the formation of GC B-cells. They also enforce the requirement of IL-21 for the formation and sustainment of GC reactions, as well as isotype switched antibody production. As such, IL-21 functions in a process that is essential to GC B-cell and GC reaction formation *in vivo*.

1.50.5   The Role of IL-21 in Autoimmunity

In the past decade, the role of IL-21 in autoimmunity has gained attention. As such, various animal studies have demonstrated the therapeutic potential of modulating the IL-21 – IL-21R axis *in vivo*. In testament to the advances made in context of IL-21 and autoimmunity, several phase-I and phase-II clinical trials are currently underway.

Clues to the role of IL-21 in autoimmunity were first demonstrated by the finding that IL-21 levels correlated with disease progression and antibody production in animal models of disease. Specifically, using the BXSB.B6-*Yaa*+ mouse model – a model of SLE – researchers demonstrated that IL-21 serum levels correlated with age dependent increase in pathology, as well as antibody levels [305]. Furthermore, *sanroque* mice – formed as a result of a mutation in the roquin gene - display enhanced Tfh cell numbers and elevated serum IL-21 levels [322].

In humans, serum IL-21 levels have been shown to correlate with criteria used to diagnose RA, including DAS28 scores and anti-cyclic citrullinated peptide (anti-CCP) antibodies [323]. Moreover, increased numbers of IL-21 secreting T-cells are evident in patients suffering from SLE [324] - a finding attributed to elevated numbers of Th17 cells – another source of IL-21.

Collectively, these studies provide evidence that IL-21 may be associated to the development of autoimmunity in humans and in animal models of disease. Although

suggesting an association, they do not provide evidence for direct role of IL-21 in autoimmunity.

With the development of techniques to specifically block IL-21R or IL-21, researchers have able to dissect the consequences of impaired IL-21 signalling in disease progression. In particular, blockade of IL-21R using an IL-21R-Fc fusion protein in an animal model of SLE results in reduced kidney pathology, as well as reduced IgG_1 and IgG_{2a} antibody production [325]. Blockade of IL-21 in two models of inflammatory arthritis reduces inflammation, antibody levels and pathological outcome [326]. Adding further to this, K/BxN mice – a model for autoantibody induced arthritis – when crossed with IL-21R deficient mice do not develop arthritis or autoantibody titres. Moreover, K/BxN mice treated with an inflammatory insult, alongside IL-21R-Fc fusion proteins, fail to develop severe forms of disease [327]. Adding further evidence to the role of IL-21 in the immunoinflammatory response, IL-21R blockade reduces gut inflammation in an animal model of colitis by affecting Th17 cells, [328] and has been shown to be important in conferring protection from type-1 diabetes [329-332].

Taken together, these studies provide evidence for the role of the IL-21 – IL-21R axis in the development and progression of immune conditions. Highlighting the pleiotropic actions of IL-21, these studies also stress the involvement of various immune cell subsets involved in IL-21 signalling and consequently disease progression. Conversely, they provide strong evidence for the role of the IL-21 – IL-21R axis in controlling pathological Tfh cell and GC B-cell responses in autoimmunity and that modulation may consequently affect Tfh cell and GC B-cell processes *in vivo.*

1.50.6   Scope of Current Study & Aims

Interestingly, atherosclerosis shares many common inflammatory hallmarks with other autoimmune diseases, including RA and SLE. Intriguingly, the role of IL-21 and IL-21R signalling in context of atherosclerosis has not been addressed.

We have shown in previous chapters that Tfh cell and GC B-cell kinetics change in line with atherosclerosis progression. Importantly, IL-21 has been shown to significantly modulate these populations *in vivo,* in context of disease. With this in mind, we aimed to dissect the effects of IL-21R modulation in context of atherosclerosis.

To study this aim, we:

1. Determined the effects of IL-21R ablation on Tfh cell and GC B-cell populations in the context of hyperlipidemia by generating IL-21R$^{-/-}$: LDLR$^{-/-}$ chimeric mice.;
2. Assessed whether IL-21R ablation resulted in altered serum antibody levels to modified forms of low-density lipoprotein (LDL);
3. Determined whether ablation of IL-21R modified atherosclerosis formation.

1.51 Results

1.52 Optimisation of Chimeric Model

1.52.1 Optimisation of Radiation Dose Required to Ablate Host Lymphocytes

To determine the optimum radiation dose required to ablate host hematopoietic stem cells, a range of radiation doses were tested. CD45.2 mice were lethally irradiated with 9, 9.5, 10.0 or 10.5 Grays of X-ray radiation. Mice were then reconstituted with 4 X 10^6 CD45.1 bone marrow derived stem cells. 8 weeks later, the efficiency of CD4+ T-cell and B220+ B-cell reconstitution was assessed via flow cytometry.

B220+ B-cells were particularly sensitive to all radiation doses, with approximately 90% of B220+ cells being CD45.1 positive at all doses (Fig 34 and Fig 35). In comparison to this, host CD4+ T-cells were more resistant to radiation-induced ablation. Maximal CD45.2 CD4+ T-cell reconstitution was only achieved at higher doses (10.5 Grays), with over 80% of CD4+ T-cells being CD45.2 positive (Fig 34 and Fig 35).

Under Home Office regulations of The United Kingdom, it is prohibited to expose animals to radiation levels exceeding 10.5 Grays in a single dose. As a result, animals were irradiated with a single dose of 10.5 Grays X-ray radiation. This allowed for maximal CD4+ T-cell and B220+ B-cell reconstitution, thus allowing for the assessment of both Tfh cell and GC B-cell compartments.
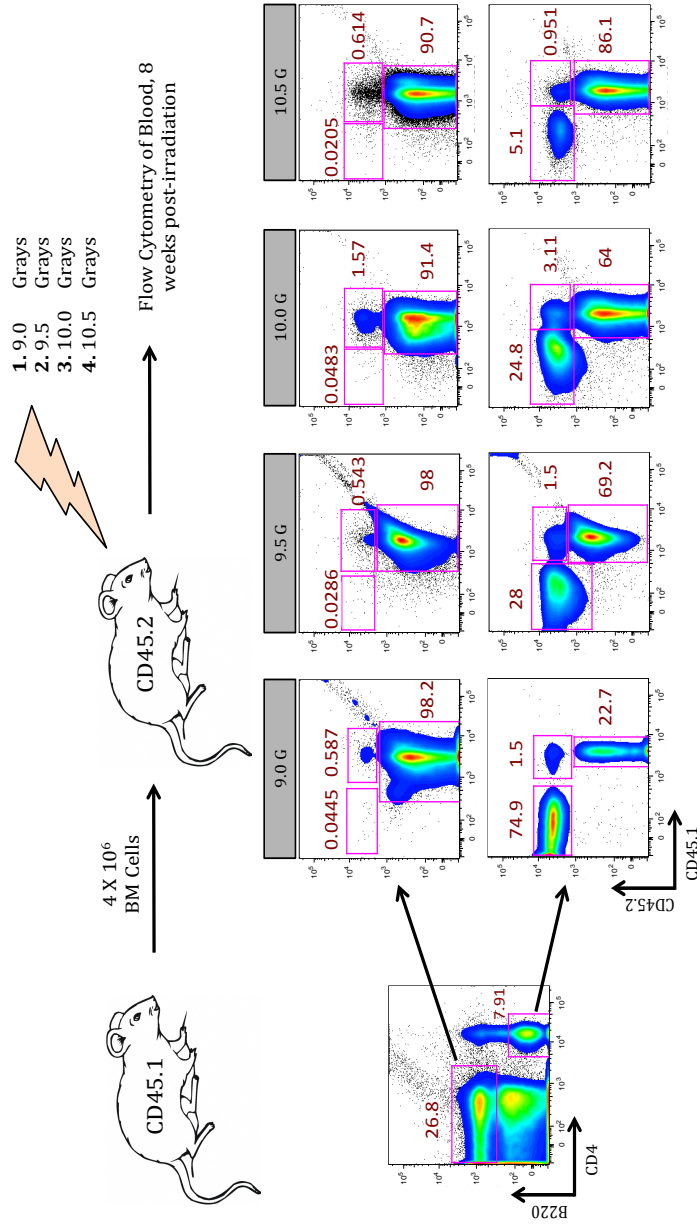
Figure 34: Optimisation of radiation dose required to ablate host lymphocytes

Four groups of CD45.2 mice were lethally irradiated with 9.0 (n = 3), 9.5 (n = 3), 10.0 (n = 3) or 10.5 (n = 3) Grays X-ray radiation. Following a period of recuperation, mice were culled and blood obtained via cardiac puncture. Lymphocytes were gated for on the basis of an initial FSC and SSC gate, with subsequent CD4+ and B220+ gates being made. Using these parent gates, CD45.1 and CD45.2 expression was assessed. Representative flow cytometry plots show CD45.1 and CD45.2 expression on CD4+ T-cells and B220+ B-cells under each condition.

	CD4+			B220+		
9.0 G	CD45.2	73.40%		CD45.2	0.269%	
	CD45.1	**24.26%**		CD45.1	**98.16%**	
	Double	0.899%		Double	0.5116%	
9.5 G	CD45.2	31.06%		CD45.2	0.0266%	
	CD45.1	**64.86%**		CD45.1	**97.3%**	
	Double	1.461%		Double	0.5386%	
10.0 G	CD45.2	16.06%		CD45.2	0.03175%	
	CD45.1	**73.85%**		CD45.1	**91.5%**	
	Double	2.00%		Double	1.047%	
10.5 G	CD45.2	6.145%		CD45.2	0.0231%	
	CD45.1	**84.65%**		CD45.1	**90.50%**	
	Double	1.22%		Double	0.6585%	
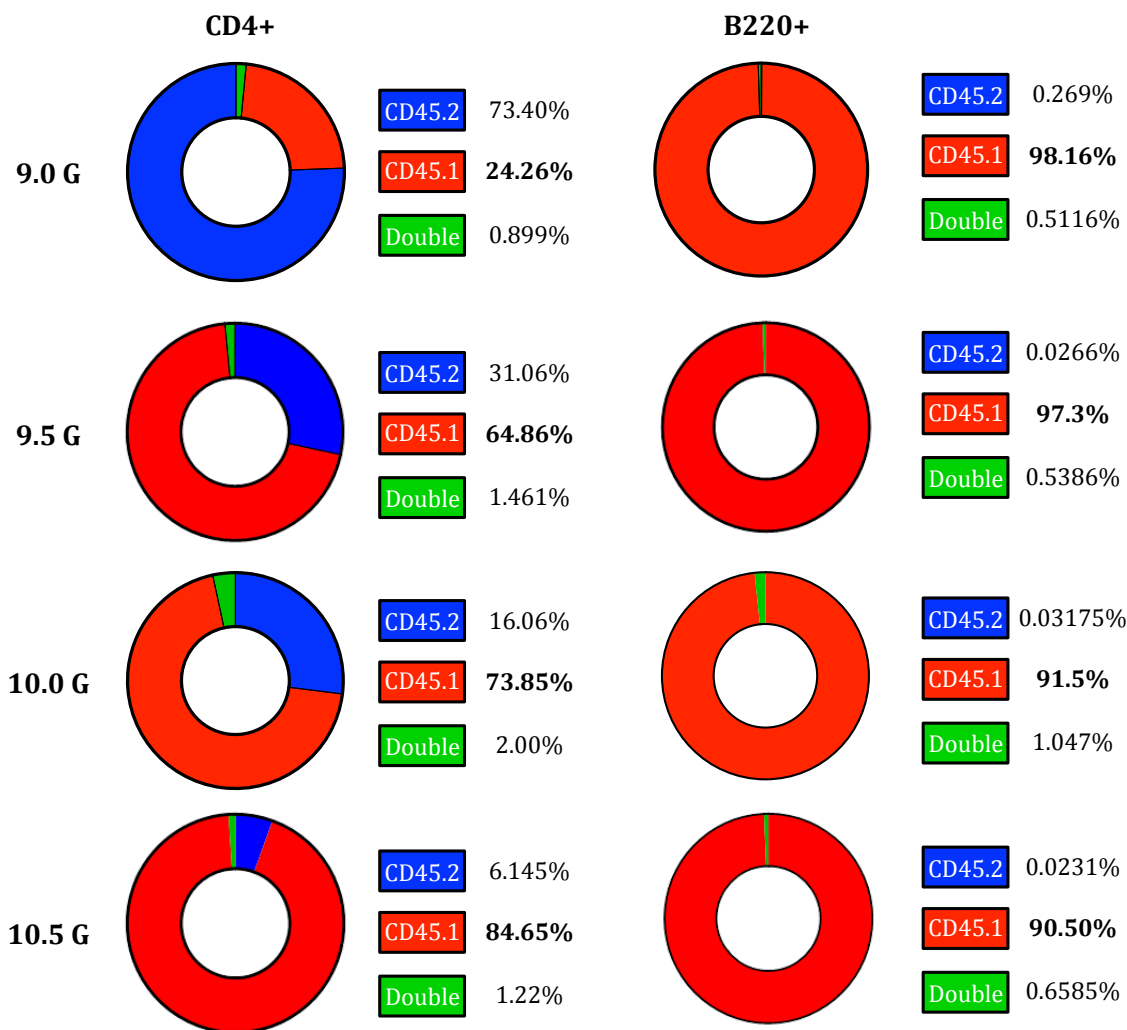
Figure 35: Pie charts display variation in the percentage of CD45.1+ / CD45.2+ CD4+ T-cells and B220+ B-cells under each condition.

1.52.2 Confirmation of Chimera Status

To confirm the successful ablation of host and reconstitution of donor bone marrow, C57BL/6NJ : LDLR$^{-/-}$ and IL-21R$^{-/-}$: LDLR$^{-/-}$ mice were assessed for LDLR and IL-21R expression. Using surface flow cytometry, LDLR expression was determined on peripheral blood monocytes 8 weeks after reconstitution. To confirm successful reconstitution of secondary lymphoid organs, IL-21R expression was assessed on B220+ B-cells from pLN, spleen and pao-LN compartments on the day of cull.

1.52.3 LDLR Expression on Circulating Peripheral Blood Monocytes

8 weeks post-reconstitution, circulating peripheral blood monocytes were characterised as LY6Chi CD115+ cells. Using the gating style shown in Figure 36A, LDLR expression was determined on LYC6Chi CD115+ cells from C57BL/6NJ : LDLR$^{-/-}$ and IL-21R$^{-/-}$: LDLR$^{-/-}$ mice.

Mice from both C57BL/6NJ : LDLR$^{-/-}$ and IL-21R$^{-/-}$: LDLR$^{-/-}$ groups displayed equivalent LDLR expression on peripheral blood monocytes as C57BL/6 positive control groups (Fig 36B). As well as this, a single positive population of LDLR expressing cells was identified in both groups, thus indicating complete LDLR re-constitution on circulating peripheral blood monocytes. Taken together, these results suggest our approach was successful in replacing host LDLR deficient bone marrow with LDLR sufficient stem cells (Fig 36B).

A
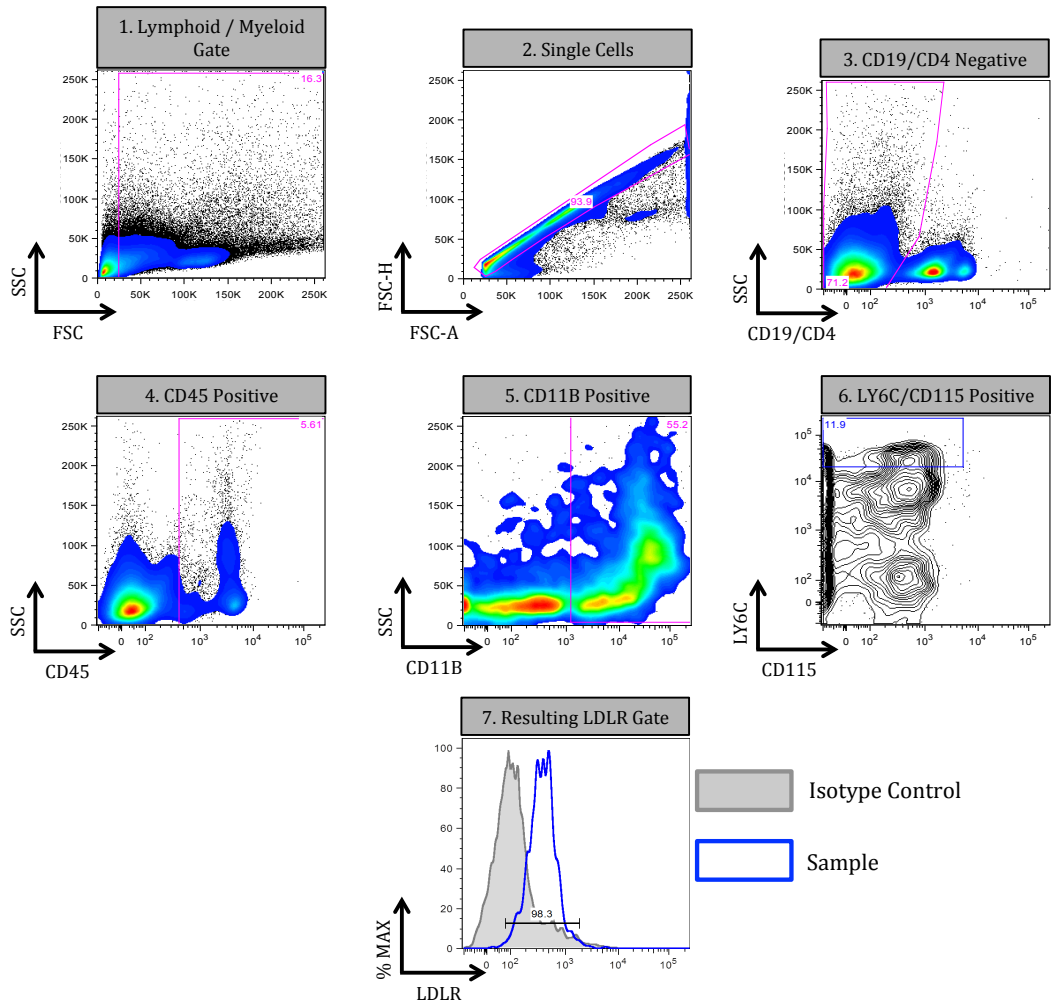
B
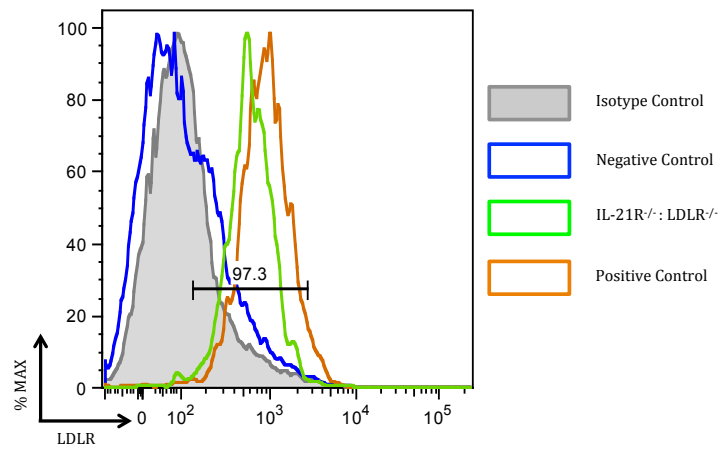
Figure 36: Confirmation of LDLR reconstitution on peripheral blood monocytes from chimeric mice

Two groups of 8 week old LDLR$^{-/-}$ mice were lethally irradiated with 10.5 Grays X-ray radiation. Mice were subsequently injected i.v. with 4 X 10^6 C57BL/6NJ (n = 10) or IL-21R$^{-/-}$ (n = 9) bone marrow. After 8 weeks, blood was collected via tail venepuncture and LDLR expression assessed on peripheral blood monocytes via flow cytometry. Myeloid cells were gated on the basis of an initial FSC and SSC gate, after which an exclusion gate was made (CD4- CD19-) **(A).** Subsequent CD45+, CD11B+ and Ly6C+ gates were made. LDLR expression was subsequently assessed on such cells **(A)**. Representative histogram plot shows LDLR expression on circulating peripheral blood monocytes from IL-21R$^{-/-}$: LDLR$^{-/-}$, C57BL/6 positive control and LDLR-/- negative control mice **(B).**

1.52.4   IL-21R Expression on Secondary Lymphoid Resident B220+ B-cells

As well as confirming LDLR expression on circulating blood monocytes, the lack of IL-21R expression on lymphoid resident B220+ B-cells was also determined. Unlike Tfh cells, B-cells express IL-21R at basal levels throughout their differentiation pathway. As a result, the B220+ B-cell population was selected to confirm IL-21R deficiency upon.

To gain a comprehensive profile of IL-21R ablation in systemic tissues, IL-21R expression was assessed on cells from pLNs, spleen and pao-LNs. Therefore providing an understanding of donor graft reconstitution in each organ of interest. Using the gating style shown in Figure 34A, IL-21R expression on B220+ B-cells from C57BL/6NJ : LDLR$^{-/-}$ and IL-21R$^{-/-}$: LDLR$^{-/-}$ mice was determined.

No IL-21R expression was detected on B220+ B-cells from IL-21R$^{-/-}$: LDLR$^{-/-}$ mice in all compartments (pLNs, spleen and pao-LNs) (Fig 37B), with expression being identical to that of isotype controls. In contrast, IL-21R expression could be detected on B220+ B-cells from C57BL/6NJ$^{-/-}$: LDLR$^{-/-}$ mice in all compartments (pLNs, spleen and pao-LNs) (Fig 37B). Taken together, these results indicate that IL-21R$^{-/-}$: LDLR$^{-/-}$ mice were successfully reconstituted with IL-21R deficient bone marrow. Adding further to this, the detection of a single peak (Fig 37B) indicates the complete reconstitution of the IL-21R$^{-/-}$ population, with no IL-21R positive peaks being observed.

A

1. Lymphocyte Gate
2. Single Cells
3. B220+ Cells
4. Resulting IL-21R Gate

C576N/J : LDLR⁻/⁻
IL-21R⁻/⁻ : LDLR⁻/⁻
Isotype Control

B

pLNs
Spleen
pao-LNs

C576N/J : LDLR⁻/⁻
IL-21R⁻/⁻ : LDLR⁻/⁻
Isotype Control
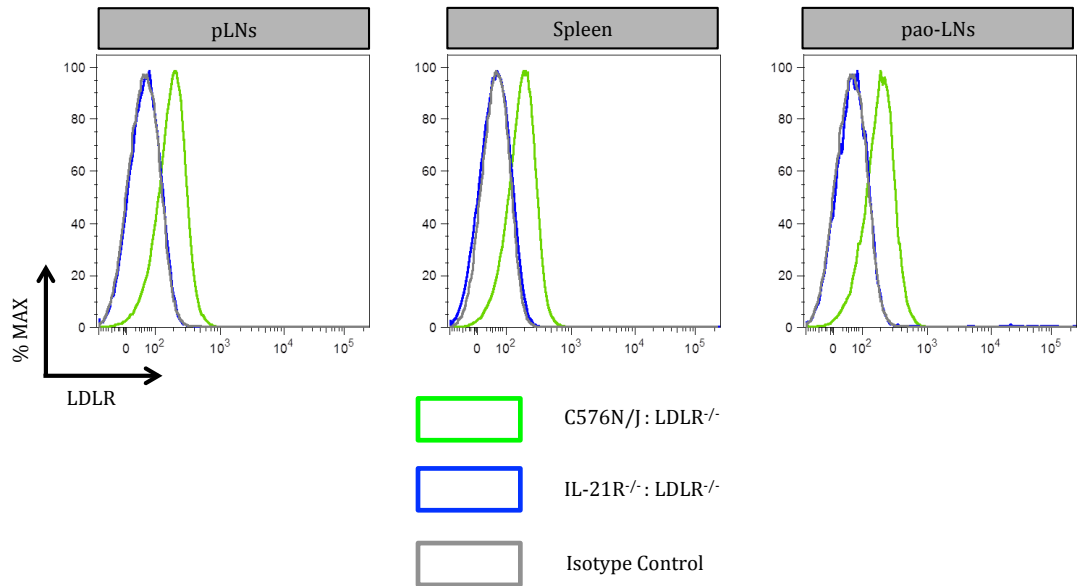
Figure 37: Confirmation of IL-21R deficiency in IL-21R$^{-/-}$: LDLR$^{-/-}$ mice

Two groups of 8 week old LDLR$^{-/-}$ mice were lethally irradiated with 10.5 Grays X-ray radiation. Mice were subsequently injected i.v. with 4 X 10^6 C57BL/6NJ (n = 10) or IL-21R$^{-/-}$ (n = 9) bone marrow. Following recovery, both groups were placed on HFD for 14 weeks. Following completion of the dietary period, pLNs, spleen and pao-LNs were harvested and IL-21R expression on B220+ B-cells assessed via flow cytometry. Lymphocytes were gated for on the basis of a FSC and SSC gate **(A)**, with subsequent single cell and B220+ gates being made **(A)**. Using these parent gates, IL-21R+ cells were selected for. Representative histogram plots show IL-21R expression on B220+ B-cells from pLNs, spleen and pao-LNs of IL-21R$^{-/-}$: LDLR$^{-/-}$ mice **(B)**.

1.52.5   IL-21R Deficiency

IL-21 is attributed as the signature cytokine of Tfh cells - and its relation to Tfh cell biology – has been the basis of intense investigation [235, 333]. Reported as being important in the induction of Bcl-6 in Tfh cells [321], IL-21 may play a role in Tfh cell fate commitment.

Of those studies conducted on IL-21 and its receptor, IL-21R expression has been linked to the maintenance of Tfh cell populations *in vivo.* As a result, we aimed to assess Tfh cell development in C57BL/6NJ : LDLR$^{-/-}$ and IL-21R$^{-/-}$: LDLR$^{-/-}$ mice. By generating an IL-21R deficient mouse, coupled with a deficiency in the LDLR, we were able to assess the effects of impaired Tfh cell formation on atherosclerotic progression. To induce lesion formation, C57BL/6NJ : LDLR$^{-/-}$ and IL-21R$^{-/-}$: LDLR$^{-/-}$ mice were placed on HFD for a period of 14 weeks.

1.53 IL-21R Deficiency Impairs Tfh Cell Formation in IL-21R$^{-/-}$: LDLR$^{-/-}$ Mice

To determine whether IL-21R deficiency impaired Tfh cell formation *in vivo*, Tfh cell marker expression was assessed in the pLNs, spleen and pao-LNs of C57BL/6NJ : LDLR$^{-/-}$ and IL-21R$^{-/-}$: LDLR$^{-/-}$ mice fed HFD for 14 weeks.

Using the same marker combination as discussed in chapter 3, Tfh cells were phenotyped as CD4+ CXCR5+ PD-1+ or CD4+ CD44+ CXCR5+ PD-1+ cells. In addition to this, ICOS expression on CD4+ CXCR5+ and CD4+ CD44+ CXCR5+ Tfh cells was determined. As a result, this provided a comprehensive profile of how IL-21R deficiency affected Tfh cell formation.

1.53.1   Peripheral Lymph Nodes

IL-21R$^{-/-}$: LDLR$^{-/-}$ mice displayed significantly reduced CD4+ CXCR5+ PD-1+ pLN Tfh cell populations than those observed in C57BL/6NJ : LDLR$^{-/-}$ control mice (0.944 % vs 0.38 %) (Fig 38). Following a similar pattern, IL-21R$^{-/-}$: LDLR$^{-/-}$ mice displayed significantly reduced CD4+ CD44+ CXCR5+ PD-1+ Tfh cell profiles than C57BL/6NJ : LDLR$^{-/-}$ control mice (1.77 % vs 0.71 %)(Fig 38).

1.53.2   Spleen

Following a similar pattern to that observed in pLNs, IL-21R deficiency resulted in a significant reduction in splenic CD4+ CXCR5+ PD-1+ Tfh cells (3.74 % vs 1.04 %) (Fig 39). As well as this, IL-21R$^{-/-}$: LDLR$^{-/-}$ mice displayed significantly reduced splenic CD4+ CD44+ CXCR5+ PD-1+ Tfh cell profiles than C57BL/6NJ : LDLR$^{-/-}$ control mice 6.01 % vs 2.32 % (Fig 39).

1.53.3   Para-aortic Lymph Nodes

Para-aortic lymph nodes comprise an important site for the trafficking of immune cells to and from luminal plaques. As such, the effects of IL-21R deficiency on local Tfh cell compartments was assessed. As observed in both peripheral lymph node and splenic compartments, IL-21R deficiency resulted in a significant reduction in CD4+ CXCR5+ PD-1+ Tfh cell expression (2.46 % vs 0.54 %) (Fig 40). In addition to this, IL-21R$^{-/-}$: LDLR$^{-/-}$ mice displayed significantly reduced CD4+ CD44+ CXCR5+ PD-1+ Tfh cell profiles (5.81 % vs 1.30 %) (Fig 40).
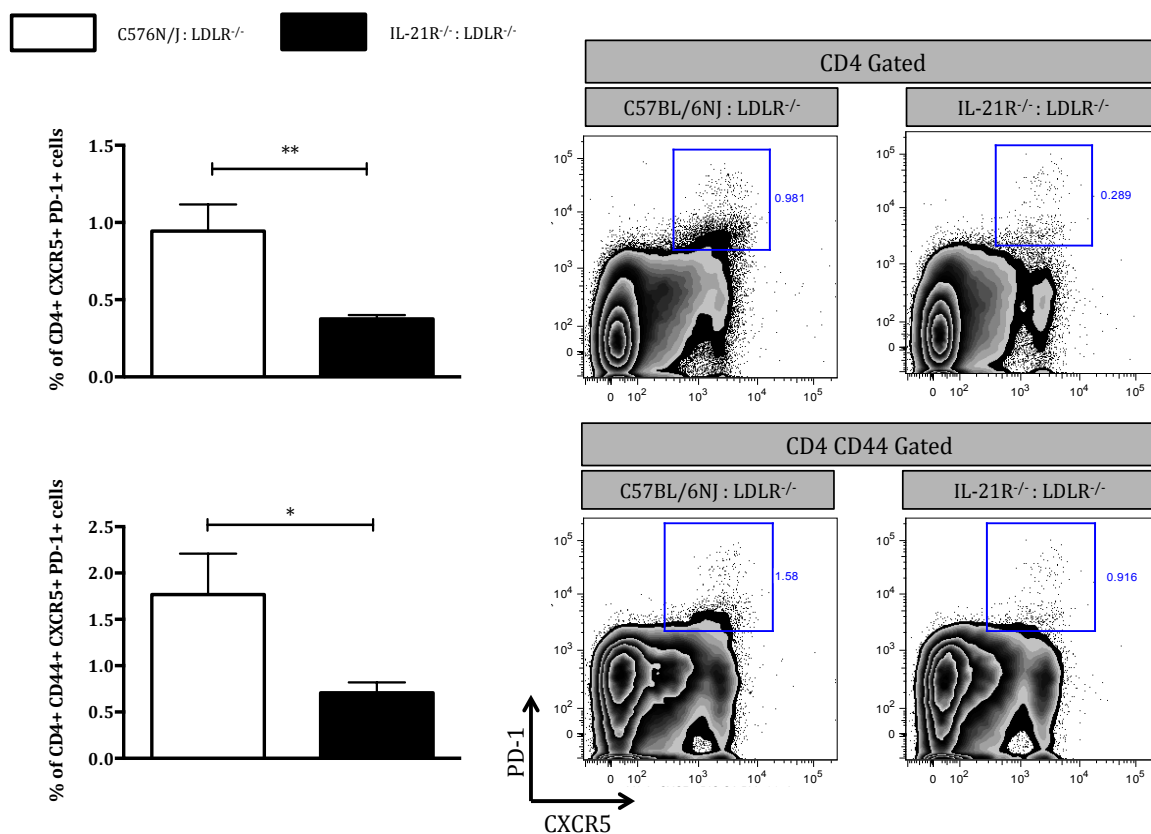
Figure 38: Percentage of CXCR5+ PD-1+ Tfh cells in pLNs of C57BL/6NJ : LDLR$^{-/-}$ and IL-21R$^{-/-}$: LDLR$^{-/-}$ mice

Two groups of 8 week old LDLR$^{-/-}$ mice were lethally irradiated with 10.5 Grays X-ray radiation. Mice were subsequently injected i.v. with 4 X 10^6 C57BL/6NJ (n = 10) or IL-21R$^{-/-}$ (n = 9) bone marrow derived stem cells. Following recovery, both groups were placed on HFD for 14 weeks. Following completion of the dietary period, pLNs were harvested and Tfh cell populations assessed via surface flow cytometry staining. Lymphocytes were gated for on the basis of an initial FSC and SSC gate and subsequent CD4+ and CD4+ CD44hi gates made. Using these two parent gates, CXCR5+ PD-1+ Tfh cells were gated. An exclusion gate using B220+ cells was used at the CD4+ gating point. Open bars represent C57BL/6NJ : LDLR$^{-/-}$ mice and shaded black bars represent IL-21R$^{-/-}$: LDLR$^{-/-}$ mice. Representative plots are taken from end point analysis for each organ analysed. Statistical analysis was performed using GraphPad Prism and by conducting an unpaired students t-test. * $P < 0.05$, ** $P < 0.01$, *** $P < 0.001$, **** $P < 0.0001$.

Figure 39: Percentage of CXCR5+ PD-1+ Tfh cells in spleen of C57BL/6NJ : LDLR$^{-/-}$ and IL-21R$^{-/-}$: LDLR$^{-/-}$ mice
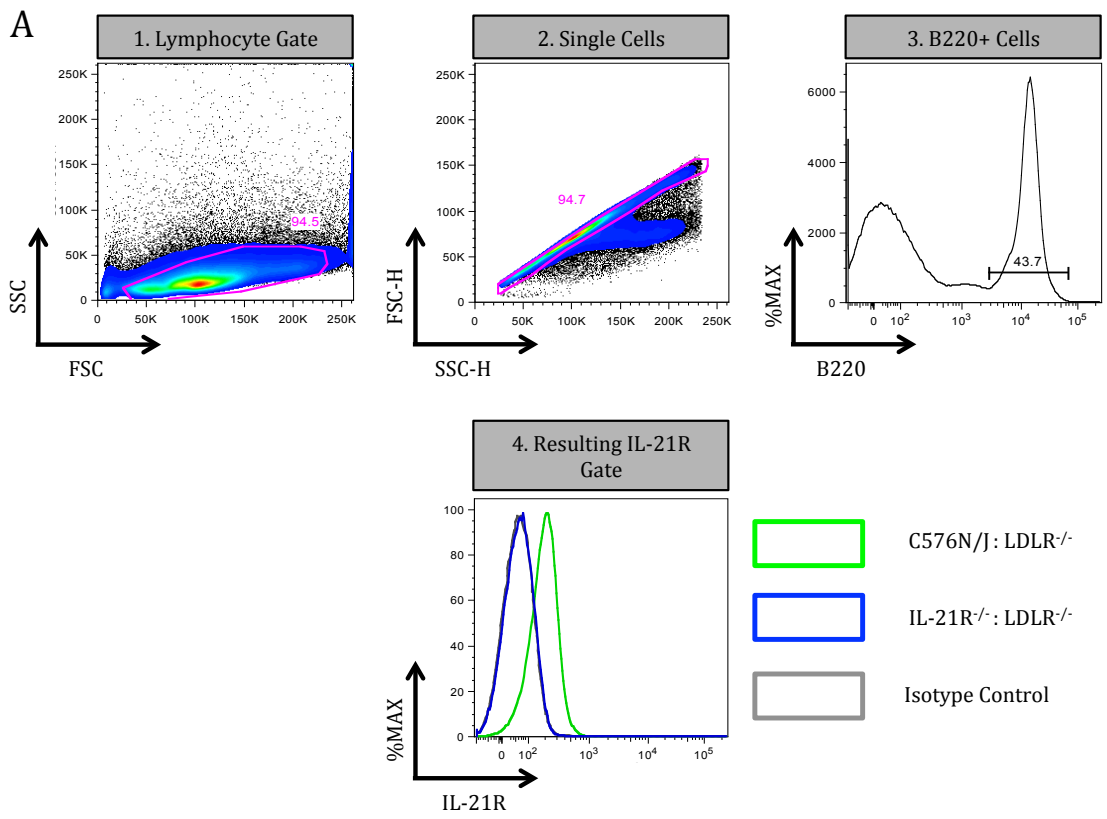
Two groups of 8 week old LDLR$^{-/-}$ mice were lethally irradiated with 10.5 Grays X-ray radiation. Mice were subsequently injected i.v. with 4 X 10^6 C57BL/6NJ (n = 10) or IL-21R$^{-/-}$ (n = 9) bone marrow derived stem cells. Following recovery, both groups were placed on HFD for 14 weeks. Following completion of the dietary period, spleens were harvested and Tfh cell populations assessed via surface flow cytometry staining. Lymphocytes were gated for on the basis of an initial FSC and SSC gate and subsequent CD4+ and CD4+ CD44hi gates made. Using these two parent gates, CXCR5+ PD-1+ Tfh cells were gated. An exclusion gate using B220+ cells was used at the CD4+ gating point. Open bars represent C57BL/6NJ : LDLR$^{-/-}$ mice and shaded black bars represent IL-21R$^{-/-}$: LDLR$^{-/-}$ mice. Representative plots are taken from end point analysis for each organ analysed. Statistical analysis was performed using GraphPad Prism and by conducting an unpaired students t-test. * $P < 0.05$, ** $P < 0.01$, *** $P < 0.001$, **** $P < 0.0001$.

Figure 40: Percentage of CXCR5+ PD-1+ Tfh cells in pao-LNs of C57BL/6NJ : LDLR⁻/⁻ and IL-21R⁻/⁻ : LDLR⁻/⁻ mice

Two groups of 8 week old LDLR⁻/⁻ mice were lethally irradiated with 10.5 Grays X-ray radiation. Mice were subsequently injected i.v. with 4 X 10⁶ C57BL/6NJ (n = 10) or IL-21R⁻/⁻ (n = 9) bone marrow derived stem cells. Following recovery, both groups were placed on HFD for 14 weeks. Following completion of the dietary period, pao-LNs were harvested and Tfh cell populations assessed via surface flow cytometry staining. Lymphocytes were gated for on the basis of an initial FSC and SSC gate and subsequent CD4+ and CD4+ CD44hi gates made. Using these two parent gates, CXCR5+ PD-1+ Tfh cells were gated. An exclusion gate using B220+ cells was used at the CD4+ gating point. Open bars represent C57BL/6NJ : LDLR⁻/⁻ mice and shaded black bars represent IL-21R⁻/⁻ : LDLR⁻/⁻ mice. Representative plots are taken from end point analysis for each organ analysed. Statistical analysis was performed using GraphPad Prism and by conducting an unpaired students t-test. * $P < 0.05$, ** $P < 0.01$, *** $P < 0.001$, **** $P < 0.0001$.

1.54 IL-21R deficiency Attenuates ICOS MFI on Tfh cells

Interaction of membrane bound ICOS with ICOSL is essential to the initiation of early Tfh cell development [207, 214, 334]. Involved in the initiation of Tfh cell associated nuclear transcripts, ICOS blockade has been shown to impair Tfh cell formation *in vivo* [207]. As a result, ICOS expression can provide an interesting insight into the potential of activated CD4+ T-cells to develop down a Tfh cell pathway.

With this in mind, we assessed the MFI of ICOS on the surface of CD4+ CXCR5+ and CD4+ CD44+ CXCR5+ T-cells. These cells were phenotyped in pLN, spleen and pao-LN compartments, thus providing an insight into the likelihood of CXCR5+ T-cells to adopt a Tfh cell phenotype.

1.54.1   ICOS Expression on CD4+ CXCR5+ CD4+ CD44+ CXCR5+ T-cells

IL-21R deficiency resulted in a significant reduction in ICOS expression on both pLN CD4+ CXCR5+ and CD4+ CD44+ CXCR5+ T-cells (Fig 41). Mirroring this, IL-21R$^{-/-}$: LDLR$^{-/-}$ mice displayed significantly less ICOS on the surface of splenic and pao-LN CD4+ CXCR5+ and CD4+ CD44+ CXCR5+ T-cells (Fig 41).

Taken together, these results indicate that CD4+ T-cells from IL-21R$^{-/-}$: LDLR$^{-/-}$ mice are less likely to express membrane bound ICOS – a molecule required for Tfh cell formation *in vivo*. Notably, although IL-21R deficiency reduced ICOS expression, a sizable population remained ICOS+ (Fig 41).
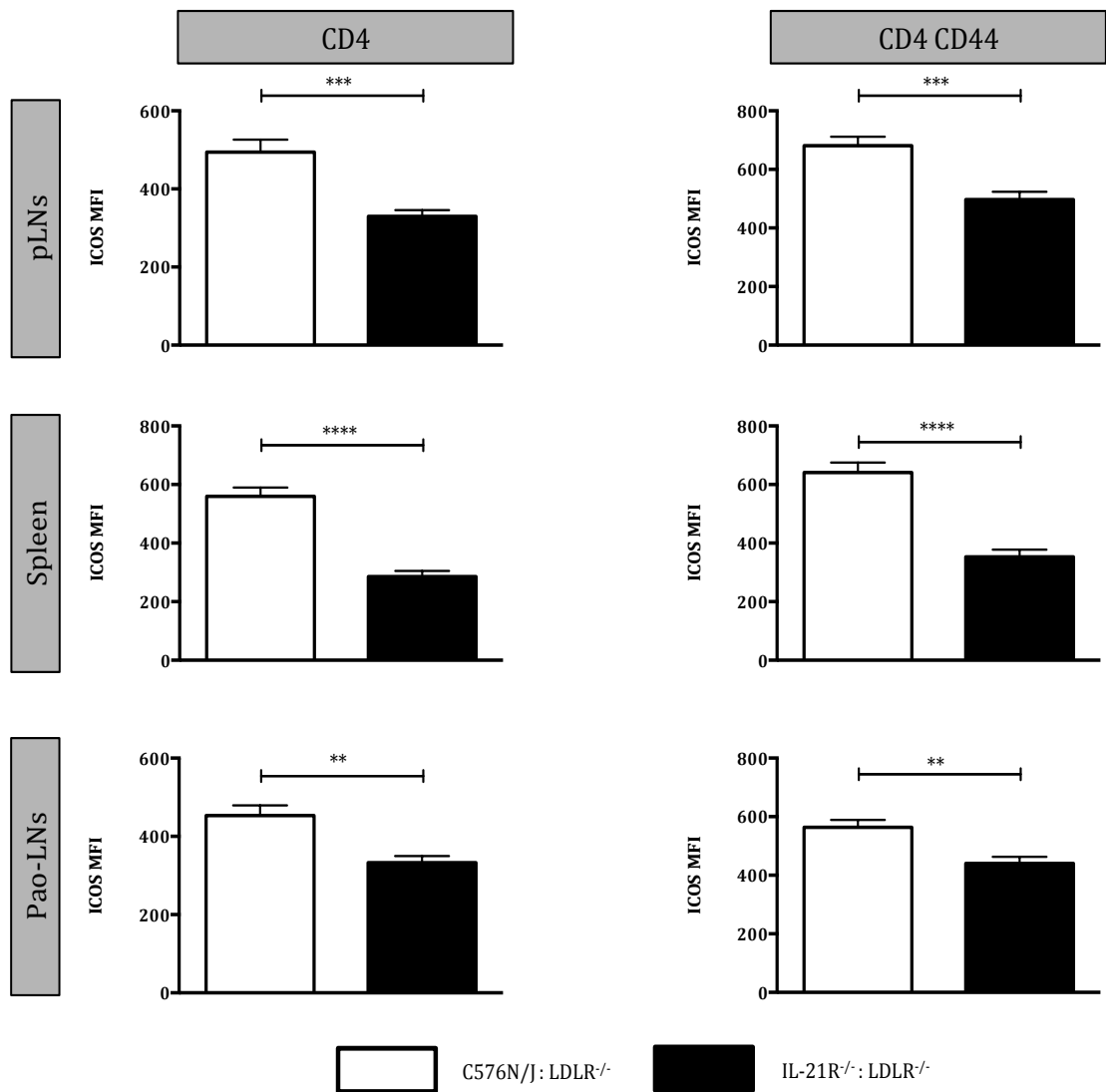
Figure 41: ICOS MFI on CD4+ CXCR5+ and CD4+ CD44+ CXCR5+ T-cells from C57BL/6NJ : LDLR$^{-/-}$ and IL-21R$^{-/-}$: LDLR$^{-/-}$

Two groups of 8 week old LDLR$^{-/-}$ mice were lethally irradiated with 10.5 Grays X-ray radiation. Mice were subsequently injected with 4 X 106 C57BL/6NJ (n = 10) or IL-21R$^{-/-}$ (n = 9) bone marrow derrived stem cells. Following recovery, both groups were placed on HFD for 14 weeks. Following completion of the dietary period, pLNs, spleen and pao-LNs were harvested. CD4+ CXCR5+ and CD4+ CD44+ CXCR5+ populations were assessed via surface flow cytometry staining. Lymphocytes were gated for on the basis of an initia FSC and SSC gate and subsequent CD4+ CXCR5+ and CD4+ CD44+ CXCR5+ parent gates made. Using these gates, MFI of ICOS was determined. Open bars represent C57BL/6NJ : LDLR$^{-/-}$ mice and shaded black bars represent IL-21R$^{-/-}$: LDLR$^{-/-}$ mice. Statistical analysis was performed using GraphPad Prism and by conducting an unpaired students t-test. * $P < 0.05$, ** $P < 0.01$, *** $P < 0.001$, **** $P < 0.0001$.

1.54.2   Summary of Findings

Taken together, our results provide strong evidence that IL-21R deficiency significantly attenuates Tfh cell formation *in vivo*. In addition to this, our results indicate that IL-21R deficiency significantly affects ICOS expression on Tfh cells *in vivo* – an important co-stimulatory molecule required for Tfh function.

1.55 IL-21R Deficiency Impairs GC B-cell Formation in IL-21R$^{-/-}$: LDLR$^{-/-}$ Mice

As well as Tfh cells, GC B-cell comprise a crucial component of the GC reaction. Interacting with Tfh cells, GC B-cells form the pre-cursors for antibody secreting, long-lived plasma cells and B-cell memory. Central to this developmental pathway, is the IL-21-IL-21R pathway, which induces GC B-cell proliferation and differentiation. As a result, we aimed to assess whether IL-21R deficiency would result in impaired GC B-cell formation *in vivo*.

Using flow cytometry, GC B-cell formation was assessed in C57BL/6NJ : LDLR$^{-/-}$ and IL-21R$^{-/-}$: LDLR$^{-/-}$ mice fed HFD for 14 weeks. To gain an understanding of how GC B-cell expression varied depending on location, GC B-cells were phenotyped in pLN, spleen and pao-LN compartments.

1.55.1   B220+ PNA+ FAS+ GC B-cells

In comparison to C57BL/6NJ : LDLR$^{-/-}$ mice, IL-21R$^{-/-}$: LDLR$^{-/-}$ mice displayed a significant reduction in the percentage of pLN B220+ PNA+ FAS+ GC B-cell populations (1.39 % vs 0.36 %) (Fig 42). Following a similar pattern, IL-21R deficiency resulted in the complete ablation of splenic B220+ PNA+ FAS+ GC B-cell populations (1.99 % vs 0.08 %) (Fig 43). This pattern was mirrored in the pao-LNs of mice, with IL-21R$^{-/-}$: LDLR$^{-/-}$ mice displaying near complete ablation of pao-LN B220+ PNA+ FAS+ GC B-cell profiles (3.49 % vs 0.38 %) (Fig 44).

Collectively, these results provide strong evidence that IL-21R expression is required for the formation and maintenance of GC B-cells, irrespective of anatomical location.
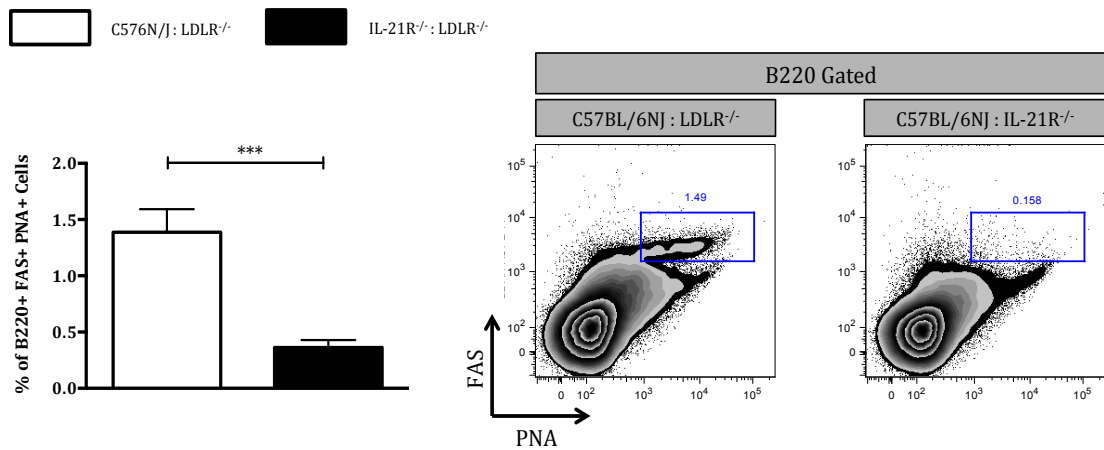
Figure 42: Percentage of B220+ FAS+ PNA+ GC B-cells in pLNs of C57BL/6NJ : LDLR$^{-/-}$ and IL-21R$^{-/-}$: LDLR$^{-/-}$ mice

Two groups of 8 week old LDLR$^{-/-}$ mice were lethally irradiated with 10.5 Grays X-ray radiation. Mice were subsequently injected i.v. with 4 X 10^6 C57BL/6NJ (n = 10) or IL-21R$^{-/-}$ (n = 9) bone marrow derived stem cells. Following recovery, both groups were placed on HFD for 14 weeks. Following completion of the dietary period, pLNs were harvested and GC B-cell populations assessed via surface flow cytometry staining. Lymphocytes were gated for on the basis of an initial FSC and SSC gate and a subsequent B220+ gate. Using this parent gate FAS+ PNA+ cells were gated. Open bars represent C57BL/6NJ : LDLR$^{-/-}$ mice and shaded black bars represent IL-21R$^{-/-}$: LDLR$^{-/-}$ mice. Representative plots are taken from end point analysis for each organ analysed. Statistical analysis was performed using GraphPad Prism and by conducting an unpaired students t-test. * $P < 0.05$, ** $P < 0.01$, *** $P < 0.001$, **** $P < 0.0001$.
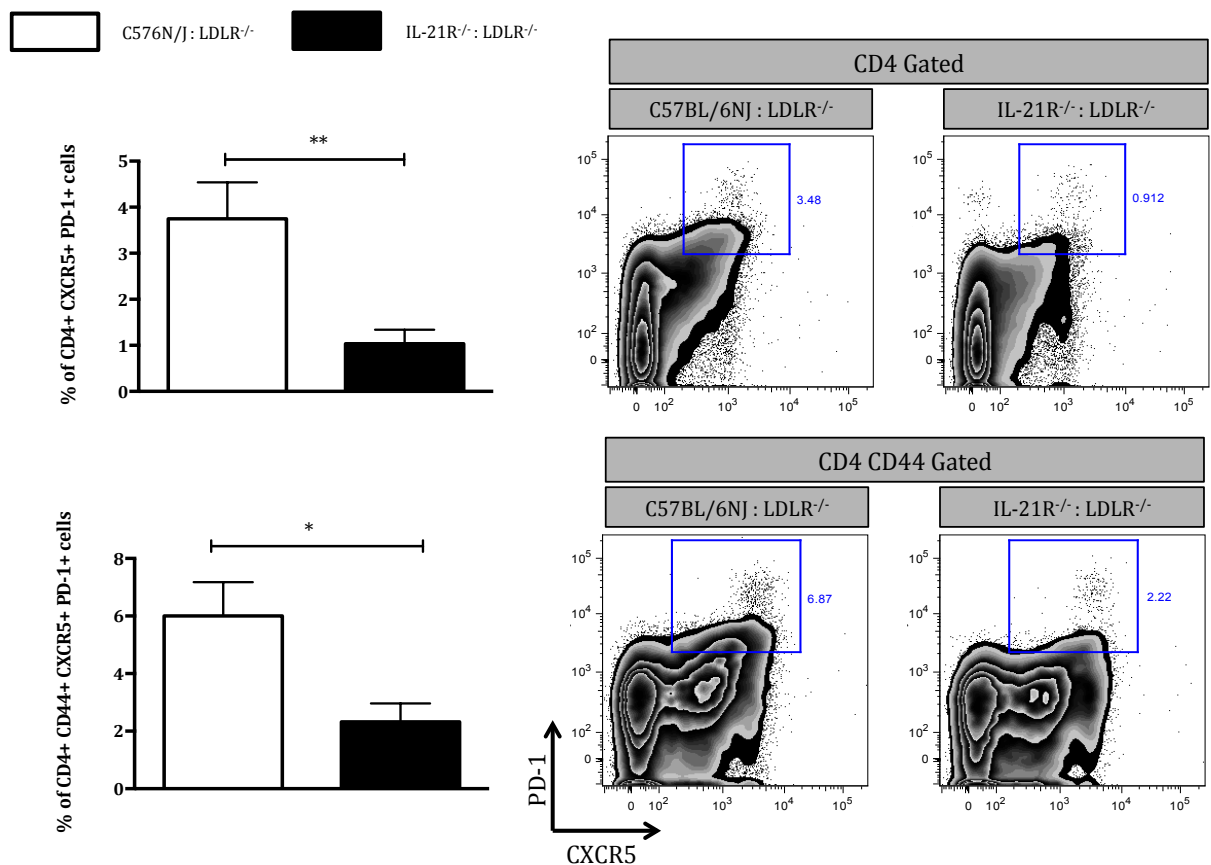
Figure 43: Percentage of B220+ FAS+ PNA+ GC B-cells in spleen of C57BL/6NJ : LDLR$^{-/-}$ and IL-21R$^{-/-}$: LDLR$^{-/-}$ mice

Two groups of 8 week old LDLR$^{-/-}$ mice were lethally irradiated with 10.5 Grays X-ray radiation. Mice were subsequently injected i.v. with 4 X 10^6 C57BL/6NJ (n = 10) or IL-21R$^{-/-}$ (n = 9) bone marrow derived stem cells. Following recovery, both groups were placed on HFD for 14 weeks. Following completion of the dietary period, spleens were harvested and GC B-cell populations assessed via surface flow cytometry staining. Lymphocytes were gated for on the basis of an initial FSC and SSC gate and a subsequent B220+ gate. Using this parent gate FAS+ PNA+ cells were gated. Open bars represent C57BL/6NJ : LDLR$^{-/-}$ mice and shaded black bars represent IL-21R$^{-/-}$: LDLR$^{-/-}$ mice. Representative plots are taken from end point analysis for each organ analysed. Statistical analysis was performed using GraphPad Prism and by conducting an unpaired students t-test. * $P < 0.05$, ** $P < 0.01$, *** $P < 0.001$, **** $P < 0.0001$.
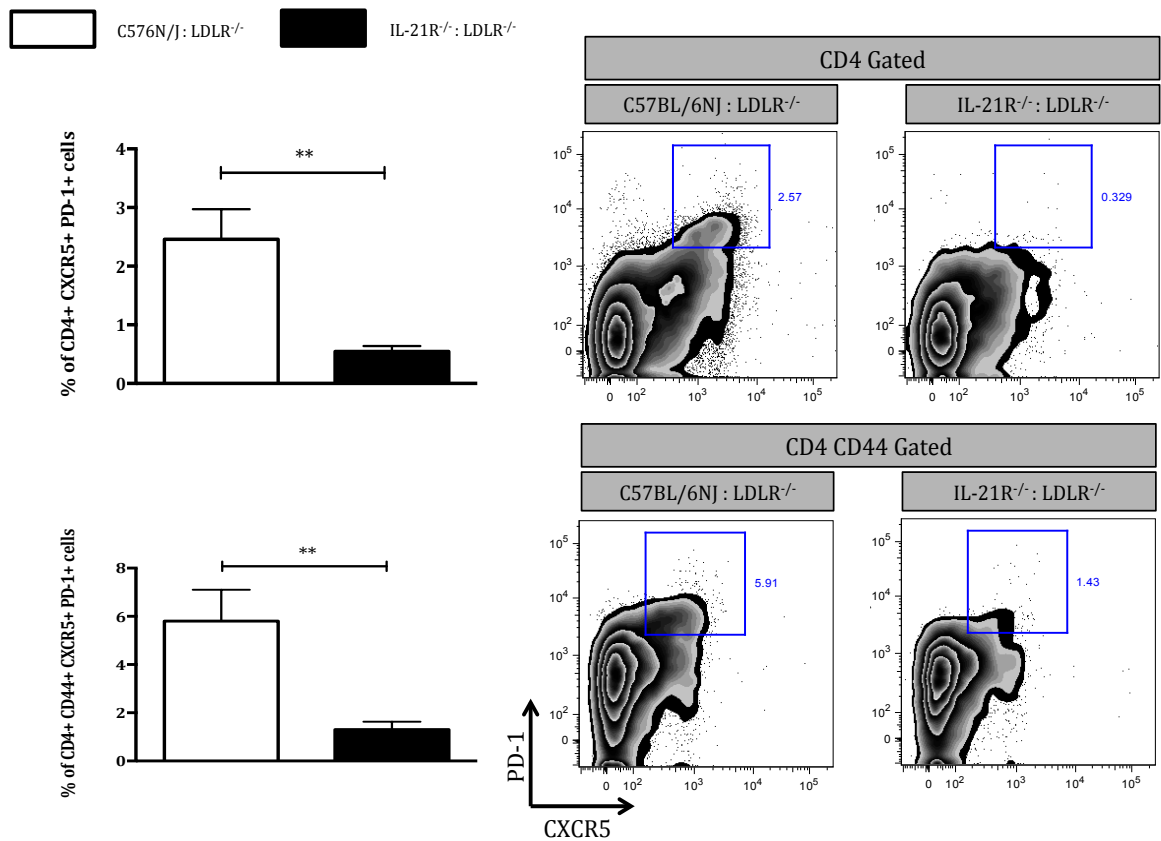
Figure 44: Percentage of B220+ FAS+ PNA+ GC B-cells in pao-LNs of C57BL/6NJ : LDLR$^{-/-}$ and IL-21R$^{-/-}$: LDLR$^{-/-}$ mice

Two groups of 8 week old LDLR$^{-/-}$ mice were lethally irradiated with 10.5 Grays X-ray radiation. Mice were subsequently injected i.v. with 4 X 10^6 C57BL/6NJ (n = 10) or IL-21R$^{-/-}$ (n = 9) bone marrow derived stem cells. Following recovery, both groups were placed on HFD for 14 weeks. Following completion of the dietary period, pao-LNs were harvested and GC B-cell populations assessed via surface flow cytometry staining. Lymphocytes were gated for on the basis of an initial FSC and SSC gate and a subsequent B220+ gate. Using this parent gate FAS+ PNA+ cells were gated. Open bars represent C57BL/6NJ : LDLR$^{-/-}$ mice and shaded black bars represent IL-21R$^{-/-}$: LDLR$^{-/-}$ mice. Representative plots are taken from end point analysis for each organ analysed. Statistical analysis was performed using GraphPad Prism and by conducting an unpaired students t-test. * $P < 0.05$, ** $P < 0.01$, *** $P < 0.001$, **** $P < 0.0001$.

1.55.2   Summary of Findings

In combination, our results indicate that IL-21R deficiency is important for the formation of B220+ FAS+ PNA+ GC B-cells *in vivo.* This is evident by the complete ablation of FAShi PNAhi expressing B220+ B-cells. As with Tfh cell populations, IL-21R deficiency results in ablation of GC B-cells in all organs assessed.

As a result, we were confident that our chimeric approach provided a reliable model for dual Tfh cell and GC B-cell deficiency *in vivo*.

1.55.3   IL-21R Ablation Attenuates Total IgM and IgG Titres While Exacerbating Total IgE Responses

Both Tfh cells and GC B-cells are intimately involved in the production of high affinity antibodies via GC reactions. Therefore, to study whether IL-21R ablation affected antibody production *in vivo* we measured serum antibody levels in both C57BL/6NJ : LDLR$^{-/-}$ and IL-21R$^{-/-}$: LDLR$^{-/-}$ mice. Specifically, we studied total IgM, IgG and IgE titres, as well as MDA-Ox-LDL specific IgM, IgG$_{2C}$, IgG$_1$ and IgG$_3$. As such, we gained an insight into the variation of total and antigen specific antibody kinetics in our chimeric mice.

IL-21R ablation resulted in an approximate two and a half-fold reduction in total serum IgM titres (Fig 45). Mirroring this, loss of IL-21R resulted in a significant reduction in total serum IgG (Fig 45). Interestingly, and in comparison to IgM and IgG titres, IL-21R$^{-/-}$: LDLR$^{-/-}$ mice displayed approximately 4 times more total serum IgE than C57BL/6NJ$^{-/-}$: LDLR$^{-/-}$ control mice (Fig 45).
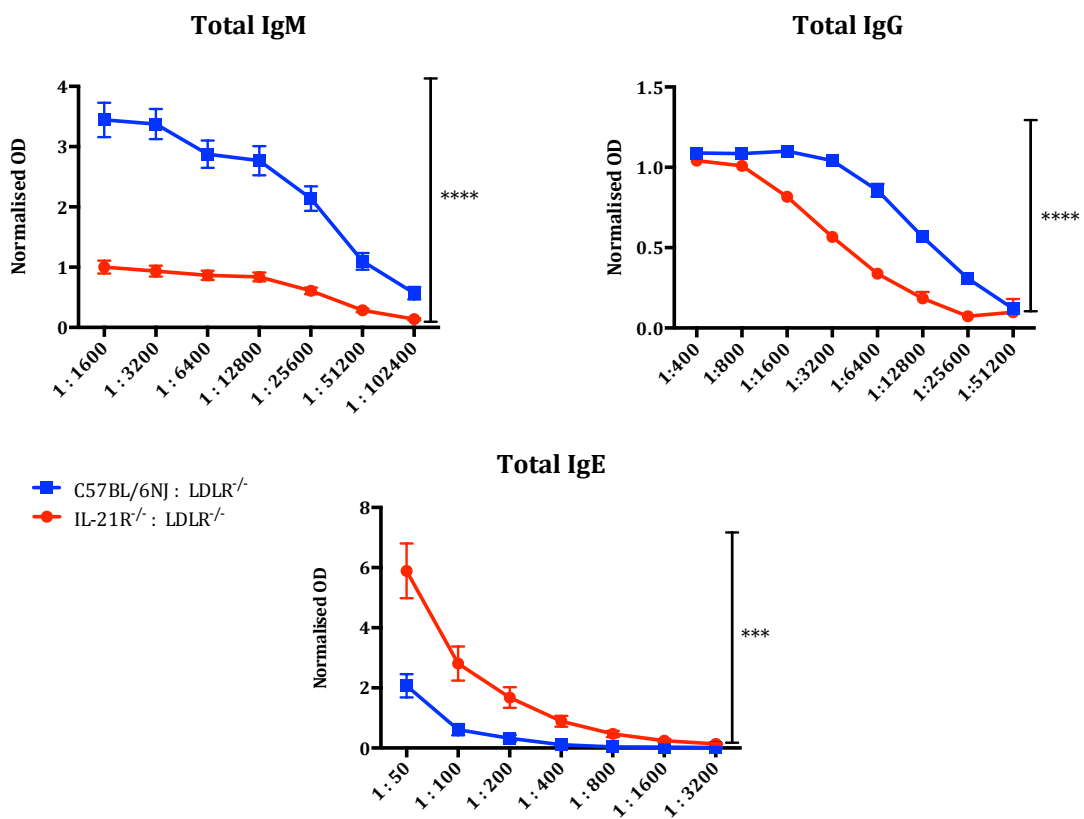
Figure 45: Total IgM, IgG and IgE serum antibody kinetics in C57BL/6NJ : LDLR$^{-/-}$ and IL-21R$^{-/-}$: LDLR$^{-/-}$ mice

Serum from C57BL/6NJ : LDLR$^{-/-}$ and IL-21R$^{-/-}$: LDLR$^{-/-}$ mice was tested for the presence of total IgM, IgG and IgE antibodies. Plots display titration of serum from both groups, from concentrated to most dilute. Results are displayed as normalised mean OD values for each dilution. Normalised values were calculated by dividing OD values with OD values of a constant dilution of C57BL/6NJ serum on each ELISA plate. Statistical analysis was performed using GraphPad Prism and by conducting a two-way-ANOVA * $P < 0.05$, ** $P < 0.01$, *** $P < 0.001$, **** $P < 0.0001$.

1.55.4 IL-21R Deficiency Significantly Attenuates MDA-Ox-LDL IgM and IgG$_{2c}$ Responses

As well as determining total antibody titres, we studied antibody titres to the pathological Ox-LDL. Described as the implicated antigen in atherosclerosis, Ox-LDL is important to the formation of intra-arterial plaques. Specifically, we determined anti-MDA-Ox-LDL-IgM, IgG$_{2c}$, IgG$_1$, IgG$_3$ and IgE serum antibody titres.

In comparison to C57BL/6NJ : LDLR$^{-/-}$ mice, IL-21R$^{-/-}$: LDLR$^{-/-}$ mice displayed a significant reduction in anti-MDA-Ox-LDL-IgM and anti-MDA-Ox-LDL-IgG$_{2c}$ serum levels (Fig 46). In contrast, no difference in anti-MDA-Ox-LDL IgG$_1$ titres between both groups was found (Fig 46). Although displaying a trend towards reduction, no significant difference in anti-MDA-Ox-LDL IgG$_3$ serum antibody levels between both groups was detected (Fig 46). Anti-MDA-Ox-LDL-IgE titres were below the limit of detection in both C57BL/6NJ : LDLR$^{-/-}$ and IL-21R$^{-/-}$: LDLR$^{-/-}$ mice (data no shown).
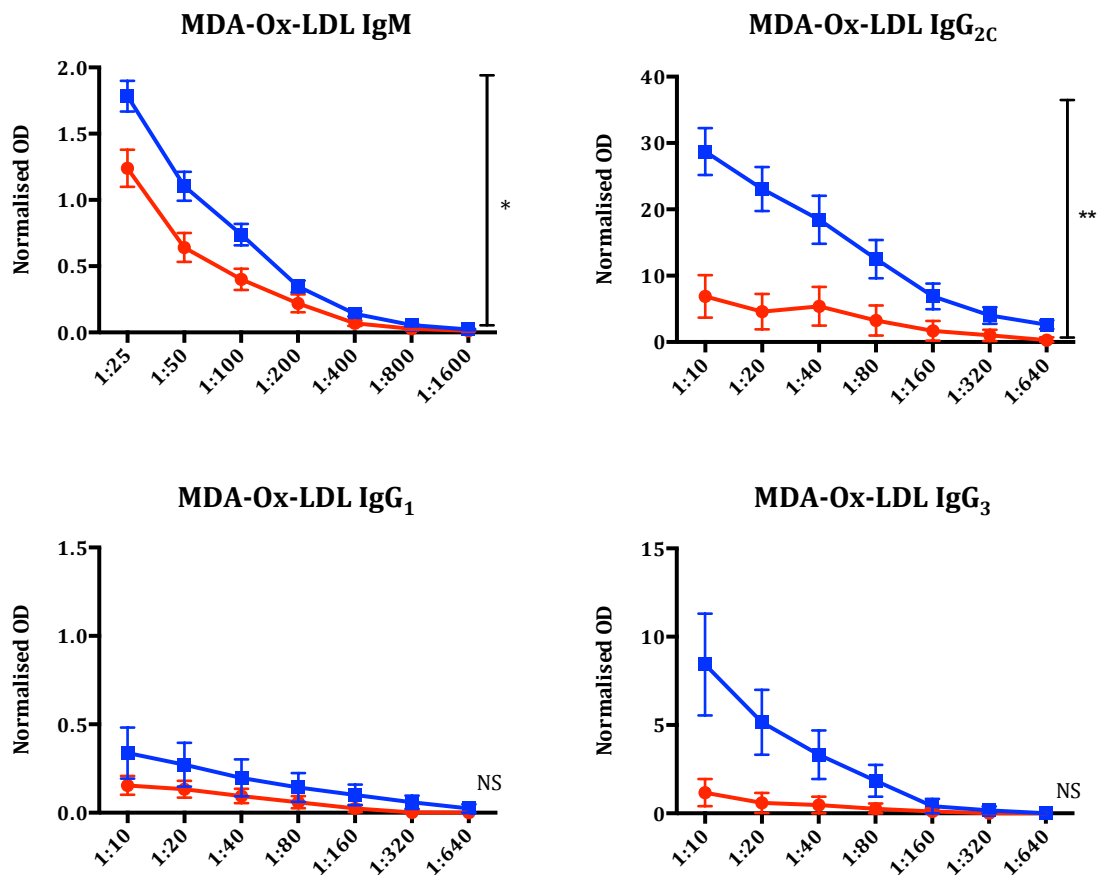
Figure 46: Anti-MDA-Ox-LDL-IgM, IgG$_{2c}$, IgG$_1$ and IgG$_3$ serum antibody levels in C57BL/6NJ : LDLR$^{-/-}$ and IL-21R$^{-/-}$: LDLR$^{-/-}$ mice

Serum from C57BL/6NJ : LDLR$^{-/-}$ and IL-21R$^{-/-}$: LDLR$^{-/-}$ mice was tested for the presence of total anti-MDA-Ox-LDL-IgM, IgG$_{2c}$, IgG$_1$ and IgG$_3$ antibodies. Plots display titration of serum from both groups, from concentrated to most dilute. Results are displayed as normalised mean OD values for each dilution. Normalised values were calculated by dividing OD values with OD values of a constant dilution of C57BL/6NJ serum on each ELISA plate. Statistical analysis was performed using GraphPad Prism and by conducting a two-way-ANOVA * $P < 0.05$, ** $P < 0.01$, *** $P < 0.001$, **** $P < 0.0001$.

1.55.5 IL-21R Deficiency Enhances Atherosclerosis Formation in the Aortic Sinus but does not Affect Plaque Burden in the Aortic Tree

Our results provide strong evidence as to the important role of IL-21R signalling in the maintenance of Tfh cell and GC B-cell populations *in vivo*. As well as this, our results show that loss of such populations coincides with significantly attenuated antibody responses. Taking this further, we wished to determine whether IL-21R ablation affected plaque formation *in vivo.*
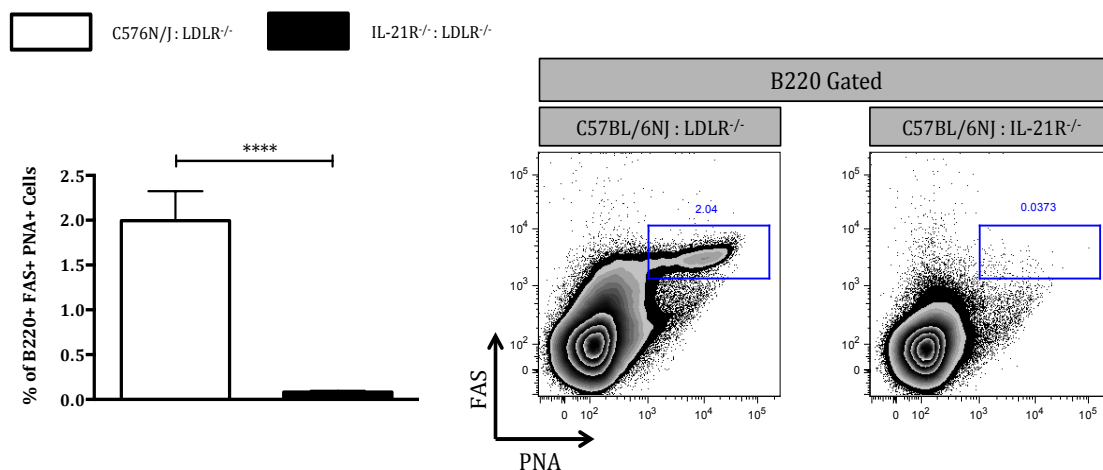
To study this, we used various histological approaches to quantify plaque burden and phenotype in areas predisposed to lesion formation. As such, we were able to determine whether IL-21R deficiency affected lesion formation in IL-21R$^{-/-}$: LDLR$^{-/-}$ mice.

To obtain a comprehensive assessment of the effects IL-21R deficiency had on atherosclerosis formation, the following histological parameters were assessed.

Stain	Organ Assessed	Aim of Histological Procedure	Question Addressed
Oil Red O (ORO)	Aortic Sinus	To quantify plaque burden in an area susceptible to lesion formation.	Does IL-21R deficiency result in modified plaque burden?
Oil Red O (ORO)	Whole Aorta	To determine whole aorta plaque burden.	Does IL-21R deficiency result in whole aorta modified plaque burden?
Picro Sirius Red	Aortic Sinus	To quantify collagen fiber content in an area susceptible to lesion formation.	Does IL-21R deficiency result in a more stable or unstable plaque phenotype?
CD68	Aortic Sinus	To quantify macrophage burden in an area susceptible to lesion formation.	Does IL-21R deficiency result in enhanced macrophage infiltration to a site susceptible to plaque formation?

Table 4: Stains used for histological assessment of atherosclerotic plaque formation and lesion composition in C57BL/6NJ : LDLR$^{-/-}$ and IL-21R$^{-/-}$: LDLR$^{-/-}$ mice.

1.56 Histological Assessment of Atherosclerosis in IL-21R$^{-/-}$: LDLR$^{-/-}$ Mice

1.56.1 IL-21R Deficiency Does Not Affect Plaque Burden in the Aortic Tree

To quantify whole aorta lesion composition, whole mount aortas were stained with the lipid stain - ORO. By measuring total plaque area and total aorta area, the percentage of whole aorta comprising plaque was calculated.

IL-21R deficiency did not affect lesion formation throughout the aortic tree (Fig 47).
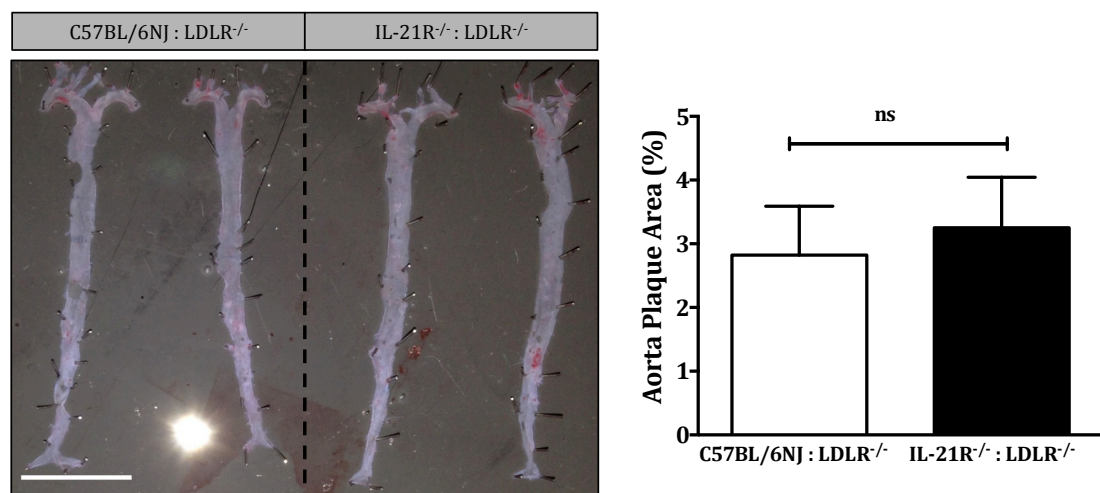
Figure 47: Whole aorta En Face Oil Red O staining

Aortas from C57BL/6NJ : LDLR$^{-/-}$ (n = 10) and IL-21R$^{-/-}$: LDLR$^{-/-}$ (n = 9) mice were dissected as previously described. Following excision of visceral fat, samples were stained with ORO and cut longitudinally through their luminal opening and pinned out using fine dissection needles. En face images were acquired using an 8-megapixel camera. Using imagej quantification software, total aorta area was measured alongside ORO positive plaque area. Percentage of aorta plaque area was calculated. Bar = 100 μm Statistical analysis was performed using GraphPad Prism and by conducting an unpaired students t-test. * $P < 0.05$, ** $P < 0.01$, *** $P < 0.001$, **** $P < 0.0001$.
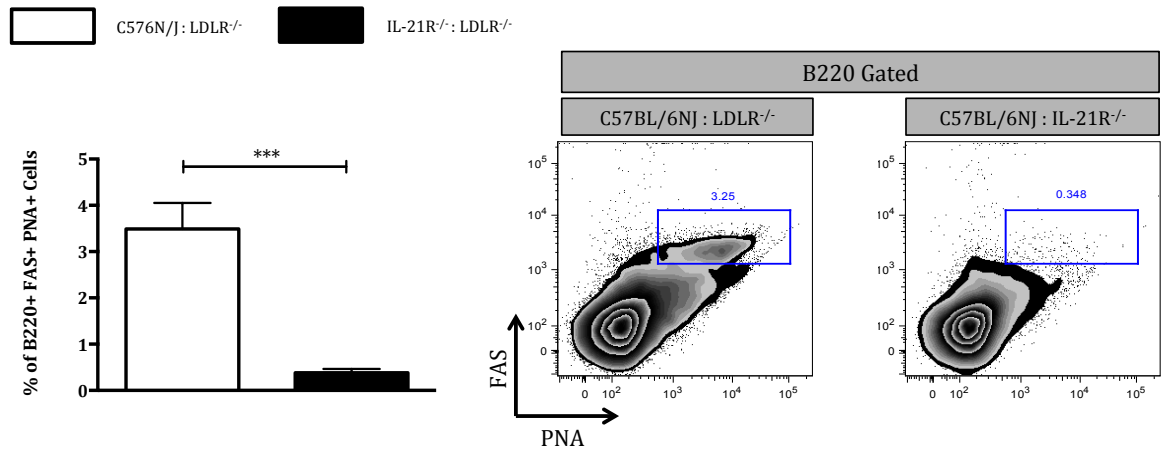
1.56.2 IL-21R Deficiency Results in Enhanced Sinus Plaque Content

Using ORO stain, total plaque content of aortic sinuses from C57BL/6NJ : LDLR^{-/-} and IL-21R^{-/-} : LDLR^{-/-} mice was assessed. To gain an appreciation of plaque content throughout the aortic sinus, 11 sequential sections from each animal were stained with ORO and plaque area plotted against sinus thickness. Sections stained started from 0 μm and ended at 660 μm.

In comparison to C57BL/6NJ : LDLR^{-/-} mice, IL-21R^{-/-} : LDLR^{-/-} mice displayed an approximate a two fold increase in sinus plaque area (Fig 48). This variation was consistent throughout the entire aortic sinus of IL-21 deficient mice.
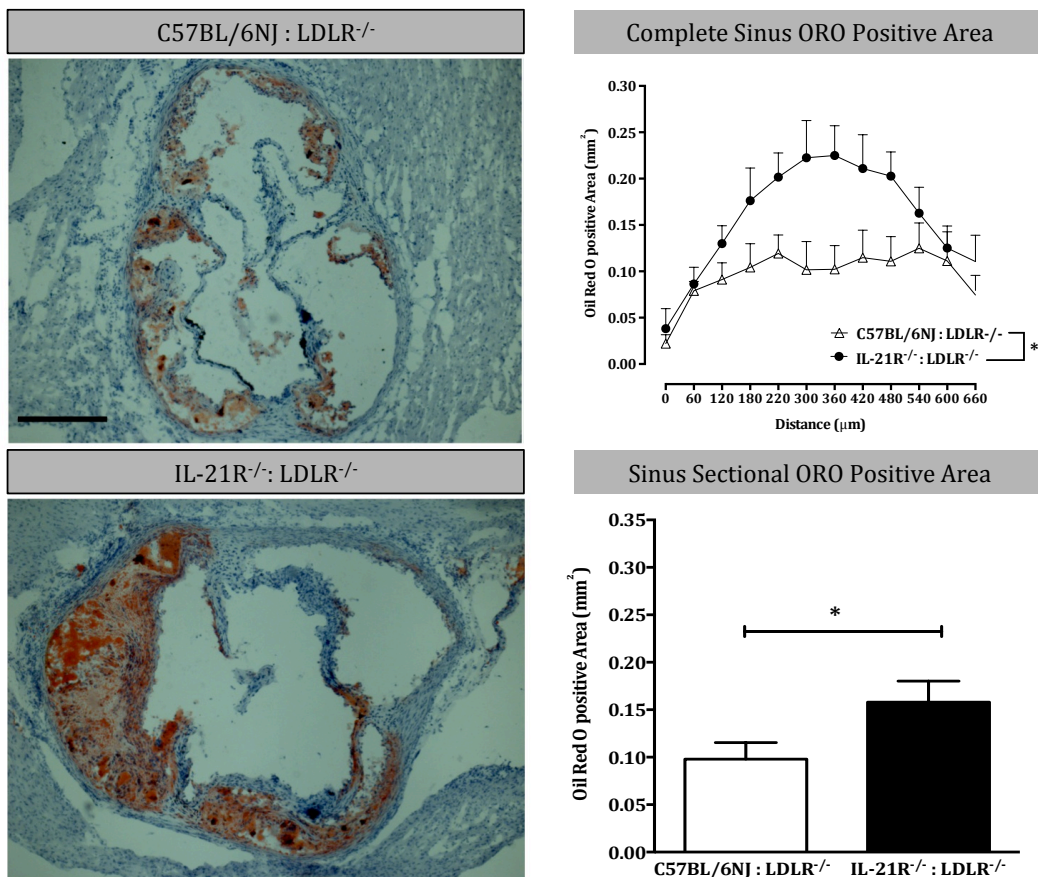
Figure 48: Aortic sinus – sequential Oil Red O staining

Aortic sinuses from C57BL/6NJ : LDLR$^{-/-}$ (n = 10) and IL-21R$^{-/-}$: LDLR$^{-/-}$ (n = 9) mice were dissected as previously described. 8 micron thick sections were cut, with sections being stained in 60 micron increments. Sections were cut until a total length of 660 microns was reached, thus allowing for the depiction of lesion progression throughout the aortic sinus. Sections were stained with ORO and haematoxylin counterstain was applied. Sections were mounted in ProlongGold mountant and imaged using a light microscope (EVOS cell imaging station, life Technologies). Bar = 100 μm. Statistical analysis was performed using GraphPad Prism and by conducting an unpaired students t-test. * *P* < 0.05, ** *P* < 0.01, *** *P* < 0.001, **** *P* < 0.0001.

1.56.3 IL-21R Ablation Does not Affect Aortic Sinus Collagen Content

Using polarised light and conventional light microscopy, collagen content in the aortic sinus of C57BL/6NJ : LDLR$^{-/-}$ and IL-21R$^{-/-}$: LDLR$^{-/-}$ mice was determined. Using Picrosirius Red staining, collagen content was assessed on sequentially cut sinus sections (determined every 60 μm). Sections were cut and stained to a completion of 660 μm.

IL-21R deficiency did not alter sinus plaque content, with the percentage of sinus collagen being equivalent in C57BL/6NJ : LDLR$^{-/-}$ and IL-21R$^{-/-}$: LDLR$^{-/-}$ mice (Fig 49). As such, these findings suggest that IL-21R deficiency does not affect plaque collagen content.
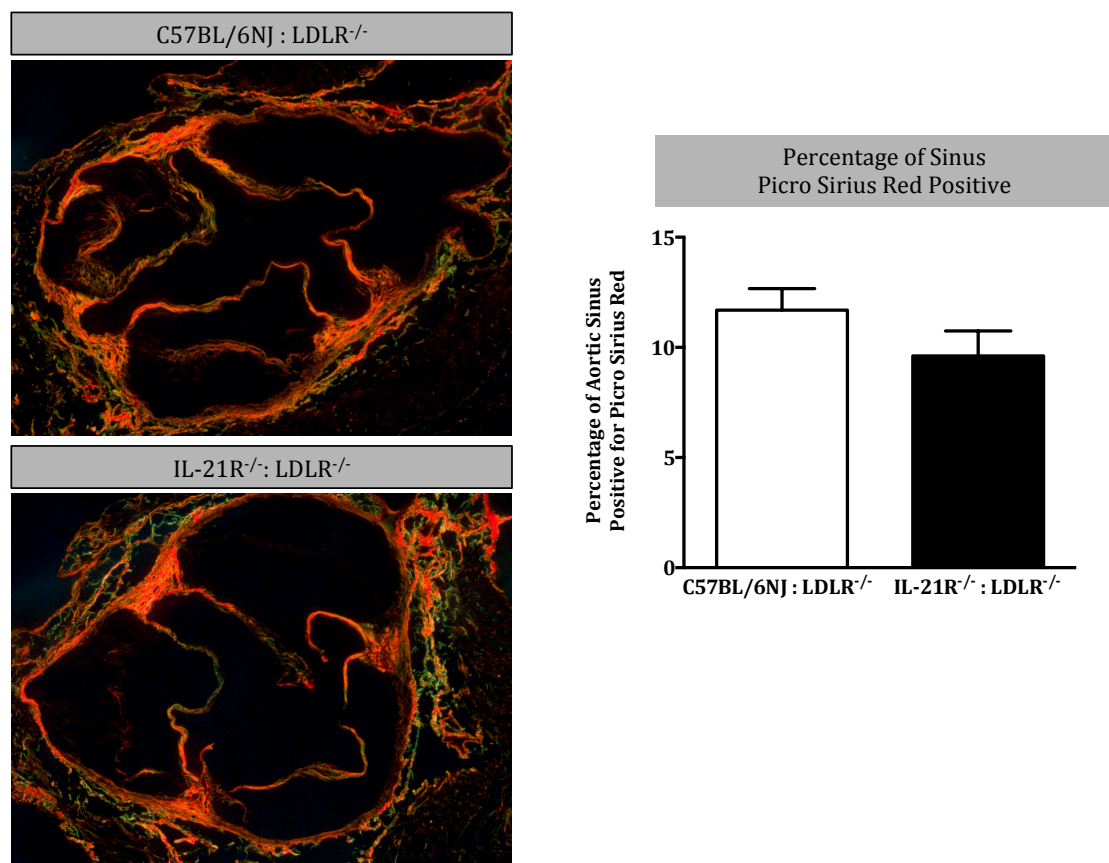
Figure 49: Aortic sinus Picro Sirius red staining

Aortic sinuses from C57BL/6NJ : LDLR$^{-/-}$ and IL-21R$^{-/-}$: LDLR$^{-/-}$ mice were dissected as previously described. Sections were stained with Picro Sirius Red Samples were subsequently mounted using DPX mounting media and visualised under polarised light using an epifluorescent microscope at X5 magnification. Statistical analysis was performed using GraphPad Prism and by conducting an unpaired students t-test. * $P <$ 0.05, ** $P <$ 0.01, *** $P <$ 0.001, **** $P <$ 0.0001.

1.56.4 IL-21R Ablation Results in Reduced Sinus CD68 Macrophage Infiltration

Macrophages represent one of the most readily recognised hallmarks of early atherogenesis and their plaque content influence lesion stability. As such, the effects of IL-21R ablation on sinus macrophage content were studied.

Using fluorescent microscopy, we stained for CD68 expressing macrophages in sequential sinus sections from C57BL/6NJ : LDLR$^{-/-}$ and IL-21R$^{-/-}$: LDLR$^{-/-}$ mice. When compared to control mice, we found that IL-21R deficient mice displayed significantly enhanced sinus CD68+ macrophage infiltration. Therefore indicating that IL-21R deficiency results in enhanced macrophage accumulation and increased plaque inflammation and instability (Fig 50).
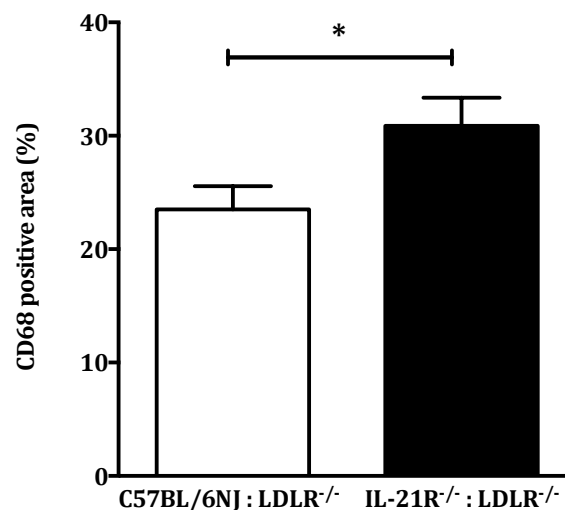
Figure 50: Aortic sinus – sequential CD68 macrophage staining

Aortic sinuses from C57BL/6NJ : LDLR$^{-/-}$ and IL-21R$^{-/-}$: LDLR$^{-/-}$ mice were dissected as previously described. Sections were incubated in rat-anti-mouse CD68 and subsequently donkey-anti-rat-IgG conjugated to CY3. Sections were then mounted in ProlongGold mountant containing DAPI. Sections were analysed using an epifluorescent microscope at X40 magnification. Statistical analysis was performed using GraphPad Prism and by conducting a students t-test. * $P < 0.05$, ** $P < 0.01$, *** $P < 0.001$, **** $P < 0.0001$.

1.56.5 Summary of Findings

Our en face studies suggest that IL-21R deficiency does not affect lesion formation in the whole aorta. This was evident by the finding that en face lesion formation was indifferent between C57BL/6NJ : LDLR$^{-/-}$ and IL-21R$^{-/-}$: LDLR$^{-/-}$ mice. In contrast to this, our sinus studies suggest that IL-21R deficiency functions to enhance lesion formation and an unstable/proinflammatory plaque phenotype (as indicated by enhanced CD68+ macrophage content). This was evident by the finding that IL-21R deficient mice displayed enhanced sinus lesion size and macrophage content.

1.57 Discussion

In this chapter, we studied the effects of IL-21R deficiency in the context of atherosclerosis. To do this, we generated IL-21R$^{-/-}$: LDLR$^{-/-}$ and C57BL/6NJ : LDLR$^{-/-}$ chimeric mice; in which hematopoietic stem cells were void of IL-21R expression. Using surface flow cytometry staining, IF and ELISAs; we determined the effects of IL-21R deficiency on Tfh cell and GC B-cell formation, antibody production and disease progression.

1.57.1   Summary of Findings

In this chapter, we demonstrated that IL-21R deficiency – in context of hyperlipidemia – significantly attenuates Tfh cell and GC B-cell formation *in vivo*. This reduction was associated with a significant increase in sinus plaque content and macrophage infiltration, with no difference in sinus collagen content and plaque formation throughout the aortic tree. Linking Tfh cell and GC B-cell kinetics, IL-21R$^{-/-}$: LDLR$^{-/-}$ mice displayed significantly attenuated total IgM and IgG serum antibody titres. This was coupled with a significant reduction in MDA-Ox-LDL specific IgG$_{2C}$, while MDA-Ox-LDL IgG$_1$ and IgG$_3$ titres remained unchanged. IL-21R ablation also resulted in enhanced total IgE titres.

Together, our results indicate that IL-21R signalling is athero-protective *in vivo*, and may exert its effects via modulation of the Tfh cell / GC B-cell axis. Our findings add to the area of adaptive immunity in atherosclerosis, with few studies addressing the role of the Tfh cell / GC B-cell axis in plaque formation. Our results also provide an interesting insight into the therapeutic advantage of Tfh cell / GC B-cell modulation in atherosclerosis.

1.57.2 Tfh cell and GC B-cell Development in IL-21R^{-/-} : LDLR^{-/-} Mice is Significantly Reduced in Comparison to C57BL/6NJ : LDLR^{-/-} Mice

Using flow cytometry, we stained for Tfh cells and GC B-cells in the pLNs, spleen and pao-LNs of chimeric mice fed HFD for 14 weeks. This allowed us to study the effects of IL-21R deficiency on Tfh cell and GC B-cell formation in systemic and local environments; where auto-reactive immune cells circulate and drain affected arteries respectively.

We found that Tfh cell and GC B-cell expression was significantly reduced in IL-21R^{-/-} : LDLR^{-/-} mice. We propose this is due to the lack of IL-21R signalling, providing important proliferation and differentiation signals to both Tfh cells and GC B-cells. Indeed, IL-21R signalling is important for the induction of the Tfh cell associated transcription factors, including Bcl-6 and c-maf [285, 335]. As well as this, IL-21 acts directly on GC B-cells to induce proliferation, isotype switching, expression of Bcl-6 and survival of antigen specific memory B-cells [170, 204, 205, 305, 306]. It is likely these processes were deficient in our model and, as a result, mice failed to develop bonafide Tfh cell and GC B-cell populations. As a consequence, IL-21R deficient mice failed to develop functional GC reactions with impaired B-cell switching and antibody production.

Interestingly, some have suggested that Tfh cells can form independent of conventional IL-21R signalling [205, 283]. Raising questions over the importance of IL-21, these studies suggest the involvement of additional pathways in Tfh cell formation. Indeed some have provided evidence to suggest that IL-21 can co-stimulate with the TCR of T-cells [206, 296]. Adding to this, others have indicated the IL-21s ability to induce signalling molecules, other that JAK and STAT proteins [310]. It is therefore plausible that the role of additional pathways involved in Tfh cell development may explain the presence of Tfh cells in such studies. In support of the notion that additional mechanisms drive Tfh cell development, adjuvant administration has been shown to enhance T-cell survival via up-regulation of Bcl-3 *in vivo* [336].

Irrespective of the studies above, we have shown unequivocally that IL-21R deficiency significantly attenuates Tfh cell and GC B-cell formation in experimental atherosclerosis.

1.57.3 Deficient Tfh cell and GC B-cell Responses Have an Impact on Atherosclerosis Formation

Moving from studying the role of IL-21R deficiency on Tfh cell and GC B-cell development, we assessed whether IL-21R ablation affected atherosclerosis progression. Using histochemical approaches, we found that IL-21R deficiency significantly attenuated plaque formation and macrophage infiltration into the aortic sinus of mice. Sinus collagen content remained unchanged, as did total aorta plaque content.

Supporting our findings, others have shown the pro-inflammatory effects of IL-21R deficiency in models of experimental autoimmune encephalomyelitis (EAE) [337], SLE [338] and chronic arthritis [339]. Linking both Tfh cells and GC B-cells to pathological progression, we suggest that enhanced atherosclerosis in our model is a result of defective Tfh cell and GC B-cell responses, induced by insufficient IL-21R signalling.

In contrast to our findings, genome wide association studies (GWAS) have identified risk variants in the IL-21 gene locus for autoimmune conditions, including SLE [340], RA [341] and diabetes [342]. This is complimented by the finding that IL-21R deficiency ameliorates disease severity in several models of autoimmunity [326, 332, 343, 344].

Although, these studies contradict our findings, some other studies have provided an interesting explanation for this apparent discrepancy. Pointing to the diverse range of effects IL-21 can exert, others have reported that IL-21 can function as both a pro-inflammatory and anti-inflammatory cytokine. Specifically, in the BXSB-yaa mouse model of SLE, neutralisation of IL-21R signalling by IL-21R-Fc antibody exacerbates disease in early stages and reduces disease at later stages. The reason for this

differential regulation is unknown, however is most likely to be linked to the dynamic induction of regulatory compartments later on in the BXSB-yaa model. Mirroring these findings, IL-21R deficiency in two models of inflammatory arthritis functions to be protective at one phase and detrimental at another [339].

Interestingly, IL-21R$^{-/-}$ mice induced to develop inflammatory arthritis display impaired regulation of suppressor of cytokine signalling (SOCS) proteins [339]. As well as inhibiting JAK / STAT signalling [345, 346], SOCS proteins also inhibit TLR signalling [347]. As such, impaired regulation of TLR signalling – as a result of deficient SOCS expression – may explain enhanced pathology observed in our study. In recent years, the role of TLR signalling in atherosclerosis has been studied in detail. Deficiency of myeloid differentiation primary response gene 88 (MyD88) – one of the major TLR signalling molecules – has been reported to both promote and inhibit atherosclerosis formation [348-350]. These findings are most likely due to the expression of TLRs on various immune cell subsets, with each subset playing distinct roles in atherosclerosis. Suggesting a pro-atherogenic role of TLR2 and TLR4 signalling in atherosclerosis, specific deletion of these receptors conveys protection from lesion development [351, 352]. It is therefore plausible that impaired regulation of TLRs by SOCS proteins in our mice may have resulted in increased TLR activation and enhanced pathology. To say with certainty that TLR mediated processes contribute significantly to disease progression in our model, assessment of TLR expression in IL-21R$^{-/-}$: LDLR$^{-/-}$ mice would be necessary.

In combination, these findings suggest that IL-21 may not simply function as a pro-inflammatory or anti-inflammatory cytokine; rather play distinct roles in different stages of the immune response. To determine whether IL-21R deficiency exerts the same dual effects in our model, it would be advantageous to quantify atherosclerosis formation in IL-21R$^{-/-}$: LDLR$^{-/-}$ mice at early and late stage atherosclerosis.

1.57.4 IL-21R Deficiency Alters the Pro-atherogenic / Athero-protective Antibody Response *in vivo.*

In this study, we demonstrated that loss of IL-21R signalling significantly attenuated GC B-cell and Tfh cell populations *in vivo*. Moreover, loss of these populations significantly altered antibody production. As such, our data demonstrates the central role of IL-21R signalling in Tfh cell and GC B-cell formation and function.

The role of antibodies in atherosclerosis has been the subject of much debate for years. Generally, IgM antibodies are perceived to confer athero-protective effects [353], while their switched counterparts – specifically IgG_{2c} – are believed to be pro-atherogenic. Preventing Ox-LDL uptake into macrophages, IgM antibodies prevent the formation of pathological foam cells as well as forming immune complexes that prevent Ox-LDL accumulation [354]. Moreover, increased IgM titres are linked to reduced atherosclerosis formation in humans as well as reduced cell death and cell debris formation [355]. In contrast to this, IgG antibodies have been shown to potentiate scavenger receptor (SR) mediated uptake of Ox-LDL into artery resident macrophages, thus enhancing atherosclerosis formation.

Considering the intimate link between the Tfh cell : GC B-cell axis and antibody production, we propose that variations in antibody kinetics are to explain for the enhanced pathology is IL-21R deficient mice. As such, we propose herein, a mechanism by which loss of IL-21R alters GC processes and subsequent pathology. To summarise, IL-21R deficiency significantly alters serum antibody titres as follows,

- Attenuated total IgM and IgG titres
- Reduced MDA-Ox-LDL specific IgG_{2c} titres
- Enhanced total IgE titres

Due to the loss of athero-protective MDA-Ox-LDL IgM antibodies, we propose that IL-$21R^{-/-}$: $LDLR^{-/-}$ mice would be deficient in their ability to control pathogenic Ox-LDL levels. As such, it is plausible to assume that IL-$21R^{-/-}$: $LDLR^{-/-}$ mice would display enhanced macrophage and foam cell formation. This phenomenon was confirmed in

our histochemical studies of the sinus, where IL-21R deficient mice displayed significantly enhanced CD68+ macrophage infiltration.

IL-21R ablation also enhanced serum IgE expression, while no MDA-Ox-LDL IgE titres could be detected in both groups. This finding is supported by the negative role of IL-21R signalling in murine IgE B-cell switching [356]. Due to the loss of this axis, we propose that IgE specific B-cells fail to receive suppressive signals. As such, negative regulation of IgE specific germ line transcription factors is prevented, leading to enhanced IgE specific B-cell proliferation and IgE production. It is likely that this process explains the enhanced total IgE titres found in IL-21R$^{-/-}$: LDLR$^{-/-}$ mice. Further supporting our data, others have demonstrated the potent effects of IL-21R deficiency on enhancing the IgE subtype *in vivo* [205, 226, 306]. Of importance to our study, IgE has been linked to increased atherosclerosis in both humans and mice [174]. Specifically, IgE has been shown to increase macrophage activation, cellular apoptosis and necrotic core formation [174]. Moreover, IgE also functions to enhance number of lesional T cells, mast cells and MHC-II expression [174]. Taking these findings into account, we propose that a culmination of impaired protection from reduced IgM and enhanced susceptibility from increased IgE explains increased disease in IL-21R deficient mice. To confirm the involvement of IgE in our model, it would be logical to use histochemical approaches to determine IgE and its receptor expression in lesions from C57BL/6 : LDLR$^{-/-}$ and IL-21R$^{-/-}$: LDLR$^{-/-}$ mice. As such, this would comprise a plausible follow up study.

As discussed before, IgG$_{2c}$ has been linked to increased lesion formation. Importantly, IL-21R ablation significantly reduced circulation IgG$_{2c}$. As such, it would be logical to assume that loss of IgG$_{2c}$ antibodies would convey athero-protection. Although this may be true, it is likely that the pro-atherogenic effect of increased IgE and diminished athero-protection from reduced IgM masked IgG$_{2c}$'s effects.

Taken together, we propose a mechanism by which IL-21R deficiency significantly enhances atherosclerosis formation. We propose that IL-21R deficiency induced ablation of Tfh cell and GC B-cell populations significantly alters the pro-atherogenic / athero-protective antibody response in atherosclerosis. As a result, pro-atherogenic antibody responses predominate, while athero-protective responses are hindered,

thus leading to lesion formation. Figure 51 summarises the proposed mechanism by which IL-21R ablation may enhance atherosclerosis formation *in vivo*.

IL-21R$^{-/-}$: LDLR$^{-/-}$

Tfh : GC B-cell Axis

Tfh cells
GC B-cells

Pathology

Lesion formation
Lesion cellularity

IgM **Athero-protective**
Total : ↓
MDA-Ox-LDL : ↓

- Decreased protection from MDA-Ox-LDL IgM titers
  - Enhanced Ox-LDL accumulation and foam cell formation

IgE **Pro-atherogenic**
Total : ↑
MDA-Ox-LDL : ↓

- Enhanced total IgE titers
  - Enhanced inflammatory cell involvement
  - Increased plaque formation

Pro-atherogenic

Athero-protective

Arterial Pathology

212

Figure 51: Mechanism by which IL-21R ablation enhances atherosclerosis formation

Following reconstitution of donor bone marrow, IL-21R$^{-/-}$: LDLR$^{-/-}$ mice displayed significantly reduced Tfh cell and GC B-cell populations in all organs assessed (pLNs, spleen and pao-LNs). This was coupled with a concomitant increase in lesion burden and instability. Comprising a functional component of these changes, IL-21R$^{-/-}$: LDLR$^{-/-}$ mice displayed significant reductions in total IgM and IgG and MDA-Ox-LDL IgM and IgG$_{2C}$. Consistent with the negative effects of IL-21R signalling on IgE production, IL-21R ablation significantly enhanced total serum IgE titres. As such, we propose that the pro-atherogenic antibody response is dominant in IL-21R$^{-/-}$: LDLR$^{-/-}$ mice (increased IgE and reduced IgM), leading to reduced protection from atherosclerosis and enhanced lesion formation.

1.57.5 IL-21R Deficiency's May Regulate Other Pro-inflammatory Cell Types

As discussed earlier in this chapter, IL-21 exerts a range of pleotropic effects on different cellular subtypes. It is, therefore, important to consider the possibility that IL-21R ablation may have affected the function and/or proliferation of these subsets. The effect that this may have had on disease progression must therefore be discussed.

Enhanced disease severity in BXSB-Yaa mice treated with IL-21-Fc has been attributed to defective CD8+ T-reg populations *in vivo* [344]. Indeed, IL-21 functions to enhance the proliferation of CD8+ T-regs and promote their survival. Functioning as a checkpoint for aberrant T-cell responses, CD8+ T-regs help maintain self-tolerance. It is plausible, that in our model, IL-21R deficiency resulted in defective CD8+ T-reg expansion, resulting in aberrant T-effector cell expansion and function. It would therefore, be advantageous to assess the expression of other T-helper cell subtypes – name Th1 cells - in our model. Of great importance to our study, CD8+ T-regs have been shown to limit atherosclerosis progression by modulating the Tfh cell / GC B-cell axis *in vivo* [142]. It is, therefore, possible that loss of CD8+ T-reg populations in our mice would result in defective T-cell regulation and may explain our findings. Subsequent follow-up studies, profiling CD8+ T-reg populations in IL-21R$^{-/-}$: LDLR$^{-/-}$ and C57BL/6NJ : LDLR$^{-/-}$ mice would provide an interesting insight into whether CD8+ T-reg compartments are deficient in our model.

As well as affecting regulatory processes, IL-21 inhibits DC function and induces DC apoptosis. Particularly, IL-21 reduces major histocompatibility complex-II (MHC-II) expression on the surface of DCs [297]. As a result, IL-21 can function to inhibit antigen presentation and subsequent T-cell activation [298]. It is therefore plausible that, in comparison to C57BL/6NJ : LDLR$^{-/-}$ control mice, IL-21R$^{-/-}$: LDLR$^{-/-}$ mice displayed enhanced antigen presenting capacity, thus influencing increased effector T-cell responses. Indeed DC function is important to lesion formation and variations in antigen presenting capacity may impact on pathology greatly. As such, Assessment of MHC-II expression on DC subsets from control and IL-21R$^{-/-}$: LDLR$^{-/-}$ mice would help to determine whether IL-21R$^{-/-}$ deficiency results in enhanced DC activity.

Intriguingly loss of PD-1 expression in atherosclerosis has been linked to enhanced CD4+ and CD8+ T-cell activation [291]. Although inducing increased T-reg responses, PD-1 deficiency has been reported to enhance IFN-γ secreting Th1 cell populations [291]. Adding to the pro-atherogenic effects of PD-1 signalling, PD-1 and PD-L1 expression is significantly reduced in patients with coronary artery disease (CAD), a finding linked to enhanced T-effector cell responses [357]. As part of our study, we demonstrated that IL-21R deficiency significantly reduces PD-1 expression *in vivo*. It is therefore possible that lack of PD-1 expression enhanced Th1 cell mediated pro-atherogenic immune response in our mice. As suggested before, to address this issue it would be advantageous to profile different T-helper subsets in IL-21R$^{-/-}$: LDLR$^{-/-}$ mice.

1.57.6   Conditional Tfh cell knock out models

Although we can be confident that IL-21R deficiency affects Tfh cell and GC B-cell development in our model, the expression of IL-21R by other cell types, means we cannot affirm that deficient Tfh cell and GC B-cell development is the only cause for our findings. To address this issue, subsequent studies, using conditional Tfh cell knock out mice would be required. To date, several models have been developed that allow for the conditional knock out of Tfh cells *in vivo*. Using a chimeric approach or cross breeding, we could develop a conditional T cell knock out in context of atherosclerosis.

Since the development of this project, various studies have provided insights into how this would be possible. Recently, several molecules have been identified - that - independent of Bcl-6 - regulate Tfh cell transcripts. Specifically, the transcription factor achaete-scute homologue 2 (Ascl-2) [237] and the ubiquitin ligase Itch [222] has been shown to be important in Tfh cell formation. Adding to this, deficiency of the transcription factor BATF – in context of atherosclerosis – would result in the selective deficiency of both Tfh cell and GC B-cells [316], thus reconfirming our data.

Crossing hyperlipidemic mice with the conditional KO described above or generating a chimera (as in this study) would allow for the selective deficiency of Tfh cells and or GC B-cells in context of atherosclerosis. As such, follow up studies are required to

fully confirm our data and support a pro-atherogenic role of the Tfh cell / GC B-cell axis in atherosclerosis.

1.57.7   Summary of Findings

- IL-21R deficiency significantly attenuated Tfh cell and GC B-cell development in context of atherosclerosis
- IL-21R deficiency significantly alters total and MDA-Ox-LDL antibody titres
    - Decreased total IgM and IgG
    - Increased total IgE
    - Decreased MDA-Ox-LDL IgG$_{2c}$
- IL-21R ablation significantly enhanced atherosclerosis formation.

1.57.8   Concluding Remarks

Together, our findings indicate the importance of IL-21R signalling in the formation of Tfh cells and GC B-cells in context of hyperlipidemia. Lack of Tfh cell and GC B-cell populations in IL-21R$^{-/-}$: LDLR$^{-/-}$ mice was linked to significant changes in athero-protective and pro-atherogenic antibody titres. We, therefore, propose that IL-21R deficiency alters Tfh cell and GC B-cell populations, leading to a skewed pro-atherogenic antibody response. Importantly, our study has provided extensive data warranting the further study of IL-21R signalling in atherosclerosis.

Chapter 6: Summary of Findings and Future Direction

1.58 Chapter 3 - Summary of Key Findings

As part of chapter 2, Tfh cell and GC B-cell populations were characterised in context of hyperlipidemia. To do this, C57BL/6 WT mice were fed chow diet and two groups of apoE$^{-/-}$ mice fed chow or HFD for 1, 2, 4, 8 and 12 weeks. These time points coincided with early stage atherosclerosis, as well as late stage progression. As a result, it was determined whether Tfh cell and GC B-cell kinetics changed in line with hyperlipidemia and atherosclerosis progression.

pLN, splenic and pao-LN Tfh cell populations increased in line with age in both apoE$^{-/-}$ chow and apoE$^{-/-}$ HFD fed mice, peaking at 12 weeks post-diet. Interestingly, GC B-cell populations peaked in the pLNs and pao-LNs of apoE$^{-/-}$ chow and HFD fed mice at 4 weeks post diet.

ApoE$^{-/-}$ chow and HFD fed mice displayed an increasing trend in anti-MDA-Ox-LDL IgG$_{2c}$ antibodies while concomitantly displaying a decreasing trend in anti-MDA-Ox-LDL IgG$_1$ antibodies.

Spleen sections from atherosclerotic mice displayed evidence of CD4+ T-cell translocation to B-cell follicles. Moreover, CD4+ T-cells from apoE$^{-/-}$ mice fed HFD for 12 weeks comprised the sole group expressing the Tfh cell transcription factor – Bcl-6 – while being aptly positioned in B-cell follicles. Interestingly, apoE$^{-/-}$ mice fed HFD for 4 weeks (peak of GC response) displayed significantly larger GC reactions than respective C57BL/6 WT controls.

In summary, our results indicate that hyperlipidemia may be an important driving force in the development of Tfh cells *in vivo*. As such, they suggest that Tfh cells may comprise a significant cell type involved in atherosclerosis development. In support of this, others have demonstrated the involvement of Tfh cells in the regulation of tertiary lymphoid organ formation (TLOs) in human aortic aneurism [142].

The finding that GC B-cell kinetics peak in apoE mice (chow and HFD) at 4 weeks post-diet, alongside changes in antibody kinetics, suggests that GC B-cell mediated processes may be of significance in atherosclerosis. Our data suggests the presence of

an early Tfh cell response potentially being able to induce GC B-cell responses. Although some may indicate that B-cells can differentiate in extra-follicular locations and produce low-affinity antibodies [358], we demonstrated via IF that GC results reported at 4 weeks were follicular in nature.

Importantly, our IF also demonstrated the exclusive expression of Bcl-6 in Tfh cells from apoE$^{-/-}$ mice fed HFD for 12 weeks. Bcl-6 expression is essential to Tfh cell and GC B-cell function, as well as GC integrity [236, 359, 360]. The exclusive expression in Tfh cells from apoE$^{-/-}$ mice fed HFD for 12 weeks indicates that severe hyperlipidemia is important in the expression of bonafide Tfh cell markers.

In conclusion, chapter 2 provided a crucial insight into the potential significance of Tfh cells and GC B-cells in experimental atherosclerosis and indicated a potential mechanism by which antibodies from the Tfh cell : GC B-cell axis may modulate disease formation and progression.

1.59 Chapter 4 - Summary of Key Findings

In the third chapter of this thesis, the effect of apoE deficiency on T-cell and B-cell responses following immunization was assessed. To study this, C57BL/6 WT and apoE$^{-/-}$ mice were immunised s.c. with OVA emulsified in CFA. Nine days later, immune cell populations were characterised via flow cytometry.

Loss of apoE did not affect CD4+ T-cell or B220+ B-cell formation, while expression of CD44 on CD4+ T-cells was significantly expanded in apoE$^{-/-}$ mice. Expression of CXCR5 was indifferent between both groups, as was Tfh cell expression, as characterised by 6 published marker combinations (see chapter 3). Interestingly, Bcl-6 and PD-1 expression was significantly reduced on CD4+ CXCR5+ gated and CD4+ CD44hi gated Tfh cells, while B220+ PNA+ FAS+ GC B-cell populations were deficient in apoE$^{-/-}$ mice.

Our results demonstrate that apoE deficiency does not affect CD4+ T-cell and B220+ B-cell formation. As a result, they reaffirm that the Tfh cell and GC B-cell pre-gates used in chapter 2 were not inadvertently affected by loss of apoE in apoE$^{-/-}$ mice. Although CD44 expression was elevated on CD4+ T-cells from apoE$^{-/-}$ mice, this is most likely due to enhanced inflammatory profiles in apoE$^{-/-}$ mice and the significance of CD44 in lesion formation [361].

As discussed previously, CXCR5 is important for translocation of Tfh cells to the B-cell follicle [362]. Our data indicates that Tfh cells from apoE$^{-/-}$ mice display equivalent expression of CXCR5, therefore indicating no regulatory role of apoE in CXCR5 expression. As such, it is plausible to assume that CD4+ T-cells from both C57BL/6 WT and apoE$^{-/-}$ mice exhibit equivalent ability to migrate to B-cell follicles and form Tfh cells. Moreover, this finding confirms that the results obtained in chapter 2 were not affected by differential CXCR5 expression.

Interestingly, GC B-cell expression was reduced in apoE$^{-/-}$ mice, suggesting that apoE mice are deficient in the formation of GC B-cell populations. Moreover, expression of Bcl-6 and PD-1 was reduced on Tfh cells, indicating that Tfh cell marker expression may be reduced in apoE$^{-/-}$ mice.

In summary, our data supports our hypothesis that atherosclerosis and hyperlipidemia, and not apoE deficiency, are the major drivers of the enhanced Tfh cell and GC responses observed in atherosclerotic mice.

1.60 Chapter 5 - Summary of Key Findings

In chapter 4, the effects of IL-21R deficiency on atherosclerosis formation were assessed. Involved in Tfh cell formation and GC B-cell differentiation, IL-21 is central to the Tfh cell : GC B-cell axis, and thus significant in diseases where aberrant GC reactions form [204-206]. To study this, a chimeric, hyperlipidemic, IL-21R deficient mouse was developed (IL-21R$^{-/-}$: LDLR$^{-/-}$), in which all hematopoietic stem cells were devoid of IL-21R expression.

IL-21R deficiency significantly reduced Tfh cell formation. Mirroring these results, IL-21R$^{-/-}$: LDLR$^{-/-}$ mice were devoid of B220+ PNA+ FAS+ GC B-cell expression in all organs assessed.

IL-21R deficiency significantly attenuated total IgM and IgG antibody titres, while exacerbating total IgE titres. Lastly, loss of IL-21R significantly enhanced aortic sinus lesion content, increased CD68+ macrophage infiltration but did not affect sinus collagen content.

We have identified an essential role of IL-21R signalling in Tfh cell and GC B-cell development in experimental atherosclerosis. We propose that loss of Tfh cell and GC B-cell populations in IL-21R$^{-/-}$: LDLR$^{-/-}$ mice enhances atherosclerosis by affecting the balance between athero-protective and pro-atherogenic antibodies. As such, we conclude that IL-21 and the Tfh cell : GC B-cell axis is protective in atherosclerosis. More recently others have demonstrated that control of the T follicular helper-germinal centre B-cell axis by CD8$^+$ regulatory T cells limits atherosclerosis and tertiary lymphoid organ development [142]. Unfortunately, our study did not extend to phenotyping regulatory cells. As such, the effect(s) of IL-21R deficiency on regulatory compartments in our hands is unknown. The effects this may have on Tfh cell populations and subsequent GC processes must therefore be addressed in subsequent studies.

It is also important to note that IL-21R signalling is important in the development and function of other immune cells, in particular Th17 cells [363]. As part of our study, we did not assess the effects of IL-21R ablation of these populations and the resulting

effects on pathology. As such, we cannot be confident that other cells (and processes) are not affected by loss of IL-21R in IL-21R$^{-/-}$: LDLR$^{-/-}$ mice. To address this, and attribute a definitive role of Tfh cells in atherosclerosis, a refined model in which Tfh cells are selectively ablated is required. Throughout the development of this thesis, several studies have indicated as to how this may be possible. In particular, several molecules required for Tfh cell differentiation have been identified, including the transcription factors, ascl-2 [237], BATF [316], Bcl-6 [236], and the messenger C-maf [285]. Using the cre/lox system it would be advantageous to develop a mouse model in which one or more of the above is devoid in CD4+ T-cells. In context of hyperlipidemia, this system would allow for the definitive discrimination of Tfh cell function in atherosclerosis.

In conclusion, this thesis has provided an interesting insight into the role of the Tfh cell : GC B-cell axis in atherosclerosis. Using the approaches described throughout, we have demonstrated the significance of Tfh cell, GC B-cell and antibody kinetics in the apoE$^{-/-}$ mouse model. Furthermore, we have provided evidence indicating a role of hyperlipidemia in driving Tfh cell marker expression. Importantly, our data provides evidence for the regulatory role of IL-21 and Tfh cells in experimental atherosclerosis and thus warrants further investigation.

1.61 Final Comments and Future Perspective

To date, atherosclerosis research has focused primarily on studying the importance of Th-1 cells – and their associated cytokines - in lesion formation. Therefore, researchers have gained valuable information as to the processes that lead to lesion formation and destabilisation. Importantly, however, the complex – and terminal - interplay between T-cells, B-cells and antibody production is only just being addressed. Recognising this, this thesis explored the idea that Tfh cells, GC B-cells and associated antibody kinetics may be of potential significance in atherosclerosis.

The first question posed related to whether or not Tfh cells, GC B-cells and antibody kinetics, 1) followed a pattern in line with lesion formation in the apoE$^{-/-}$ mouse model and 2) whether T-cells from apoE$^{-/-}$ mice expressed markers of Tfh cell phenotype and anatomical location. It was found that severe hypercholesterolemia was important in modulating Tfh cell, GC B-cell and pathological antibody kinetics in apoE$^{-/-}$ mice. Moreover, expression of the Tfh cell master regulator – Bcl-6 - was linked to hypercholesterolemia, with apoE$^{-/-}$ mice fed HFD for 12 weeks displaying exclusive expression and follicular location. The results presented demonstrate the first reports of a possible Tfh cell component to the adaptive immune response in hypercholesterolemia To confirm that hypercholesterolemia – and therefore disease severity – drive Tfh cell populations in atherosclerosis, future studies may use *in vitro* approaches to stimulate cultured naive T-cells from HFD fed apoE$^{-/-}$ mice and assess Tfh cell markers, Bcl-6 expression, B-cell helper capacity and antibody production.

The second question posed related to whether modulation of the key Tfh cell cytokine receptor – IL-21R - would affect atherosclerosis formation *in vivo*. Using the approach described in chapter 5, loss of IL-21R expression increased plaque burden, conferred an unstable plaque phenotype and favoured pro-atherogenic antibody production. As such, IL-21R signalling is protective in atherosclerosis. Importantly, IL-21R signalling also mediates mitogenesis of other cell subsets, including NK cells, Th-17 cells and mast cells. Crucially, these subsets have been shown to be of importance in atherogenic processes [113, 117, 364, 365]. Therefore, the pathological effects of IL-21R ablation on these subsets must be addressed, including CD8+ T-regs, Tf-regs, Th-17 cells and conventional Th-1 cells. To attribute a definitive role of Tfh cells, and associated processes in atherosclerosis, future studies could focus on developing a method in which Tfh cells are exclusively deficient in context of

hypercholesterolemia, while maintaining integrity of other subsets. As this thesis has evolved, several studies have emerged that describe methods in which selective Tfh cell impairment may be conferred *in vivo*. In particular, several key molecules have been identified that preferentially regulate Tfh cell fate [222, 237, 316, 335, 366]. Using bone marrow chimera technology or the cre/lox system, lack of these molecules – and thus Tfh cells – in context of atherosclerosis, will provide a definitive answer to the role of Tfh cells in atherosclerosis. Irrespective of this, chapter 5 has demonstrated the strong protective effects of the Tfh cell cytokine receptor – IL-21R – in atherosclerosis. To substantiate our hypothesis that, Tfh cells are athero-protective, serum transfer studies from $IL-21R^{-/-}$: $LDLR^{-/-}$ into hypercholesterolemic $LDLR^{-/-}$ mice may confirm the protective roles of IL-21R signalling. Used in other models, this method has proved valuable in conferring disease states in rodent models of RA [367] and as such may prove helpful in advancing the role of IL-21R in atherosclerosis.

The aorta comprises the site at which atherosclerotic lesions form and progress, and as such represents a significant tissue of interest. Moreover, lesions house dense populations of immune cells that contribute to the pro-inflammatory response. Importantly, recent studies have indicated the presence of Tfh cells and associated molecules in advanced disease, in ATLOs [45, 219]. In this context, however, the Tfh cell content of lesions in unknown, and in relation to this thesis - the subsequent effects of IL-21R ablation on such populations. As described in chapter 3, this was due to the technical limitation of absent CXCR5 expression post-digestion in the aorta. To address this, future studies may determine, via IF, the expression of plaque Tfh cell markers, including ICOS, PD-1 and Bcl-6. Moreover, IF staining for isotype switched antibodies may indicate a local response that eventually develops into a structured ATLO in advanced disease.

Taken together, the results presented throughout this thesis have provided an interesting insight into the potential significance of the Tfh cell : GC B-cell axis in atherosclerosis. In particular, they indicate that Tfh cells increase in line with lesion development, hypercholesterolemia favours Bcl-6 expression and loss of IL-21R expression significantly aggravates disease states.

References

1. Organisation, W.H., *World Health Organisation - Cardiovascular Disease (CVDs) Fact Sheet.* 2015: p. 1-5

2. Foundation, B.H., *Cardiovascular Disease Statistics 2014.* 2014: p. 1-126.

3. Government, T.S., *The Scottish Health Survey - The Glasgow Effect* 2010: p. 1-57.

4. Celermajer, D.S., et al., *Cardiovascular disease in the developing world: prevalences, patterns, and the potential of early disease detection.* J Am Coll Cardiol, 2012. **60**(14): p. 1207-16.

5. Reddy, K.S. and S. Yusuf, *Emerging epidemic of cardiovascular disease in developing countries.* Circulation, 1998. **97**(6): p. 596-601.

6. Galkina, E. and K. Ley, *Immune and inflammatory mechanisms of atherosclerosis (*).* Annu Rev Immunol, 2009. **27**: p. 165-97.

7. Kannel, W.B., et al., *Factors of risk in the development of coronary heart disease--six year follow-up experience. The Framingham Study.* Ann Intern Med, 1961. **55**: p. 33-50.

8. Balagopal, P.B., et al., *Nontraditional risk factors and biomarkers for cardiovascular disease: mechanistic, research, and clinical considerations for youth: a scientific statement from the American Heart Association.* Circulation, 2011. **123**(23): p. 2749-69.

9. Mayhan, W.G. and G.M. Sharpe, *Effect of cigarette smoke extract on arteriolar dilatation in vivo.* J Appl Physiol (1985), 1996. **81**(5): p. 1996-2003.

10. Mayhan, W.G. and K.P. Patel, *Effect of nicotine on endothelium-dependent arteriolar dilatation in vivo.* Am J Physiol, 1997. **272**(5 Pt 2): p. H2337-42.

11. Ota, Y., et al., *Impairment of endothelium-dependent relaxation of rabbit aortas by cigarette smoke extract--role of free radicals and attenuation by captopril.* Atherosclerosis, 1997. **131**(2): p. 195-202.

12. Qazi, M.U. and S. Malik, *Diabetes and Cardiovascular Disease: Original Insights from the Framingham Heart Study.* Glob Heart, 2013. **8**(1): p. 43-48.

13. Kannel, W.B. and D.L. McGee, *Diabetes and cardiovascular disease. The Framingham study.* JAMA, 1979. **241**(19): p. 2035-8.

14. Fox, C.S., et al., *Trends in cardiovascular complications of diabetes.* JAMA, 2004. **292**(20): p. 2495-9.

15. Libby, P., *Inflammation in atherosclerosis.* Nature, 2002. **420**(6917): p. 868-74.

16. VanPutte, C.R., J. Russo, A. , *Blood Vessels and Circulation*, in *Seeley's Essentials of Anatomy & Physiology* McGraw-Hill Education: New York. p. 350 - 253.

17. Mulvany, M.J. and C. Aalkjaer, *Structure and function of small arteries.* Physiol Rev, 1990. **70**(4): p. 921-61.

18. Stary, H.C., *Evolution and progression of atherosclerotic lesions in coronary arteries of children and young adults.* Arteriosclerosis, 1989. **9**(1 Suppl): p. I19-32.

19. Jonas, A. and M.C. Phillips, *CHAPTER 17 - Lipoprotein structure*, in *Biochemistry of Lipids, Lipoproteins and Membranes (Fifth Edition)*, D.E.V.E. Vance, Editor. 2008, Elsevier: San Diego. p. 485-506.

20. Tabas, I., *CHAPTER 21 - Lipids and atherosclerosis*, in *Biochemistry of Lipids, Lipoproteins and Membranes (Fifth Edition)*, D.E.V.E. Vance, Editor. 2008, Elsevier: San Diego. p. 579-605.

21.   Fielding, C.J. and P.E. Fielding, *CHAPTER 19 - Dynamics of lipoprotein transport in the circulatory system*, in *Biochemistry of Lipids, Lipoproteins and Membranes (Fifth Edition)*, D.E.V.E. Vance, Editor. 2008, Elsevier: San Diego. p. 533-553.

22.   Cyrus, T., et al., *Disruption of the 12/15-lipoxygenase gene diminishes atherosclerosis in apo E-deficient mice.* J Clin Invest, 1999. **103**(11): p. 1597-604.

23.   Mukhopadhyay, S. and S. Gordon, *The role of scavenger receptors in pathogen recognition and innate immunity.* Immunobiology, 2004. **209**(1-2): p. 39-49.

24.   Endemann, G., et al., *CD36 is a receptor for oxidized low density lipoprotein.* J Biol Chem, 1993. **268**(16): p. 11811-6.

25.   Nakata, A., et al., *CD36, a novel receptor for oxidized low-density lipoproteins, is highly expressed on lipid-laden macrophages in human atherosclerotic aorta.* Arterioscler Thromb Vasc Biol, 1999. **19**(5): p. 1333-9.

26.   Goldstein, J.L., et al., *Binding site on macrophages that mediates uptake and degradation of acetylated low density lipoprotein, producing massive cholesterol deposition.* Proc Natl Acad Sci U S A, 1979. **76**(1): p. 333-7.

27.   Babaev, V.R., et al., *Reduced atherosclerotic lesions in mice deficient for total or macrophage-specific expression of scavenger receptor-A.* Arterioscler Thromb Vasc Biol, 2000. **20**(12): p. 2593-9.

28.   Febbraio, M., et al., *Targeted disruption of the class B scavenger receptor CD36 protects against atherosclerotic lesion development in mice.* J Clin Invest, 2000. **105**(8): p. 1049-56.

29.   Mehta, J.L., et al., *Deletion of LOX-1 reduces atherogenesis in LDLR knockout mice fed high cholesterol diet.* Circ Res, 2007. **100**(11): p. 1634-42.

30.   Moore, K.J., et al., *Loss of receptor-mediated lipid uptake via scavenger receptor A or CD36 pathways does not ameliorate atherosclerosis in hyperlipidemic mice.* J Clin Invest, 2005. **115**(8): p. 2192-201.

31.   Stary, H.C., et al., *A definition of initial, fatty streak, and intermediate lesions of atherosclerosis. A report from the Committee on Vascular Lesions of the Council on Arteriosclerosis, American Heart Association.* Circulation, 1994. **89**(5): p. 2462-78.

32.   Gerrity, R.G., et al., *Dietary induced atherogenesis in swine. Morphology of the intima in prelesion stages.* Am J Pathol, 1979. **95**(3): p. 775-92.

33.   Napoli, C., et al., *Fatty streak formation occurs in human fetal aortas and is greatly enhanced by maternal hypercholesterolemia. Intimal accumulation of low density lipoprotein and its oxidation precede monocyte recruitment into early atherosclerotic lesions.* J Clin Invest, 1997. **100**(11): p. 2680-90.

34.   Hegyi, L., et al., *Foam cell apoptosis and the development of the lipid core of human atherosclerosis.* J Pathol, 1996. **180**(4): p. 423-9.

35.   Khan, B.V., et al., *Modified low density lipoprotein and its constituents augment cytokine-activated vascular cell adhesion molecule-1 gene expression in human vascular endothelial cells.* J Clin Invest, 1995. **95**(3): p. 1262-70.

36.   Cushing, S.D., et al., *Minimally modified low density lipoprotein induces monocyte chemotactic protein 1 in human endothelial cells and smooth muscle cells.* Proc Natl Acad Sci U S A, 1990. **87**(13): p. 5134-8.

37.   Collins, R.G., et al., *P-Selectin or intercellular adhesion molecule (ICAM)-1 deficiency substantially protects against atherosclerosis in apolipoprotein E-deficient mice.* J Exp Med, 2000. **191**(1): p. 189-94.

38.   Janabi, M., et al., *Oxidized LDL-induced NF-kappa B activation and subsequent expression of proinflammatory genes are defective in monocyte-derived*

macrophages from CD36-deficient patients. Arterioscler Thromb Vasc Biol, 2000. **20**(8): p. 1953-60.

39. Hansson, G.K., J. Holm, and L. Jonasson, *Detection of activated T lymphocytes in the human atherosclerotic plaque.* Am J Pathol, 1989. **135**(1): p. 169-75.

40. Stemme, S., et al., *T lymphocytes from human atherosclerotic plaques recognize oxidized low density lipoprotein.* Proc Natl Acad Sci U S A, 1995. **92**(9): p. 3893-7.

41. Kyaw, T., et al., *Cytotoxic and proinflammatory CD8+ T lymphocytes promote development of vulnerable atherosclerotic plaques in apoE-deficient mice.* Circulation, 2013. **127**(9): p. 1028-39.

42. Gupta, S., et al., *IFN-gamma potentiates atherosclerosis in ApoE knock-out mice.* J Clin Invest, 1997. **99**(11): p. 2752-61.

43. Frostegard, J., et al., *Cytokine expression in advanced human atherosclerotic plaques: dominance of pro-inflammatory (Th1) and macrophage-stimulating cytokines.* Atherosclerosis, 1999. **145**(1): p. 33-43.

44. Breitfeld, D., et al., *Follicular B helper T cells express CXC chemokine receptor 5, localize to B cell follicles, and support immunoglobulin production.* J Exp Med, 2000. **192**(11): p. 1545-52.

45. Grabner, R., et al., *Lymphotoxin beta receptor signaling promotes tertiary lymphoid organogenesis in the aorta adventitia of aged ApoE-/- mice.* J Exp Med, 2009. **206**(1): p. 233-48.

46. Alon, R., et al., *The integrin VLA-4 supports tethering and rolling in flow on VCAM-1.* J Cell Biol, 1995. **128**(6): p. 1243-53.

47. Galkina, E. and K. Ley, *Vascular adhesion molecules in atherosclerosis.* Arterioscler Thromb Vasc Biol, 2007. **27**(11): p. 2292-301.

48. Farsak, B., et al., *Detection of Chlamydia pneumoniae and Helicobacter pylori DNA in human atherosclerotic plaques by PCR.* J Clin Microbiol, 2000. **38**(12): p. 4408-11.

49. Ameriso, S.F., et al., *Detection of Helicobacter pylori in human carotid atherosclerotic plaques.* Stroke, 2001. **32**(2): p. 385-91.

50. Kuo, C.C., et al., *Detection of Chlamydia pneumoniae in aortic lesions of atherosclerosis by immunocytochemical stain.* Arterioscler Thromb, 1993. **13**(10): p. 1501-4.

51. Dabiri, H., et al., *Detection of Chlamydia pneumoniae in atherosclerotic plaques of patients in Tehran, Iran.* Jpn J Infect Dis, 2009. **62**(3): p. 195-7.

52. Sorrentino, R., et al., *A single infection with Chlamydia pneumoniae is sufficient to exacerbate atherosclerosis in ApoE deficient mice.* Cell Immunol, 2015. **294**(1): p. 25-32.

53. Binder, C.J., et al., *Pneumococcal vaccination decreases atherosclerotic lesion formation: molecular mimicry between Streptococcus pneumoniae and oxidized LDL.* Nat Med, 2003. **9**(6): p. 736-43.

54. Koltsova, E.K., et al., *Dynamic T cell-APC interactions sustain chronic inflammation in atherosclerosis.* J Clin Invest, 2012. **122**(9): p. 3114-26.

55. Skold, B.H., R. Getty, and F.K. Ramsey, *Spontaneous atherosclerosis in the arterial system of aging swine.* Am J Vet Res, 1966. **27**(116): p. 257-73.

56. Reiser, R., M.F. Sorrels, and M.C. Williams, *Influence of high levels of dietary fats and cholesterol on atherosclerosis and lipid distribution in swine.* Circ Res, 1959. **7**: p. 833-46.

57.   Koskinas, K.C., et al., *Natural history of experimental coronary atherosclerosis and vascular remodeling in relation to endothelial shear stress: a serial, in vivo intravascular ultrasound study.* Circulation, 2010. **121**(19): p. 2092-101.

58.   Gerrity, R.G., et al., *Endothelial cell morphology in areas of in vivo Evans blue uptake in the aorta of young pigs. II. Ultrastructure of the intima in areas of differing permeability to proteins.* Am J Pathol, 1977. **89**(2): p. 313-34.

59.   Getz, G.S. and C.A. Reardon, *Animal models of atherosclerosis.* Arterioscler Thromb Vasc Biol, 2012. **32**(5): p. 1104-15.

60.   Civelek, M., et al., *Coronary artery endothelial transcriptome in vivo: identification of endoplasmic reticulum stress and enhanced reactive oxygen species by gene connectivity network analysis.* Circ Cardiovasc Genet, 2011. **4**(3): p. 243-52.

61.   Duff, G.L., *Experimental cholesterol arteriosclerosis and its relationship to human arteriosclerosis.* Arch. Pathol., 1935. **20**.

62.   Nordestgaard, B.G. and D.B. Zilversmit, *Large lipoproteins are excluded from the arterial wall in diabetic cholesterol-fed rabbits.* J Lipid Res, 1988. **29**(11): p. 1491-500.

63.   Huang, Y., et al., *Apolipoprotein E2 transgenic rabbits. Modulation of the type III hyperlipoproteinemic phenotype by estrogen and occurrence of spontaneous atherosclerosis.* J Biol Chem, 1997. **272**(36): p. 22685-94.

64.   Heistad, D.D. and M.L. Armstrong, *Blood flow through vasa vasorum of coronary arteries in atherosclerotic monkeys.* Arteriosclerosis, 1986. **6**(3): p. 326-31.

65.   Barter, P.J., et al., *Cholesteryl ester transfer protein: a novel target for raising HDL and inhibiting atherosclerosis.* Arterioscler Thromb Vasc Biol, 2003. **23**(2): p. 160-7.

66.   Carter, C.P., P.N. Howles, and D.Y. Hui, *Genetic variation in cholesterol absorption efficiency among inbred strains of mice.* J Nutr, 1997. **127**(7): p. 1344-8.

67.   Zhang, S.H., et al., *Spontaneous hypercholesterolemia and arterial lesions in mice lacking apolipoprotein E.* Science, 1992. **258**(5081): p. 468-71.

68.   Ross, R., *Atherosclerosis--an inflammatory disease.* N Engl J Med, 1999. **340**(2): p. 115-26.

69.   Galkina, E., et al., *Lymphocyte recruitment into the aortic wall before and during development of atherosclerosis is partially L-selectin dependent.* J Exp Med, 2006. **203**(5): p. 1273-82.

70.   Getz, G.S. and C.A. Reardon, *Apoprotein E as a lipid transport and signaling protein in the blood, liver, and artery wall.* J Lipid Res, 2009. **50 Suppl**: p. S156-61.

71.   Barcat, D., et al., *Combined hyperlipidemia/hyperalphalipoproteinemia associated with premature spontaneous atherosclerosis in mice lacking hepatic lipase and low density lipoprotein receptor.* Atherosclerosis, 2006. **188**(2): p. 347-55.

72.   Teupser, D., A.D. Persky, and J.L. Breslow, *Induction of atherosclerosis by low-fat, semisynthetic diets in LDL receptor-deficient C57BL/6J and FVB/NJ mice: comparison of lesions of the aortic root, brachiocephalic artery, and whole aorta (en face measurement).* Arterioscler Thromb Vasc Biol, 2003. **23**(10): p. 1907-13.

73.   Ma, Y., et al., *Hyperlipidemia and atherosclerotic lesion development in Ldlr-deficient mice on a long-term high-fat diet.* PLoS One, 2012. **7**(4): p. e35835.

74. Linton, M.F., et al., *A direct role for the macrophage low density lipoprotein receptor in atherosclerotic lesion formation.* J Biol Chem, 1999. **274**(27): p. 19204-10.

75. Galkina, E. and K. Ley, *Leukocyte influx in atherosclerosis.* Curr Drug Targets, 2007. **8**(12): p. 1239-48.

76. Wick, G., et al., *Atherosclerosis, autoimmunity, and vascular-associated lymphoid tissue.* FASEB J, 1997. **11**(13): p. 1199-207.

77. Erbel, C., et al., *Functional profile of activated dendritic cells in unstable atherosclerotic plaque.* Basic Res Cardiol, 2007. **102**(2): p. 123-32.

78. Paulsson, G., et al., *Oligoclonal T cell expansions in atherosclerotic lesions of apolipoprotein E-deficient mice.* Arterioscler Thromb Vasc Biol, 2000. **20**(1): p. 10-7.

79. Rossmann, A., et al., *T-cells from advanced atherosclerotic lesions recognize hHSP60 and have a restricted T-cell receptor repertoire.* Exp Gerontol, 2008. **43**(3): p. 229-37.

80. Dansky, H.M., et al., *T and B lymphocytes play a minor role in atherosclerotic plaque formation in the apolipoprotein E-deficient mouse.* Proc Natl Acad Sci U S A, 1997. **94**(9): p. 4642-6.

81. Zhou, X., et al., *Transfer of CD4(+) T cells aggravates atherosclerosis in immunodeficient apolipoprotein E knockout mice.* Circulation, 2000. **102**(24): p. 2919-22.

82. Song, L., C. Leung, and C. Schindler, *Lymphocytes are important in early atherosclerosis.* J Clin Invest, 2001. **108**(2): p. 251-9.

83. Zhou, X., et al., *Adoptive transfer of CD4+ T cells reactive to modified low-density lipoprotein aggravates atherosclerosis.* Arterioscler Thromb Vasc Biol, 2006. **26**(4): p. 864-70.

84. Schulte, S., G.K. Sukhova, and P. Libby, *Genetically programmed biases in Th1 and Th2 immune responses modulate atherogenesis.* Am J Pathol, 2008. **172**(6): p. 1500-8.

85. Stemme, S., G. Fager, and G.K. Hansson, *MHC class II antigen expression in human vascular smooth muscle cells is induced by interferon-gamma and modulated by tumour necrosis factor and lymphotoxin.* Immunology, 1990. **69**(2): p. 243-9.

86. Li, H., et al., *An atherogenic diet rapidly induces VCAM-1, a cytokine-regulatable mononuclear leukocyte adhesion molecule, in rabbit aortic endothelium.* Arterioscler Thromb, 1993. **13**(2): p. 197-204.

87. Li, H., et al., *Inducible expression of vascular cell adhesion molecule-1 by vascular smooth muscle cells in vitro and within rabbit atheroma.* Am J Pathol, 1993. **143**(6): p. 1551-9.

88. Thornhill, M.H. and D.O. Haskard, *IL-4 regulates endothelial cell activation by IL-1, tumor necrosis factor, or IFN-gamma.* J Immunol, 1990. **145**(3): p. 865-72.

89. Whitman, S.C., et al., *Exogenous interferon-gamma enhances atherosclerosis in apolipoprotein E-/- mice.* Am J Pathol, 2000. **157**(6): p. 1819-24.

90. Buono, C., et al., *Influence of interferon-gamma on the extent and phenotype of diet-induced atherosclerosis in the LDLR-deficient mouse.* Arterioscler Thromb Vasc Biol, 2003. **23**(3): p. 454-60.

91. Wuttge, D.M., et al., *CXCL16/SR-PSOX is an interferon-gamma-regulated chemokine and scavenger receptor expressed in atherosclerotic lesions.* Arterioscler Thromb Vasc Biol, 2004. **24**(4): p. 750-5.

92. Li, H., M.W. Freeman, and P. Libby, *Regulation of smooth muscle cell scavenger receptor expression in vivo by atherogenic diets and in vitro by cytokines.* J Clin Invest, 1995. **95**(1): p. 122-33.

93. Tellides, G., et al., *Interferon-gamma elicits arteriosclerosis in the absence of leukocytes.* Nature, 2000. **403**(6766): p. 207-11.

94. Takeda, K., et al., *Defective NK cell activity and Th1 response in IL-18-deficient mice.* Immunity, 1998. **8**(3): p. 383-90.

95. Whitman, S.C., P. Ravisankar, and A. Daugherty, *Interleukin-18 enhances atherosclerosis in apolipoprotein E(-/-) mice through release of interferon-gamma.* Circ Res, 2002. **90**(2): p. E34-8.

96. Elhage, R., et al., *Reduced atherosclerosis in interleukin-18 deficient apolipoprotein E-knockout mice.* Cardiovasc Res, 2003. **59**(1): p. 234-40.

97. Mitchell, D.M., E.V. Ravkov, and M.A. Williams, *Distinct roles for IL-2 and IL-15 in the differentiation and survival of CD8+ effector and memory T cells.* J Immunol, 2010. **184**(12): p. 6719-30.

98. Malek, T.R., et al., *CD4 regulatory T cells prevent lethal autoimmunity in IL-2Rbeta-deficient mice. Implications for the nonredundant function of IL-2.* Immunity, 2002. **17**(2): p. 167-78.

99. Malek, T.R., et al., *Normal lymphoid homeostasis and lack of lethal autoimmunity in mice containing mature T cells with severely impaired IL-2 receptors.* J Immunol, 2000. **164**(6): p. 2905-14.

100. Malek, T.R., *The main function of IL-2 is to promote the development of T regulatory cells.* J Leukoc Biol, 2003. **74**(6): p. 961-5.

101. Upadhya, S., et al., *Atherogenic effect of interleukin-2 and antiatherogenic effect of interleukin-2 antibody in apo-E-deficient mice.* Angiology, 2004. **55**(3): p. 289-94.

102. Dietrich, T., et al., *Local delivery of IL-2 reduces atherosclerosis via expansion of regulatory T cells.* Atherosclerosis, 2012. **220**(2): p. 329-36.

103. Kasahara, K., et al., *CD3 antibody and IL-2 complex combination therapy inhibits atherosclerosis by augmenting a regulatory immune response.* J Am Heart Assoc, 2014. **3**(2): p. e000719.

104. Szabo, S.J., et al., *A novel transcription factor, T-bet, directs Th1 lineage commitment.* Cell, 2000. **100**(6): p. 655-69.

105. Buono, C., et al., *T-bet deficiency reduces atherosclerosis and alters plaque antigen-specific immune responses.* Proc Natl Acad Sci U S A, 2005. **102**(5): p. 1596-601.

106. Paigen, B., et al., *Variation in susceptibility to atherosclerosis among inbred strains of mice.* Atherosclerosis, 1985. **57**(1): p. 65-73.

107. King, V.L., L.A. Cassis, and A. Daugherty, *Interleukin-4 does not influence development of hypercholesterolemia or angiotensin II-induced atherosclerotic lesions in mice.* Am J Pathol, 2007. **171**(6): p. 2040-7.

108. Davenport, P. and P.G. Tipping, *The role of interleukin-4 and interleukin-12 in the progression of atherosclerosis in apolipoprotein E-deficient mice.* Am J Pathol, 2003. **163**(3): p. 1117-25.

109. King, V.L., S.J. Szilvassy, and A. Daugherty, *Interleukin-4 deficiency decreases atherosclerotic lesion formation in a site-specific manner in female LDL receptor-/- mice.* Arterioscler Thromb Vasc Biol, 2002. **22**(3): p. 456-61.

110. Binder, C.J., et al., *IL-5 links adaptive and natural immunity specific for epitopes of oxidized LDL and protects from atherosclerosis.* J Clin Invest, 2004. **114**(3): p. 427-37.

111. Miller, A.M., et al., *IL-33 reduces the development of atherosclerosis.* J Exp Med, 2008. **205**(2): p. 339-46.

112. McLaren, J.E., et al., *IL-33 reduces macrophage foam cell formation.* J Immunol, 2010. **185**(2): p. 1222-9.

113. Smith, E., et al., *Blockade of interleukin-17A results in reduced atherosclerosis in apolipoprotein E-deficient mice.* Circulation, 2010. **121**(15): p. 1746-55.

114. Xie, J.J., et al., *The Th17/Treg functional imbalance during atherogenesis in ApoE(-/-) mice.* Cytokine, 2010. **49**(2): p. 185-93.

115. Eid, R.E., et al., *Interleukin-17 and interferon-gamma are produced concomitantly by human coronary artery-infiltrating T cells and act synergistically on vascular smooth muscle cells.* Circulation, 2009. **119**(10): p. 1424-32.

116. Erbel, C., et al., *Expression of IL-17A in human atherosclerotic lesions is associated with increased inflammation and plaque vulnerability.* Basic Res Cardiol, 2011. **106**(1): p. 125-34.

117. Taleb, S., et al., *Loss of SOCS3 expression in T cells reveals a regulatory role for interleukin-17 in atherosclerosis.* J Exp Med, 2009. **206**(10): p. 2067-77.

118. Ng, H.P., R.L. Burris, and S. Nagarajan, *Attenuated atherosclerotic lesions in apoE-Fcgamma-chain-deficient hyperlipidemic mouse model is associated with inhibition of Th17 cells and promotion of regulatory T cells.* J Immunol, 2011. **187**(11): p. 6082-93.

119. Erbel, C., et al., *Inhibition of IL-17A attenuates atherosclerotic lesion development in apoE-deficient mice.* J Immunol, 2009. **183**(12): p. 8167-75.

120. Ait-Oufella, H., et al., *B cell depletion reduces the development of atherosclerosis in mice.* J Exp Med, 2010. **207**(8): p. 1579-87.

121. Danzaki, K., et al., *Interleukin-17A deficiency accelerates unstable atherosclerotic plaque formation in apolipoprotein E-deficient mice.* Arterioscler Thromb Vasc Biol, 2012. **32**(2): p. 273-80.

122. Gistera, A., et al., *Transforming growth factor-beta signaling in T cells promotes stabilization of atherosclerotic plaques through an interleukin-17-dependent pathway.* Sci Transl Med, 2013. **5**(196): p. 196ra100.

123. Konigshofer, Y. and Y.H. Chien, *Gammadelta T cells - innate immune lymphocytes?* Curr Opin Immunol, 2006. **18**(5): p. 527-33.

124. Peng, S.L., et al., *Propagation and regulation of systemic autoimmunity by gammadelta T cells.* J Immunol, 1996. **157**(12): p. 5689-98.

125. Mukasa, A., et al., *Evidence that the same gamma delta T cells respond during infection-induced and autoimmune inflammation.* J Immunol, 1997. **159**(12): p. 5787-94.

126. Lockhart, E., A.M. Green, and J.L. Flynn, *IL-17 production is dominated by gammadelta T cells rather than CD4 T cells during Mycobacterium tuberculosis infection.* J Immunol, 2006. **177**(7): p. 4662-9.

127. Chien, Y.H., R. Jores, and M.P. Crowley, *Recognition by gamma/delta T cells.* Annu Rev Immunol, 1996. **14**: p. 511-32.

128. Vu, D.M., et al., *gammadeltaT cells are prevalent in the proximal aorta and drive nascent atherosclerotic lesion progression and neutrophilia in hypercholesterolemic mice.* PLoS One, 2014. **9**(10): p. e109416.

129. Elhage, R., et al., *Deleting TCR alpha beta+ or CD4+ T lymphocytes leads to opposite effects on site-specific atherosclerosis in female apolipoprotein E-deficient mice.* Am J Pathol, 2004. **165**(6): p. 2013-8.

130. Cheng, H.Y., R. Wu, and C.C. Hedrick, *Gammadelta (gammadelta) T lymphocytes do not impact the development of early atherosclerosis.* Atherosclerosis, 2014. **234**(2): p. 265-9.

131. Corthay, A., *How do regulatory T cells work?* Scand J Immunol, 2009. **70**(4): p. 326-36.

132. Taleb, S., A. Tedgui, and Z. Mallat, *Regulatory T-cell immunity and its relevance to atherosclerosis.* J Intern Med, 2008. **263**(5): p. 489-99.

133. Mor, A., et al., *Role of naturally occurring CD4+ CD25+ regulatory T cells in experimental atherosclerosis.* Arterioscler Thromb Vasc Biol, 2007. **27**(4): p. 893-900.

134. Potteaux, S., et al., *Leukocyte-derived interleukin 10 is required for protection against atherosclerosis in low-density lipoprotein receptor knockout mice.* Arterioscler Thromb Vasc Biol, 2004. **24**(8): p. 1474-8.

135. Pinderski, L.J., et al., *Overexpression of interleukin-10 by activated T lymphocytes inhibits atherosclerosis in LDL receptor-deficient Mice by altering lymphocyte and macrophage phenotypes.* Circ Res, 2002. **90**(10): p. 1064-71.

136. Weber, C., A. Zernecke, and P. Libby, *The multifaceted contributions of leukocyte subsets to atherosclerosis: lessons from mouse models.* Nat Rev Immunol, 2008. **8**(10): p. 802-15.

137. Kolbus, D., et al., *CD8+ T cell activation predominate early immune responses to hypercholesterolemia in Apoe(-)(/)(-) mice.* BMC Immunol, 2010. **11**: p. 58.

138. Roselaar, S.E., P.X. Kakkanathu, and A. Daugherty, *Lymphocyte populations in atherosclerotic lesions of apoE -/- and LDL receptor -/- mice. Decreasing density with disease progression.* Arterioscler Thromb Vasc Biol, 1996. **16**(8): p. 1013-8.

139. Fyfe, A.I., J.H. Qiao, and A.J. Lusis, *Immune-deficient mice develop typical atherosclerotic fatty streaks when fed an atherogenic diet.* J Clin Invest, 1994. **94**(6): p. 2516-20.

140. Kolbus, D., et al., *TAP1-deficiency does not alter atherosclerosis development in Apoe-/- mice.* PLoS One, 2012. **7**(3): p. e33932.

141. Zhou, J., et al., *CD8(+)CD25(+) T cells reduce atherosclerosis in apoE(-/-) mice.* Biochem Biophys Res Commun, 2014. **443**(3): p. 864-70.

142. Clement, M., et al., *Control of the T follicular helper-germinal center B-cell axis by CD8(+) regulatory T cells limits atherosclerosis and tertiary lymphoid organ development.* Circulation, 2015. **131**(6): p. 560-70.

143. Kantor, A., *A new nomenclature for B cells.* Immunol Today, 1991. **12**(11): p. 388.

144. Masmoudi, H., et al., *All T15 Id-positive antibodies (but not the majority of VHT15+ antibodies) are produced by peritoneal CD5+ B lymphocytes.* Int Immunol, 1990. **2**(6): p. 515-20.

145. Weber, G.F., et al., *Pleural innate response activator B cells protect against pneumonia via a GM-CSF-IgM axis.* J Exp Med, 2014. **211**(6): p. 1243-56.

146. Hardy, R.R., *B-1 B cell development.* J Immunol, 2006. **177**(5): p. 2749-54.

147. VanPutte, C.R., J. Russo, A., *Sheeley's Essentials of Anatomy and Physiology.* Ninth ed. Vol. 4. New York: McGraw-Hill Education.

148. Janeway, C.A.T., P. Walport, M. Shlomchik, M.J. , *Immunobiology the Immune system in health and disease.* 6th ed. 2005: Garland Science 823.

149. Yla-Herttuala, S., et al., *Rabbit and human atherosclerotic lesions contain IgG that recognizes epitopes of oxidized LDL.* Arterioscler Thromb, 1994. **14**(1): p. 32-40.

150. Salonen, J.T., et al., *Autoantibody against oxidised LDL and progression of carotid atherosclerosis.* Lancet, 1992. **339**(8798): p. 883-7.

151. Xu, Q., et al., *Association of serum antibodies to heat-shock protein 65 with carotid atherosclerosis.* Lancet, 1993. **341**(8840): p. 255-9.

152. Saikku, P., et al., *Serological evidence of an association of a novel Chlamydia, TWAR, with chronic coronary heart disease and acute myocardial infarction.* Lancet, 1988. **2**(8618): p. 983-6.

153. Habets, K.L., et al., *Vaccination using oxidized low-density lipoprotein-pulsed dendritic cells reduces atherosclerosis in LDL receptor-deficient mice.* Cardiovasc Res, 2010. **85**(3): p. 622-30.

154. Klingenberg, R., et al., *Subcutaneous immunization with heat shock protein-65 reduces atherosclerosis in Apoe(-)/(-) mice.* Immunobiology, 2012. **217**(5): p. 540-7.

155. Rezende, A.B., et al., *Splenectomy increases atherosclerotic lesions in apolipoprotein E deficient mice.* J Surg Res, 2011. **171**(2): p. e231-6.

156. Caligiuri, G., et al., *Protective immunity against atherosclerosis carried by B cells of hypercholesterolemic mice.* J Clin Invest, 2002. **109**(6): p. 745-53.

157. Major, A.S., S. Fazio, and M.F. Linton, *B-lymphocyte deficiency increases atherosclerosis in LDL receptor-null mice.* Arterioscler Thromb Vasc Biol, 2002. **22**(11): p. 1892-8.

158. Karvonen, J., et al., *Immunoglobulin M type of autoantibodies to oxidized low-density lipoprotein has an inverse relation to carotid artery atherosclerosis.* Circulation, 2003. **108**(17): p. 2107-12.

159. Tsimikas, S., et al., *Relationship of IgG and IgM autoantibodies to oxidized low density lipoprotein with coronary artery disease and cardiovascular events.* J Lipid Res, 2007. **48**(2): p. 425-33.

160. Kyaw, T., et al., *B1a B lymphocytes are atheroprotective by secreting natural IgM that increases IgM deposits and reduces necrotic cores in atherosclerotic lesions.* Circ Res, 2011. **109**(8): p. 830-40.

161. Lewis, M.J., et al., *Immunoglobulin M is required for protection against atherosclerosis in low-density lipoprotein receptor-deficient mice.* Circulation, 2009. **120**(5): p. 417-26.

162. Fiskesund, R., et al., *Low levels of antibodies against phosphorylcholine predict development of stroke in a population-based study from northern Sweden.* Stroke, 2010. **41**(4): p. 607-12.

163. Gronlund, H., et al., *Low levels of IgM antibodies against phosphorylcholine predict development of acute myocardial infarction in a population-based cohort from northern Sweden.* Eur J Cardiovasc Prev Rehabil, 2009. **16**(3): p. 382-6.

164. Boullier, A., et al., *The binding of oxidized low density lipoprotein to mouse CD36 is mediated in part by oxidized phospholipids that are associated with both the lipid and protein moieties of the lipoprotein.* J Biol Chem, 2000. **275**(13): p. 9163-9.

165. Wang, J., et al., *High frequencies of activated B cells and T follicular helper cells are correlated with disease activity in patients with new-onset rheumatoid arthritis.* Clin Exp Immunol, 2013. **174**(2): p. 212-20.

166. Zhang, Y., et al., *Elevated circulating Th17 and follicular helper CD4(+) T cells in patients with rheumatoid arthritis.* APMIS, 2015. **123**(8): p. 659-66.

167. Choi, J.Y., et al., *Circulating follicular helper-like T cells in systemic lupus erythematosus: association with disease activity.* Arthritis Rheumatol, 2015. **67**(4): p. 988-99.

168. Schaerli, P., et al., *CXC chemokine receptor 5 expression defines follicular homing T cells with B cell helper function.* J Exp Med, 2000. **192**(11): p. 1553-62.

169. Crotty, S., *T follicular helper cell differentiation, function, and roles in disease.* Immunity, 2014. **41**(4): p. 529-42.

170. Eto, D., et al., *IL-21 and IL-6 are critical for different aspects of B cell immunity and redundantly induce optimal follicular helper CD4 T cell (Tfh) differentiation.* PLoS One, 2011. **6**(3): p. e17739.

171. Choi, Y.S., et al., *Bcl6 expressing follicular helper CD4 T cells are fate committed early and have the capacity to form memory.* J Immunol, 2013. **190**(8): p. 4014-26.

172. Sage, P.T., et al., *Circulating T follicular regulatory and helper cells have memory-like properties.* J Clin Invest, 2014. **124**(12): p. 5191-204.

173. Linterman, M.A., et al., *Foxp3+ follicular regulatory T cells control the germinal center response.* Nat Med, 2011. **17**(8): p. 975-82.

174. Chung, Y., et al., *Follicular regulatory T cells expressing Foxp3 and Bcl-6 suppress germinal center reactions.* Nat Med, 2011. **17**(8): p. 983-8.

175. Sage, P.T., et al., *The receptor PD-1 controls follicular regulatory T cells in the lymph nodes and blood.* Nat Immunol, 2013. **14**(2): p. 152-61.

176. Wollenberg, I., et al., *Regulation of the germinal center reaction by Foxp3+ follicular regulatory T cells.* J Immunol, 2011. **187**(9): p. 4553-60.

177. Ron, Y. and J. Sprent, *T cell priming in vivo: a major role for B cells in presenting antigen to T cells in lymph nodes.* J Immunol, 1987. **138**(9): p. 2848-56.

178. LeBien, T.W. and T.F. Tedder, *B lymphocytes: how they develop and function.* Blood, 2008. **112**(5): p. 1570-80.

179. Janeway CA Jr, T.P., Walport M, et al, *Immunobiology: The Immune System in Health and Disease.* 2001(Fifth Edition.): p. 261 - 265

180. von Freeden-Jeffry, U., et al., *Lymphopenia in interleukin (IL)-7 gene-deleted mice identifies IL-7 as a nonredundant cytokine.* J Exp Med, 1995. **181**(4): p. 1519-26.

181. Koni, P.A., et al., *Conditional vascular cell adhesion molecule 1 deletion in mice: impaired lymphocyte migration to bone marrow.* J Exp Med, 2001. **193**(6): p. 741-54.

182. Market, E. and F.N. Papavasiliou, *V(D)J recombination and the evolution of the adaptive immune system.* PLoS Biol, 2003. **1**(1): p. E16.

183. Sadofsky, M.J., *The RAG proteins in V(D)J recombination: more than just a nuclease.* Nucleic Acids Res, 2001. **29**(7): p. 1399-409.

184. Shinkai, Y., et al., *RAG-2-deficient mice lack mature lymphocytes owing to inability to initiate V(D)J rearrangement.* Cell, 1992. **68**(5): p. 855-67.

185. Mombaerts, P., et al., *RAG-1-deficient mice have no mature B and T lymphocytes.* Cell, 1992. **68**(5): p. 869-77.

186. Tobon, G.J., J.H. Izquierdo, and C.A. Canas, *B lymphocytes: development, tolerance, and their role in autoimmunity-focus on systemic lupus erythematosus.* Autoimmune Dis, 2013. **2013**: p. 827254.

187. Gunn, M.D., et al., *A chemokine expressed in lymphoid high endothelial venules promotes the adhesion and chemotaxis of naive T lymphocytes.* Proc Natl Acad Sci U S A, 1998. **95**(1): p. 258-63.

188. Baekkevold, E.S., et al., *The CCR7 ligand elc (CCL19) is transcytosed in high endothelial venules and mediates T cell recruitment.* J Exp Med, 2001. **193**(9): p. 1105-12.

189. Nakano, H., et al., *Genetic defect in T lymphocyte-specific homing into peripheral lymph nodes.* Eur J Immunol, 1997. **27**(1): p. 215-21.

190. Warnock, R.A., et al., *The role of chemokines in the microenvironmental control of T versus B cell arrest in Peyer's patch high endothelial venules.* J Exp Med, 2000. **191**(1): p. 77-88.

191. Okada, T., et al., *Chemokine requirements for B cell entry to lymph nodes and Peyer's patches.* J Exp Med, 2002. **196**(1): p. 65-75.

192. Legler, D.F., et al., *B cell-attracting chemokine 1, a human CXC chemokine expressed in lymphoid tissues, selectively attracts B lymphocytes via BLR1/CXCR5.* J Exp Med, 1998. **187**(4): p. 655-60.

193. Ansel, K.M., et al., *A chemokine-driven positive feedback loop organizes lymphoid follicles.* Nature, 2000. **406**(6793): p. 309-14.

194. Yurasov, S., et al., *Defective B cell tolerance checkpoints in systemic lupus erythematosus.* J Exp Med, 2005. **201**(5): p. 703-11.

195. Janeway CA Jr, T.P., Walport M, et al. , *Immunobiology: The Immune System in Health and Disease.* 2001. **Fifth Edition**: p. 647 - 649.

196. De Silva, N.S. and U. Klein, *Dynamics of B cells in germinal centres.* Nat Rev Immunol, 2015. **15**(3): p. 137-48.

197. Klein, U. and R. Dalla-Favera, *Germinal centres: role in B-cell physiology and malignancy.* Nat Rev Immunol, 2008. **8**(1): p. 22-33.

198. Di Noia, J.M. and M.S. Neuberger, *Molecular mechanisms of antibody somatic hypermutation.* Annu Rev Biochem, 2007. **76**: p. 1-22.

199. Nieuwenhuis, P. and D. Opstelten, *Functional anatomy of germinal centers.* Am J Anat, 1984. **170**(3): p. 421-35.

200. Jacobson, E.B., L.H. Caporale, and G.J. Thorbecke, *Effect of thymus cell injections on germinal center formation in lymphoid tissues of nude (thymusless) mice.* Cell Immunol, 1974. **13**(3): p. 416-30.

201. Han, S., et al., *Cellular interaction in germinal centers. Roles of CD40 ligand and B7-2 in established germinal centers.* J Immunol, 1995. **155**(2): p. 556-67.

202. Allen, R.C., et al., *CD40 ligand gene defects responsible for X-linked hyper-IgM syndrome.* Science, 1993. **259**(5097): p. 990-3.

203. Ferrari, S., et al., *Mutations of CD40 gene cause an autosomal recessive form of immunodeficiency with hyper IgM.* Proc Natl Acad Sci U S A, 2001. **98**(22): p. 12614-9.

204. Linterman, M.A., et al., *IL-21 acts directly on B cells to regulate Bcl-6 expression and germinal center responses.* J Exp Med, 2010. **207**(2): p. 353-63.

205. Zotos, D., et al., *IL-21 regulates germinal center B cell differentiation and proliferation through a B cell-intrinsic mechanism.* J Exp Med, 2010. **207**(2): p. 365-78.

206. Vogelzang, A., et al., *A fundamental role for interleukin-21 in the generation of T follicular helper cells.* Immunity, 2008. **29**(1): p. 127-37.

207. Bossaller, L., et al., *ICOS deficiency is associated with a severe reduction of CXCR5+CD4 germinal center Th cells.* J Immunol, 2006. **177**(7): p. 4927-32.

208. Coyle, A.J., et al., *The CD28-related molecule ICOS is required for effective T cell-dependent immune responses.* Immunity, 2000. **13**(1): p. 95-105.

209. Hutloff, A., et al., *ICOS is an inducible T-cell co-stimulator structurally and functionally related to CD28.* Nature, 1999. **397**(6716): p. 263-6.

210. Tafuri, A., et al., *ICOS is essential for effective T-helper-cell responses.* Nature, 2001. **409**(6816): p. 105-9.

211. Chtanova, T., et al., *T follicular helper cells express a distinctive transcriptional profile, reflecting their role as non-Th1/Th2 effector cells that provide help for B cells.* J Immunol, 2004. **173**(1): p. 68-78.

212. Haynes, N.M., et al., *Role of CXCR5 and CCR7 in follicular Th cell positioning and appearance of a programmed cell death gene-1high germinal center-associated subpopulation.* J Immunol, 2007. **179**(8): p. 5099-108.

213. Mahajan, S., et al., *The role of ICOS in the development of CD4 T cell help and the reactivation of memory T cells.* Eur J Immunol, 2007. **37**(7): p. 1796-808.

214. Choi, Y.S., et al., *ICOS receptor instructs T follicular helper cell versus effector cell differentiation via induction of the transcriptional repressor Bcl6.* Immunity, 2011. **34**(6): p. 932-46.

215. Schroder, A.E., et al., *Differentiation of B cells in the nonlymphoid tissue of the synovial membrane of patients with rheumatoid arthritis.* Proc Natl Acad Sci U S A, 1996. **93**(1): p. 221-5.

216. Croia, C., et al., *Implication of Epstein-Barr virus infection in disease-specific autoreactive B cell activation in ectopic lymphoid structures of Sjogren's syndrome.* Arthritis Rheumatol, 2014. **66**(9): p. 2545-57.

217. Humby, F., et al., *Ectopic lymphoid structures support ongoing production of class-switched autoantibodies in rheumatoid synovium.* PLoS Med, 2009. **6**(1): p. e1.

218. Chang, A., et al., *In situ B cell-mediated immune responses and tubulointerstitial inflammation in human lupus nephritis.* J Immunol, 2011. **186**(3): p. 1849-60.

219. Hu, D., et al., *Artery Tertiary Lymphoid Organs Control Aorta Immunity and Protect against Atherosclerosis via Vascular Smooth Muscle Cell Lymphotoxin beta Receptors.* Immunity, 2015. **42**(6): p. 1100-15.

220. Spear, R., et al., *Adventitial Tertiary Lymphoid Organs as Potential Source of MicroRNA Biomarkers for Abdominal Aortic Aneurysm.* Int J Mol Sci, 2015. **16**(5): p. 11276-93.

221. Johnston, R.J., et al., *Bcl6 and Blimp-1 are reciprocal and antagonistic regulators of T follicular helper cell differentiation.* Science, 2009. **325**(5943): p. 1006-10.

222. Xiao, N., et al., *The E3 ubiquitin ligase Itch is required for the differentiation of follicular helper T cells.* Nat Immunol, 2014. **15**(7): p. 657-66.

223. DeGrendele, H.C., et al., *CD44 activation and associated primary adhesion is inducible via T cell receptor stimulation.* J Immunol, 1997. **159**(6): p. 2549-53.

224. Witztum, J.L., *Splenic immunity and atherosclerosis: a glimpse into a novel paradigm?* J Clin Invest, 2002. **109**(6): p. 721-4.

225. Hansson, G.K., *Immune mechanisms in atherosclerosis.* Arterioscler Thromb Vasc Biol, 2001. **21**(12): p. 1876-90.

226. Ozaki, K., et al., *A critical role for IL-21 in regulating immunoglobulin production.* Science, 2002. **298**(5598): p. 1630-4.

227. Coico, R.F., B.S. Bhogal, and G.J. Thorbecke, *Relationship of germinal centers in lymphoid tissue to immunologic memory. VI. Transfer of B cell memory with lymph node cells fractionated according to their receptors for peanut agglutinin.* J Immunol, 1983. **131**(5): p. 2254-7.

228. Busnelli, M., et al., *Diet induced mild hypercholesterolemia in pigs: local and systemic inflammation, effects on vascular injury - rescue by high-dose statin treatment.* PLoS One, 2013. **8**(11): p. e80588.

229. Drechsler, M., et al., *Hyperlipidemia-triggered neutrophilia promotes early atherosclerosis.* Circulation, 2010. **122**(18): p. 1837-45.

230. Swirski, F.K., et al., *Ly-6Chi monocytes dominate hypercholesterolemia-associated monocytosis and give rise to macrophages in atheromata.* J Clin Invest, 2007. **117**(1): p. 195-205.

231. Simpson, N., et al., *Expansion of circulating T cells resembling follicular helper T cells is a fixed phenotype that identifies a subset of severe systemic lupus erythematosus.* Arthritis Rheum, 2010. **62**(1): p. 234-44.

232. Chu, Y., et al., *A preliminary study on the characterization of follicular helper T (Tfh) cells in rheumatoid arthritis synovium.* Acta Histochem, 2014. **116**(3): p. 539-43.

233. Zhang, Y., et al., *Elevated circulating Th17 and follicular helper CD4 T cells in patients with rheumatoid arthritis.* APMIS, 2015.

234. Yusuf, I., et al., *Germinal center T follicular helper cell IL-4 production is dependent on signaling lymphocytic activation molecule receptor (CD150).* J Immunol, 2010. **185**(1): p. 190-202.

235. Nurieva, R.I., et al., *Generation of T follicular helper cells is mediated by interleukin-21 but independent of T helper 1, 2, or 17 cell lineages.* Immunity, 2008. **29**(1): p. 138-49.

236. Yu, D., et al., *The transcriptional repressor Bcl-6 directs T follicular helper cell lineage commitment.* Immunity, 2009. **31**(3): p. 457-68.

237. Liu, X., et al., *Transcription factor achaete-scute homologue 2 initiates follicular T-helper-cell development.* Nature, 2014. **507**(7493): p. 513-8.

238. Kato, R., et al., *Transient increase in plasma oxidized LDL during the progression of atherosclerosis in apolipoprotein E knockout mice.* Arterioscler Thromb Vasc Biol, 2009. **29**(1): p. 33-9.

239. Kyaw, T., et al., *Depletion of B2 but not B1a B cells in BAFF receptor-deficient ApoE mice attenuates atherosclerosis by potently ameliorating arterial inflammation.* PLoS One, 2012. **7**(1): p. e29371.

240. Sage, A.P., et al., *BAFF receptor deficiency reduces the development of atherosclerosis in mice--brief report.* Arterioscler Thromb Vasc Biol, 2012. **32**(7): p. 1573-6.

241. Smedbakken, L.M., et al., *Increased levels of the homeostatic chemokine CXCL13 in human atherosclerosis - Potential role in plaque stabilization.* Atherosclerosis, 2012. **224**(1): p. 266-73.

242. Mahley, R.W., et al., *Plasma lipoproteins: apolipoprotein structure and function.* J Lipid Res, 1984. **25**(12): p. 1277-94.

243. O, D., *Apolipoproteins: Biochemistry, Methods and Clinical Significance* Biochemical Education 1989. **17**(2): p. 63-68.

244. Goldberg, I.J., et al., *Lipoprotein ApoC-II activation of lipoprotein lipase. Modulation by apolipoprotein A-IV.* J Biol Chem, 1990. **265**(8): p. 4266-72.

245. Jonas, A., S.A. Sweeny, and P.N. Herbert, *Discoidal complexes of A and C apolipoproteins with lipids and their reactions with lecithin: cholesterol acyltransferase.* J Biol Chem, 1984. **259**(10): p. 6369-75.

246. Fielding, C.J. and P.E. Fielding, *Chapter 19 - Dynamics of lipoprotein transport in the circulatory system*, in *Biochemistry of Lipids, Lipoproteins and Membranes (Fifth Edition)*, D.E.V.E. Vance, Editor. 2008, Elsevier: San Diego. p. 533-XIII.

247. Gaudreault, N., et al., *ApoE suppresses atherosclerosis by reducing lipid accumulation in circulating monocytes and the expression of inflammatory molecules on monocytes and vascular endothelium.* Arterioscler Thromb Vasc Biol, 2012. **32**(2): p. 264-72.

248.	Havel, R.J., et al., *Radioimmunoassay of human arginine-rich apolipoprotein, apoprotein E. Concentration in blood plasma and lipoproteins as affected by apoprotein E-3 deficiency.* J Clin Invest, 1980. **66**(6): p. 1351-62.

249.	Laskowitz, D.T., et al., *Altered immune responses in apolipoprotein E-deficient mice.* J Lipid Res, 2000. **41**(4): p. 613-20.

250.	Mahley, R.W., *Apolipoprotein E: cholesterol transport protein with expanding role in cell biology.* Science, 1988. **240**(4852): p. 622-30.

251.	Schneider, W.J., *Chapter 20 - Lipoprotein receptors*, in *Biochemistry of Lipids, Lipoproteins and Membranes (Fifth Edition)*, D.E.V.E. Vance, Editor. 2008, Elsevier: San Diego. p. 555-578.

252.	Vermeer, B.J., R.R. Frants, and L.M. Havekes, *Familial dysbetalipoproteinemia: a genetically heterogenous disease caused by mutations of the ligand apolipoprotein E.* J Invest Dermatol, 1992. **98**(6 Suppl): p. 57S-60S.

253.	Mahley, R.W., et al., *Lipoproteins of special significance in atherosclerosis. Insights provided by studies of type III hyperlipoproteinemia.* Ann N Y Acad Sci, 1985. **454**: p. 209-21.

254.	Piedrahita, J.A., et al., *Generation of mice carrying a mutant apolipoprotein E gene inactivated by gene targeting in embryonic stem cells.* Proc Natl Acad Sci U S A, 1992. **89**(10): p. 4471-5.

255.	Plump, A.S., et al., *Severe hypercholesterolemia and atherosclerosis in apolipoprotein E-deficient mice created by homologous recombination in ES cells.* Cell, 1992. **71**(2): p. 343-53.

256.	Nakashima, Y., et al., *ApoE-deficient mice develop lesions of all phases of atherosclerosis throughout the arterial tree.* Arterioscler Thromb, 1994. **14**(1): p. 133-40.

257.	Busch, M., et al., *Dendritic cell subset distributions in the aorta in healthy and atherosclerotic mice.* PLoS One, 2014. **9**(2): p. e88452.

258.	Macritchie, N., et al., *Plasmacytoid dendritic cells play a key role in promoting atherosclerosis in apolipoprotein E-deficient mice.* Arterioscler Thromb Vasc Biol, 2012. **32**(11): p. 2569-79.

259.	Kim, J., J.M. Basak, and D.M. Holtzman, *The role of apolipoprotein E in Alzheimer's disease.* Neuron, 2009. **63**(3): p. 287-303.

260.	Chartier-Harlin, M.C., et al., *Apolipoprotein E, epsilon 4 allele as a major risk factor for sporadic early and late-onset forms of Alzheimer's disease: analysis of the 19q13.2 chromosomal region.* Hum Mol Genet, 1994. **3**(4): p. 569-74.

261.	Hori, Y., et al., *Role of Apolipoprotein E in beta-Amyloidogenesis: ISOFORM-SPECIFIC EFFECTS ON PROTOFIBRIL TO FIBRIL CONVERSION OF Abeta IN VITRO AND BRAIN Abeta DEPOSITION IN VIVO.* J Biol Chem, 2015. **290**(24): p. 15163-74.

262.	Weeber, E.J., et al., *Reelin and ApoE receptors cooperate to enhance hippocampal synaptic plasticity and learning.* J Biol Chem, 2002. **277**(42): p. 39944-52.

263.	de Bont, N., et al., *Apolipoprotein E-deficient mice have an impaired immune response to Klebsiella pneumoniae.* Eur J Clin Invest, 2000. **30**(9): p. 818-22.

264.	Vonk, A.G., et al., *Apolipoprotein-E-deficient mice exhibit an increased susceptibility to disseminated candidiasis.* Med Mycol, 2004. **42**(4): p. 341-8.

265.	Van Oosten, M., et al., *Apolipoprotein E protects against bacterial lipopolysaccharide-induced lethality. A new therapeutic approach to treat gram-negative sepsis.* J Biol Chem, 2001. **276**(12): p. 8820-4.

266. Rensen, P.C., et al., *Human recombinant apolipoprotein E redirects lipopolysaccharide from Kupffer cells to liver parenchymal cells in rats In vivo.* J Clin Invest, 1997. **99**(10): p. 2438-45.

267. Van Lenten, B.J., et al., *The role of lipoproteins and receptor-mediated endocytosis in the transport of bacterial lipopolysaccharide.* Proc Natl Acad Sci U S A, 1986. **83**(8): p. 2704-8.

268. Harris, H.W., et al., *Human very low density lipoproteins and chylomicrons can protect against endotoxin-induced death in mice.* J Clin Invest, 1990. **86**(3): p. 696-702.

269. Harris, H.W., et al., *Chylomicrons alter the fate of endotoxin, decreasing tumor necrosis factor release and preventing death.* J Clin Invest, 1993. **91**(3): p. 1028-34.

270. Flegel, W.A., et al., *Prevention of endotoxin-induced monokine release by human low- and high-density lipoproteins and by apolipoprotein A-I.* Infect Immun, 1993. **61**(12): p. 5140-6.

271. Parker, T.S., et al., *Reconstituted high-density lipoprotein neutralizes gram-negative bacterial lipopolysaccharides in human whole blood.* Infect Immun, 1995. **63**(1): p. 253-8.

272. Netea, M.G., et al., *Lipoprotein(a) inhibits lipopolysaccharide-induced tumor necrosis factor alpha production by human mononuclear cells.* Infect Immun, 1998. **66**(5): p. 2365-7.

273. Curtiss, L.K. and T.S. Edgington, *The biologic activity of the immunoregulatory lipoprotein, LDL-In is independent of its free fatty acid content.* J Immunol, 1981. **126**(4): p. 1382-6.

274. Mistry, M.J., et al., *Apolipoprotein E restricts interleukin-dependent T lymphocyte proliferation at the G1A/G1B boundary.* Cell Immunol, 1995. **160**(1): p. 14-23.

275. Kelly, M.E., et al., *Apolipoprotein E inhibition of proliferation of mitogen-activated T lymphocytes: production of interleukin 2 with reduced biological activity.* Cell Immunol, 1994. **159**(2): p. 124-39.

276. Pepe, M.G. and L.K. Curtiss, *Apolipoprotein E is a biologically active constituent of the normal immunoregulatory lipoprotein, LDL-In.* J Immunol, 1986. **136**(10): p. 3716-23.

277. Terkeltaub, R.A., et al., *Apolipoprotein (apo) E inhibits the capacity of monosodium urate crystals to stimulate neutrophils. Characterization of intraarticular apo E and demonstration of apo E binding to urate crystals in vivo.* J Clin Invest, 1991. **87**(1): p. 20-6.

278. Tenger, C. and X. Zhou, *Apolipoprotein E modulates immune activation by acting on the antigen-presenting cell.* Immunology, 2003. **109**(3): p. 392-7.

279. Fazio, S., et al., *Increased atherosclerosis in mice reconstituted with apolipoprotein E null macrophages.* Proc Natl Acad Sci U S A, 1997. **94**(9): p. 4647-52.

280. Baitsch, D., et al., *Apolipoprotein E induces antiinflammatory phenotype in macrophages.* Arterioscler Thromb Vasc Biol, 2011. **31**(5): p. 1160-8.

281. Avila, E.M., et al., *Apoprotein E suppresses phytohemagglutinin-activated phospholipid turnover in peripheral blood mononuclear cells.* J Biol Chem, 1982. **257**(10): p. 5900-9.

282. Liu, X., et al., *Bcl6 expression specifies the T follicular helper cell program in vivo.* J Exp Med, 2012. **209**(10): p. 1841-52, S1-24.

283. Poholek, A.C., et al., *In vivo regulation of Bcl6 and T follicular helper cell development.* J Immunol, 2010. **185**(1): p. 313-26.

284. Zhou, X., S. Stemme, and G.K. Hansson, *Evidence for a local immune response in atherosclerosis. CD4+ T cells infiltrate lesions of apolipoprotein-E-deficient mice.* Am J Pathol, 1996. **149**(2): p. 359-66.

285. Kroenke, M.A., et al., *Bcl6 and Maf cooperate to instruct human follicular helper CD4 T cell differentiation.* J Immunol, 2012. **188**(8): p. 3734-44.

286. Good-Jacobson, K.L., et al., *PD-1 regulates germinal center B cell survival and the formation and affinity of long-lived plasma cells.* Nat Immunol, 2010. **11**(6): p. 535-42.

287. Freeman, G.J., et al., *Engagement of the PD-1 immunoinhibitory receptor by a novel B7 family member leads to negative regulation of lymphocyte activation.* J Exp Med, 2000. **192**(7): p. 1027-34.

288. Bu, D.X., et al., *Impairment of the programmed cell death-1 pathway increases atherosclerotic lesion development and inflammation.* Arterioscler Thromb Vasc Biol, 2011. **31**(5): p. 1100-7.

289. Gotsman, I., et al., *Proatherogenic immune responses are regulated by the PD-1/PD-L pathway in mice.* J Clin Invest, 2007. **117**(10): p. 2974-82.

290. Qiu, M.K., et al., *PD-1 and Tim-3 Pathways Regulate CD8+ T Cells Function in Atherosclerosis.* PLoS One, 2015. **10**(6): p. e0128523.

291. Cochain, C., et al., *Programmed cell death-1 deficiency exacerbates T cell activation and atherogenesis despite expansion of regulatory T cells in atherosclerosis-prone mice.* PLoS One, 2014. **9**(4): p. e93280.

292. Nazari-Jahantigh, M., et al., *MicroRNA-155 promotes atherosclerosis by repressing Bcl6 in macrophages.* J Clin Invest, 2012. **122**(11): p. 4190-202.

293. Meazza, R., et al., *Role of common-gamma chain cytokines in NK cell development and function: perspectives for immunotherapy.* J Biomed Biotechnol, 2011. **2011**: p. 861920.

294. Habib, T., et al., *The common gamma chain (gamma c) is a required signaling component of the IL-21 receptor and supports IL-21-induced cell proliferation via JAK3.* Biochemistry, 2002. **41**(27): p. 8725-31.

295. Ozaki, K., et al., *Cloning of a type I cytokine receptor most related to the IL-2 receptor beta chain.* Proc Natl Acad Sci U S A, 2000. **97**(21): p. 11439-44.

296. Parrish-Novak, J., et al., *Interleukin 21 and its receptor are involved in NK cell expansion and regulation of lymphocyte function.* Nature, 2000. **408**(6808): p. 57-63.

297. Brandt, K., et al., *Interleukin-21 inhibits dendritic cell activation and maturation.* Blood, 2003. **102**(12): p. 4090-8.

298. Brandt, K., et al., *Interleukin-21 inhibits dendritic cell-mediated T cell activation and induction of contact hypersensitivity in vivo.* J Invest Dermatol, 2003. **121**(6): p. 1379-82.

299. Nurieva, R., et al., *Essential autocrine regulation by IL-21 in the generation of inflammatory T cells.* Nature, 2007. **448**(7152): p. 480-3.

300. Wurster, A.L., et al., *Interleukin 21 is a T helper (Th) cell 2 cytokine that specifically inhibits the differentiation of naive Th cells into interferon gamma-producing Th1 cells.* J Exp Med, 2002. **196**(7): p. 969-77.

301. Coquet, J.M., et al., *IL-21 is produced by NKT cells and modulates NKT cell activation and cytokine production.* J Immunol, 2007. **178**(5): p. 2827-34.

302. Allard, E.L., et al., *Overexpression of IL-21 promotes massive CD8+ memory T cell accumulation.* Eur J Immunol, 2007. **37**(11): p. 3069-77.

303. Spolski, R. and W.J. Leonard, *Interleukin-21: basic biology and implications for cancer and autoimmunity.* Annu Rev Immunol, 2008. **26**: p. 57-79.

304. Sutherland, A.P., et al., *IL-21 promotes CD8+ CTL activity via the transcription factor T-bet.* J Immunol, 2013. **190**(8): p. 3977-84.

305. Ozaki, K., et al., *Regulation of B cell differentiation and plasma cell generation by IL-21, a novel inducer of Blimp-1 and Bcl-6.* J Immunol, 2004. **173**(9): p. 5361-71.

306. Rankin, A.L., et al., *IL-21 receptor is critical for the development of memory B cell responses.* J Immunol, 2011. **186**(2): p. 667-74.

307. Asao, H., et al., *Cutting edge: the common gamma-chain is an indispensable subunit of the IL-21 receptor complex.* J Immunol, 2001. **167**(1): p. 1-5.

308. Konforte, D. and C.J. Paige, *Identification of cellular intermediates and molecular pathways induced by IL-21 in human B cells.* J Immunol, 2006. **177**(12): p. 8381-92.

309. de Totero, D., et al., *Interleukin-21 receptor (IL-21R) is up-regulated by CD40 triggering and mediates proapoptotic signals in chronic lymphocytic leukemia B cells.* Blood, 2006. **107**(9): p. 3708-15.

310. Zeng, R., et al., *The molecular basis of IL-21-mediated proliferation.* Blood, 2007. **109**(10): p. 4135-42.

311. Brenne, A.T., et al., *Interleukin-21 is a growth and survival factor for human myeloma cells.* Blood, 2002. **99**(10): p. 3756-62.

312. Luthje, K., et al., *The development and fate of follicular helper T cells defined by an IL-21 reporter mouse.* Nat Immunol, 2012. **13**(5): p. 491-8.

313. Crotty, S., *Follicular helper CD4 T cells (TFH).* Annu Rev Immunol, 2011. **29**: p. 621-63.

314. Pot, C., et al., *Cutting edge: IL-27 induces the transcription factor c-Maf, cytokine IL-21, and the costimulatory receptor ICOS that coordinately act together to promote differentiation of IL-10-producing Tr1 cells.* J Immunol, 2009. **183**(2): p. 797-801.

315. Bauquet, A.T., et al., *The costimulatory molecule ICOS regulates the expression of c-Maf and IL-21 in the development of follicular T helper cells and TH-17 cells.* Nat Immunol, 2009. **10**(2): p. 167-75.

316. Ellyard, J.I. and C.G. Vinuesa, *A BATF-ling connection between B cells and follicular helper T cells.* Nat Immunol, 2011. **12**(6): p. 519-20.

317. Reinhardt, R.L., H.E. Liang, and R.M. Locksley, *Cytokine-secreting follicular T cells shape the antibody repertoire.* Nat Immunol, 2009. **10**(4): p. 385-93.

318. Jin, H. and T.R. Malek, *Redundant and unique regulation of activated mouse B lymphocytes by IL-4 and IL-21.* J Leukoc Biol, 2006. **80**(6): p. 1416-23.

319. Good, K.L., V.L. Bryant, and S.G. Tangye, *Kinetics of human B cell behavior and amplification of proliferative responses following stimulation with IL-21.* J Immunol, 2006. **177**(8): p. 5236-47.

320. Saito, T., et al., *Effective collaboration between IL-4 and IL-21 on B cell activation.* Immunobiology, 2008. **213**(7): p. 545-55.

321. Ettinger, R., et al., *IL-21 induces differentiation of human naive and memory B cells into antibody-secreting plasma cells.* J Immunol, 2005. **175**(12): p. 7867-79.

322. Vinuesa, C.G., et al., *A RING-type ubiquitin ligase family member required to repress follicular helper T cells and autoimmunity.* Nature, 2005. **435**(7041): p. 452-8.

323. Liu, R., et al., *A regulatory effect of IL-21 on T follicular helper-like cell and B cell in rheumatoid arthritis.* Arthritis Res Ther, 2012. **14**(6): p. R255.

324. Dolff, S., et al., *Increase in IL-21 producing T-cells in patients with systemic lupus erythematosus.* Arthritis Res Ther, 2011. **13**(5): p. R157.

325. Herber, D., et al., *IL-21 has a pathogenic role in a lupus-prone mouse model and its blockade with IL-21R.Fc reduces disease progression.* J Immunol, 2007. **178**(6): p. 3822-30.

326. Young, D.A., et al., *Blockade of the interleukin-21/interleukin-21 receptor pathway ameliorates disease in animal models of rheumatoid arthritis.* Arthritis Rheum, 2007. **56**(4): p. 1152-63.

327. Jang, E., et al., *A positive feedback loop of IL-21 signaling provoked by homeostatic CD4+CD25- T cell expansion is essential for the development of arthritis in autoimmune K/BxN mice.* J Immunol, 2009. **182**(8): p. 4649-56.

328. Fina, D., et al., *Regulation of gut inflammation and th17 cell response by interleukin-21.* Gastroenterology, 2008. **134**(4): p. 1038-48.

329. Spolski, R., et al., *IL-21 signaling is critical for the development of type I diabetes in the NOD mouse.* Proc Natl Acad Sci U S A, 2008. **105**(37): p. 14028-33.

330. Datta, S. and N.E. Sarvetnick, *IL-21 limits peripheral lymphocyte numbers through T cell homeostatic mechanisms.* PLoS One, 2008. **3**(9): p. e3118.

331. Sutherland, A.P., et al., *Interleukin-21 is required for the development of type 1 diabetes in NOD mice.* Diabetes, 2009. **58**(5): p. 1144-55.

332. McGuire, H.M., et al., *Interleukin-21 is critically required in autoimmune and allogeneic responses to islet tissue in murine models.* Diabetes, 2011. **60**(3): p. 867-75.

333. Bryant, V.L., et al., *Cytokine-mediated regulation of human B cell differentiation into Ig-secreting cells: predominant role of IL-21 produced by CXCR5+ T follicular helper cells.* J Immunol, 2007. **179**(12): p. 8180-90.

334. Akiba, H., et al., *The role of ICOS in the CXCR5+ follicular B helper T cell maintenance in vivo.* J Immunol, 2005. **175**(4): p. 2340-8.

335. Nurieva, R.I., et al., *Bcl6 mediates the development of T follicular helper cells.* Science, 2009. **325**(5943): p. 1001-5.

336. Mitchell, T.C., et al., *Immunological adjuvants promote activated T cell survival via induction of Bcl-3.* Nat Immunol, 2001. **2**(5): p. 397-402.

337. Coquet, J.M., et al., *Cutting edge: IL-21 is not essential for Th17 differentiation or experimental autoimmune encephalomyelitis.* J Immunol, 2008. **180**(11): p. 7097-101.

338. Bubier, J.A., et al., *A critical role for IL-21 receptor signaling in the pathogenesis of systemic lupus erythematosus in BXSB-Yaa mice.* Proc Natl Acad Sci U S A, 2009. **106**(5): p. 1518-23.

339. Marijnissen, R.J., et al., *Interleukin-21 receptor deficiency increases the initial toll-like receptor 2 response but protects against joint pathology by reducing Th1 and Th17 cells during streptococcal cell wall arthritis.* Arthritis Rheumatol, 2014. **66**(4): p. 886-95.

340. Hughes, T., et al., *Fine-mapping and transethnic genotyping establish IL2/IL21 genetic association with lupus and localize this genetic effect to IL21.* Arthritis Rheum, 2011. **63**(6): p. 1689-97.

341. Daha, N.A., et al., *Confirmation of STAT4, IL2/IL21, and CTLA4 polymorphisms in rheumatoid arthritis.* Arthritis Rheum, 2009. **60**(5): p. 1255-60.

342. Cooper, J.D., et al., *Meta-analysis of genome-wide association study data identifies additional type 1 diabetes risk loci.* Nat Genet, 2008. **40**(12): p. 1399-401.

343. Chen, X.L., et al., *Induction of autoimmune diabetes in non-obese diabetic mice requires interleukin-21-dependent activation of autoreactive CD8(+) T cells.* Clin Exp Immunol, 2013. **173**(2): p. 184-94.

344. Bubier, J.A., et al., *Treatment of BXSB-Yaa mice with IL-21R-Fc fusion protein minimally attenuates systemic lupus erythematosus.* Ann N Y Acad Sci, 2007. **1110**: p. 590-601.

345. Croker, B.A., H. Kiu, and S.E. Nicholson, *SOCS regulation of the JAK/STAT signalling pathway.* Semin Cell Dev Biol, 2008. **19**(4): p. 414-22.

346. Yoshimura, A., et al., *Regulation of TLR signaling and inflammation by SOCS family proteins.* J Leukoc Biol, 2004. **75**(3): p. 422-7.

347. Baetz, A., et al., *Suppressor of cytokine signaling (SOCS) proteins indirectly regulate toll-like receptor signaling in innate immune cells.* J Biol Chem, 2004. **279**(52): p. 54708-15.

348. Subramanian, M., et al., *Treg-mediated suppression of atherosclerosis requires MYD88 signaling in DCs.* J Clin Invest, 2013. **123**(1): p. 179-88.

349. Bjorkbacka, H., et al., *Reduced atherosclerosis in MyD88-null mice links elevated serum cholesterol levels to activation of innate immunity signaling pathways.* Nat Med, 2004. **10**(4): p. 416-21.

350. Michelsen, K.S., et al., *Lack of Toll-like receptor 4 or myeloid differentiation factor 88 reduces atherosclerosis and alters plaque phenotype in mice deficient in apolipoprotein E.* Proc Natl Acad Sci U S A, 2004. **101**(29): p. 10679-84.

351. Madan, M. and S. Amar, *Toll-like receptor-2 mediates diet and/or pathogen associated atherosclerosis: proteomic findings.* PLoS One, 2008. **3**(9): p. e3204.

352. Ding, Y., et al., *Toll-like receptor 4 deficiency decreases atherosclerosis but does not protect against inflammation in obese low-density lipoprotein receptor-deficient mice.* Arterioscler Thromb Vasc Biol, 2012. **32**(7): p. 1596-604.

353. Kyaw, T., et al., *Protective role of natural IgM-producing B1a cells in atherosclerosis.* Trends Cardiovasc Med, 2012. **22**(2): p. 48-53.

354. Horkko, S., et al., *Monoclonal autoantibodies specific for oxidized phospholipids or oxidized phospholipid-protein adducts inhibit macrophage uptake of oxidized low-density lipoproteins.* J Clin Invest, 1999. **103**(1): p. 117-28.

355. Fiskesund, R., et al., *IgM phosphorylcholine antibodies inhibit cell death and constitute a strong protection marker for atherosclerosis development, particularly in combination with other auto-antibodies against modified LDL.* Results Immunol, 2012. **2**: p. 13-8.

356. Suto, A., et al., *Interleukin 21 prevents antigen-induced IgE production by inhibiting germ line C(epsilon) transcription of IL-4-stimulated B cells.* Blood, 2002. **100**(13): p. 4565-73.

357. Lee, J., et al., *Contributions of PD-1/PD-L1 pathway to interactions of myeloid DCs with T cells in atherosclerosis.* J Mol Cell Cardiol, 2009. **46**(2): p. 169-76.

358. Lee, S.K., et al., *B cell priming for extrafollicular antibody responses requires Bcl-6 expression by T cells.* J Exp Med, 2011. **208**(7): p. 1377-88.

359. Hollister, K., et al., *Insights into the role of Bcl6 in follicular Th cells using a new conditional mutant mouse model.* J Immunol, 2013. **191**(7): p. 3705-11.

360. Ye, B.H., et al., *The BCL-6 proto-oncogene controls germinal-centre formation and Th2-type inflammation.* Nat Genet, 1997. **16**(2): p. 161-70.

361. Cuff, C.A., et al., *The adhesion receptor CD44 promotes atherosclerosis by mediating inflammatory cell recruitment and vascular cell activation.* J Clin Invest, 2001. **108**(7): p. 1031-40.

362. Hardtke, S., L. Ohl, and R. Forster, *Balanced expression of CXCR5 and CCR7 on follicular T helper cells determines their transient positioning to lymph node follicles and is essential for efficient B-cell help.* Blood, 2005. **106**(6): p. 1924-31.

363. Wei, L., et al., *IL-21 is produced by Th17 cells and drives IL-17 production in a STAT3-dependent manner.* J Biol Chem, 2007. **282**(48): p. 34605-10.

364. Selathurai, A., et al., *Natural killer (NK) cells augment atherosclerosis by cytotoxic-dependent mechanisms.* Cardiovasc Res, 2014. **102**(1): p. 128-37.

365. Bobryshev, Y.V., et al., *VCAM-1 expression and network of VCAM-1 positive vascular dendritic cells in advanced atherosclerotic lesions of carotid arteries and aortas.* Acta Histochem, 1996. **98**(2): p. 185-94.

366. Suri, R.M., H.M. Burkhart, and H.V. Schaff, *Robot-assisted aortic valve replacement using a novel sutureless bovine pericardial prosthesis: proof of concept as an alternative to percutaneous implantation.* Innovations (Phila), 2010. **5**(6): p. 419-23.

367. Christianson, C.A., et al., *K/BxN serum transfer arthritis as a model of inflammatory joint pain.* Methods Mol Biol, 2012. **851**: p. 249-60.

Appendix

Appendix 1 – Composition of High Fat Diet

Diet Name	Western RD
Company	Special Diet Services (Essex, United Kingdom)
Diet Code	829100
Additional Information	Contains 0.15% supplementary cholesterol, resulting in approximately 0.2% total cholesterol content

Diet	829100 – Western RD
Ingredient	**g% (w/w)**
Sucrose	33.94
Milk Fat Anhydrous	20.00
Casein	19.50
Maltodextrin	10.00
Corn Starch	5.00
Cellulose	5.00
Corn Oil	1.00
Calcium Carbonate	0.40
L-Cystine	0.30
Choline Bitartrate	0.20
Cholesterol	0.15
Antioxidant	0.01
AIN – 76A – MX	3.50
AIN – 76A – VX	1.00
Total	**100**

Appendix 2 – Antibodies for Detection of Cells via Flow Cytometry

T-Follicular Helper Cell Antibodies					
Antibody	**Fluorochrome**	**Company**	**Concentration**	**Clone**	**Dilution**
Rat Anti-Mouse CXCR5	Biotin	BD Bioscience	0.5 mg/ml	2G8	1 : 50
Anti-Human/Mouse CD4	Alexa-Fluor 780	Ebioscience	0.2 mg/ml	IM7	1 : 400
Anti-Human/Mouse CD44	PercP Cy 5.5	Ebioscience	0.2 mg/ml	IM7	1 : 400
Anti-Mouse PD-1	Pe Cy 7	Ebioscience	0.2 mg/ml	J43	1 : 500
Anti-Human/Mouse/Rat ICOS	Alexa-Fluor 488	Biolegend	0.5 mg/ml	C398.4A	1 : 100
Streptavidin	Brilliant Violet 421	BD Bioscience	0.5 mg/ml	N/A	1 : 400
Rat IgG$_{2a}$	Biotin	BD Bioscience	0.5 mg /ml	N/A	1 : 50
Armenian Hamster IgG	488	Biolegend	0.5 mg/ml	HTK888	1 : 100
Mouse IgG$_1$	Pe Cy 7	Ebioscience	0.2 mg/ml	P3.6.2.8.1	1 : 500

Germinal Centre B-cell Antibodies					
Antibody	**Fluorochrome**	**Company**	**Concentration**	**Clone**	**Dilution**
Rat Anti-Mouse BB20	APC	BD Bioscience	0.2 mg/ml	RA3-6B2	1 : 100
Peanut Agglutinin (PNA)	Biotin	Vector Labs	5 mg/ml	N/A	1 : 600
Human Anti-Mouse CD95	PE	BD Bioscience	0.2 mg/ml	DX2	1 : 400
Streptavidin	FITC	BD Bioscience	0.5 mg/ml	N/A	1 : 400
Mouse IgG$_1$	PE	BD Bioscience	0.2 mg/ml	N/A	1 : 400

Antibodies for the Detection of Adaptive Immune Cells					
Antibody	**Fluorochrome**	**Company**	**Concentration**	**Clone**	**Dilution**
Anti-Human/Mouse CD4	Alexa-Fluor 780	Ebioscience	0.2 mg/ml	IM7	1 : 400
Anti-Human/Mouse B220	APC	Ebioscience	0.2 mg/ml	RA3-6B2	1 : 400
Anti-Human/Mouse CD44	PercP Cy 5.5	Ebioscience	0.2 mg/ml	IM7	1 : 400

Appendix 3 – Antibodies for Detection of Antibody Isotypes via ELISA

Secondary ELISA Antibodies				
Antibody	**Conjugate**	**Company**	**Clone**	**Dilution**
Goat Anti-Mouse IgG$_1$	HRP	Southern Biotech	N/A	1 : 4000
Goat Anti-Mouse IgG$_{2C}$	HRP	Southern Biotech	N/A	1 : 4000
Goat Anti-Mouse IgG	HRP	Southern Biotech	N/A	1 : 4000
Rat Anti-Mouse IgM	HRP	BD Biosciences	II/41	1 : 1000

Appendix 4 – Antibodies for Detection of Antibody Isotypes via ELISA

Secondary Antibodies for MDA-Ox-LDL Specific ELISAs				
Antibody	**Conjugate**	**Company**	**Clone**	**Dilution**
Goat Anti-Mouse IgG_1	HRP	Southern Biotech	N/A	1 : 4000
Goat Anti-Mouse IgG_{2C}	HRP	Southern Biotech	N/A	1 : 4000
Goat Anti-Mouse IgG	HRP	Southern Biotech	N/A	1 : 4000
Rat Anti-Mouse IgM	HRP	BD Biosciences	II/41	1 : 1000

Antibodies for Total Serum ELISAs (IgM, IgG, IgG_{2C} and IgG_1)				
Capture Antibodies				
Antibody	**Conjugate**	**Company**	**Clone**	**Dilution**
AffiniPure Goat Anti-Mouse IgG, Fcγ Subclass 2c Specific	Purified	Jackson ImmunoResearch	N/A	1 : 60
AffiniPure Goat Anti-Mouse IgG, Fcγ Subclass 1 Specific	Purified	Jackson ImmunoResearch	N/A	1 : 60
AffiniPure Goat Anti-Mouse IgG + IgM (H+L)	Purified	Jackson ImmunoResearch	N/A	1 : 60
Detection Antibodies				
Antibody	**Conjugate**	**Company**	**Clone**	**Dilution**
Goat Anti-Mouse IgG_1	HRP	Southern Biotech	N/A	1 : 4000
Goat Anti-Mouse IgG_{2C}	HRP	Southern Biotech	N/A	1 : 4000
Goat Anti-Mouse IgG	HRP	Southern Biotech	N/A	1 : 4000
Rat Anti-Mouse IgM	HRP	BD Biosciences	II/41	1 : 1000

Antibodies for Total Serum ELISAs (IgE)				
Capture Antibody From Mouse-IgE-Ready-SET-Go! Kit				
Antibody	**Conjugate**	**Company**	**Clone**	**Dilution**
Anti-Mouse IgE	Purified	Ebioscience	N/A	1 : 250
Detection Antibody From Mouse-IgE-Ready-SET-Go! Kit				
Antibody	**Conjugate**	**Company**	**Clone**	**Dilution**
Anti-Mouse IgE	Biotinylated	Ebioscience	N/A	1 : 250

Appendix 5 – Antibodies for Detection of Tfh cells and GC B-cells via IF

T-Follicular Helper Cell Antibodies					
Antibody	**Fluorochrome**	**Company**	**Concentration**	**Clone**	**Dilution**
Anti-Mouse CD4	FITC	Ebioscience	0.5 mg/ml	GK1.5	1 : 100
Anti-Human/Mouse B220	PE	Ebioscience	0.2 mg/ml	RA3-6B2	1 : 100
Anti-Mouse Bcl-6	Alexa Fluor 647	BD Bioscience	5 µl / test	K112-91	1 : 50

Germinal Centre B-cell Antibodies					
Antibody	**Fluorochrome**	**Company**	**Concentration**	**Clone**	**Dilution**
Peanut Agglutinin	Biotinylated	Vector Labs	5 mg	N/A	1 : 400
Anti-Human/Mouse B220	PE	Ebioscience	0.2 mg/ml	RA3-6B2	1 :100
Anti-Mouse CD4	Alexa Fluor 647	BD Bioscience	0.1 mg/ml	RM4-5	1 : 100
Streptavidin	FITC	BD Bioscience	0.5 mg/ml	N/A	1 : 400

Appendix 6 – Antibodies for the Detection of CD68 Macrophages via IF

CD68 Immunohistochemistry Antibodies				
Antibody	**Conjugate**	**Company**	**Clone**	**Dilution**
Rat Anti-Mouse CD68	Purified	AbD Serotec	FA-11	1 : 500
Rat Anti-Mouse IgG$_{2a}$	Purified	AbD Serotec	N/A	1 : 500
Donkey Anti-Rat IgG	Texas Red	Jackson ImmunoResearch	N/A	1 : 200